

https://dspace.org/

Exploring patterns of morphological integration in the crania of papio hamadryas ursinus and homo sapiens

Hemingway, Jason

2017

http://hdl.handle.net/10539/23726

Hemingway, Jason (2017) Exploring patterns of morphological integration in the crania of Papio hamadryas ursinus and Homo sapiens, University of the Witwatersrand, Johannesburg, http://hdl.handle.net/10539/23726

Downloaded from a DSpace repository. https://dspace.org/

EXPLORING PATTERNS OF MORPHOLOGICAL INTEGRATION IN THE CRANIA OF *PAPIO HAMADRYAS URSINUS* AND *HOMO SAPIENS*

Jason Hemingway



UNIVERSITY OF THE
WITWATERSRAND,
JOHANNESBURG

A Theses submitted to the Faculty of Science, University of the Witwatersrand, Johannesburg, in fulfilment of the requirements for the degree of Doctor of Philosophy

Johannesburg, 2017

DECLARATION

I declare that this Theses is my own, unaided work. It is being submitted for the Degree of Doctor of Philosophy at the University of the Witwatersrand, Johannesburg. It has not been submitted before for any degree or examination at any other University.

_____

_____ day of _____ 20 _____ in _____

ABSTRACT

Morphological integration is the pattern of correlation or covariation among parts due to genetic, developmental and functional processes, and is essential for the viability of an organism. Integration among processes is not uniform but forms distinct modules allowing for their independent evolvability and is thus central to the study of biological evolution. The incongruence between phylogenies estimated using the genotype and the cranial morphology in both the Papionini primates as well as the Hominidae possibly result from the disregard of character integration. Regarding the degree of morphological integration humans display extremely low levels of integration among the primates, while the baboon possesses extremely high levels.

This thesis set out to address three broad aims regarding integration of the baboon and human cranium; namely 1) to study the effect of allometry on measures of integration, and when allometry and sexual dimorphism had been accounted for, 2) to assess the patterning of morphological integration into morphological modules; and finally, 3) to assess differences in the pattern of covariation between the cranial base, cranial vault and facial skeleton in humans and baboons.

Although allometric growth is divided into neural and somatic, the findings suggest that the effect of allometry conceals more detailed patterns of morphological integration likely resulting from genetic and developmental processes, and should therefore be accounted for in studies of morphological integration. It is unlikely that allometry among cranial regions constrains evolutionary diversity, but rather offers a path of least resistance. The second aim offered up novel methods of exploring the pattern of morphological covariation using clustering and network methods that supported current hypotheses and proposed that the oral and basicranial regions are comprised of additional modules; however, rigorous scientific scrutiny is required for its support.

The third aim involved the analysis of integration between the cranial base, cranial vault, and facial skeleton. The results supported the proposal that humans and non-human primates share a similar pattern of integration likely reflecting shared developmental processes among the primates, but with key differences probably relating to functional demands. Integration between these three cranial regions primarily involve their relative positioning and proportions.

The broad pattern of integration likely reflects the role of the cranium as the supporting framework around the organs and functional capsules, the “real” modules, which accommodate one another epigenetically as they develop. The recognition of both independent modules and their pervasive integration are important and depend primarily on the nature of the investigation.

To Natasha and Tomas, my family

ACKNOWLEDGEMENTS

My deepest gratitude goes to my supervisor, Paul Manger, who took over supervision, support and guidance. Thank you for your words of encouragement, but most importantly your belief and trust in me. This research was made possible by awards from the National Research Foundation, the Paleontological Scientific Trust (PAST), and the J.J. Smiesjeck bursary.

I would like to thank the following people for their help, advice and words of encouragement: Muhammad Spocter, because we started this journey together; my friends and mentors, Anthony Kegley and Justin Adams; Brendon Billings, for our many discussions and your words of encouragement; The many students that have walked through the doors of my office, especially Candice Small, who on many occasions tested my R skills to the limit; A special thanks goes out to my colleague and friend, Adhil Bhagwandin, for reading through the many drafts, and most importantly ensuring I do not stray too far from sanity. I would also like to thank all the staff in the School of Anatomical Sciences for their continued support.

I would like to thank my parents, Lynn and Stuart Hemingway, for planting the seeds of curiosity and discovery, and giving them room to grow. Janis and Ashleigh, my sisters, for being there when I needed them.

Natasha, my beautiful wife, for all the support, love and patience a husband could ever ask for.

To my son, Tomas. The greatest lesson in this thesis are not to be found in its words but lay in the journey experienced by its author. From conception to putting my thoughts on paper, this process brought about two major shifts in my thinking. The first taught me that with every journey, you will need someone to go with you, someone to share not only your experiences and ideas with, but also your burdens and frustrations. The second is persistence, it does not always pay off, but eventually it will.

CONTENTS

Declaration ii
Abstract iii
Acknowledgements vi
Contents viii
List of figures xi
List of tables xvi
Introduction 1
Background 4
2.1 Morphological integration and modularity 4
2.1.1 Morphological integration 4
2.1.2 Modularity 6
2.1.3 The hierarchical nature of integration 9
2.1.4 The relationships among levels of integration 14
2.1.5 Evolutionary constraints and evolvability 16
2.1.6 The evolution of modularity 18
2.2 Cranial growth and development 19
2.2.1 Embryogenesis 22
2.2.2 Craniofacial embryology and development 27
2.2.3 Craniofacial growth 42
2.3 The study of morphological integration 54
2.3.1 History of morphological integration 54
2.3.2 Morphological integration in the primate cranium 59
2.4 Rationale 68
2.5 Aims 69
Materials and Methods 71
3.1 Samples 71
3.1.1 *Papio hamadryas ursinus* 71

3.1.2 *Homo sapiens sapiens* 78
3.2 Landmarks 82
3.2.1 Estimation of missing landmarks 86
3.3 Repeatability 92
3.3.1 *P. h. ursinus* 92
3.3.2 *H. s. sapiens* 93
3.4 General statistical procedures 93
3.4.1 Superimposition 93
3.4.2 Visualisation 107
3.4.3 General principal component analysis 111
3.5 Aim 1: The role of allometry in morphological integration 112
3.5.1 The pattern of postnatal ontogenetic allometry 112
3.5.2 The patterning of morphological integration in ontogenetic samples 114
3.5.3 Allometric proportion of variation 118
3.6 Accounting for allometry 118
3.7 Aim 2: Patterning of covariation 119
3.8 Aim 3: Exploring integration among *a priori* modules 120
Results 123
4.1 Repeatability 124
4.2 Superimposition 128
4.3 General principal component analysis 133
4.4 Aim 1: The role of allometry in morphological integration 139
4.4.1 Pattern of postnatal ontogenetic allometry 139
4.4.2 The patterning of morphological integration in ontogenetic samples 149
4.4.3 Allometric proportion of variation 157
4.5 Accounting for allometry and sexual dimorphism 159
4.6 Aim 2: Patterning of covariation 160
4.6.1 Polygon clustering 160
4.6.2 Network analysis 166
4.7 Aim 3: Exploring morphological integration between *a priori* modules . 169

Discussion 178
5.1 Summary of findings 178
5.2 Technological limitations 180
5.3 Allometry as an integrating factor 182
5.3.1 Relative cranial growth 182
5.3.2 Clustering and networks during ontogeny 185
5.3.3 Role of allometry in static variation 186
5.4 Exploration of modules 188
5.5 Study of integration among *a priori* modules 194
5.6 Pervasive integration 197
Conclusion 202
References 204

LIST OF FIGURES

Figure 2.1 The chondrocranium of a ~10-week human foetus (left; adapted from Standring, 2005: 494) and the respective neonatal cranial elements (right). 33

Figure 3.1. X-ray of specimen ZA1508 clearly illustrating the size of the crown of the un-erupted canine, suggestive of male sex. 72

Figure 3.2. The approximate distribution of *Papio* across the African continent and Arabian Peninsula. 74

Figure 3.3. Distribution of the baboon specimens, showing sex for the dental age groupings. 78

Figure 3.4. Distribution of the human specimens, showing sex arranged into 5-year cohorts. 81

Figure 3.5. Distribution of the human specimens, showing sex for the dental age groupings. 82

Figure 3.6. Landmarks recorded from the crania of baboons. 84

Figure 3.7. Illustration of the wireframe for aiding in visualisation of landmark statistics in the analysis of the baboon crania. 85

Figure 3.8. Procrustes superimposition of two triangles. 95

Figure 3.9. Illustration of preshapes Z_1 and Z_2 occupying a highly simplified space represented as the surface of a sphere with radius 1. 97

Figure 3.10. The common schematic used to depict the concept of fibres $f(Z_1)$ and $f(Z_2)$ of two pre-shapes Z_1 and Z_2 on the surface of a pre-shape sphere. 98

Figure 3.11. A highly simplistic representation outlining the concept of preshape rotation along fibres that lie parallel to one another in preshape space. 98

Figure 3.12. Sectioning of the Procrustes hemisphere by a plane passing through the two configurations on the surface of this space. 100

Figure 3.13. The relationship between partial and full Procrustes superimposition of Z_2 on Z_1. 102

Figure 3.14. A schematic representation of a cross section through the Procrustes hemisphere. 104

Figure 3.15. Surface model of the specimen used as the basis for visualising shape changes. 108

Figure 3.16. Cartesian transformation grids of D'Arcy Thompson (1917). 110

Figure 3.17. Thin plate spline transformation of the vertices of a Cartesian grid... 111

Figure 4.1. Repeatability in the baboon sample. 125

Figure 4.2. Visual representation of measurement error in the first 20 human crania. 126

Figure 4.3. Visual representation of measurement error in the entire human sample after removal of the lambda-pterion landmark. 127

Figure 4.4. Repeatability in the human sample. 127

Figure 4.5. Scatterplots illustrating the distortion in configurations of the baboon crania brought about through various projections of Procrustes aligned data to the tangent space. 130

Figure 4.6. Scatterplots illustrating the distortion in configurations of the human crania brought about through various projections of Procrustes aligned data to the tangent space. 131

Figure 4.7. Scatterplots illustrating the distortion in configurations of the mixed sample produced by the projections of Procrustes aligned data to the tangent space. 132

Figure 4.8. Plots of first three principal components scores of shape space of the baboon sample. 136

Figure 4.9. Plots of first three principal components scores of shape space of the human sample. 138

Figure 4.10. Plots of first three principal components scores of size-shape space for the baboon crania. 141

Figure 4.11. Allometric shape change of the baboon cranium as associated with the first Principal component in size-shape space. 143

Figure 4.12. A: Plots of first three principal component scores of size-shape space for the human sample. 145

Figure 4.13. Allometric shape change of the human cranium as associated with the first principal component in size-shape space. 146

Figure 4.14. A: Plots of first three principal component scores of size-shape space for a pooled baboon and human sample. 148

Figure 4.15. Plot between the number of polygon clusters and the proportion of variance explained, representing the baboon cranium during ontogeny. 151

Figure 4.16. The resulting dendrogram and associated polygon clusters of the baboon cranium based on the strength of associations during ontogeny. 151

Figure 4.17. Plot between the number of polygon clusters and the proportion of variance explained, representing the human cranium during ontogeny. 153

Figure 4.18. The resulting dendrogram and associated polygon clusters of the human cranium, representing ontogenetic associations. 153

Figure 4.19. The network and associated polygon clusters of the baboon cranium based on the presence and absence of associations during ontogeny. . 155

Figure 4.20. The network and associated polygon clusters of the human cranium based on the presence and absence of associations during ontogeny. . 156

Figure 4.21. Plot between the number of polygon clusters and the proportion of explained variance in the baboon cranium. 162

Figure 4.22. The resulting dendrogram based on covariation between polygons and the distribution of clusters on the baboon cranium. 163

Figure 4.23. Plot between the number of polygon clusters and the proportion of explained variance in the human cranium for the selection of the optimal number of clusters. 165

Figure 4.24. A dendrogram based on the strength of covariation between polygons and the distribution of the resulting clusters on the human cranium. .. 165

Figure 4.25. The network and associated polygon clusters of the baboon cranium based on the presence and absence of associations. 167

Figure 4.26. The network and associated polygon clusters of the human cranium based on the presence and absence of associations. 169

Figure 4.27. Plots of the first partial warp scores from each of the 2B-PLS analyses between the *a priori* defined regions..... 173

Figure 4.28. Wireframe and polygon models depicting the PLS1 relationship between the cranial vault on the left and the facial skeleton on the right. 176

Figure 4.29. Wireframe and polygon models depicting the PLS2 relationship between the cranial vault on the left and the facial skeleton on the right. 177

Figure 4.30. Wireframe and polygon models depicting the PLS2 relationship between the cranial base on the left and the facial skeleton on the right. 177

LIST OF TABLES

Table 2.1 A list of the cranial elements observed in an adult human, whether they are paired or unpaired and the region(s) they are generally associated with. The ear ossicles are omitted. 21

Table 3.1. List of landmarks used in the analysis 89

Table 4.1. Proportion of variation in the baboon sample accounted for by the first ten principal components. 134

Table 4.2. Proportion of variation in the human sample accounted for by the first ten principal components. 137

Table 4.4: Tests for differences between the major axis slopes on the 2B-PLS scores of the baboon and human samples. 174

INTRODUCTION

> *"…the whole organisation is so tied together during its growth and development, that when slight variations in any one part occur, and are accumulated through natural selection, other parts become modified. This is a very important subject, most imperfectly understood."* Darwin, 1859, pg. 143.

A biological organism can be thought of as being composed of numerous parts that are all connected through various levels of integration, necessary for the organism to function as a coherent whole. This morphological integration results from diverse genetic, developmental and functional mechanisms, operating at differing degrees and at various hierarchical levels (Strait, 2001). The concept of covariation due to function and development is not new, but the study of population genetics and then the formation of the discipline of evolutionary-developmental biology (evo-devo) rekindled an interest in the study of morphological integration. This rebirth is primarily due to the developmental origins of much of the integration, and its more primary role in studies of the evolution of novel and complex phenotypes.

Not only is morphological integration interesting and significant in itself, but it is fundamental in estimating the phylogenetic relationships among extinct taxa. Hypotheses of the relationships between extinct primate taxa, and ideas concerning the adaptive nature of trait acquisition, are complicated by the potential integration of morphological characters. The non-independence of traits can give disproportionately high weighting to characters used to reconstruct morphological

phylogenies, specifically when the trait is highly adaptive in nature, potentially homoplastic, or even very susceptible to fixation through genetic drift.

Current hypotheses of hominin phylogeny are thought to be confounded by potentially integrated suites of traits, particularly with regard to discerning the positions of *Australopithecus africanus* and *Paranthropus aethiopicus* among the australopithecines (and the relationship between the former and early *Homo*), and whether the genus *Paranthropus* constitutes a mono- or polyphyletic grouping (Strait, 2001). The proper consideration of morphological integration may improve phylogenetic inference by highlighting biases brought about by interrelated characters.

This study aims to explore patterns of craniofacial morphological integration in *Papio hamadryas ursinus* and *Homo sapiens sapiens*. The morphological variation within extant analogues forms the yardstick from which individual, sexual and ontogenetic variation in closely related fossil taxa is assessed. Understanding integration and potentially delineating modules in the primate craniofacial complex can guide the choice of characters we use to infer relationships between fossils. The recognition of homoplasy and the importance of morphological integration in the papionin (Disotell *et al*., 1992; Leigh, 2007; Cheverud *et al*., 2009) and hominin tribes (Ruvolo *et al*., 1991; Ruvolo, 1997; Ackermann, 2002; Mitteroecker and Bookstein, 2008) have received much consideration. It has also been highlighted that instances of parallel and convergent evolution are not as apparent as originally suspected (Leigh, 2007; Mitteroecker and Bookstein, 2008), calling to question the reliability of the phylogenetic positions of various primate fossil taxa (e.g. Gilbert, 2007). It is hypothesized that the patterns of morphological integration in the human and baboon cranium do not fit *a priori* models based on simplistic

developmental and functional factors; neither do they fit a pattern suggestive of multiple overlapping developmental and functional processes. The patterns of morphological integration do, however, reflect what would be expected for a scaffolding or framework, which houses and supports the true modules of the head – the organs, functional spaces and jaws.

The background chapter introduces the concepts of morphological integration and modularity and covers the developmental and functional aspects relevant to studies of craniofacial integration, before dealing with the literature concerning studies of morphological integration and modularity in primates, and laying out the aims of this thesis. The sample and methodology will be dealt with in chapter three and will be followed by the results chapter. The discussion and conclusion make up the final chapter.

BACKGROUND

2.1 Morphological integration and modularity

2.1.1 Morphological integration

Morphological integration is the pattern of correlation or covariation among parts due to genetic, developmental and functional processes. The pattern of interdependence among these processes responsible for morphological integration is a result of an organism's evolutionary history, and the tendency of evolution to generate novel structures through the co-option or parcellation of existing genetic or developmental processes (Wagner, 1996; Wagner & Altenberg, 1996). Integration in general is also born out of a necessity for coherence at multiple levels among the various processes and the resulting structures essential for an organism to function as a viable whole.

Morphological integration is central to the study of evolution and development for a number of reasons. Firstly, integration among traits constrains evolution by channelling the existing variation on which selection and genetic drift can act (Maynard Smith *et al*., 1985). The propensity for the production of genetic variation as well as the ability of an organism to respond to selection has been dubbed "evolvability" by Chernoff and Magwene (1999). Hence, integration plays an important role in the evolvability of organisms by constraining and directing evolutionary diversity (Cheverud, 1996a), and has the potential to provide insight into the intrinsic factors responsible for radiations and extinctions in the fossil record. Secondly, uncovering patterns of integration is necessary if we are to understand the evolution of complex characters (Cheverud, 1996a; Wagner, 1996; Wagner & Altenberg, 1996). For example, a

detailed analysis of the role of evolutionary forces responsible for modern human craniofacial variation (i.e. gene flow, selection or stochastic processes) requires an understanding of the pattern of integration among human craniofacial traits. Selection on a specific trait may involve a suite of secondary changes that can be misconstrued as the target of selection, and thus might confound evolutionary analyses of morphological diversity (Martínez-Abadías *et al*., 2012). Thirdly, the pattern of integration provides a framework on which the genotype-phenotype map can be drafted (Mezey *et al*., 2000). An organism is not a simple construct from its genetic blueprint, and the hypothetical genotype-phenotype map lays out the complicated developmental processes that translate the genetic makeup of an organism to its physical appearance. Integration is an important characteristic of this genotype-phenotype map, and one essential if we are to untangle and fully understand the complex relationship between the genotype and phenotype. Finding links between seemingly distinct parts can reveal clues about the processes responsible for their formation.

Finally, an understanding of the integration among characters is crucial to uncovering the phylogenetic history based solely on morphological traits. Morphology is still the only line of evidence available for reconstructing the relationships between fossil taxa (Lockwood, 2007) older than the current range of ancient DNA techniques (Meyer *et al*., 2014). Defining the phylogenetic relationship between organisms is essential when constructing and testing hypotheses concerning possible evolutionary trends and underlying mechanisms (Collard & O'Higgins, 2001), yet cladistic analyses of extinct primates are currently only used to provide a general idea of relatedness between taxa. This is because cladistic analyses assume an independence of morphological traits and consider a change in each character state as

representing a single evolutionary event (Skelton & McHenry, 1992), and additionally, there are many uncertainties regarding the covariance between, and biological relevance of, particular traits (Trinkaus, 1990). Thus, multiple associated changes between highly integrated parts without recognition of their non-independence can skew phylogenetic interpretations, and is probably responsible for many of the disparities between genetic and morphological phylogenies of some living taxa, such as the papionin primates (Page & Goodman, 2001). This questions the reliability of those phylogenetic trees for which we do not have any genetic ratification, such as our own human evolutionary history, and further highlights the importance of studies that address morphological integration.

A key aspect of morphological integration is that it is a characteristic of the morphology, and its measure, whether by correlation or covariation, is a gauge of the true integration resulting from biological processes at multiple spatio-temporal levels. Additionally, the distribution of morphological integration is not homogenous but rather reflects the hierarchical structure of the processes involved. This pattern of morphological integration and the inferences regarding the underlying processes are central to this thesis.

2.1.2 Modularity

"Essentially, modularity is nested integration" Willmore *et al*., (2009: 20)

It is evident that body parts form separate entities. If integration were total and uniform across structures, all mutations that elicit a phenotypic change would be detrimental and disrupt the

development and functioning of the organism (Schlosser & Wagner, 2004). Hence, the relative dissociation of structures into groups allows for their independent evolvability and mosaic evolution (Cheverud, 1996a; Raff, 1996). Needham's (1933) recognition of the dissociability of development – that morphogenesis of a part is somewhat independent from that of other structures – set the initial framework for the conceptual ideas that became developmental modularity. Raff (1996: 260) illustrates this dissociation effectively by describing development as multiple parallel pathways, with some developmental pathways affecting others and some being completely dependent on others, but their dissociation permits individual modification of these pathways without detriment to the developing embryo.

Today, modularity is considered an organisational property of any biological substructure (Wagner *et al.,* 2007). It results from the inherent self-organisational property of biological processes and can essentially be found in any complex non-random arrangement at any level of the biological hierarchy (e.g. gene expression, development, behaviour, ecology). Because biological modularity spans multiple disciplines, Bolker (2000: 773) characterised a biological module as possessing three properties: "(1) a module is a biological entity (a structure, a process, or a pathway) characterized by more internal than external integration . . . (2) Modules are biological individuals . . . that can be delineated from their surroundings or context, and whose behavior or function reflects the integration of their parts . . . [and] (3) a module can be delineated from other entities with which it interacts in some way" (see additional definitions by Wagner, 1996, and Schlosser, 2004)

The relationship between morphological integration and modularity has recently come under scrutiny. Mitteroecker and Bookstein (2007) argued that modularity had been misrepresented as a descriptive characteristic of morphological integration where the proper traditional usage of the term has been to describe the arrangement of the genetic and developmental processes themselves. Like Lieberman and colleagues (2000), I would like to draw attention to the importance of defining what is meant by pattern and process. Like them, the pattern used here is a description of a relationship among parts, while the process refers to a series of events leading to a part's formation, and does not specifically entail a causal mechanism. Although Bolker (2000) allows any biological entity that fulfils the above requisites to be considered a module, the characteristics of a process and its resulting pattern can diverge. It is thus essential to clearly define the phenomenon – the process or the statistical pattern in the resulting morphology – to which the propensity (modularity) belongs. As such researchers have begun using the adjective "variational" to define morphological modules identified through statistical means (e.g. Wagner & Mezey, 2004; Hallgrímsson *et al*., 2007; Mitteroecker, 2009), as opposed to modularity defined on the basis of genetic or developmental processes. A recent review has used the term "morphological" to describe the measured or observed patterns of morphological integration (Klingenberg, 2014), which implies that it is derived from morphological characteristics, but not necessarily their variational properties. Thus, the term 'morphological modularity' describes a resulting pattern of morphological integration independent of the methodology, and 'variational modularity' refers to the structure of potential relationships among traits, as measured directly using patterns of covariation. The term "morphological modules" will be used here because methods other than covariation and correlation have been employed to delineate phenotypic modules (e.g. the relative number of quantitative trait loci; Mezey *et al*., 2000).

Thus, associated with morphological integration is the arrangement of phenotypic traits into morphological modules. The pattern of morphological integration and morphological modularity is descriptive, and only an estimate of the arrangement of integrating and modular morphogenic processes. Ultimately the modularity of interest is that which describes the grouping of developmental, structural and functional processes into units that possess some degree of semiautonomy (Wagner, 2007). But because of the complexity of the underlying processes, a module is generally inferred or tested under the premise that it possesses greater integration internally, among its constituents, than externally between it and other modules.

2.1.3 The hierarchical nature of integration

Integration and modularity can occur at many hierarchical levels. A recent review (Klingenberg, 2014) highlighted the similarities between integration and allometry, the influence of size on shape, and even categorized integration under the qualifying terms – static, ontogenetic and evolutionary – originally proposed for allometry (Cock, 1966). The mutual contextual terminology can be applied because both allometry and integration deal with variation and covariation, and each level attempts to partition these phenomena into factors responsible for idiosyncratic variation (static), variation due to growth (ontogenetic), and variation due to evolutionary processes (evolutionary). Just as allometry at one level affects the allometry at other levels (Pélabon *et al.*, 2013), the levels of integration are intimately intertwined.

Studies of static integration address integration among individuals in a biological population or species at the same ontogenetic stage; ontogenetic integration involves the expression of morphological integration across multiple ontogenetic stages in a biological population or species; and investigations of evolutionary integration deal with morphological integration across multiple taxa, while trying to maintain a comparable ontogenetic stage (Klingenberg, 2014). Whereas ontogenetic and evolutionary integration deal with integration resulting specifically from growth and evolutionary forces respectively, there are several factors responsible for variation and covariation at the level of static integration. Accordingly, static integration is further subdivided into genetic, developmental, functional and environmental integration.

Genetic integration is the heritable portion of morphological integration resulting from genuine pleiotropy and linkage disequilibrium. "Genuine" pleiotropy (*sensu* Pyeritz, 1989) describes the occurrence of a single locus affecting two or more distinct phenotypic traits (through distinct developmental pathways or the same pathway in different morphological and physiological contexts – type I and II pleiotropy *sensu* Wagner & Zhang, 2011), either through a multifunctional gene product, or through the production of multiple products with disparate functions (single loci may have multiple overlapping reading frames, and nucleotide substitutions in the mRNA can modify the resulting products; Stearns, 2010). An example of pleiotropy would be the human disease Phenylketonuria, where a mutation in the PAH gene results in both mental retardation and reduced hair and skin pigmentation. New research has shown that coding genes play a minor role in the production of normal craniofacial variation (eg Paternoster *et al*., 2012). Rather, single nucleotide polymorphisms in enhancer sequences found on non-coding DNA are significantly associated with non-pathological variation and have been

shown to regulate the spatio-temporal pattern of gene expression (Attanasio *et al*., 2013; Rada-Iglesias *et al*., 2013). Interestingly, these enhancer sequences also display a high degree of pleiotropy, affecting multiple protein-coding genes (Clarke, 2013).

The other factor responsible for genetic integration, linkage disequilibrium, is a non-independence between genotypes at multiple loci resulting from their relative position on a chromosome (Freeman & Herron, 2004). Because of recombination during meiosis, genes that are proximal to one another on a particular chromosome have a higher probability of being inherited together. Like pleiotropy, strong linkage disequilibrium between genes affecting different traits can bring about heritable covariation in the phenotype, particularly during periods of hybridization and gene flow (Wagner *et al*., 2007)

Developmental integration refers to morphological covariation that arises solely through interactions among developmental processes that affect different traits (Klingenberg, 2008; 2014). In traditional genotype-phenotype mapping, developmental processes are abandoned and developmental interactions are subsumed under the general term 'pleiotropy'. However, the current understanding of molecular mechanisms warrants further distinction between integration arising from developmental and genetic processes. That the expression of genetic variation is not exclusively through developmental processes, and that developmental interactions are under genetic control make for a compelling argument in favor of their separation (Klingenberg, 2008). Where confusion may arise is that developmental integration is genetically determined and is thus heritable, like genetic integration.

Developmental integration involves interactions among pathways that distribute the genetic variation among multiple traits, whereas the gene in genuine pleiotropy affects multiple pathways directly (either through pleiotropic regulatory mechanisms, a multifunctional product, or multiple products). Developmental integration involves all the complex, localized epigenetic interactions during growth and development that govern the spatio-temporal patterning, morphogenesis and localised growth of organs in response to their immediate surroundings (Hallgrímsson *et al.,* 2007a; Lieberman, 2011a). For example, the growth of the cranial vault in response to pressures from the developing brain. Because fluctuating asymmetry results from random deviations from symmetry as a result of perturbations in developmental processes alone, the study of its covariation has provided some insight into developmental integration (Klingenberg, 2009). One of the drawbacks is that the variation resulting from fluctuating asymmetry is minute and thus small sample sizes and measurement error impact negatively on its accurate detection.

Functional integration is the association among parts that jointly affect performance (Cheverud, 1996a). The most intuitive example is the coordination between the upper and lower jaws and teeth, as their dissociation and resulting malocclusion would significantly affect fitness (Boughner & Hallgrímsson, 2008; Lieberman, 2011a; Polly, 2011). Functional hypotheses are difficult to test because they require additional information on how the covariation between the traits affects performance and fitness (Rolian & Willmore, 2009). As an added factor, integration among different regions can come about through the simultaneous plastic modeling that results from parallel mechanical stresses and strains due to their joint function (Enlow & Hans, 1996).

Thus, function can bring about integration through selection as well as the physiological responses of bone to mechanical processes.

Environmental integration at the level of static integration results from environmental variation. The association between morphological traits can occur through their joint physiological response to an environmental stimulus. Depending on the type and extent of the environmental variable, its resulting integration may be substantial and pervasive and its pattern comparable to that from ontogeny. The increased chest dimensions and reduced stature associated with hypoxia in humans is a good example of environmental integration. It is important to note that integration based on environmental correlation matrices, calculated as the residual component of a quantitative genetics analysis (e.g. Cheverud, 1995), is not equivalent to environmental integration (Klingenberg, 2014), as the prior considers all non-heritable components, and should possibly be termed *non-heritable* integration.

Ontogenetic integration is a level of integration that involves a coordinated change among traits due to growth processes (Klingenberg, 2014). Ontogenetic integration is akin to ontogenetic allometry as it focuses on the associations between the growth trajectories among traits, and should not be confused with developmental integration, which is the static correlated variation due to interactions between developmental factors. Growth across the organism is most often not equivalent and is reflected as allometric patterns (Mitteroecker & Bookstein, 2007). The parallel responses to an endocrine signal, such as growth hormone, bring about ontogenetic integration and coordinated growth among parts during ontogeny. The growth plates of the fore- and hind-limb, for example. The effect of ontogenetic integration is likely considerable and overshadows

much of the local developmental integration arising from developmental pathways (Klingenberg, 2008), which is particularly problematic if the distribution of genetic and developmental integration is of primary interest (Mitteroecker & Bookstein, 2007). The study of the temporal dissociation among characters in related organisms (a shift in relative onset, cessation or rate of development) has been a topic of much research under the title of heterochrony (*sensu* Alberch *et al*., 1979).

Evolutionary integration results from the coordinated evolution of characters through their joint-selection and/or co-inheritance (Cheverud, 1996a; Wagner, 1996; Wagner & Altenberg, 1996). This is usually measured as covarying traits across a number of species, after accounting for the effect of phylogeny (independent contrasts, phylogenetic generalized least squares; see Klingenberg & Marugán-Lobón, 2013, and references therein). Of course evolutionary integration results from the heritable portion of those factors responsible for morphological integration, which ties many of these levels together.

2.1.4 The relationships among levels of integration

It is evident that integration and modularity occurs at multiple levels; three – ontogenetic, static and evolutionary integration – are contextual levels (of study) while the four levels under static integration – genetic, developmental, functional and environmental integration – are in the same context and their label reflects the mechanistic cause, and should rather be refered to as types. Nevertheless, each of these levels is associated with, influenced, or is affected by the integration at other levels (Klingenberg, 2008; 2014). The relationship between ontogenetic, static and

evolutionary integration is relatively straightforward but multifactorial; ontogenetic variation gives rise to the static variation on which evolutionary forces act (at least the heritable portion) to generate evolutionary variation, and reciprocally, evolutionary change commonly involves a shift in ontogenetic processes. Genetic or developmental integration among traits in a population can, over time, become a characteristic among taxa (evolutionary integration) through selection and genetic drift (Lande, 1979). Likewise, selection for the association between parts of a functional complex (Cheverud, 1996a; Wagner, 1996), as well as selection for increased plasticity among parts in response to function or the environment can both bring about evolutionary integration. Ontogenetic integration affects static integration as associations and dissociations among growth rates will influence the pattern of integration in a population at a given ontogenetic stage. Evolutionary change through heterochrony (shifts in the rates and timing of processes between ancestral and descendent populations) links ontogenetic and evolutionary integration.

Klingenberg (2014) has noted that links also exist among the types of static integration within a population. Genetic and developmental integration are related through the developmental regulation of genetic expression and, reciprocally, the genetic control of developmental interactions. Environmental integration is linked to developmental integration because plasticity is a physiological process invoking existing developmental pathways. Environmental integration can be linked to functional integration as plastic responses to functional requirements can be seen as adaptive (Klingenberg, 2014). Cheverud (1984; 1989) and Wagner (1988; 1996) have proposed the matching hypothesis, whereby selection for integration among traits that form a functional complex (functional integration) can increase the linkage disequilibrium (genetic integration) as association among those traits brings increased fitness, which in turn will become

entrenched among taxa as evolutionary integration. The proposal that selection can generate genetic integration among functional groups is difficult to test as most analyses show a general agreement between genetic and functional modules (Breuker *et al*., 2006) without any indication of the causal relationship. Additionally, the processes of integration are not necessarily dependent or independent of one another; integration of phenotypic traits at one level does not necessitate integration of those characters at other levels, and developmentally and functionally independent traits, for example, may possess genetic correlations (Cheverud, 1982).

Both integration and modularity occur in a complex hierarchy of innumerable and interacting mechanisms. All through this section I have been addressing integration, but it is important to note that at each level, and associated with each type of integration, there exists a non-random modular pattern. For example, the arrangement of interactions among developmental pathways will invoke developmental modularity, just as high levels of pleiotropy and linkage disequilibrium among a set of traits could be considered genetic modularity.

2.1.5 Evolutionary constraints and evolvability

Integration among genetic, developmental and functional mechanisms can limit or channel the variation available for evolutionary change (Lande, 1979; Cheverud 1984; 1996a; Wagner 1996; Wagner & Altenberg 1996), and has thus been causally linked with the concept of evolutionary constraints (Maynard Smith *et al*., 1985; Richardson & Chipman, 2003). Horizontal and vertical constraints result from both genetic and developmental integration between traits, and preclude change from occurring in one trait if there were deleterious secondary consequences in another.

Functional constraints restrict evolutionary change as the modification of a structure in a complex that requires functional integration could be deleterious to the organism. Richardson and Chipman (2003) also suggest that developmental buffering is an evolutionary constraint, where integration among developmental processes can buffer against the phenotypic presentation of a particular genetic change, so that it is not presented for selection.

It is important to recognise that constraints do not only withhold variation but also channel variation, biasing the direction and rate in a manner that may increase the evolvability of an organism (Altenberg, 1994; 2005). As mentioned earlier, evolvability is the propensity for the production of genetic variation and directly affects the ability of an organism to respond to selection (Chernoff & Magwene, 1999). Thus, the pattern and magnitude of integration influences the evolvability of a population (Marroig *et al*., 2009). Integration among phenotypic characters generally takes on a modular arrangement, whereby integration is greatest among characters within a functional complex than between characters serving different functions. This morphological modularity has been suggested to increase evolvability by reducing the integration between different complexes (Wagner & Altenberg, 1996), thus reducing the constraints between, and channelling evolution within, phenotypic characters in a complex.

Wagner *et al.* (2007) suggest that, at least at the molecular level, modules are conservative and evolutionary changes generally affect integration between modules rather than within them. They further suggest that this can be extrapolated to the morphological level, and that the joint modification of characters within a complex is evolutionarily maintained. Because increased modularity (reduced integration between modules) is theoretically associated with increased

evolvability, species with greater modularity should have a selective advantage over others. However, the relationship between the degree of modularity and evolvability is probably parabolic as integration between modules is necessary to maintain organismal integrity and just the right amount of integration allows for autonomy but not at the expense of the whole organism (Polansky & Franciscus, 2006). This relationship between integration, modularity and evolvability is dependent on many factors including the environment and the degree of specialization of a particular module (e.g. Young & Hallgrímsson, 2005).

2.1.6 The evolution of modularity

As stated above the origin of modularity is associated with organismal complexity and the evolution of complex characters. Riska (1986) proposed that modularity can arise through two processes; namely fusion, the differential integration of originally independent characters into sets, or fission, whereby integration breaks down between unrelated characters and is strengthened among characters that share a functional role (Wagner, 1996, referred to these respective processes as integration and parcellation). Although both models possibly occur, the fission model has received the greatest amount of support, primarily regarding the origin of modularity among the metazoa (Wagner & Altenberg, 1996; Porto *et al*., 2009). The first line of support draws on the principle of parsimony, that a complete independence of each developmental process in the fusion model would be extremely complicated and would imply many local, independent factors instead of the simple coordination of growth by means of a single global factor (Chernoff & Magwene, 1999). The second line of support for the fission model arises from the notion that genetic or developmental processes are generally co-opted or shared by evolution when generating novel structures, entailing strong general integration as a

foundation. The third comes from comparative biology, where it is evident that repeated elements, such as teeth, tend to differentiate over evolutionary time, accumulating more discrete developmental processes (Wagner, 1996; Wagner & Altenberg, 1996). The last line of support for the fission model comes from the association between degree of modularity and the phylogenetic history among mammals, with metatherian crania displaying increased integration compared to most eutherian crania (Porto *et al*., 2009).

The matching hypothesis (Cheverud, 1984; Wagner & Altenberg, 1996; see also Riedl's, 1978, "imitatory epigenotype"), whereby distinct parts that form a functional complex will, over time, become a genetically integrated module, follows the logic of the fusion model for the origin of modules. Although supporting examples exist, such as modularity of the vertebrate jaw from evolutionarily distinct structures, there is little support to suggest that fusion is the predominant process responsible for the origin of modularity from simple organisms. This is important from a statistical sense; if the origin follows a fission model, the null hypothesis should propose complete integration. On the other hand, if fusion is the likely origin, one should test against a total lack of integration (Chernoff & Magwene, 1999).

2.2 Cranial growth and development

"evolution is the control of development by ecology." Van Valen (1973: 488)

A basic understanding of craniofacial morphogenesis is required to fully grasp some of the developmental reasons that have been used to separate phenotypic traits *a priori*. An

understanding of the events and mechanisms responsible for generating patterns is vital to any study of modularity and integration. The general evolutionary history behind the acquisition of the various cranial components will be included as this provides an important causative explanation for the persistence and retrospective utility of these parts. The following description of embryology is based primarily on human development although many of the finer details have been determined though experimental embryology on model organisms such as the chicken and mouse. Additionally, it is expected that craniofacial development of other members of the Catarrhini, such as *Papio*, will follow in a similar fashion, although the relative rate and timing of developmental processes may differ slightly.

The primate skull not only functions to protect and support the brain and special sensory organs, but it initiates digestion, functions in respiration, and is important for vocal and visual communication. The adult human cranium generally comprises 28 bones (Standring, 2005) that can be divided into paired and unpaired elements (Table 2.1), together with the three paired ear ossicles. Besides the synovial temporomandibular joint, the bones of the skull are separated by sutural synarthroses or cartilaginous synchondroses that are involved in growth.

The skull is generally described as comprising a cranial vault, a cranial base and the facial skeleton. The cranial vault is the dome-like bony covering that surrounds the brain while the cranial base supports the ventral surface of the brain through which many of the neurovascular structures pass. The facial skeleton includes the dermal bone that surrounds the orbital and nasal cavities together with the jaws. The ethmoid possesses all the characteristics of a bone of the cranial base but extends inferiorly to play a primary role in the positioning and growth of the

facial skeleton (Lieberman *et al.,* 2000). There is further confusion, as some authors (e.g. McBratney-Owen *et al*., 2008; Morriss-Kay, 2001) group the cranial vault and base together under a single neurocranium despite each region possessing a somewhat distinct growth pattern as well as developmental and evolutionary history. This independence is obscured by a few compound bones resulting from the early fusion of distinct precursor elements from the cranial vault and base, forming the occipital, temporal and sphenoid bones. The frontal bone is another element involved with two regions, playing a role in both the upper face and the cranial vault.

Table 2.1 A list of the cranial elements observed in an adult human, whether they are paired or unpaired and the region(s) they are associated with. The ear ossicles are omitted.

Bone	Paired/unpaired	Region
Nasal	Paired	Facial
Lacrimal	Paired	Facial
Palatine	Paired	Facial
Zygomatic	Paired	Facial
Maxilla	Paired	Facial
Mandible	Unpaired	Facial
Vomer	Unpaired	Facial
Frontal	Unpaired	Vault/facial
Parietal	Paired	Vault
Occipital	Unpaired	Vault/base
Temporal	Paired	Vault/base/facial
Sphenoid	Unpaired	Vault/base/facial
Ethmoid	Unpaired	Base
Conchae	Paired	Base

The development from zygote to adult can be subdivided into a number of specific periods that are dominated by particular trends and developmental processes. The first logical subdivision is into separate prenatal and postnatal periods, where the latter involves mostly size increases, the development of secondary sexual characteristics, and a structural “finalisation” in the presence of

the surrounding environment. The prenatal period can be further divided into an embryonic stage, where most of the structural arrangements and organ and system precursors are fashioned, and a foetal stage, where the necessary organs develop in size and to a state necessary for the viability of the newborn. This subdivision of prenatal development into two separate stages at eight weeks is somewhat arbitrary as size increases in an approximately linear fashion throughout the combined embryonic and foetal period, and structural genesis continues well into the foetal stage. Nevertheless, the subdivision aids in the conceptualisation of the numerous developmental processes.

2.2.1 Embryogenesis

The age of an embryo or foetus can be measured in days or weeks since last menstruation, coitus, ovulation or conception. There is variation in the rate of development and often the timing of many of these events can only be estimated. As such, many embryologists prefer to use developmental stages as a means of communicating the relative temporal position of a developing embryo. Because this section is only meant as an outline of craniofacial embryogenesis for the sake of understanding modularity and integration, the stated days or weeks will represent the elapsed time since conception so as to provide the reader with a relative sense of order and timing.

Development of the head only begins forming around four weeks post conception, however the formation of the germ layers, the notochord and neurulation are all important for understanding the origin of the tissues that give rise to the head. In each stage, many of the formed tissues and

structures play an important role in inducing and patterning cell lineages in ensuing stages. For example, the notochord, which appears by the end of the third week, plays an important role in regulating organogenesis and establishing polarity of the future nervous system and limbs (Echelard, 1993). To set the stage and put everything into perspective, a synopsis of the major events during the first four weeks are provided, after which the description of the development will focus on specific craniofacial regions, until many of the anlagens are in place. Again, much of the detail regarding early development is omitted for sake of brevity. Much of the information on early development is from Sperber *et al.* (2010) and Larsen (2001), and supplemented with more current literature where relevant.

The first two weeks

In the human, the embryonic stage begins with fertilisation of the egg to form a zygote. The single celled zygote divides into a multicellular morula followed by the formation of a cavity within. At this point the structure is called a blastocyst and consists of an outer single layer of cells surrounding a cavity with an asymmetrically positioned inner cell mass. By the end of the first week the inner cell mass has differentiated into two cell layers: the epiblast, which gives rise to all embryonic structures, and the hypoblast, from which certain extraembryonic structures develop (see Stern & Downs, 2012). An amniotic cavity then forms within the epiblast separating it from the outer layer of cells, while the cavity adjacent to the hypoblast becomes the primitive yolk sac. By the end of the second week, the resulting structure can be described as a bilaminar embryonic disc between two hemispheric cavities, the amniotic cavity dorsally and the primitive yolk sac ventrally.

Third week

The double-layered embryonic disk becomes a trilaminar structure when numerous cells in the epiblast migrate ventrally, *via* the median primitive streak. The migrating cells replace those cells of the ventral hypoblast and form an intermediate layer. These three germ layers are now dorso-ventrally referred to as the ectoderm, mesoderm and endoderm, and will give rise to the embryo. Skeletal tissue is generally derived from mesodermal cells, but in the vertebrates a unique ectodermal cell line, the neural crest, is responsible for the bony structures of the rostral skull (this will be covered in more detail below). The buccopharyngeal membrane appears as a cranial depression where the ectoderm has fused with the endoderm, preventing mesoderm from occupying the space between. As the cells of the epiblast populate the underlying layers, some cells invaginate through the primitive node at the cranial end of the primitive streak to form the chordal process, which extends cranially along the median line and fuses with the underlying endoderm. Around the beginning of the fourth week this structure then separates from the endoderm to become the notochord, an important structure responsible for providing position and fate information to surrounding tissues (Stemple, 2005).

At approximately day 19, the neural plate appears as a mid-sagittal ectodermal thickening with a broadened cranial end and narrower caudal end, and after a few days begins to crease down the midline forming a neural groove, the crests of which are called the neural folds. Indentations along the cranial end of the neural folds demarcate the divisions between the future prosencephalon, mesencephalon and rhombencephalon; the primitive fore-, mid- and hind-brain

respectively. This developing central nervous system is responsible for the much of the induction and the initial structural arrangement of the vertebrate head (Schumacher, 1997).

Fourth week

Many interconnected and temporally overlapping phenomena take place or are initiated during the fourth week post-fertilisation, including neural tube formation, mesoderm differentiation and embryonic folding. Neural tube closure involves the neural folds meeting and thereby pinching the neural groove off from the surface ectoderm to form a hollow ectodermal neural tube within the mesodermal layer. In humans, this process begins in the occipitocervical area around day 22 and extends both cranially and caudally with the cranial end closing around day 24. A specialised cell type found in the ectoderm of the neural folds, called neural crest cells, dislodge from the crests and migrate ventrally to populate the substance of much of the rostral head during formation of the neural tube. At the cranial end of the developing mammalian embryo, these cells begin migrating just as the neural folds rise (Tan & Morriss-Kay, 1985). Neural crest cells contribute not only to the peripheral nervous system but differentiate into many specialised vertebrate structures of the craniofacial complex.

During neural tube formation, the mesoderm begins to differentiate into three longitudinally arranged columns on both sides of the notochord. They are, from medial to lateral, the paraxial, intermediate and lateral plate mesoderm. Segmentation of the paraxial mesoderm begins in the third week and forms somitomeres that, with the exception of the first seven, become more discrete structures called somites. The somites begin to appear on day 20 and continue to form

until day 30. The somites will subdivide into sclerotomes, which give rise to the axial skeleton, as well as dermomyotomes, which will separate further and give rise to some of the dermis (dermatomes) and much of the musculature (myotomes) of the postcranial body. This is significant as the somites are responsible for the segmental nature of the postcranial body. Segmentation is an important concept in the study of modularity and integration as these repeated structures possess common processes but some autonomy. The first four somites form in the occipital region and, together with the cranial half of the cervical somite, contribute to part of the occipital bone. Cranial to the first somite are the seven somitomeres that never condense into somites, but give rise to many structures of the face and throat.

Concurrent with the neural tube formation and mesodermal differentiation, the flat embryonic disk undergoes complex folding to form a cylindrical structure with a central intraembryonic coelom and gut tube. The cranial and caudal ends, as well as the lateral aspects of the embryonic disk flex toward the ventral midline, taking with them the expanding amniotic cavity so that it almost completely surrounds the developing embryo. This is associated with a strong flexion of the neural structures at the future mesencephalon, between the prospective prosencephalon and rhombencephalon. This flexion rotates the buccopharyngeal membrane from a cranial to a ventral position relative to the position of the developing neural tube.

The appearance, around day 22, of the first pharyngeal arches surrounding the developing pharynx marks the start of facial development. These bilateral mesenchymal swellings develop in a cranio-caudal sequence in response to the arrival of migrating neural crest cells. By day 27 a single frontonasal prominence has begun to develop cranial to the now disintegrating

buccopharyngeal membrane, which is bounded laterally and inferiorly by the paired maxillary and mandibular processes of the first pharyngeal arch. The frontonasal prominence, together with the paired maxillary and mandibular processes, give rise to most of the structures of the face.

By day 25, the neural tube would have closed and each of these primary brain vesicles would be represented as slight dilations. These primary vesicles proceed through a transient segmentation into neuromeres, which are thought to mirror the segmentation of paraxial mesoderm into somitomeres (Jacobson, 1993). Neural crest cells from the posterior mesencephalon and the first three neuromeres of the rhombencephalon contribute to many of the skeletal structures of the face, as well as the squamous portion of the temporal bone (Santagati & Rijli, 2003).

2.2.2 Craniofacial embryology and development

"form is simply a short time-slice of a single spatio-temporal entity" Needham (1936: 6)

The skeleton is of primary interest in most studies of vertebrate morphological evolution because the hardness and inorganic constituency of bone and teeth ensure that they are usually the only remaining evidence of extinct morphology (Kardong, 2002) and their fixed form guarantees that measurements and qualitative characters are maintained. Additionally, bone is an important tissue among the vertebrates, not only for providing structure and shape to the surrounding soft-tissue, but also providing protection to vital organs and function as the levers by which muscles produce movement (Kardong, 2002).

Besides the division of the skull based on adult form and function, developmental and evolutionary principles can be used to subdivide the skull into a number of distinct components. The first, the viscerocranium, comprises those bony elements derived from cartilaginous rods that develop within the pharyngeal arches and represent the early vertebrate jaw. The second component, the cranial base, develops from the chondrocranium, a phylogenetically primitive cartilaginous base that supports the developing brain and houses the sensory organs of the cranium (Kardong, 2002). The portion of the cranium surrounding the foramen magnum is often included as part of the cranial base, however it is derived from occipital sclerotomes and is thus a serial homologue of the vertebrae with which it articulates (Burke *et al*., 1995). The third component, the cranial vault, comprises dermal bones of intramembranous origin that function to house the brain in an overlying protective bony covering, derived from the protective dermal plates of early jawless fishes (Morriss-Kay & Wilkie, 2005). The final component, the facial dermal skeleton, is also of dermal origin like the cranial vault, but developed principally as a supportive structure to the viscerocranial jaws, and now plays a much more prominent role (and exclusive role in mammals) in the masticatory apparatus of most extant vertebrates.

Some authors (e.g. McBratney-Owen *et al*., 2008; Morriss-Kay, 2001) refer to the cranial vault and base together as the neurocranium, and yet others (e.g. Schumacher, 1997) group the cranial vault and facial skeleton under the term dermatocranium, suggestive of its proposed dermal evolutionary origin (but see Yoshida *et al*., 2008). However, combining these regions as a single entity possibly conceals their individuality resulting from their distinct developmental and evolutionary origins. The primate skull is subsequently partitioned here into the cranial vault, cranial base and facial skeleton, as each is unique in its embryology and evolutionary history.

The exceptions include the occipital portion of the basicranium, which phylogenetically and developmentally represents an extension of the vertebrae (Burke *et al*., 1995), and the alisphenoid, or a portion of the greater wing of the sphenoid, which is derived from a viscerocranial (maxillary) cartilage that has come to comprise a major portion of the middle cranial base in the mammalian skeleton (Presely & Steel, 1976). The details of the viscerocranium will be discussed in relation to the developing facial skeleton.

Development of the cranial base

The adult cranial base consists of a number of bones that ossify endochondrally from precursor cartilages commonly referred to as the chondrocranium. It is appropriate to describe the development of the cranial base prior to that of the facial skeleton and cranial vault as the cartilaginous precursors of the cranial base develop earlier (Gross & Hanken, 2008). From an evolutionary point of view, the cranial base is the oldest component of the vertebrate skull and houses many of the sense organs specific to this group (Lieberman *et al*., 2000). Additionally, the cranial base represents a structural intermediate between the facial skeleton and cranial vault, forming the framework on which the brain and face develop (Lieberman *et al*., 2008). Thus, the processes responsible for development of the cranial base can potentially influence overall cranial morphology, and integrate somewhat distinct regions.

The cartilaginous precursors of the cranial base are derived from mesenchyme of both neural crest and paraxial mesoderm origin. As a general rule, the anterior cranial base structures lying rostral to the notochord are of neural crest origin, while those caudal to this prechordal-chordal

boundary are derived from paraxial mesoderm (McBratney-Owen *et al*., 2008). Only the hypochiasmatic cartilages break this rule by being rostrally positioned but of mesodermal origin. McBratney-Owen and colleagues (2008) suggest the reason for the mesoderm origin of the hypochiasmatic cartilages is that they are derived from the same paraxial mesoderm as that which forms the attaching extra-ocular muscles. The general rostral-caudal patterning of neural crest and mesoderm precursor cell lines is also expressed in the facial skeleton and cranial vault and its evolutionary significance will be dealt with later. The occipital sclerotomal condensations, located on either side of the cranial notochord, are the first mesenchymal condensations to appear during the fourth week post-conception. These condensations form within the ectomeningeal capsule, a mesenchyme-derived membrane surrounding the developing brain (Sperber *et al*., 2010). This process of condensation then extends rostrally from the occipital region.

The formation of the cranial base cartilages from the mesenchymal condensations initiates around day 40, well after the development of the brain, eyes, inner ear, cranial nerves and blood vessels have all begun (Morriss-Kay & Wilkie, 2005); thus, these soft-tissue structures largely determine the morphology and orientation of the cranial base, as well as the presence and positioning of the its fossae and foramina (Presley, 1993). The paired parachordal cartilages are the first to appear and fuse together as the midline basioccipital cartilage. The process of chondrification first extends caudally so that the bilateral four occipital and first cervical sclerotome condensations become the paired exoccipital cartilages. The anterior trabecular cartilage then begins to condense, eventually forming a rostral mesethmoid cartilage and a caudal presphenoid cartilage, which will ultimately fuse with the hypochiasmatic cartilages (Lieberman,

2000). The postsphenoid cartilages (also referred to as the hypophyseal or polar cartilages) that lie below the developing pituitary gland chondrify and will later fuse as the basisphenoid cartilage. Supraoccipital cartilages appear late (McBratney-Owen *et al*., 2008), completing the occipital arch and forming the foramen magnum.

In addition to the midline structures there are laterally placed cartilages, the orbitosphenoid and alisphenoid as well as paired nasal and otic capsules, which chondrify around the same time and form a substantial part of the cranial base. As stated above, the alisphenoid is unique among the mammalian cranial base cartilages as it is phylogenetically a viscerocranial element, being derived from a part of the maxillary cartilages of the first pharyngeal arch, namely the epipterygoid of the palatoquadrate (Presely & Steel, 1976). The nasal capsule is formed by the ectethmoid cartilages, the lamina (inferior nasal concha) and the mesethmoid, while the otic capsule comprises the canalicular and cochlear cartilages (McBratney-Owen *et al*., 2008). The ocular capsule is present in many vertebrates as the scleral cartilages or bones of the eye, and while the mammalian sclera never chondrifies, its constituent cells retain the ability for chondrification (Seko *et al*., 2008).

These basicranial cartilages and sensory capsules fuse to form a single plate that supports the brain and allows the passage of neurovascular structures. Ossification begins in the alisphenoid cartilages around 8 weeks post conception followed by the orbitosphenoid, and then the supraoccipital, basioccipital and exoccipital cartilages (Sperber *et al*., 2010). Ossification centres appear much later in the presphenoid and basisphenoid cartilages as well as in the nasal and otic capsules (at around 16 weeks post conception). The boundaries between cartilaginous precursors

and their osseous derivatives are demarcated by a number of foramina and fissures in the adult cranial base (Figure 2.1). The cartilaginous junctions that remain between bony elements of the cranial base act as sites of postnatal growth, and the persistence of the cartilaginous nasal septum suggests it has a primary role in growth of the nasal capsule and facial skeleton (Holton *et al*., 2011; Al Dayeh *et al*., 2013).

The bony elements forming the cranial base include the anterior neural crest derived ethmoid bone from the mesethmoid and ectethmoid cartilages, the inferior nasal conchae, portions of the sphenoid bone including the body, basisphenoid, greater and lesser wings from the hypophyseal, alisphenoid and orbitosphenoid cartilages (although there are intramembranously ossifying components to the lateral aspects of the greater wings of the sphenoid), together with the pterygoid hamuli of the sphenoid. The elements posterior to the prechordal-chordal boundary are of mesodermal origin and include the petrosal portion of the temporal bone from the otic capsule, and the subnuchal portion of the occipital bone derived from the basioccipital, exoccipital and supraoccipital cartilages (Figure 2.1).

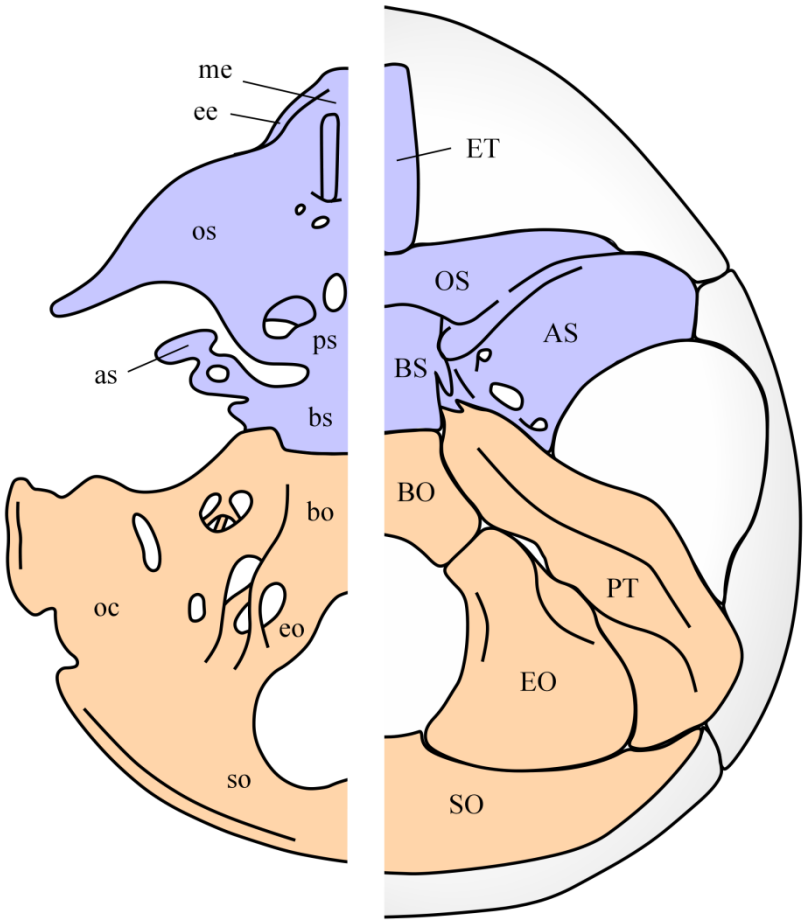


Figure 2.1 The chondrocranium of a ~10-week human foetus (left; adapted from Standring, 2005: 494) and the respective neonatal cranial elements (right). Elements rostral to the prechordal-chordal boundary are generally of neural crest origin (blue), while those caudal of this landmark are derived from mesoderm (orange). Adjacent bony elements of dermal origin are illustrated on the right (grey). as, alisphenoid; bo, basioccipital; bs, basisphenoid; ee, ectethmoid; eo, exoccipital; me, mesethmoid; oc, otic capsule; os, orbitosphenoid; ps, presphenoid; so, supraoccipital; AS, alisphenoid; BO, basioccipital; BS, basisphenoid; EO, exoccipital; ET, ethmoid; OS, orbitosphenoid; SO, supraoccipital; PT, petrous temporal. The hypochiasmatic cartilages are not indicated.

Development of the facial skeleton

The mammalian face develops from the frontonasal prominence and the first pharyngeal arch, with the remaining arches contributing largely to the anterior neck. The streams of neural crest cells migrating into the frontonasal prominence and the first branchial arch are responsible for much of their swelling (Tan and Morriss-Kay, 1985; Kuratani *et al.*, 2013; Richtsmeier & Flaherty, 2013) with the proliferating neural crest cells forming almost all branchial arch mesenchyme (Chai *et al*., 2000). The pharyngeal arches begin to form around day 22 with the first arch presenting separate maxillary and mandibular swellings around day 27, just as the frontonasal prominence develops. The embryonic mouth (stomodeum) forms by disintegration of the buccopharyngeal membrane, which now lies between the frontonasal, maxillary and mandibular processes.

In the fifth week, nasal placodes appear on the frontonasal processes as ectodermal thickenings and begin to enlarge, and over the following week, a nasal pit will form in the centre of each of these placodes dividing it into medial and lateral nasal processes. These nasal structures migrate medially and the medial nasal processes eventually fuse to form the anlage of the nasal bridge and nasal septum. By the end of week six the nasal pits have fused internally, forming a single nasal sac. The tissue lying between the nasal sac and oral cavity eventually perforates to form the primitive choana.

Throughout this period the maxillary swellings have been enlarging and extending ventrally and medially toward one another and eventually fuse with an inferior extension of the medial nasal

process, the intermaxillary process, sometime during the seventh week. During weeks eight and nine, palatine shelves grow inferiorly from the maxillary processes, and eventually rotate to a horizontal position to fuse with each other and the intermaxillary process to form the secondary palate. During development of the palate, a medial nasal process descends from the frontonasal prominence to form the midline nasal septum, which fuses with primary and secondary palates to divide the nasal cavity. Unlike the maxilla, the premaxilla develops from the intermaxillary extension of the frontonasal process, which is derived from a distinct neural crest stream.

Focusing specifically on the development of the bony structures, the facial skeleton involves two phylogenetic and embryological distinct constructs, the viscerocranium and the dermal bones of the face. Both are derived entirely from neural crest cells (Jiang *et al*., 2002) that have migrated to the substance of the frontonasal process and pharyngeal arches from the diencephalon, mesencephalon, and the first three rhombomeres of the developing neural tube (Santagati & Rijli, 2003). However, the viscerocranial elements that ossify do so endochondrally while the dermal bones of the facial skeleton ossify intramembranously. I separate them completely because from an evolutionarily perspective the viscerocranium represents the endoskeletal cartilages of the primitive vertebrate jaw, while the dermal bones are homologous with the exoskeletal structures of the early vertebrate facial skeleton (Kardong, 2002). The viscerocranial cartilages form from mesenchymal condensations in the maxillary and mandibular swellings of the first pharyngeal arch. The mandibular cartilage (Meckel's cartilage) in mammals acts as a signalling structure for the formation of the mandible remaining only as small mental ossicles at the mental symphysis and contributing to a major portion of the malleus in the middle ear (Larson, 2001). The maxillary cartilage gives rise to the palatoquadrate, which later forms the

alisphenoid (portion of the greater wing of the sphenoid) of the cranial base, as well as most of the incus (the third ear ossicle, the stapes, develops primarily from the cartilage of the second pharyngeal arch). The primitive viscerocranium serves no structural function in the mammalian jaw but has taken on secondary roles, guiding the development of the mammalian lower jaw, forming part of the cranial base and functioning in sound conduction (Kardong, 2002). The dermal skeleton, on the other hand, has shifted from its initially supportive role of the primitive viscerocranial jaws, to fulfilling the role of the entire mammalian jaw, epitomised by the exclusively mammalian temporomandibular joint between the mandible and temporal squama. Readers are directed to Kardong (2002) for a more comprehensive account of the evolution of the vertebrate jaws.

The dermal bones of the facial skeleton (the paired maxillae, nasal, lacrimal, zygomatic, and palatine bones as well as the vomer and mandible) are derived from neural crest cells that have invaded the paraxial mesoderm of the developing face. The rostral-caudal origin of the neural crest cells appears to play an important role on the cranial derivatives, as the cells tend to remain segregated even though they can contribute to different portions of a single bone through the later fusion of elements (Santagati & Rijli, 2003). Neural crest cells from the diencephalon and anterior mesencephalon migrate to the frontonasal process, while those of the posterior mesencephalon and the first three rhombomeres migrate to the first pharyngeal arch (Santagati & Rijli, 2003). Thus, elements such as the frontal, nasal and premaxilla are of diencephalic and anterior mesencephalic origin, whereas the mandible, maxilla and zygomatic derive from neural crest cells of posterior mesencephalic origin. Neural crest cells derived from the first three rhombomeres form the elements of the viscerocranium, the malleus, incus and alisphenoid, as

well as the squamous portion of the temporal bone (Santagati & Rijli, 2003). The origin of many of the neural crest cells that give rise to some of the smaller bones of the facial skeleton are inferred from the general pattern observed in the avian model; however, new methods have been developed and studies are currently being carried out to establish the mammalian pattern (e.g. Jiang *et al*., 2002).

Development of the cranial vault

The bones of the cranial vault provide a protective covering over the brain and are thought to have evolved from the dermal armour that formed the skull roof of early vertebrates, such as the ostracoderms (Kardong, 2002). In mammals, the cranial vault generally comprises the paired frontal bones, the paired parietal bones, and the unpaired interparietal. The interparietal develops initially from two pairs of independent bones (Koyabu *et al*., 2012) that fuse with each other and the supraoccipital portion of the occipital bone early in human development. As stated above, two additional bones, the squamous part of the temporal bone and the greater wing of the sphenoid bone, have been co-opted into the floor and lateral walls of the cranial vault from their original roles as bones of the masticatory complex. This incorporation of additional elements from phylogenetically distinct origins, together with the expansion of the frontal and parietal bones is thought to have allowed for the increased size of the telencephalon associated with mammalian evolution (Goodrich, 1958).

Neural tube closure at the cranial end around day 24 marks an important point in the development of the brain, and formation of the cranial vault is primarily dependent on the

presence of the neural structures (Müller & O'Rahilly, 1991). The condensations of the frontal and parietal bones form in an osteogenic membrane between the dermal and meningeal mesenchymal layers, starting initially at the basolateral region above the eye and growing superiorly towards the apex of the head (Yoshida *et al*., 2008). Mineralisation of the bones of the cranial vault begins at around 6-7 weeks (Scheuer & Black, 2000) and occurs in a radial pattern once the condensations are formed, following the shape of the growing brain closely (Richtsmeier & Flaherty, 2013). The presumptive sutures appear early on in the mesenchyme between the widely separated bones (Yoshida *et al*., 2008). All but the coronal suture will form over regions where there are dural reflections between the major parts of the brain: the sagittal and metopic sutures demarcate the location of the falx cerebri between the cerebral hemispheres, and likewise, the lambdoidal suture lies over the bony tethering of the tentorium cerebelli which lies between the cerebrum and cerebellum (Morriss-Kay & Wilkie, 2005). The coronal suture is, however, an analogous boundary to the pre-chordal/chordal boundary of the basi-sphenoid synchondrosis of the cranial base, separating those elements of the rostral vault derived from neural crest cells, from the caudally positioned bones of mesoderm origin (Jiang *et al*., 2002). Interestingly, the coronal suture does have some association with the underlying meninges. Jiang *et al.* (2002) have shown that the suture marks the site where the telencephalon-diencephalon boundary occurred at the end of neural crest migration, and the continued growth of the cerebrum has concealed this relationship.

Thus, like the cranial base, the elements of the vault form from neural crest- and paraxial mesoderm derived mesenchyme, but, unlike the cranial base these elements are derived directly from the mesenchyme and do not pass through a cartilaginous stage (Richtsmeier & Flaherty,

2013). The frontal bone, the squamosal portion of the temporal bones and the medial portion of the interparietal bone are all of neural crest origin, while only the parietal bones and the lateral portions of the interparietal bone are derived from mesenchyme of mesodermal origin (Jiang *et al*., 2002). The neural crest origin of the squamous temporal bone is likely a result of its co-option into the vault from the masticatory complex. Neural crest cells that contribute to the squamosal portion of the temporal bone also migrate to the first arch from the first three rhombomeres (Santagati & Rijli, 2003), which is generally associated with the bones of the masticatory complex – suggesting this shift to its current utility. Likewise, the interparietal is considered homologous with the postparietals and tabulars of the basal reptiles and the extrascapulars of prehistoric lobe-finned fish (Santagati & Rijli, 2003), which are thought to have been incorporated into the vault from posteriorly positioned elements (Forey, 1998). The neural crest source for the frontal bones relates to its later origin in the sarcopterygian ancestors of the tetrapods (Morriss-Kay, 2001), which suggests that the frontal bone represents an expansion of an anteriorly positioned, facial element onto the skull roof during this transition (Jiang *et al*., 2002).

The new head hypothesis

Throughout the introduction to the development of the skull, I have constantly highlighted its division into an anterior neural-crest derived component and a posterior region of mesodermal origin. Gans and Northcutt (1983; Northcutt & Gans, 1983; Gans 1993; Northcutt, 2005) proposed that the evolution of the vertebrates was associated with the acquisition of a "new head" rostral to the notochord. This novel complex included a suit of highly specialised sense organs, an expanded telencephalon, as well as the connective tissues necessary for their support

and function, most of which were derived from a specialised group of epidermal cells, the neural crest cells (Kuratani & Schilling, 2008). Neural crest cells are pluripotent mesenchymal stem cells derived from the neuroectoderm along the ridges of the neural plate during embryogenesis, specific to the vertebrates (Hall & Gillis, 2013). Fate mapping studies (e.g. Jiang *et al*., 2002; McBratney-Owen *et al*., 2008) are finding support for the new head hypothesis, indicating that a clear boundary exists between the rostral head – adapted for the acquisition and initial processing of prey – and the primitive caudal portion.

The importance of recognising the embryonic derivatives of specific cell lines lies not only in providing clues regarding the evolution of modern vertebrates, but the origin of specific cells can affect the patterns of gene expression during the development of complex structures (Clarke & Tickle, 1999). The presence of a clear boundary between the neural crest-derived and mesoderm-derived tissue suggests that there is either a repulsive interaction preventing the mixing of the two cell populations (Morriss-Kay & Wilkie, 2005), or further induction and signalling depends on features specific to each cell line, with a general incompatibility between certain structures on either side of the pre- and post-chordal boundary. Where the patterning of the mesodermally derived skull is largely determined by local signalling factors from the notochord (Couly *et al.,* 1992), the developing brain, neural placodes and the endoderm have taken on the primary inductive role in patterning the prechordal head (Santagati & Rijli, 2003; Lieberman, 2011b). Additionally, the rostral skull represents a novel vertebrate structure, suggesting that either novel developmental processes are involved, or pre-existing processes are adopted and utilised in novel ways (Holland *et al*., 2008; Hall & Gillis, 2013). Because a common pattern of gene expression and response to signalling will bring about integration and should play a role in constraining the

evolvability of particular structures, those elements anterior to the spheno-occipital synchondrosis and the coronal suture should possess some genetic and developmental isolation from those caudal to these boundaries, and morphological integration should be patterned in a way that reflects this division.

Not only is there evidence for separation between the prechordal and postchordal elements, but the different streams of neural crest are patterned differently and do not mix (Santagati & Rijli, 2003). Neural crest cells of the future diencephalon and anterior mesencephalon migrate over to the frontonasal prominence forming the frontal, nasal and premaxillary bones, while those of the posterior mesencephalon migrate into the first branchial arch forming much of the jaws and face, including the mandible, maxilla and zygomatic bones. Neural crest cells from the first three rhombomeres migrate to the first arch and are responsible for most of the malleus, incus, squamous temporal and alisphenoid (Santagati & Rijli, 2003). Thus, while the structures of the face are generally derived from neural crest, the differential expression of certain genes by the neural tube induces differential roles and further division among the cell lines, suggesting that the resulting facial skeleton could be separated further based on each particular stream.

Segmentation

Modularity and integration are clearly fundamental in structures that are sequentially repeated, such as the limbs, ribs or vertebrae. The processes responsible for the development and regulation of each segment are clearly repeated but each would possess some form of autonomy. The potential segmental nature of the vertebrate head has received much debate over the years,

and has recently been revived with some of the new biomolecular findings (Kuratani & Schilling, 2008). There is clearly an anterior-posterior arrangement to the pattern of gene expression, cell lineage restrictions, the pharyngeal arches and the subdivisions of the neural tube in the embryo, which are all suggestive of segmentation (Kuratani *et al.,* 2013). However, with continued development and the migration of tissues the segmentation becomes obscured and the resulting head does not appear to be segmented (Northcutt, 2008). Kuratani and Schilling (2008) also highlight that the neural crest origin of much of the skull goes against the idea that the head is a continuation of the segmental processes associated with the trunk. The head is clearly different from the postcranium with regards to many of its characteristics, and segmentation is one of them (Schumacher, 1997).

2.2.3 Craniofacial growth

Although the processes involved with the development of the various regions are expected to integrate the skull, the overall increase in size and the associated relative proportional changes are also important integrating factors (Lieberman *et al.,* 2008; Hallgrímsson *et al.,* 2007). Bone growth involves three mechanisms: chondral, sutural, and subperiosteal (modelling) growth. Chondral growth is responsible for longitudinal growth at the synchondroses between the various bones of the cranial base as well as growth of the cartilaginous nasal septum (Scott, 1953) and at the temporomandibular joint (Schumacher, 1997). These secondary cartilaginous growth sites are the remnants of the cartilaginous template from which the bones of the cranial base arose. Growth at these cartilaginous sites involves cellular proliferation before undergoing mineralisation to form new bone (Clarke, 2008).

Unlike endochondral growth, which is limited to only a handful of elements, sutural growth and subperiosteal growth are universal (Scheuer & Black, 2000) and occur in the connective tissues found between and surrounding each of the bones (except where a joint is cartilaginous). The intramembranously ossifying bones of the cranial vault and the facial skeleton are each separated from one another by fibrous sutures, which additionally separate these elements from the bones of the cranial base. Sutural growth occurs through osteoblast activity in the connective tissue within sutural joints in response to direct and indirect tensile strains. The direction of growth is perpendicular to the orientation of the suture (Richtsmeier & Flaherty, 2013), and closure signifies the end of sutural growth.

Subperiosteal growth involves the process of both resorptive and depositional (appositional) processes at the adjacent periosteum and endosteum. This growth is usually referred to as modelling (Pearson & Lieberman, 2004), however the term "subperiosteal growth" used here is preferred as it follows the convention applied to other types of growth by highlighting the location at which this particular process occurs. Subperiosteal growth occurs in all bones and is homologous to the process of intramembranous ossification (Scheuer & Black, 2000), but it continues throughout life, even long after other forms of growth have ceased. Subperiosteal deposition and resorption is also responsible for changing the shape of a particular element, with osteoclast or osteoblast activation in the periosteum responding to mechanical and physiological influences (Clarke, 2008). A number of signalling and hormonal factors, including the sex hormones and those responsible for the regulation of circulating minerals, play an important role in regulating the rate of bone resorption and deposition, and the balance between bone resorption

and deposition determines whether there is a net gain or loss of bone (Scheuer & Black, 2000; Vanderschueren *et al*., 2004).

The three processes of endochondral, sutural and subperiosteal growth result in the drift and active or passive displacement of bony elements. Drift, also referred to a cortical drift, involves the change of a bony structure and position through the subperiosteal deposition and resorption of bone on opposing surfaces, generally resulting in movement towards the depositional surface and away from the resorptive surface. Displacement, on the other hand, entails a shift in the relative position of an element resulting from growth at a sutural or cartilaginous joint. The cartilaginous synchondroses are growth sites that actively generate the force responsible for displacing elements (Clarke, 2008; McBratney-Owen *et al*., 2008), but unlike cartilage, bone cannot actively generate growth forces and the displacement at sutural joints is passive and subject to extrinsic factors. The subsequent accretion of bone along the suture is thus secondary, and results from tensile stimuli (Richtsmeier & Flaherty, 2013). Similarly, drift occurs in response to mechanical and physiological factors and is largely under the control of volume requirements of the surrounding or encapsulated soft tissues, as well as the mechanical strains experienced by the bone. While drift and passive displacement are largely directed through localised signalling from adjacent tissues, and the growth of synchondroses appears to be internally compelled, all post-natal bony growth processes are regulated by more general factors, such as hormones (Schumacher, 1997). It is plainly evident from the changing proportions of the neonatal, juvenile and adult cranium that the various regions grow at different times and rates; the neurocranium follows a neural growth pattern while the facial skeleton grows at the same rate as the rest of the body (Nanda, 1955)

Growth of the vault

No aspect of growth can be considered simple and we do not fully understand the causal and mechanistic processes behind the growth of any tissue; however, the growth of the cranial vault is one of those processes that superficially appears to possess fewer determinants than the rest of the skull. All evidence suggests that growth of the cranial vault is driven passively through the displacement of elements at the sutures in response to brain growth, supported by subperiosteal growth (Duterloo & Enlow, 1970) along the surfaces to accommodate the changing curvature of the underlying structures (including the brain, cerebrospinal fluid, meninges, and vasculature). This is not to undermine the complexity of brain growth, or the process of reciprocal signalling between the meninges, sutures and brain (Richtsmeier & Flaherty, 2013), but it allows for a simpler causal link for the morphology of the cranial vault. There is evidence, however, to suggest that the dural reflections found between the cerebral hemispheres (falx cerebri) and the cerebrum and cerebellum and brainstem (tentorum cerebelli) play an important role in shaping the developing brain. Because these strong, fibrous membranes structurally support the brain, they would likely anchor and constrain the length, width and shape of the neurocranium during neural growth (Jeffery, 2002). Greater support for the role of the dura in directing growth is evinced from studies showing the role the dural membranes play in the biomolecular maintenance and growth of the sutures (Richtsmeier & Flaherty, 2013), as well as their association with the major sutures of the cranial vault (Morriss-Kay & Wilkie, 2005).

The human brain is only a third of its adult volume at birth but that value climbs to about 55% over the first 90 days of postnatal life (Holland *et al*., 2014). Most of the postnatal neural growth takes place in the first year of life (Martin, 1983), after which there is a tapering in the rate so that the human brain attains an almost adult size by the seventh year (Richtsmeier & Flaherty, 2013). This differs from non-human primates, as the brain of a newborn macaque, for example, is already at 70% of its adult size (McCollum *et al*., 2007), and the rate of growth plateaus soon after birth (Martin, 1983). Maintaining sutural patency during periods of brain growth is essential for normal development, which is evident in the suite of craniofacial syndromes in which one or more sutures close prematurely (craniosynostosis). In these syndromes, the premature closure of a suture puts an end to its growth, but the continued brain growth is accommodated by compensatory sutural and subperiosteal growth in other regions of the skull (Richtsmeier, 2002; Richtsmeier & Flaherty, 2013).

Much of the flat, sheet-like cranial vault is diploic with a layer of trabecular bone between two cortical plates, the inner and outer tables, which extends from the orbital margins over and into the squamous portions of the occipital and temporal bones (Peterson & Dechow, 2002). In these diploic elements, the inner and outer tables of cortical bone are likely under different functional pressures because the inner cortical lamina is in direct contact with the dural covering of the brain, while the outer table supports the attachment of various muscles - involved with mastication and posture - and is more proximal to the external environment (Cheverud, 1996a; Peterson & Dechow, 2002). The extent of this separation is emphasized in the cresting of the outer bony table observed on crania where the temporalis and or nuchal musculature have converged to a point where no further purchase can be obtained from the existing vault. In

contrast, the inner table continues to follow the contours of the underlying organs. Although separate from the diploë, the frontal sinus further separates the endocranial cavity from the outer cortex of the frontal bone, likely lessening the integration and constraints between the endocranium and the upper face.

Growth of the facial skeleton

The naso-maxillary complex, which includes the ethmoid bone, basically hangs as a "facial block" from the sphenoethmoidal articulation (Lieberman *et al.*, 2000; McCarthy & Lieberman, 2001; but see Bastir & Rosas, 2016) to occlude with the mandibular arch below. At birth the facial skeleton appears short and wide on the well-developed neurocranium. Compared with the initially high postnatal growth rate of the brain and cranial vault, growth of the naso-maxillary complex is delayed during infancy but increases steadily in response to circulating hormones, and follows the growth rate expected for a somatic structure (Schumacher, 1997).

Growth of this naso-maxillary complex involves displacement resulting from growth in the midline cranial base synchondroses, displacement at the sutures of the facial bones, and drift due to opposing processes of deposition and resorption (Enlow, 1990). The synchondroses of the cranial base are actively involved with displacing the facial block forward and downward (Enlow, 1990), while the displacement at many of the mid-facial sutures is due to the active enlargement of the nasal region by the growing nasal septal cartilage (Scott, 1953; Sarnat, 1971; Al Dayeh *et al*., 2013). Vertical growth of the face is largely due to growth of the nasal region, development of the alveolar processes and eruption of the dentition. Subperiosteal growth is an

important process for structuring the oral cavity, nasal cavity, paranasal sinuses as well as the orbits, and is responsible for increasing the depth of the midface (Schumacher, 1997). Around seven years of age subperiosteal growth becomes the dominant form of growth, with resorptive and depositional processes along the surfaces slowly allowing elements to drift and change shape with time (Enlow, 1968; Enlow & Hans, 1996; Schumacher, 1997). Growth of the oral cavity involves active growth in the cartilage of the mandibular condyle as well as drift from apposition and resorption along its surfaces (Sarnat, 1971; Enlow, 1990). The tongue may play an important part in guiding the latter processes (Liu *et al*., 2008; Salles *et al*., 2008). Although the presence of dentition and the ability to masticate has been shown to affect morphology of the cranium through responses to biomechanical strain (Menegaz *et al*., 2010; Small *et al*., 2016), the presence or absence of the teeth play a relatively minor role in bone morphogenesis in regions other than the alveolar processes (Paradis *et al*., 2013). From the point of integration, however, not only would there be strong functional and evolutionary integration between tooth morphology and that of the bony jaws that house them, but the teeth are probably important for functionally integrating the upper and lower jaws for proper occlusion.

The upper face is somewhat unique, being closely related to the neurocranium and housing not only the upper nasal cavity but also the orbits, which are considered to be neural structures. It is for this reason the upper face develops in an intermediate fashion, with a fast initial growth rate that slows with the end of the neural phase of growth (Schumacher, 1997). Formation of the frontal sinus separates the outer layers of the frontal bone from an inner layer, allowing for some independence of these two regions.

There are no non-pathological conditions where bone will form a very thick and dense layer. Even in weight bearing structures that resist immense compressive forces, the matrix is fashioned as trabeculae interdigitated with other types of tissue. In many bones hematopoietic tissues have invaded this space, while in the cranium open air cells often occupy "bony blocks". These air cells form through invagination from a nearby cavity during development, and communicate with the external environment to maintain pressure equilibrium. The paranasal air sinuses develop primarily from the nasal cavity and extend into the maxilla, the frontal bone and the ethmoid and sphenoid of the cranial base during development (Larson, 2001). Interestingly, the baboon belongs to the superfamily Cercopithecoidea, a unique group of primates that, with the exception of the macaque and some fossil genera, lack maxillary sinuses (Rae, 2008). The external cortical surface of the maxillary bone in these primates tracks the internal wall of the nasal cavity closely, but can be separated by trabecular bone. Recent studies (Ito & colleagues, 2015; Maddux & Butaric, 2017) have shown that the maxillary sinuses may play a role in reducing the integration between the external facial morphology and the nasal cavity in humans and non-human primates, thereby increasing the adaptability of the nasal airways.

Growth of the cranial base

The cranial base forms the junction between the brain and the structures of the facial complex and pharynx, and thus act as a mediator between the initial rapid growth of the brain and the steady and prolonged growth of the face, possessing a mixed neural and somatic growth pattern (VandeBerg *et al*., 2004a). The brain is not the only structure of the head to develop early. The organs of hearing and balance are also established early within the petrous temporal of the cranial base (Schumacher, 1997). In fact, the bone surrounding the inner ear labyrinth remains

unaltered after the 24th week post conception (Sperber *et al*., 2010). Growth of the cranial base results from the active growth in the cartilages that remain between the bony elements (synchondroses) after their ossification, together with the passive displacement of elements at sutural joints, and a deepening and expansion of the cranial fossa through drift (Sperber *et al*., 2010). Most of the remaining cartilaginous joints fuse shortly before birth. The exceptions are the mid-sphenoidal and spheno-ethmoidal synchondroses, which fuse perinatally and at the end of the neural growth phase, respectively, and the spheno-occipital synchondrosis, which ossifies around 20 years of age, generally around the time facial growth ceases (Schumacher, 1997; Lieberman *et al.*, 2008). There is very little postnatal growth of the spheno-ethmoidal synchondrosis (Scheuer & Black, 2000), whereas growth at the spheno-occipital synchondrosis contributes greatly to postnatal growth of the cranial base. Most non-human primates differ from the human condition in that the mid-sphenoid synchondrosis remains patent and the spheno-ethmoid synchondrosis fuses perinatally (Lieberman *et al.*, 2008, and references therein). These discrepancies in the timing of fusion between human and non-human primates probably reflect differences in the growth rates and timing of the neural and facial structures.

The unequal growth of the various parts of the brain is accommodated by the cranial base (Schumacher, 1997), at the sutures, and through drift. Although the exact causal relationship of this interaction is not fully understood, the cranial base likely determines some aspects of brain morphology. Control of growth at the synchondroses is genetically complex (Adams *et al*., 2013), but it is generally accepted that cell proliferation at these growth centres and the cartilaginous nasal septum is internally driven, but regulated by circulating hormones such as growth hormone (and the sex hormones). High levels of these hormones are involved with

lengthening of the cranial base and enlargement of the nasal cavity. Due to the complex relationship between the cranial base and the face and vault, disruption to growth at the synchondroses affects the proper positioning of the face as well as cranial vault morphology (Adams *et al*., 2013). Neonates with severe cases of achondrogenesis possess relatively enlarged crania with a prominent forehead and enlarged fontanels, while the facial skeleton presents with a depressed nasal bridge and shortened nose (Chen *et al*., 1981).

The hormonal regulation of growth

Since the growth and development of the neural structures and the sensory organs of vision, hearing and balance precedes the postnatal growth of the face and masticatory complex, it is unsurprising that different mechanisms regulate the prenatal and postnatal growth phases. While prenatal growth, from zygote formation till just before birth, is largely determined by locally secreted and locally regulated insulin-like growth factors and non-pituitary growth hormone, systemically circulating pituitary growth hormone assumes a prominent role in regulating postnatal growth and stimulating the production of systemic (through the liver) and local insulin-like growth factors (Randhawa & Cohen, 2005). Although pituitary growth hormone is not a necessary determinant for early prenatal growth, it does play a minor role during later gestation, with slightly lower birth weights recorded for infants suffering congenital hypopituitarism or growth hormone insensitivity (Randhawa & Cohen, 2005).

The shift from prenatal to postnatal growth is associated with the largely independent and localised processes involving insulin-like growth factors coming under the global regulation of

the growth hormone axis. As such, postnatal growth involves systemic and localised factors that jointly regulate the timing and rate of organ growth and the associated skeletal components (Parker, 2011). The intrinsic growth factors can thus be thought of as modulators of the effect of systemic factors (Gonzalez *et al*., 2013). Conversely, growth hormone directly stimulates chondrocyte proliferation and is thus an important factor for craniofacial growth at the synchondroses, mandibular condyle, and the cartilaginous nasal septum (Takakura & Kuroda, 1998; VandeBerg *et al*., 2004b; Funatsu *et al*., 2006). Thus growth hormone affects the cranial base, vault, and face differently, acting directly on the cranial base synchondroses and indirectly on many of the facial sutures, but having little effect on the structures of the cranial vault (Gonzalez *et al*., 2013). Growth hormone also affects proliferation and differentiation of osteoblasts and osteoclasts and thus plays a role in subperiosteal growth (Giustina *et al.,* 2008). Because subperiosteal apposition and resorption is also plays a fundamental role in the development of sexual dimorphism, bone regeneration (Fowlkes *et al*., 2006) and homeostasis (Rosen *et al*., 1997), many other localised cellular signalling molecules and circulating hormones are involved with its regulation.

The shared response to circulating hormones, such as growth hormone and insulin-like growth factor, ties together disparate regions with the result that they possess common growth trajectories and scaling (Lieberman, 2011b). With this in mind, changes to the interrelationship between the local and systemic factors, or the relative timing and of expression of either can significantly affect adult morphology (Singleton *et al*., 2006; Gonzalez *et al*., 2013). Modifying the expression of localised factors can shift the scaling relationships between structures, resulting in a perceived dissociation of developmental processes (Raff, 1996) and a decoupling of traits

(classic heterochrony), whilst changes in systemic factors can significantly affect morphology through the allometric relationship between structures (Parker, 2011). Although a large proportion of phylogenetic diversity is considered a result of heterochronic processes, shifts along a common allometric trend have been shown to play a major role in craniofacial variation amongst the Papionini (Singleton, 2002; Frost *et al*., 2003) and Hominidae (Schaefer *et al*., 2004).

How timing affects association

The timing, rate and extent of growth will influence patterns of covariation in the cranium. The brain is considered an early determinant of craniofacial form while development of the jaws and masticatory complex are important postnatally (Schumacher, 1997). Because growth and development builds upon existing structures, it is valuable to recognise that the cranial base develops ventral to the early developing brain, and that both the brain and cranial base are well developed by the time the facial skeleton reaches a point of significant growth. It has been proposed, and it is very likely, that the cranial base has a determinant role over the shape of the cranial vault and the facial complex (Lieberman *et al*., 2000). However, this relationship is not unidirectional, as analyses of head binding (Cheverud *et al*., 1992; Kohn *et al.*, 1993), and craniosynostosis (Heuzé *et al*., 2010) have shown a strong link between cranial vault deformation and the cranial base and facial skeleton. Additionally, asymmetries associated with cleft lip syndromes are not only observed in the facial complex but extend into the cranial vault (Parsons *et al*., 2008). Hence the relative timing and development of regions is an important source of covariation, but the relationship is reciprocal rather than unidirectional.

2.3 The study of morphological integration

2.3.1 History of morphological integration

> *"The whole is something over and above its parts, and not just the sum of them all..."*
>
> Aristotle, Metaphysics, Book H, 1045a: 8-10.

The recognition of interconnectedness between morphological traits formed one of the recurring themes in the writings of Aristotle. He was well aware of correlations between parts, both functional and non-functional, and attempted to explain many of the apparent associations he found (Russell, 1916). These ideas reappear in the early nineteenth century, when Cuvier used his 'principle of correlation of parts' as a central basis for his argument against evolution, stating that organs are so perfectly integrated that any change to one would severely disrupt the functioning of the organism (Schlosser & Wagner, 2004). By the time Darwin published *On the Origin of Species* in 1859, correlation among physical traits was an accepted phenomenon among animal breeders, and rightly recognized by Darwin as an important factor in determining variation. He explicitly acknowledged its evolutionary significance, stating that natural selection could unintentionally bring about associated modifications in "often of the most unexpected nature" (Darwin, 1859: 87). Darwin attributed most correlations to early embryonic growth and development and acknowledged the ignorance at the time regarding the source of these correlations.

The study of the association between morphological characters by the early biostatisticians led Galton (1888; also see Bulmer, 2003) and subsequently Pearson (1896) to establish and refine

the mathematical model of correlation. Pearson (1903) then went on to focus on the mathematical procedures for the analysis of selection among correlated characters. Similarly, Wright (1918; 1932; 1934) developed the method of path analysis initially as an exploratory model for the observed pattern of correlation among morphological characters, attributing it to general and local growth factors, but then went on to concentrate on formalizing the mathematical argument and its application to other fields. Concurrently, Thompson (1917) dealt comprehensively with correlated characters from a geometric perspective in his classical book, *On Growth and Form*. Thompson recognised that students of morphology, and particularly the palaeontologists of the time, treated phenotypic characters as completely independent entities. Consequently, he proposed that morphological comparisons be based primarily on geometric principles such that "independent variants should be relatively few", and should be attributable to general "laws of growth" (Thompson, 1917: 727). Thompson's ground-breaking publication, together with the works of Galton, Pearson and Wright, precipitated the theoretical developments that led Huxley (1932) and others (cf. Gayon, 2000) to formally establish the study of allometry.

The first to recognize and define patterned groupings of correlations among morphological characters was Terentjev (1931: 26, cited in Mitteroecker and Bookstein, 2007), who proposed the term "correlation Pleiades" for groups of variables that displayed a strong association among each other and a weak association with variables in other Pleiades; however, Terentjev failed to relate these sets of correlated variables to biological hypotheses. This was left to Olson and Miller, who in 1958 formalised the study and terminology of morphological integration. They too set out to identify groups of variables that were highly correlated with each other and less so with variables in other groups (Olson & Miller, 1951; 1958). Unlike Terentjev, they attempted to

explain the observed patterns using biological principles. Olson and Miller (1958) presented an extensive treatise on patterns of integration and the potential underlying functional, developmental and evolutionary factors responsible for these patterns, as well as outlining its evolutionary significance. They succeeded in demonstrating that the arrangements of morphological correlations were biologically meaningful. Interestingly, the concept of "morphological integration" was never formally defined in Olson and Miller's book of that title (1958), but rather represented a culmination of their ideas (Chernoff & Magwene, 1999).

Although the statistics employed by Olson and Miller were heavily criticized (e.g. Bock, 1960), the importance of their contribution lay in their comprehensive biological interpretation of their studies. The concept of morphological integration formed the basis of many future studies (Blackith, 1960; Van Valen, 1962, 1965; Gould, 1967; Gould & Garwood, 1969; Edredge 1972; Swindler & Orlosky, 1974; Corruccini, 1977; Gingerich & Winkler, 1979; among others) and was significantly influential on the later work of Van Valen (1970), and especially Gould (1970, 1971, 1974, 1977, 1980a, 1980b; Gould & Lewontin, 1979). Gould, however, did not not directly attribute the concept of morphological or 'structural' integration to Olson and Miller in his later works, and possibly considered it to be 'common knowledge' by that stage.

While Olson and Miller recognised the evolutionary significance of morphological integration, the theoretical context and methodology to test specific hypotheses were still to be fully developed (Chernoff & Magwene, 1999). Quantitative geneticists at the time recognised that pleiotropy and linkage disequilibrium could be responsible for correlations between traits, but their primary interest was on estimating correlated responses to selection at the

microevolutionary level. Leamy (1977) and Cheverud and colleagues (Cheverud, 1982, 1984; Cheverud *et al*., 1983, 1989) rekindled the interest in morphological integration by incorporating these new quantitative genetic methods in its analysis. Using controlled breeding programs on model organisms, they partitioned the phenotypic correlation matrix into separate genetic and environmental matrices, with the genetic matrix representing the heritable patterns of correlation, and the environmental matrix being the non-heritable residual component. The findings of Cheverud and colleagues initiated many theoretical and mathematical studies on morphological evolution, largely associated with the theme of constraints (Maynard Smith *et al*., 1985; Wagner 1984, 1988; Riska, 1986, 1989; Zelditch & Carmichael, 1989), but with surprisingly few empirical studies being conducted (Atchley, 1984; Lofsvold, 1986; Zelditch, 1987, 1988; Wagner, 1990). The relative dearth of quantitative genetic studies primarily resulted from the difficulty in generating genetic correlation matrices, which require large samples of known genealogy (Chernoff & Magwene, 1999). Cheverud (1988) thus compared genetic and phenotypic correlation matrices from a number of studies and determined that the phenotypic matrices serve as good proxies for genetic matrices. He proposed that the equivalence of the two matrices results from both environmental and genetic sources of phenotypic variation having to be channelled through common developmental pathways. This has recently been supported by the study of Martínez-Abadías *et al*. (2009).

The late 1980s and early 1990s saw an explosion of work focused on cladistic methods, evolvability, and non-selective factors of evolutionary change (primarily the role of constraints). Although the modern synthesis of the mid-20th century united evolutionary thought with population genetics, systematics and palaeontology (Mayr, 1991: 134), there were two

fundamental omissions. The first was any serious discussion of correlated traits (given that allometry was a well-established phenomenon), and the second was embryology and the role of development in evolutionary thought (Arther, 2002). Although the beginnings of evolutionary developmental biology were seeded in the mid-70's through major publications by, among others, Gould (1977), Riedl (1978) and Alberch and colleagues (1979), it was the recent advancements in molecular genetics and developmental biology that opened the door for experimental investigations of how shifts in development processes affect heritable morphology.

Cheverud and Wagner continued the theme of morphological integration in this new context, focusing not only on the mechanisms by which integration can evolve (Rolian & Willmore, 2009), but also on how integration could affect phylogenetic analyses, evolvability, and even how integrated units could be selected for (e.g. Cheverud, 1996a; Wagner & Altenberg, 1996). The influence of developmental biology in studies of morphological integration was becoming more evident by the adoption of certain terms, such as modularity (e.g. Stearns, 1989). Recent work has built upon these foundations, focusing on the genetic, developmental and functional processes that contribute to the pattern of integration (Rolian & Willmore, 2009). As an example, Albertson and co-authors (2005) used embryology and the method of quantitative trait loci, which links phenotypic and genotypic data, to show that functionally associated parts of the cichlid jaw have more genetic loci in common than regions of the jaw that are not functionally associated. This finding supports the "matching hypothesis" for the evolution of modularity in the vertebrate jaw (see section 2.1.6).

2.3.2 Morphological integration in the primate cranium

Not only did Cheverud revive the study of morphological integration, he also initiated its consideration in the primate cranium (Cheverud, 1982, 1989, 1995, 1996). Investigations of morphological integration have subsequently been applied to a variety of primate taxa utilizing various methods. Studies have examined the overall strength and pattern of morphological integration not only among adult representatives within a population (static integration), but between species (evolutionary integration) and the analysis of ontogenetic samples (ontogenetic integration). Studies considering the pattern of morphological integration can involve either 1) testing hypotheses of modularity, 2) assessing the nature of the associations among parts, or 3) exploring morphological covariation.

Testing hypotheses of modularity

Cheverud (1982a) began by looking at the static integration of macaque cranial morphology using phenotypic and genetic correlation matrices obtained from a sample of known genealogy. The original focus on the static component of integration is probably because of the intimate relationship between static variation, the developmental and functional factors that pattern that variation, and how these associations might constrain evolution at the level of the population. Cheverud (1982a) set about proposing *a priori* cranial regions based on Moss' functional matrix hypothesis (Moss & Young, 1960; Moss, 1968; Moss & Salentijn, 1969; see also Moss, 1997a, 1997b, 1997c). He subsequently tested whether cluster analysis of the correlations between cranial measures would arrange the variables for comparison with these *a priori* defined sets. At the highest level, Cheverud divided the skull into the neurocranium and facial skeleton. The

neurocranial unit was based on the functional matrix comprising the brain and associated endocranial soft tissues (including the leptomeninges and cerebrospinal fluid), which was further divided into frontal, parietal and occipital submatrices. The facial skeleton was defined by the orofacial functional matrix, which was further divided into nasal, oral and orbital submatrices. The functional matrices of the oral and nasal structures included the cavities and their linings, while the orbital submatrix comprised the eye and its surrounding soft tissue. Cheverud (1982a) went further to define a masticatory set which included the oral cavity and regions for attachment of the muscles of mastication. Subsequent studies have basically continued this general subdivision of the cranium with very little modification.

Most of Cheverud's (1982a) measures clustered accordingly, particularly regarding the neurocranial set. The problem, however, was that the genetic matrix appeared to perform poorly, with only 58% of the measures clustering correctly and the orbital set falling away completely. An extension of this study on a species of tamarin monkey (Cheverud, 1995) was improved by employing Mantel's (1967) test to assess the correspondence between phenotypic or genetic correlation matrices and hypothesized correlation matrices based on developmental and functional principles. The results suggested strong integration among traits of the cranial vault, as well as the oral region, but failed to support significant integration among traits of the cranial base, zygomatic region and nasal region.

Cheverud's (1995) method of using Mantel's test to compare correlation matrices with hypothesized matrices is still frequently applied in studies of morphological integration among primates and other mammals, specifically where the interest is to test *a priori* hypotheses of

modularity (Cheverud, 1996b; Ackermann & Cheverud, 2000; Marroig & Cheverud, 2001; González-José *et al*., 2004; Hallgrímsson, *et al*., 2004; Marroig *et al*., 2004, 2009; Ackerman, 2005; Porto *et al*., 2009, 2013; Shirai & Marroig, 2010; Willmore *et al*., 2012). All of these studies have applied the same or very similar groupings to examine the integration between the facial skeleton and neurocranium, the neurocranium as a whole, the cranial vault and cranial base as separate units, and the facial skeleton as a whole as well as divided into oral, orbital, zygomatic and nasal modules. There is general support for the hypotheses of modularity regarding the neurocranium and the facial skeleton. Within these regions, the cranial vault and the oral subsets have been consistently supported as potential modules, with the latter often exhibiting the highest levels of integration. On the other hand, statistical support for modularity of the nasal and zygomatic/masticatory regions have been inconsistent, while the cranial base, orbit, and subdivisions of the cranial vault have, with few exceptions, failed to reach significance.

Although the pattern of integration accross primate taxa is largely similar, there are some differences that are thought to relate to the role of allometry in interspecific variation (Marroig *et al*., 2004; Porto *et al*., 2013), and the relative influence of the brain and the masticatory system on the pattern of craniofacial covariation (Marroig & Cheverud, 2001). When allometry plays a significant role in patterning intra or interspecific variation, a large proportion of the morphological diversity is thought to be associated through the joint response to systemic factors, such as growth hormone. Although allometry is an important integrating factor (ontogenetic integration *sensu* Klingenberg, 2014) and can function as a line of least resistance during diversification (Marroig & Cheverud, 2005, 2010), it likely overshadows subtler patterns

of covariation more relevant to the study of integration resulting from genetic or developmental factors. In a similar manner, elevated variability or substantial growth of one particular region can dominate covariance matrices and alter the perceived pattern of morphological integration, reflecting morphological change but not necessarily shifts in integration relevant to answering the problems of evolvability and phylogenetic relatedness. Inconsistencies among the analyses can also result from differences between the measurements as well as the differences between the constructed test matrices. Ackermann (2005) provides further discussion regarding this point.

Investigations of magnitude

The study of overall integration, as proposed by Cheverud (1995), and measures of the integration between the facial skeleton and neurocranium have formed an important part of interspecific studies (Cheverud, 1996b; Ackermann & Cheverud, 2000; Marroig & Cheverud, 2001; Marroig *et al*., 2004, 2009; Gonzáles-José *et al*., 2004; Hallgrímsson *et al*., 2004; Ackermann, 2005; Martínez-Abadías *et al*., 2009b; Porto *et al*., 2009, 2013; Shirai & Marroig, 2010; Willmore *et al*., 2012), primarily because of its direct link with evolutionary constraints and evolvability. The consistent association between the facial skeleton and the neurocranium lends support to the proposal that mammalian and primate crania are a significantly integrated structures (Cheverud, 1995; Hallgrímsson *et al*., 2007a; Martínez-Abadías *et al*., 2009b). Despite this, the primates, and especially humans, express relatively low levels of overall morphological integration except for baboons, which display some of the highest levels among the placental mammals (Marroig *et al*., 2009; Porto *et al*., 2009). Again, much of this pattern probably relates to allometry and differential growth between the neural and somatic regions of the cranium, but

morphological integration has general significance with respect to evolvability and evolutionary flexibility among mammals (Marroig *et al*., 2009).

Exploring associations among parts

Another channel of investigation focuses on the extent and influence of integration between proposed modules (Ross & Ravosa, 1993; Lieberman *et al*., 2000; Bookstein *et al*., 2003; Bastir & Rosas, 2004, 2006; Bastir *et al*., 2008, 2010; Mitteroecker & Bookstein, 2008; Martínez-Abadías *et al*., 2009, 2011, 2012; Singh *et al*., 2012). Although Huxley (1863) was probably the first to suggest that brain size could influence facial morphology, Weidenreich (1941) developed the argument supporting the association between the relative size of the neurocranium and the shape and positioning of the facial skeleton using the observed variation among domestic dogs (in a similar vein to Darwin, 1859), as well as among primates and pathological human crania. It was Weidenreich's (1941, 1946, 1947) application of this association to interpreting modern human variation, as well as the sparse fossil hominin record of the time, that sparked an interest in the subject among the anthropological sciences.

Corruccini (1976) found support for Weidenreich's (1941) proposed interdependence of the jaws, face and neurocranium among members of the hominin lineage. He found very little difference between the scores obtained from shape-based principal coordinate analyses of two sets of data – one consisting of 25 neurocranial measures and the other including the same neurocranial measures but supplemented with 19 facial measurements. Although integration between the facial skeleton and neurocranium exists, Corruccini's (1976) analysis suffers some

methodological problems. Not only were the measurements of the neurocranium impartially selected based on their ability to distinguish the fossil species (unlike those of the facial skeleton) but their high number would have led to a greater weighting of the neurocranium (as noted by Polanski & Franciscus, 2006). Both factors likely resulted in an increased contribution of the neurocranial measures to the principal coordinates analysis of the facial/neurocranial set and were possibly responsible for the high congruence between the resulting scores.

Almost independently, Enlow and colleagues (Enlow *et al*., 1969, 1971a, 1971b, 1988; Enlow & Azuma, 1975; Enlow & Hans, 1996) developed the part-counterpart principle as a causative explanation of malocclusion in the field of orthodontics. They recognised that the bones of the skull are not isolated and independent units, but rather that the growth and development in one region has the ability to displace structurally related elements due to their spatial arrangement. In other words, the part-counterpart principle proposes that parts of the skull possess structurally and geometrically related counterparts such that a change in the size or shape of the part results in simultaneous changes in the shape, size or position of its counterparts. Although Enlow *et al*. (1971b) correctly recognised that the skull likely possesses many potential part-counterpart relationships, the scope of their work within the orthodontic sciences likely narrowed their focus to those relationships responsible for the relative protrusion and retrusion of the maxilla and mandible. Basically, Enlow and colleagues proposed that the brain affects the cranial base, which in turn influences the shape and positioning of the nasomaxillary complex and mandible. More specifically, Enlow and colleagues identified the frontal and temporal lobes as separate parts that influence the anterior and posterior face, their respective counterparts, via the associated portion

of the cranial base. Additionally, Enlow *et al*. (1971a) studied the association between the maxillary and mandibular arcades as a part-counterpart relationship.

Enlow and McNamara (1973) and Bhat and Enlow (1985) appealed more to the anthropological sciences, and using the part-counterpart principle, built on the early proposals of Huxley (1863) and Weidenreich (1941, 1946, 1947) by suggesting that the relationships between the shape of the cranial vault, cranial flexure and the relative positioning and proportions of the facial skeleton have some bearing on modern human biodiversity. They noted that a short, broad neurocranium (brachycephaly, in the classical anthropological and typological terms of Anders Retzius) was often associated with a wider, anterio-posteriorly shorter, and more flexed basicranium, as well as a shorter and wider facial skeleton (euryprosopy). On the other hand, a long narrow neurocranium (dolichocephaly) often presented with a narrower, longer and less flexed basicranium, as well as more anteriorly projecting and tall facial skeletons (leptoprosopy).

The more recent anthropological studies have built on the work of Weidenreich and Enlow, exploring the associations among these regions of the skull, either among primate taxa or within modern humans, and often utilising the framework of modularity and integration. While a few investigations have utilised basic bivariate correlations among measures and angles of the cranium (e.g. Ross & Ravosa, 1993; Lieberman *et al*., 2000), most of the more recent studies divide the skull into the hypothesised modules, generally the cranial base, cranial vault and facial skeleton, and use multivariate methods somewhat analogous to regression (Partial least squares) to explore the influence of each of these regions on one another (Bookstein *et al*., 2003; Bastir & Rosas, 2006; Bastir *et al*., 2008, 2010; Mitteroecker & Bookstein, 2008; Martínez-Abadías *et al*.,

2009; Singh *et al*., 2012). The multivariate regression of a single factor such as brain size (or its size relative to basicranial length) against overall shape has also been used to investigate the influence of that factor on craniofacial morphology (Bastir *et al*., 2010; Martínez-Abadías *et al*., 2012), while other studies have made use of principal component analysis as a descriptor of covariation across the entire complex structure (Bastir & Rosas, 2004, 2006; Martínez-Abadías *et al*., 2011).

Using multiple bivariate analyses, Ross & Ravosa (1993) showed that the associations between basicranial flexion and various cranial variables were characteristic of the Haplorrhii and not observed among the Strepsirrhini. Most significantly, Ross & Ravosa (1993) found the basicranium to flex more among Haplorrhii that possessed large neurocrania relative to the basicranial length, as well as an association between flexion of the cranial base and facial orientation (facial kyphosis and orbital axis orientation). The flexion of the basicranium is generally expressed as the angle between the anterior and posterior portions of the cranial base in the midline. See Lieberman (2000) and Lieberman & McCarthy (1999) for discussion on the many measures of cranial base flexion. Subsequent work has confirmed that relative neurocranial volume plays a role in the positioning and shape of the basicranium and facial skeleton (e.g. Spoor, 1997; Lieberman *et al*., 2000), and that facial size also influences basicranial flexion (Lieberman & McCarthy, 1999; Lieberman *et al*., 2008).

With the exception of Ross & Ravosa (1993), much of the focus has been on describing the morphological associations observed in humans (Lieberman *et al*., 2000a; Bookstein *et al*., 2003; Bastir & Rosas, 2005, 2006; Bastir *et al*., 2008, 2010; Martínez-Abadías *et al*., 2009, 2011;

2012) and to a lesser degree the apes (Bastir & Rosas, 2004; Singh *et al*., 2012; Mitteroecker & Bookstein, 2008; Neaux, 2016). Bookstein and colleagues' (2003) analyses of covariation between the facial skeleton, cranial vault and cranial base in the genus *Homo* found high correlations between the three regions. Specifically, the face and vault possessed a stronger relationship than either had with the cranial base (Bookstein *et al*., 2003). They went on to show that a relatively reduced facial size is associated with a more flexed cranial base, thinner cranial vault bones, and smaller frontal sinuses. Additionally, an increased facial prognathism is associated with a more antero-posteriorly elongated cranial vault and a relatively shorter clivus.

Like Bookstein and colleagues (2003), many authors have noted an association involving the breadths, lengths and heights of the cranial base, cranial vault and facial skeleton among members of the Hominoidea (e.g. Mitteroecker & Bookstein, 2008; Martínez-Abadías *et al*., 2009b; Singh *et al*., 2012; Neaux, 2016), generally assumed to be supporting evidence for the traditional concepts of dolicocephaly and brachycephaly. However, a recent analysis of morphological integration using genetic matrices found only support for integration between the breadth measures of these three regions, and not between the measures of either height or length (Martínez-Abadías *et al*., 2009a). This supports the proposal by Hallgrímsson *et al*. (2007a) that integration between the relative widths of the facial skeleton, the cranial base and cranial vault are dominant in the mammalian skull.

The exploration of morphological covariation

There is general caution against diverting from the accepted statistical, hypothesis-driven, hypothetical-deductive model of empirical investigation, with most of the studies testing *a priori* hypotheses of modularity based on Moss' functional matrix hypothesis (e.g. Cheverud, 1982, 1989, 1995), and Enlow's part-counterpart principle. There are, however, several studies using an exploratory method, but with sufficient theoretical background to make an informed appraisal of the results (Polanski & Franciscus, 2006; Neubauer *et al*., 2009; Bruner *et al*., 2010). Principally, when a clear theoretical framework is provided on which findings can be discussed, *a posteriori* hypotheses can provide the theoretical background for future studies. Chernoff and Magwene (1999: 319) have gone so far as to even define morphological integration as the "correspondence of patterns of covariation among traits to *a priori* and *a posteriori* biological hypotheses." Nonetheless, it must be stressed that an *a posteriori* hypothesis should not be accepted without undergoing rigorous testing.

2.4 Rationale

The failure of phylogenetic methods to consider the effect of integration is probably responsible for much of the incongruence between phylogenies estimated using the genotype and the cranial morphology in both the Papionini primates (particularly the relationships among *Lophocebus*, *Papio*, *Cercocebus* and *Mandrillus*) as well as the Hominidae (the position of *Homo* among *Gorilla*, *Pan* and *Pongo*). Interspecific studies of cranial integration (Marroig *et al*., 2009; Porto *et al*., 2009) have identified *Homo sapiens* as being on the lower end of the scale, expressing relatively low levels of overall morphological integration among the primates. Members of

Papio, on the other hand, display particularly extreme levels of integration among the primates, exhibiting what would be considered high levels of integration among the placental mammals. Marroig and colleagues (2009) attribute much of these differences in overall integration to the proportion of variation attributed to size, or the role of allometry in extant variation. In addition, allometry has been reported to play a fundamental role in directing craniofacial interspecific variation in both the Papionini (Singleton, 2002; Frost *et al*., 2003) and the Hominidae (Schaefer *et al*., 2004).

The cranial morphology of humans is overshadowed by the size and globularity of the neurocranium, and some authors have suggested that this feature is somewhat responsible for much of the facial and basicranial morphology (Lieberman, 1995; Lieberman *et al*., 2002). In sharp contrast, the dominance of the facial complex in the cranium of baboon species likely brings about a high degree of integration to the remainder of the cranium. Recent studies have found a common pattern of morphological integration among the Hominoidea (Singh *et al*., 2012; Neaux, 2016), but I propose here that this pattern has deeper developmental roots (Hallgrímsson *et al*., 2007a) and should be shared even among organisms as morphologically dissimilar as baboons and modern humans.

2.5 Aims

This body of work thus aimed to explore and compare different aspects of morphological integration and its modular arrangement in modern humans, *H. s. sapiens*, and a baboon species, *P. h. ursinus*. More specifically, the broad aims of this thesis are to:

1) Assess the role of allometry across different cranial regions in both these species by highlighting regions of differential growth during ontogeny, assessing the effect of ontogenetic allometry on the patterning of integration, as well as quantifying the proportion of adult variation attributed to size;
2) Explore patterns of covariation of the *P. h. ursinus* and *H. s. sapiens* cranium, to assess the patterning of morphological integration into morphological modules once allometry and sexual dimorphism had been accounted for; and finally,
3) Analyse differences in morphological integration between *a priori* modules in the two species.

The specific hypotheses are:

H1) The general pattern of postnatal ontogenetic allometry will be one of slower neural growth and faster facial growth, while the orbits, zygomatic region and cranial base will possess an intermediate, possibly isometric growth
H2) Allometry will have a general concealing effect on the pattern of morphological integration, apart from those regions associated with neural versus somatic growth
H3) The proportion of variation attributed to size will be larger in *P. h. ursinus* than in *H. s. sapiens*
H4) After accounting for allometry and sexual dimorphism, the patterns of covariation in the crania of both *P. h. ursinus* and *H. s. sapiens* will partition into clear morphological modules that fit with current understandings of development
H5) *P. h. ursinus* and *H. s. sapiens* possess a general and shared pattern of morphological integration between *a priori* modules, with a few slight differences

MATERIALS AND METHODS

3.1 Samples

3.1.1 *Papio hamadryas ursinus*

Seventy crania assigned to the chacma baboon, *Papio hamadryas ursinus*, were digitized from the comparative collection at the School of Anatomical Sciences, University of the Witwatersrand. Of the 70 individuals, 21 were identified as being male and 32 as female, leaving only 17 that were too young to possess the distinct sexually dimorphic features characteristic of the papionins (Freedman, 1962). Sex was easily estimated in the adult and majority of the sub-adult baboons, although x-rays were taken of 13 juvenile and sub-adult individuals to observe the developing canine (Figure 3.1). This increased the number of individuals for which sex was known by five, and ensured that all the sub-adult crania were sexed. The canine was not sufficiently developed in the infant and juvenile specimens to estimate the sex for those individuals beyond doubt.

Males with well-developed cranial superstructures were excluded when cresting obscured or elevated the landmark positions. This particularly affected lambda and the associated lambdoidal suture, which in some cases was completely obliterated by the nuchal cresting and external occipital protuberance. The development of sagittal and nuchal crests will move the associated landmarks from the neurocranial surface to these extensions of bone, which are now novel features that primarily function for the attachment of muscles. The landmarks would then not be homologous between specimens and samples, a prerequisite for morphometric studies. Specimens with any visible or recorded pathology or damaged in a manner that prevented the

reliable location of landmarks were also excluded. As with many skeletal collections, calottes are often removed using a mortuary saw to aid in the maceration of endocranial structures. The resulting incision around the circumference of the cranium is often variable in thickness, and repositioning of the calotte involves some estimation that could affect the accuracy of configurations. It was for this reason that specimens cut this way were excluded from the study.

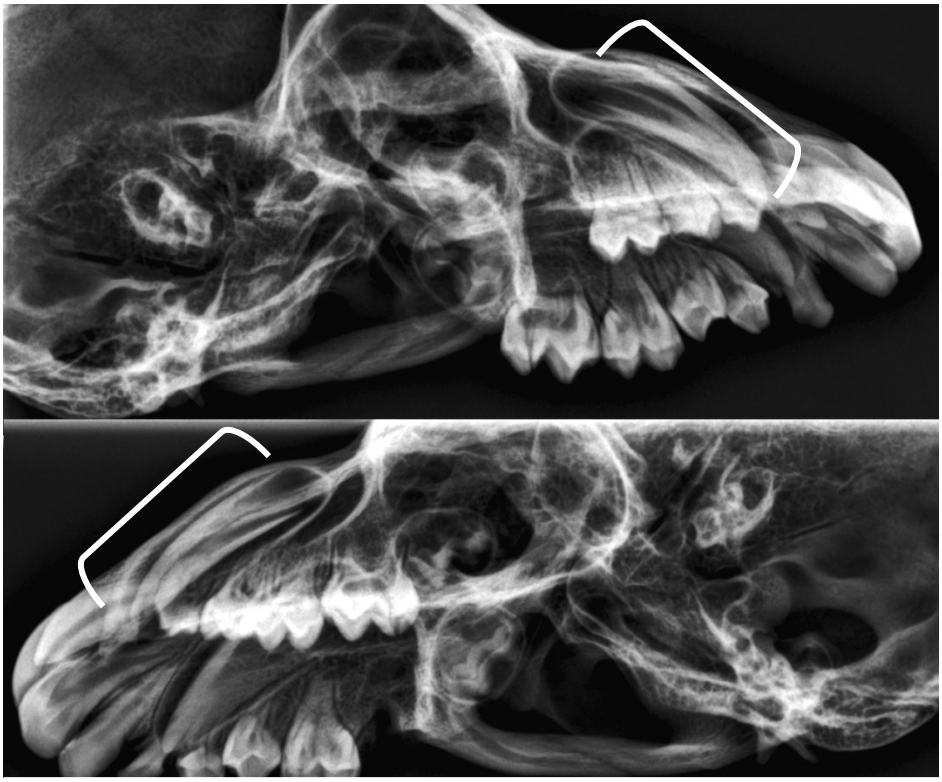


Figure 3.1. X-ray of specimen ZA1508 clearly illustrating the size of the crown of the un-erupted canine, suggestive of male sex.

Origin of the specimens

Papio is a genus of the papionin primates in the parvorder Catarrhini (É. Geoffroy, 1812), family Cercopithecidae (Gray, 1821). Members of the genus *Papio* are commonly referred to as the savannah baboons and generally possess a large body size, elongated and extended face, and deep maxillary and mandibular fossa (Szalay & Delson, 1979). The current range of *Papio* extends almost entirely across sub-Saharan Africa and to the Arabian Peninsula (Figure 3.2). The degree of variability across this geographic range has caused some controversy regarding the taxonomy of the various phenotypic groups. Extant *Papio* is considered by many (Szalay & Delson, 1979; Jolly, 1993; Frost *et al.,* 2003) to consist of only one species, *Papio hamadryas*, comprising a few subspecies; namely *P. h. hamadryas*, *P. h. cynocephalus*, *P. h. ursinus*, *P. h. papio*, *P. h. anubis*, and *P. h. kindae*. Other researchers interpret *Papio* as consisting of multiple species due to their noticeable phenotypic differences (Groves, 2001; Grubb *et al.,* 2003; see review in Jolly, 1993); however, the subspecific status of the various *Papio* groups is supported, according to the biological species concept, by the occurrence of hybridization zones at the borders of subspecies' ranges (Jolly, 1993), and by mtDNA analysis indicating a somewhat clinal variation (Newman *et al.,* 2004). Additionally, the cranial variation between subspecies appears to show a north-south stepped cline, with an east-west allometric cline between *P. h. cynocephalus* and *P.h. kindae* (Frost *et al.,* 2003). Given the abovementioned evidence, a subspecific designation will be used throughout this thesis to refer to groups of *Papio hamadryas*. Importantly, Jolly (1993) also highlighted the high degree of variability within some of the subspecies, specifically *P.h. anubis* and *P.h. ursinus*, and there have been suggestions to taxonomically recognise these varieties (e.g. Sithaldeen *et al*., 2009, 2015).

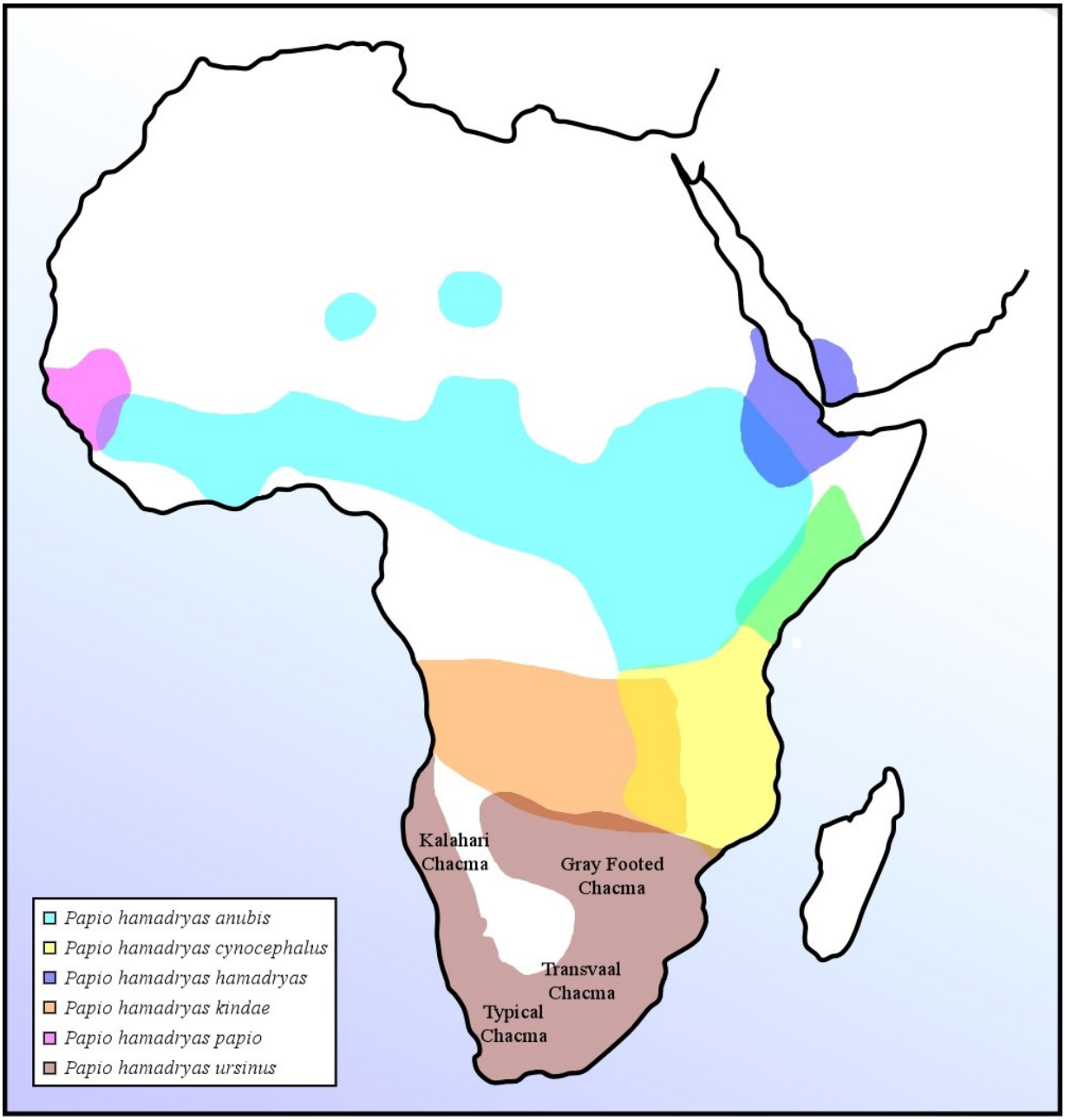


Figure 3.2. The approximate distribution of *Papio* across the African continent and Arabian Peninsula. Sub-specific attribution is provided in the key. Shaded regions follow Jolly's (1993) "phenostructure" but are extended to include specimens used by Frost and colleagues (2003). The distribution of *P. h. ursinus* and the populations highlighted by Jolly (1993) have been modified in accordance with Sithaldeen *et al*. (2009).

Most of the *P. h. ursinus* specimens used in this study were donated to the School of Anatomical Sciences. Thirty-six are from the South African Institute for Medical Research and eight are from the Council for Scientific and Industrial Research. Wild-shot specimens used in this analysis consist of a single individual from Swaziland, and seven from the Western Cape, South Africa. There were 18 specimens for which there is no information on how they were acquired, nor were there any records as to how the medical institutes mentioned above acquired the baboons, although primate specimens for medical research in South Africa were generally wild-caught and not bred in captivity (Seier, 2003).

The potential effect of sample heterogeneity, in terms of wild-shot versus captive and inconsistency of geographic source, is expected to increase sample variation. The developmental differences related to varying environmental conditions and between wild and captive primates are thought to be driven primarily by diet quality, and are discussed below under age distribution. Regarding geographic variation, Jolly (1993, 2003) has stated there are a number of geographically bounded populations of *P. h. ursinus* morphologically different enough to warrant distinction; namely the grey-footed chacma, Kalahari chacma, Transvaal chacma, and typical chacma (Figure 3.2). His views regarding chacma diversity have recently been supported by an analysis of mitochondrial DNA (Sithaldeen *et al.,* 2009), which demonstrated a deep divergence of about 1.5 million year before present between the north-eastern grey-footed chacma, the south-western Cape chacma (equivalent to the combined Transvaal and typical chacma baboons *sensu* Jolly, 1993) and the ruacana (Kalahari) chacma. However, there does appear to be secondary contact and gene flow between the Cape and grey-footed chacma (Sithaldeen *et al.,* 2009). Nonetheless, a large component of the subspecific diversity in *Papio* is

due to shifts in a common allometry (Leigh, 2006) and, besides distinct coat colouration, size is one of the morphological criteria used to distinguish the Cape chacma from the grey-footed chacma. Thus, accounting for the effect of allometry should minimize most of the additional variability incurred through the use of multiple populations. To assist with readability, the *P. h. ursinus* sample will be referred to as the baboon sample.

Age distribution

There are no documented ages for any of the baboon specimens and their having been acquired from both wild and captive sources complicates the use of dental scores for estimating age. Tooth eruption schedules are generally used to estimate age in living and skeletal primate samples (e.g. Kuykendall, 1992) although the accuracy has been questioned (Gavan & Hutchinson, 1973). One of the factors contributing to inaccurate age estimation is the marked disparity between the age at which developmental milestones are reached in captive and wild individuals (Altmann *et al.,* 1981). Dental emergence has been shown to occur later in wild baboons than their captive counterparts (Phillips-Conroy & Jolly, 1988; Kahumbu & Eley, 1991), especially with regards to the later-erupting premolars, the 2nd and 3rd molars, and the male canine-P3 complex. This acceleration in dental development in captive baboons is thought to be the result of an improved diet (Phillips-Conroy & Jolly, 1988; Kahumbu & Eley, 1991; O'Regan & Kitchener, 2005), which would not only accelerate dental maturation but also the growth and development of the organism as a whole (Altmann *et al.,* 1981; Altmann & Alberts, 2005). This concomitant development between the dental eruption and the rest of the body would not only allow for the use of eruption schedules as relative developmental markers independent of source, but supports its use over recorded ages when a heterogeneous sample is used.

Bogin and Smith (1996) define three stages of "social mammalian" growth, namely infanct, juvenile, and adulthood based on morphological, behavioural and physiological changes. The baboon sample was placed into the above three groups, supplemented with a fourth 'subadult' group based on permanent maxillary molar eruption. A specimen was considered an infant prior to eruption of the first molar, a juvenile between eruption of the first and second molars, a subadult between eruption of the second and third molars, and an adult thereafter. Following Schultz (1935), a tooth was considered erupting when its occlusal surface was above the alveolar margin, and where the eruption status of the left and right sides differed, the more advanced side was recorded. The sample consisted of five infants and 12 juveniles, all of unknown sex, 25 subadults consisting of 12 females and 13 males, and 28 adults comprising 20 females and only eight males (Figure 3.3). The reduced number of adult males resulted from the exclusion of individuals possessing cranial superstructures that would affect data acquisition. The resulting lack of homology between landmarks on the cranial vault or crest supersedes the potential problems of inequality between the sexes, and because the effects of allometry and sexual dimorphism are accounted for it is unlikely to significantly affect the results. The categorisation of individuals into age cohorts is primarily for the purpose of visualisation.

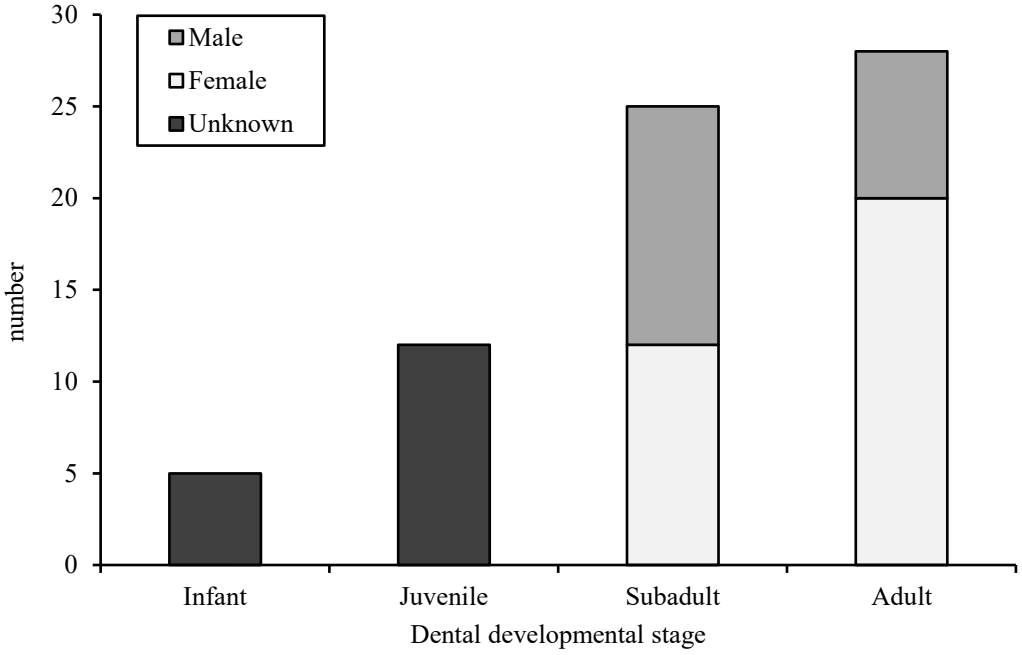


Figure 3.3. Distribution of the baboon specimens, showing sex for the dental age groupings.

3.1.2 *Homo sapiens sapiens*

Seventy-three modern human crania were digitised for this study, 45 of them male, and 28 female. The *H. s. sapiens* material was obtained from the cadaver-derived portion of the Raymond A. Dart Collection of Human Skeletons, School of Anatomical Sciences, University of the Witwatersrand (Dayal *et al.,* 2009).

The ages of the *H. s. sapiens* individuals were obtained from the catalogue and were limited to specimens aged between zero and forty years. The upper age limit was employed so that the morphological variation associated with development could be recorded while minimising the effects of senescence. The morphological changes of the skull associated with aging (Albert *et*

al., 2007) are out of the scope of this analysis, and the trajectory associated with senescence will likely be different from that of growth and will further complicate the analysis of morphological integration. In addition, crania that displayed any disease or pathology that would affect cranial morphology or increase asymmetry were excluded, as were specimens with curatorial damage where a substantial portion of the morphology was missing (involving more than three landmarks).

Sample size was severely limited by the completeness of the cranium. As with the baboon sample, *H. s. sapiens* crania with sectioned calottes were excluded because the repositioning of the calotte involves some estimation of the incision thickness. In addition, there were some complete crania that had undergone destructive sampling at the intersection of sutures at pterion on both sides, limiting the sample further. A handful of specimens possessed broken noses or damaged alveoli, but to prevent further reductions in sample sizes the missing landmarks were estimated, particularly when contralateral landmarks were present (more details are provided in section 3.2.1). The sample of 73 represents all the available crania from the Raymond A. Dart Collection that met the requirements of the study.

Origin of the specimens

The sample includes individuals racially designated as black Southern Africans. Although racial classifications were historically imposed on individuals, the term "black African" is currently an officially recognised, self-identifying term, commonly associated with individuals of Bantu-speaking descent. The movement of Bantu speaking peoples into southern Africa occurred

relatively recently, around 2000–1200 years ago, and is thought to have primarily occurred through demic diffusion (Newman, 1997) involving population growth and the sequential diffusion of populations into and across an area, with the potential displacement or intermixing with pre-existing populations (Ammerman & Cavalli-Sforza, 1984). Living Bantu-speaking populations have been shown to be genetically homogenous although there is a variable degree of admixture with autochthonous populations such as the Khoesan, particularly among the Zulu and Xhosa tribes (Schlebusch *et al.,* 2013).

The importance of a homogenous sample in studies of morphological integration is well recognized (Hallgrímsson *et al.,* 2004; Jones & German, 2005). Samples comprising individuals from disparate populations can potentially generate erroneous covariation as the variation will be biased about those trajectories that explain their particular morphological differences. If, for example, two populations differ with respect to frequency of character states of multiple potentially independent traits (such as breadth across the zygoma and nasal bone prominence), lumping representatives from each population as a single sample will artificially generate a statistical association between these traits. The aim is to minimise false character associations (autocorrelations) that can occur when distinct populations are sampled. Again, to assist with readability, the *H. s. sapiens* sample will from this point be referred as the human sample.

Age distribution

Both the sex and age information was obtained from the collection catalogue. Although the sex information can be considered reliable, as it was determined from soft-tissue characteristics, the

age at death data are problematic. Age was often estimated because the birth dates of many South Africans were not officially recorded and many individuals in the collection represent unclaimed bodies sourced from hospitals in the Johannesburg region (Dayal *et al.,* 2009). The age distribution for each of the sexes is illustrated in Figures 3.4 and 3.5, where the first presents the data as a basic histogram, and the second groups the specimens according to the infant, juvenile, subadult and adult categories using the same dental developmental criteria applied to the baboon sample.

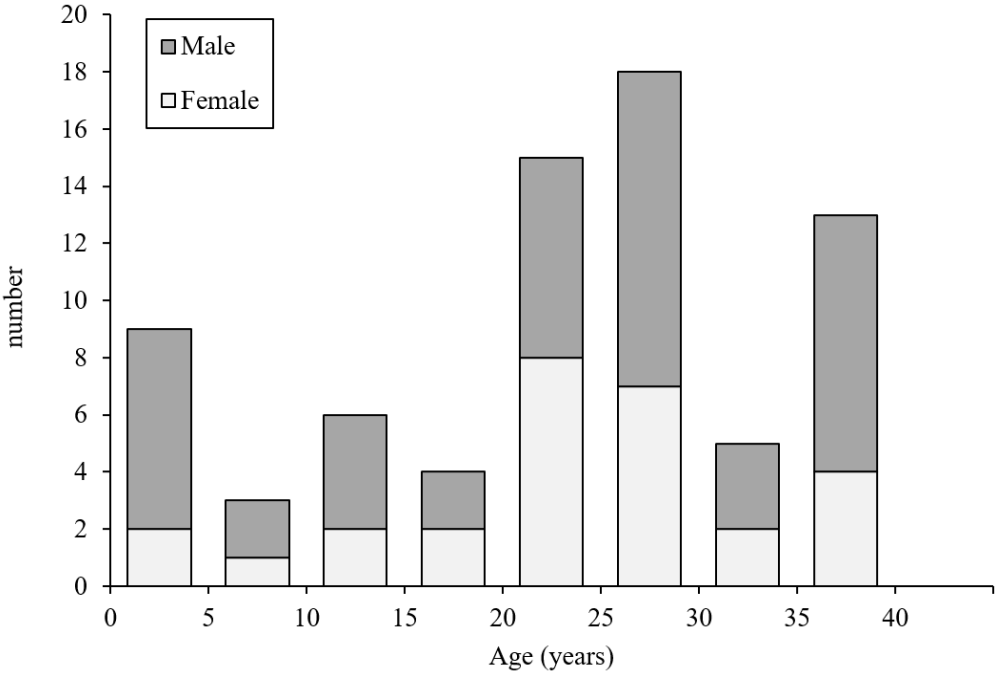


Figure 3.4. Distribution of the human specimens, showing sex, arranged into 5-year cohorts.

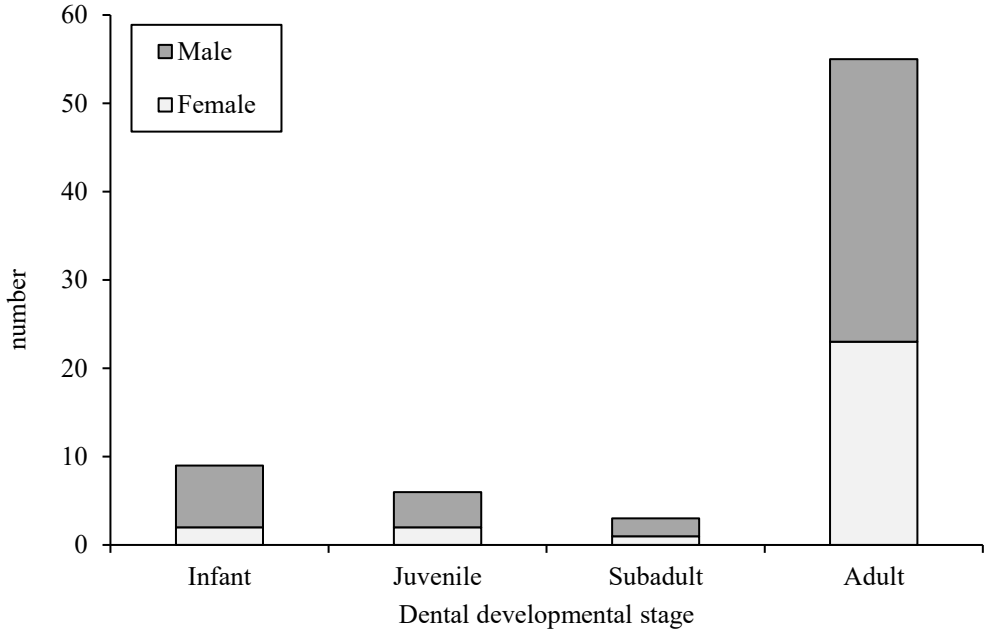


Figure 3.5. Distribution of the human specimens, showing sex for the dental age groupings.

3.2 Landmarks

Specimens were mounted in a manner such that all landmarks were easily accessible without having to reorientate the cranium, or necessitate the fitting of landmarks captured in two separate sessions. This involved creating a "ring" of plasticine that cradled the nuchal region of the cranium between opisthion and lambda. After fixing the specimens in place using modelling clay, several three-dimensional Cartesian landmarks were recorded from each specimen using an Immersion Microscribe G2 digitizer. This specific digitizer is reported to have a mean accuracy of 0.13 mm.

For the sample of baboons, the data consisted of 13 midline and 30 lateral landmarks, which were recorded from the right side of the cranium following Fleagle *et al*. (2010). Table 3.1 defines each landmark and the cranial region accounted for by that landmark, which are also presented in Figure 3.6. All but the last three landmarks were chosen to represent homologous points between specimens at sutural intersections or other anatomical features, corresponding to Bookstein's (1991: 64) type I and type II landmarks, defined therein as the "discrete juxtapositions of tissues" and the "maxima of curvature or other local morphogenetic processes" respectively. The last three landmarks listed in Table 3.1, namely glabella-bregma, bregma-lambda, and lambda-pterion, fall under Bookstein's type III landmarks, which are "extremal points" or constructed mathematical landmarks (see also Dryden & Mardia, 1998). To ease visualisation of the results, wireframe and polygon surface models were defined between the landmarks (Figure 3.7).

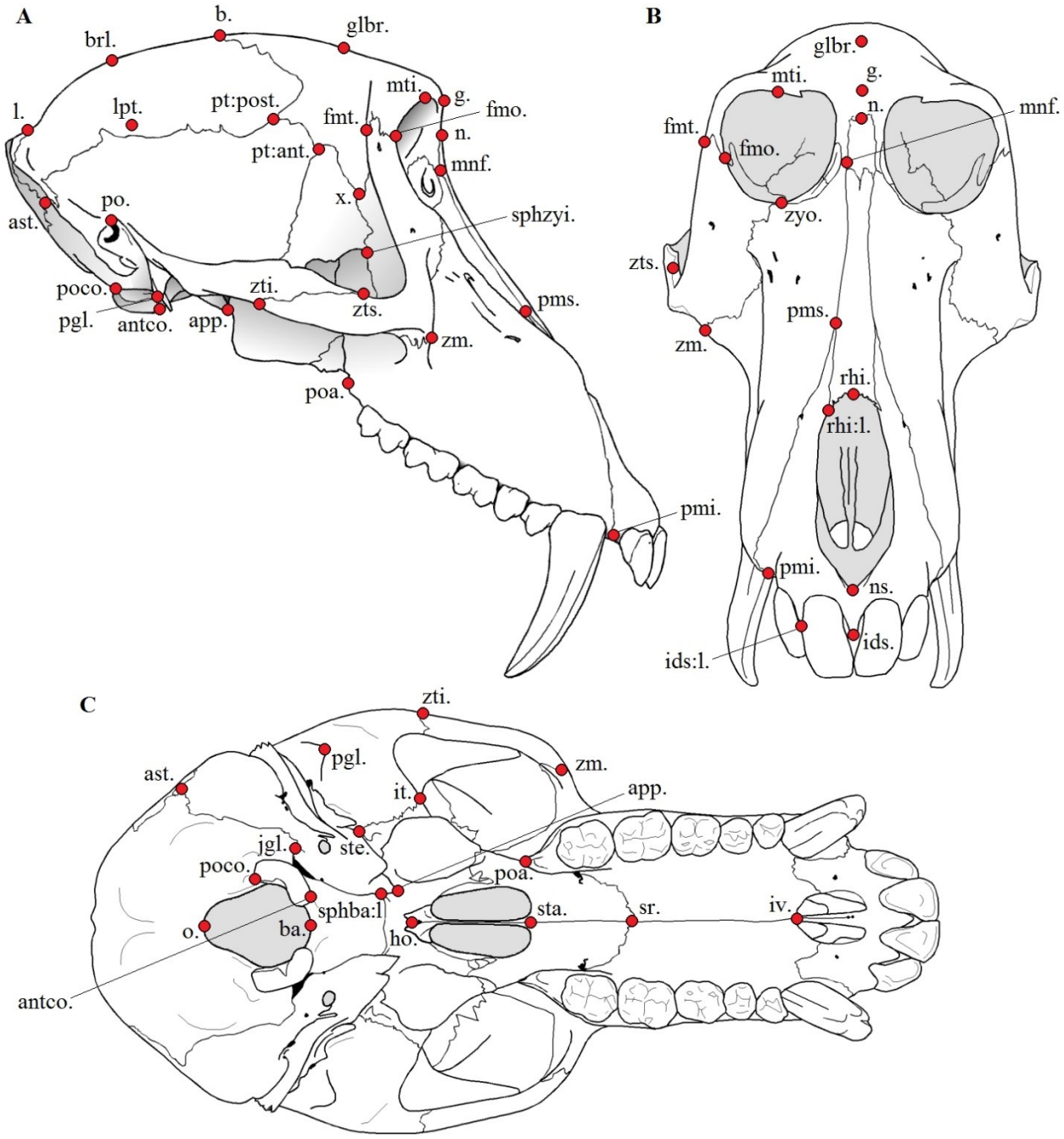


Figure 3.6. Landmarks recorded from the crania of baboons. These landmarks correspond with those recorded from the human sample with the exception of pms., pmi., pt:post., pt:ant., and lpt. **A**: lateral view; **B**: anterior view; **C**: inferior view. Abbreviations correspond with landmarks defined in Table 3.1.

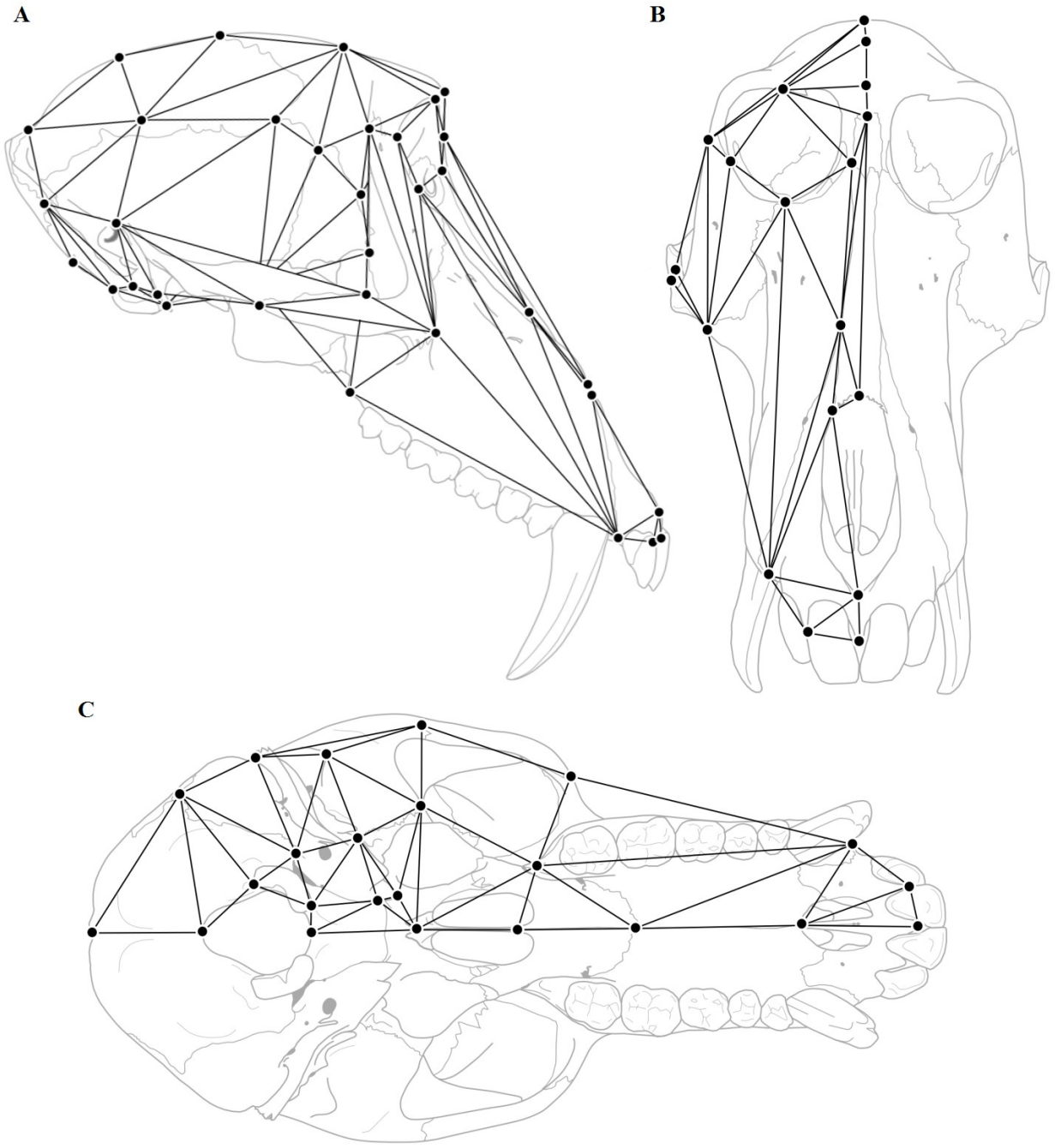


Figure 3.7. Illustration of the wireframe for aiding in visualisation of landmark statistics in the analysis of the baboon crania. **A**: lateral view; **B**: anterior view; **C**: inferior view.

The landmarks that were located on the human crania are also presented in Table 3.1. If any meaningful comparison is to be achieved, homologous landmarks between the baboon and human samples need to be established. However, the early closure of the premaxillary-maxillary suture in humans and differences in the arrangement of the bones at pterion between the two species prevent its total homology of the landmarks. Removing landmarks involved with the premaxillary-maxillary suture in the baboons was not an option as the patency of this suture well into adulthood suggests that it is an important site of growth in many non-human primates (Carmody *et al.,* 2008), while pterion is important because of the paucity of fixed landmarks that can be used to document cranial breadth. These differences are ignored for the analysis of individual samples, but when comparing the two samples the landmarks associated with the premaxillary-maxillary suture were deleted, and the mean of those landmarks comprising pterion were used to represent the average point of the intersection of the parietal, temporal, sphenoid and frontal bones. In addition, the landmark between lambda and pterion was removed from the human sample as it was found to have very poor repeatability, and thus had to be removed from the baboon sample when analysing the samples jointly.

3.2.1 Estimation of missing landmarks

Geometric morphometric methods require complete datasets, but to increase sample size human specimens missing three or fewer landmarks (less than five percent of the landmarks) were included. There are currently four proposed methods for estimating the coordinates of missing landmarks (Bookstein *et al.,* 1999; Gunz *et al.,* 2004, 2009; Arbour & Brown, 2014). The first proposes a mean substitution of Procrustes aligned data. This method is very problematic as it not only negates sample variation but also artificially decreases the distances between specimens.

The second utilises the principle of thin plate splines, warping the configuration of a complete specimen onto the configuration of the specimen missing landmarks, all while ensuring that bending energy is minimised. Unfortunately, the result is completely dependent on the specific shape of the complete specimen used, and ignores sample variation. The use of thin plate splines is particularly suited to data missing unilaterally, using the reflection as the complete set.

The third method for estimating missing landmarks uses multivariate regression to predict the position of the unknown landmarks given their association with known landmarks in the rest of the sample. This method is problematic as sample size in geometric morphometric analyses is often smaller than the number of variables, resulting in matrices that are not invertible, a necessary step in many multivariate statistical methods including multivariate regression. Using a reduced number of principal components of the original variables has been proposed as a possible solution to this problem, but there is the possibility of overfitting the data.

The final method, and the one used here, involves using a two-block partial least squares (2B-PLS). This method finds vectors that generalise the covariance between the known and unknown sets of landmarks, which are subsequently used to predict the positions of the missing landmarks. Missing landmarks were initially estimated to assess centroid size. This involved assigning a value of zero to each dimension of the missing landmarks, and superimposing the configurations using a partial Procrustes method, while ignoring size differences. The 2B-PLS method was used to estimate the coordinates of the missing landmarks. However, the initial assigning of zero to the missing data affects the Procrustes superimposition and thus the prediction. To account for this, the configurations must undergo Procrustes superimposition again, and the coordinates must

be estimated again. This must continue until there is an insignificant decrease in the sample variation from the new estimate, resulting in a maximum likelihood estimate of the missing values. Once this estimate was optimised, the specimen sizes were recorded.

Because size was initially ignored, the configurations are superimposed completely using a partial Procrustes superimposition (accounting for translation, rotations and now size too), and the same maximum likelihood method was used to estimate missing landmarks. Estimates were considered suitable once there was negligible improvement in sample variation. The actual estimation was implemented in R using the *estimate.missing* function in the geomorph package (Adams & Otárola-Castillo, 2013).

Table 3.1. List of landmarks used in the analysis

Landmark	Abb.	Region	Definition
Lambda	l.	vault	The ectocranial point where the sagittal and lambdoidal sutures intersect, not necessarily forced to the median sagittal plane[1]
Bregma	b.	vault	The ectocranial point where the coronal and sagittal sutures intersect, not necessarily forced to the median sagittal plane [2,3]
Glabella	g.	vault/face	The most anterior projecting point in the midline of the frontal bone usually above the nasofrontal suture as seen in the Frankfurt horizontal [4]
Nasion	n.	face	The junction of internasal suture with nasofrontal suture [2]
Rhinion	rhi.	face	The point located at the lower end of the internasal suture [2]
Nasospinale	ns.	face	Inferiormost midline point of piriform aperture in baboons. [4] The midline point on a line between the deepest points on the two inferior curves of the nasal aperture margin in humans [7]
Infradentale superius	ids.	face	The point at the apex of the septum between the upper central incisors [5,3]
Incisivion	iv.	face	Point at the most posterior margin of the incisive foramen [6], not extrapolated if asymmetry present.
Staurion	sr.	face	Intersection of the median palatine suture and transverse palatine suture, where asymmetrical, the anterior-most intersection [6]
Staphylion	sta.	face	The point on the interpalatal suture where it intersects with a line drawn between the deepest recesses of the posterior margin of the palate [3]
Hormion	ho.	base	The point at the attachment of the vomer with the sphenoid body, between the two alae of the vomer [1]
Basion	ba.	base	The midline point on the anterior margin of the foramen magnum placed on the anteroinferior portion of the foramen's rim for consistency [3]
Opisthion	o.	vault/base	The midline point at the posterior margin of the foramen magnum [3]
Maxillonasofrontale	mnf.	face	The point at the intersection of the frontomaxillary, frontonasal and nasomaxillary sutures [1]
Rhinionlaterale	rhi:l.	face	The most inferolateral extent of the nasal bone
Infradentale superius laterale	ids:l.	face	Point at the apex of the septum between the upper central and lateral incisors.

Table 3.1 continued

Landmark	Abb.	Region	Definition
Premax-maxillary superior	pms.	face	Point where maxillary-premaxillary suture meets nasal bones. [4] Note that this point was not recorded in humans
Premax-maxillary inferior	pmi.	face	Point along maxillary-premaxillary suture at alveolar margin [4,7] Note that this point was not recorded in humans
Zygomaxillare	zm.	face	The most inferior point on the zygomaticomaxillary suture [1]
Zygoorbitale	zyo.	face	The point where the orbital rim intersects the zygomaticomaxillary suture [1]
Mid-torus inferior	mti.	vault/face	Point on supraorbital rim at middle of orbit [4]
Frontomalare orbitale	fmo.	face	The point where the frontozygomatic suture crosses lateral orbital margin [1]
Frontomalare temporal	fmt.	vault/face	The most lateral point on the frontozygomatic suture before passing posteriorly to the temporal fossa [1]
Porion	po.	vault/base	The point on the superior margin of the external acoustic meatus[5]
Zygotemporale superior	zts.	vault/face	Superior point of zygomaticotemporal suture on lateral surface of zygomatic arch [4]
Zygotemporale inferior	zti.	vault/face	Inferior point of zygomaticotemporal suture on lateral surface of zygomatic arch [4]
Postglenoid	pgl.	base	Tip of the postglenoid tubercle [4]
Postalverion	poa.	face	The most posterior point on the alveolar process of the maxilla [6]
Pterion anterior	pt:ant.	vault	The point where the sphenoid, temporal and frontal bones meet at pterion. Note that this point differs from sphenion (sphn.) in the bones which intersect in humans
Sphenion	sphn.	vault	The point where the frontal, sphenoid and parietal bones meet at pterion. Note that this point differs from the anterior pterion configuration that generally occurs in baboons
Pterion posterior	pt:post.	vault	The point where the frontal, temporal and parietal bones meet at pterion. Note that this point differs from Krotaphion (k) in the bones which intersect in humans
Krotaphion	k.	vault	The point where the sphenoid, parietal and temporal bones meet at pterion. Note that this point differs from the posterior pterion configuration that generally occurs in baboons

Table 3.1 continued

Landmark	Abb.	Region	Definition
Asterion	ast.	vault/base	The point at the intersection of the lambdoidal, parietomastoid, and occipitomastoid sutures, that separate the occipital, temporal and parietal bones [2,3]
Sphenobasionlaterale	sphba:l.	base	Most lateral point along the sphenooccipital synchondrosis as it passes deep to the petrous part of the temporal bone
Sphenozygomatic inferior	sphzyi	face	Most inferior point along the sphenozygomatic suture in the infratemporal fossa (pterygopalatine fossa)
landmark x	x	vault	Point at the intersection of the sphenozygomatic, sphenofrontal and frontozygomatic sutures [6]
Infratemporale	it.	vault/base	Intersection of the sphenosquamous suture and infratemporal crest of the sphenoid bone [6]
Stenion	ste.	base	The most medially located point on the sphenosquamous suture [1]
Apex partispetrosae	app.	base	Point on the apex of the petrous part of the temporal bone on the inferior surface of the cranium
Jugularislaterale	jgl	base	Most lateral point on the jugular notch on the external surface of the occipital bone
Occipitocondylion anterior	antco.	base	The most anterior point on the margin of the occipital condyle [6]
Occipitocondylion posterior	poco.	base	The most posterior point on the margin of the occipital condyle [6]
Glabella-bregma,	glbr.	vault	Midpoint between glabella and bregma measured along the surface of the cranium
Bregma-lambda	brl.	vault	Midpoint between bregma and lambda measured along the surface of the cranium
lambda-pterion	lpt.	vault	Midpoint between lambda and Pterion posterior measured along the surface of the cranium. This landmark was found to have low repeatability in *H. s. sapiens*, and thus removed

1. Knußmann (1988); 2. Krogman & İşcan (1986); 3. White *et al*., (2012); 4. Frost *et al.*, (2003); 5. Bass (1995); 6. Bigoni *et al*., (2010); 7. Collard & O'Higgins (2001)

3.3 Repeatability

3.3.1 *P. h. ursinus*

To assess the repeatability of the landmark data among the baboon sample, ten crania were measured for a second time on a different day. After Procrustes alignment, the partial Procrustes distances between repeated observations were compared with the partial Procrustes distances between between all paired specimens in the sample. As sexual dimorphism and ontogeny inflate sample variation, minimising the relative effect of measurement error, the partial Procrustes distance between repeated observations were also compared with those between all individuals in the sample after accounting for these additional factors. The procedures by which sexual dimorphism and ontogeny were dealt with are described in section 3.6. Measurement error is commonly deemed acceptable when it contributes less than five percent to the variation of interest.

In addition, data were inspected for measurement error across individual landmarks by calculating the difference between repeated landmarks after superimposing the configurations. These differences were added to the mean configuration, and the resulting configurations were used to illustrate the landmark error using 95% confidence interval ellipses. Although errors are spread somewhat throughout the configurations during superimposition, this method should highlight any potentially problematic landmarks.

3.3.2 *H. s. sapiens*

Repeatability in the human crania was dealt with somewhat differently, with each cranium measured twice, on different days. All configurations and their repeats were initially superimposed, and as with the baboon sample, sexual dimorphism and ontogeny were accounted for before assessing measurement error as they both contribute significantly to sample variation. Measurement error, or the partial Procrustes distances between repeats, was compared with the partial Procrustes distances between all specimens. Measurement error was considered negligible if the distances between repeated measures all fell below five percent of the between-specimen distances. After measuring 20 crania, measurement error across individual landmarks was assessed visually following the method outlined above (section 3.3.1).

3.4 General statistical procedures

All morphometric, statistical and graphical analyses were programmed in R version 3.3.1 (The R Foundation for Statistical Computing; www.r-project.org) by the author. Algorithms that are derived from Claude (2008) are specifically stated. Because shape analysis forms an integral part of the methodology employed, it is necessary to present a brief overview of the theory underpinning many of the methodological considerations. Specific R packages are mentioned where appropriate.

3.4.1 Superimposition

There are several methods by which landmark configurations can be mathematically modified for the statistical analysis of shape, including, but not limited to, angle-based and distance-based

methods, Procrustes analysis, and resistant fit superimposition. These methods aim to remove nuisance parameters, or at least analyse transformations of the data such that the resulting configurations are invariant under the effect of these nuisance parameters. Of all these methods, it is Euclidean distance matrix analysis (Lele & Richtsmeier, 1991) and generalised Procrustes analysis (Dryden & Mardia, 1998) that possess a sound and rigorously studied mathematical and statistical basis. Besides outperforming other methods (in terms of error and bias) when estimating the mean and variance from samples with known parameters (Rohlf, 2003), the greatest advantage of the generalised Procrustes method, and possibly the single most important reason for its popularity, is the ease with which results can be visualized and interpreted (Collard & O'Higgins, 2001).

Shape theory

Procrustes analysis aims to remove the nuisance parameters of translation, rotation and size, resulting in a least-squares approximation of shape. The term generalised is used to describe the superimposition of multiple configurations as opposed to ordinary Procrustes analysis where there is a single ‘target’ and a single ‘reference’ configuration. With regard to terminology, both the ‘target’ and ‘reference’ configurations are translated and standardised for size, whereas it is only the ‘target’ configuration that is rotated and, in the case of full Procrustes superimposition, again resized in order to minimise the squared distance between the two configurations.

Procrustes superimposition

The ordinary Procrustes fitting of only one target configuration to a single reference serves well for the description of this method of superimposition, which will be expanded on later in this chapter to explain the generalised instance. For greater mathematical detail and a discussion of the intricacies of Procrustes methods see Dryden and Mardia (1998). The nuisance parameters to be accounted for involve the effects of translation, size and rotation on two landmark configurations. Initially, the effect of translation is accounted for by subtracting the coordinates of the centroid for each configuration (the arithmetic mean of each dimension) from its constituent landmarks. This centres the configurations at the origin (Figure 3.8).

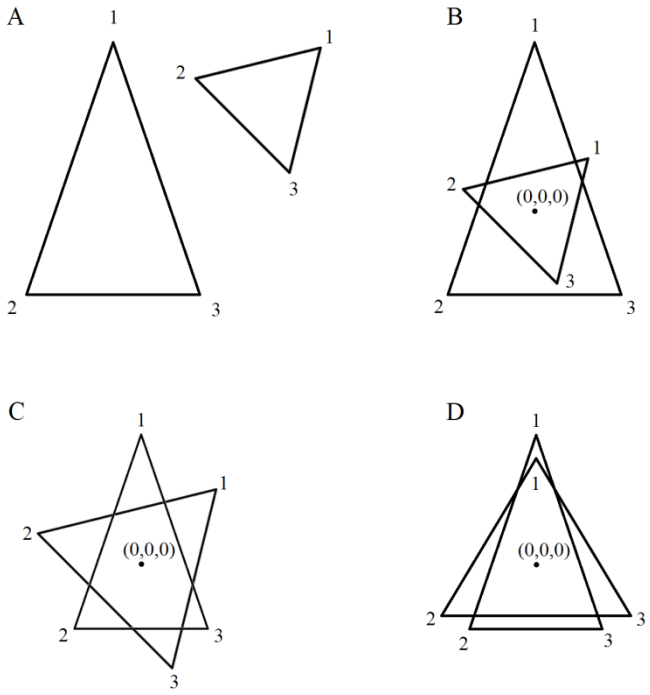


Figure 3.8. Procrustes superimposition of two triangles. **A**: two configurations for which shape information is of interest. **B**: the removal of translation by the repositioning of two configurations so that their centroids lie over the origin in Cartesian space. **C**: configurations are standardised to unit

centroids size. **D**: the reference configuration remains in place while the target configuration rotates, minimising the square root of the sum of the squared distances between homologous landmarks.

Centroid size, being the preferred measure of size for Procrustes methods, is calculated as the square root of the sum of the squared Euclidean distances between the centroid and every landmark:

$$CS = \sqrt{\sum_{i=1}^{k}\sum_{j=1}^{m}(X_{ij} - \bar{X}_j)^2}$$

where *Xij* is value corresponding to the *j*th dimension of the *i*th landmark of the configuration *X*, and $\bar{X}_j$ represents the *j*th dimension of the centroid for configuration *X* (Dryden & Mardia, 1998). Size is standardised by dividing the coordinates of each landmark by the centroid size of that particular configuration, thereby transforming the configurations to unit centroid size (Figure 3.8 C). The resulting centred and scaled configurations are referred to as preshapes.

Removal of the effect of rotation from the translated, unit-sized preshapes is accomplished by rotating the target configuration to the reference configuration to minimise the sum of the squared distances between homologous landmarks (Figure 3.8 D). There are several theoretical considerations that need to be outlined prior to removing the effect of rotation from the preshapes, which will be covered briefly.

Constraining configurations to unit size has an interesting effect on the relative space occupied by possible preshapes. Note that the equation defining the size of the configurations now resembles that of a sphere of unit radius ($x^2 + y^2 + z^2 = 1$) but with greater dimensionality. The dimensionality of the preshape space depends on the number of landmarks and dimensions; triangles of three two-dimensional landmarks originally occupy six dimensions which are reduced to three dimensions by the removal of translation (-2) and size (-1). Thus, in the case of triangles, each preshape can be considered as a point on the three-dimensional surface of a four-dimensional hypersphere (for sake of illustration, this is simplified to a three-dimensional sphere in Figure 3.9). The distance between two preshapes, Z_1 and Z_2, on this hypersphere is along the surface of the sphere (ρ, which is equivalent to the angle in radians between the two configurations from the centre of the space) and not the straight-line chordal distance, termed the partial Procrustes distance (*Dp*).

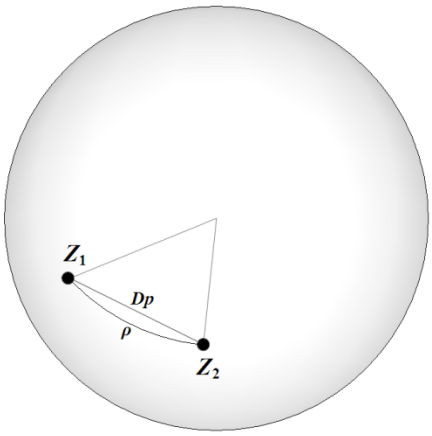


Figure 3.9. Illustration of preshapes Z_1 and Z_2 occupying a highly simplified space represented as the surface of a sphere with radius 1. The great circle distance and the chordal distance between the two preshapes are designated respectively.

Rotation of preshapes shifts their position on the preshape hypersphere along potential trajectories, or what Dryden and Mardia (1998) termed "fibres". These fibres have commonly been illustrated as converging arcs on the surface of the sphere (Figure 3.10), which is theoretically problematic, as minimising the distance between two preshapes involves the rotation of only one preshape and is independent of which configuration is designated the target and which the reference. The reference preshape is fixed, and the target is allowed to rotate. Following Figure 3.10, both preshapes Z_1 and Z_2 must be rotated to minimise the distance between them, at the point of convergence of the two fibres. Additionally, the fixing of Z_1 and rotation of only Z_2 would result in a significantly different distance than if Z_2 were fixed and Z_1 was allowed to rotate. As an alternate illustration, I suggest that these fibres are better represented as parallel lines on the surface of the (hyper)sphere (Figure 3.11), where minimisation of the distance between the two preshapes Z_1 and Z_2 is independent of the choice of target and reference configuration, and can be achieved by the rotation of only one configuration.

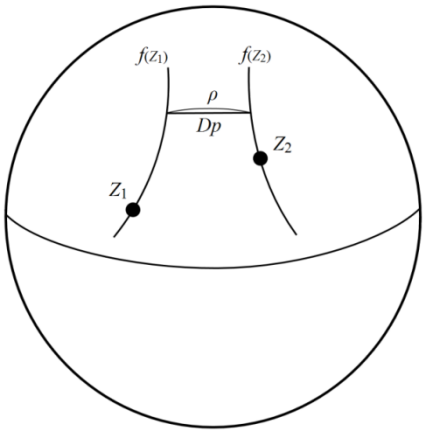


Figure 3.10. The common schematic used to depict the concept of fibres $f(Z_1)$ and $f(Z_2)$ of two pre-shapes Z_1 and Z_2 on the surface of a pre-shape sphere. Adapted from Dryden and Mardia (1998: Figure 40: 63).

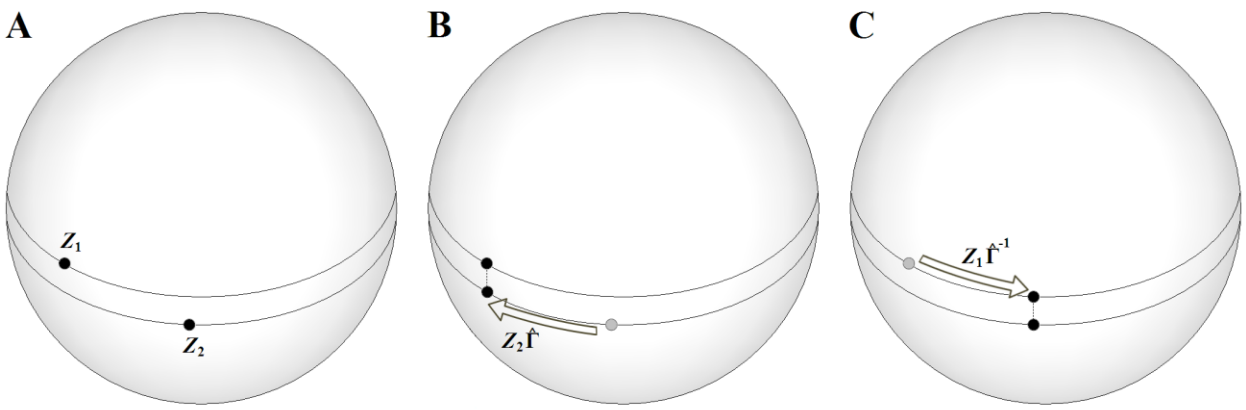


Figure 3.11. A highly simplistic representation outlining the concept of preshape rotation along fibres that lie parallel to one another in preshape space. For the purpose of illustration, the preshape space here is simplified to a sphere. **A**: original positions of the preshapes Z_1 and Z_2 in the preshape space; **B**: rotation of preshape Z_2 along its fibre to minimise the distance between configurations; **C**: rotation of preshape Z_1 along its fibre to minimise the distance between configurations. Note: $\hat{\Gamma}$ represents the least squares estimate of the rotation matrix that minimises the distance between configurations by the rotation of Z_2, and $\hat{\Gamma}^{-1}$ is its inverse that will rotate Z_1 along its fibre to achieve the same objective.

Standardisation of size to unit, and the removal of both translation and rotation, further reduces the dimensionality of the space occupied by potential shapes. The preshape space of triangles, as considered above, is a three-dimensional surface of a four-dimensional hypersphere. The preceding figures depict the space as a two-dimensional surface on a three-dimensional sphere for explanatory purposes only. Rotating preshapes to minimise the difference between configurations removes additional dimension(s) from the potential space occupied by configurations: one for the rotation of two-dimensional configurations – as rotation is about one axis, and three for the rotation of three-dimensional data because there are three axes around

which configurations are rotated. Thus, in the case of two-dimensional triangles, the removal of one dimension from the four-dimensional preshape space results in the 'shapes' occupying the surface of a hemisphere, like that illustrated in Figure 3.12. Triangles occupy a hemisphere instead of a complete sphere as the angle, ρ, between shapes does not exceed $\pi/2$ radians (90 degrees).

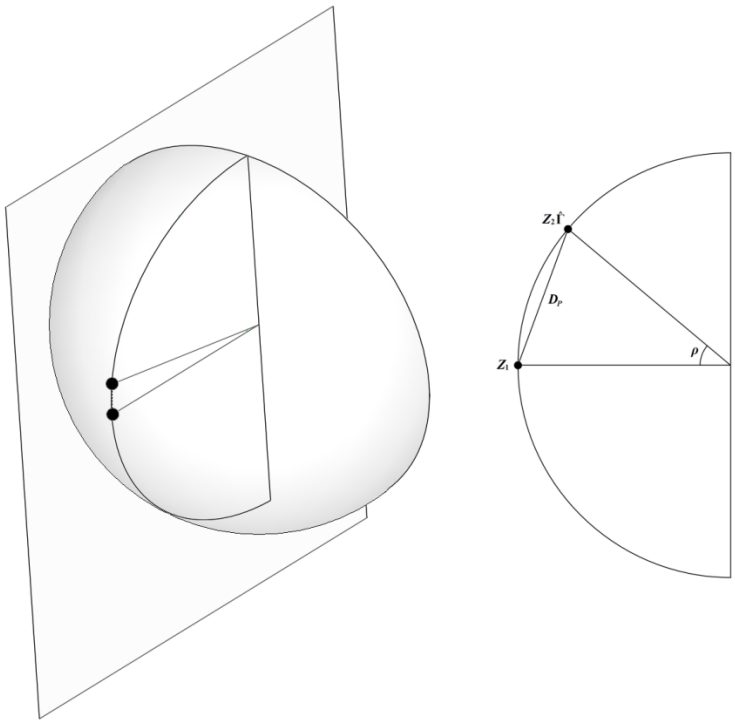


Figure 3.12. Sectioning of the Procrustes hemisphere by a plane passing through the two configurations on the surface of this space, and the resulting schematic used in Figures 3.13 and 3.14.

The above steps have outlined how the effects of translation and rotation are accounted for, but only describes standardising size to a unit. A complete least squares superimposition (a full Procrustes superimposition) aims to minimise the difference between configurations by adjusting

translation, rotation and size – as size can be adjusted again to further reduce the differences between configurations. If size is not modified further, and kept at a value of one, the configurations would remain on the (hyper)hemisphere of unit radius and the superimposition is considered a partial Procrustes superimposition, and as stated before, the chordal distance between the two shapes in the shape space hemisphere is the partial Procrustes distance.

For the continued illustration of Procrustes methods, the Procrustes hemisphere of possible shape space is bisected by a plane that runs through the two configurations in Figure 3.12. The chord between the two shapes in the shape space hemisphere is regarded as the partial Procrustes distance, *Dp*. Note that the angle ρ is equivalent to the great circle distance between the two configurations as the radius of the hemisphere is one. Given that this angle is minimised, the distance between the shapes can only be reduced further by projecting $Z_2\hat{\Gamma}$ onto Kendall's shape space by reducing the size of the $Z_2\hat{\Gamma}$ configuration to the cosine of ρ, which minimises the chordal distance between configurations, the full Procrustes distance (D_F). Kendall's shape space is a (hyper)spherical space of radius half, with reference at Z_1 (Kendall, 1984). Figure 3.13 depicts the relationship between the partial and full Procrustes distances, and the projection of shapes from the Procrustes hemisphere onto Kendall's shape space. Note also that the great circle distance between the two configurations in both the Procrustes hemisphere and Kendall's shape space is the same, ρ.

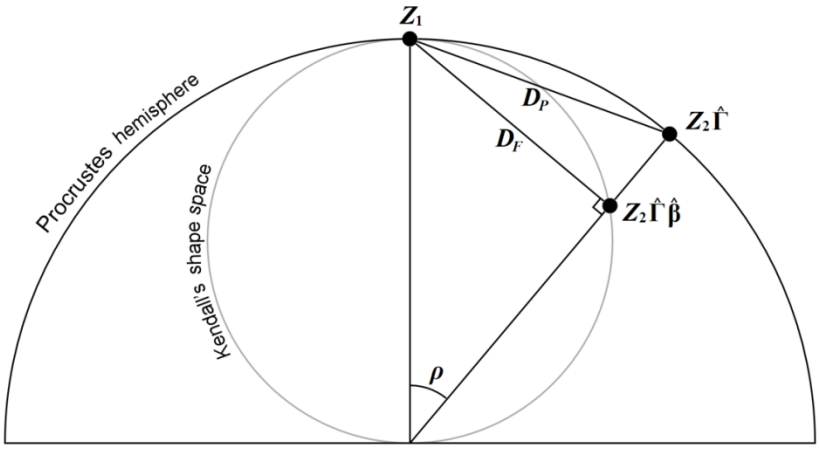


Figure 3.13. The relationship between partial and full Procrustes superimposition of Z_2 on Z_1. Note that partial superimposition requires that the rotated preshape $Z_2\hat{\Gamma}$ remains on the Procrustes hemisphere and the chordal distance between the configurations is given by D_P. Full Procrustes superimposition involves reducing the size of configuration $Z_2\hat{\Gamma}$ by $\hat{\beta}$, which is estimated as the cosine of ρ, thereby projecting the configuration onto Kendall's shape space and minimising the inter-object chordal distance to D_F. Adapted from Zelditch *et al*. (2004: 86, Figure 4.10)

It is important to note here that the preceding description is based on the superimposition of a target two-dimensional triangle onto a reference two-dimensional triangle. The preshape and shape space becomes increasingly more complex (a manifold) for additional landmarks, and for three-dimensional data singularities may exist. Biological shapes do not usually have extreme variability (Marcus *et al.,* 2000) and thus it is generally assumed that the data are not near any singularities in the occupied space (Zelditch *et al.,* 2004: 97).

Generalised Procrustes Superimposition

The generalised extension of the Procrustes method follows the above steps iteratively until the rotation of configurations fails to reduce sample variability. Rohlf and Slice (1990) outlined the algorithm for optimal Procrustes superimposition, which is simplified here:

1. Translate all landmark configurations to the origin and standardise their size to unit centroid size.
2. Make the first configuration the 'reference' and sequentially rotate all subsequent configurations using the least squares procedure.
3. Calculate the mean landmark configuration from the sample and designate it as the new 'reference'. Rotate all configurations to the reference.
4. The measure of sample disparity is calculated as the square root of the summed squared distances between each of the configurations.
5. The scaling factor is set to unit.
6. The configurations are now iteratively rotated to the reference, the mean. Each of the configurations is also rescaled in full generalised Procrustes superimposition.
7. The measure of sample disparity and the sample mean is recalculated after each bout of rotations.
8. Steps 6 and 7 continue until there is negligible or no decrease in sample disparity.

The data are then considered to be optimally superimposed according to the least squares principle. The major difference between partial and full Procrustes superimposition involves the rescaling of specimens in step 6.

Tangent plane projection

Multivariate statistics have been developed around the analysis of data in Euclidean space and are not suitable for the analysis of configurations in shape space, whether in the Procrustes (hyper)hemisphere or Kendall's shape space. For this reason, superimposed configurations must

be projected to a Euclidean plane that lies tangent to the space at a reference configuration, which is preferably the mean configuration (Zelditch *et al.,* 2004: 97).

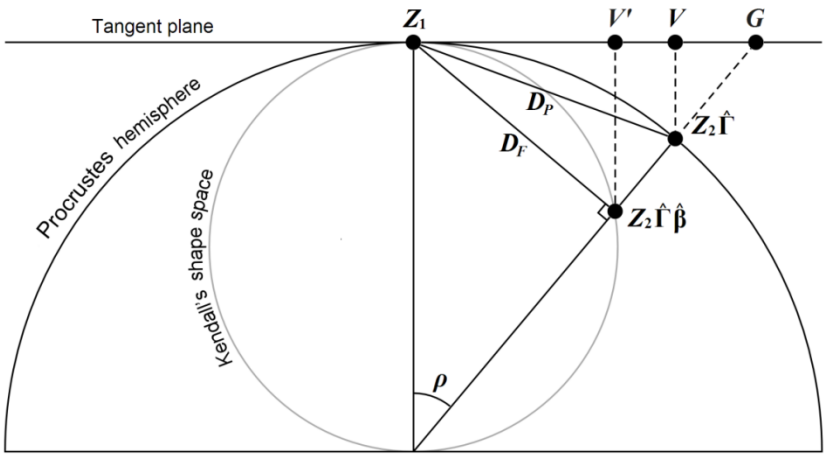


Figure 3.14. A schematic representation of a cross section through the Procrustes hemisphere. The position of the 'target' configuration on the Procrustes hemisphere ($Z_2\hat{\Gamma}$) and Kendall's shape space ($Z_2\hat{\Gamma}\hat{\beta}$), as well as the various projections from these two spaces to the tangent plane (points *V'*, *V* and *G*) are demonstrated. Adapted from Rohlf (1999) and Zelditch *et al*. (2004: 95, Figure 4.17)

There is debate as to which method of projection to the tangent space satisfies the requirements of shape analysis best. Projection can be preformed by either: 1) the orthogonal projection of the configuration from the Procrustes hemisphere ($Z_2\hat{\Gamma}$) to the tangent at *V*; 2) the orthogonal projection from the position of the configuration on Kendall's shape space ($Z_2\hat{\Gamma}\hat{\beta}$) to the tangent at *V'*; or 3) the stereographic projection of the configuration, from either the Procrustes hemisphere or Kendall's shape space, to the tangent at *G* (Figure 3.14). Generally, orthogonal projection from the Procrustes hemisphere to the tangent plane results in the fewest biases (Rohlf, 1999, 2001), but the optimum method depends on the composition and variability of the

underlying sample. As can be seen in Figure 3.14, orthogonal projection will result in underestimates of the difference between the reference and target configurations whereas the stereographic projection results in an overestimate (the amount of distortion depends on the distance between the configuration and the point at which the plane is tangent, ρ). As the average configuration possesses the minimal sum of squared distance between it and all members of the sample, it serves well as the reference point for projection to the tangent space in generalised Procrustes analysis.

Superimposition of the samples

Asymmetry could not be accounted for in the baboon sample because landmarks were taken from the midline and right side. In contrast, landmarks were digitised from both sides of the human cranium, thus left-right differences could be accounted for by superimposing each configuration with its reflection and using the mean. This, however, would create additional discrepancies between the two samples, which may affect their comparison. Thus, the left set of the bilateral landmarks were deleted from the human sample before further analyses were run.

Determining the optimum superimposition and projection

As highlighted above, Procrustes superimposition is ideal for the analysis of shape and size. However, the resulting data either occupy a non-linear, hyperspherical space (partial Procrustes superimposition) or Kendall's shape space (full Procrustes superimposition). Both of these are incompatible with traditional statistical methods and requires projection to a tangent plane. This projection of superimposed configurations to the tangent plane, using either an orthogonal or

stereographic projection, distorts the relationships between configurations somewhat and thus the method of projection should be chosen to minimise this effect. Because the appropriateness of the method applied is dependent on the composition and variability of the sample, scatterplots and uncentred correlations (Rohlf, 1999; Marcus et al., 2000; Slice, 2001; modified from Claude, 2008: 170) were used to describe the relationships between inter-object distances in Kendall's shape space or the Procrustes hemisphere, and their respective distances on the tangent space using both stereographic and orthogonal projections. In other words, to determine the optimal superimposition method, the samples were superimposed using a partial Procrustes superimposition (Claude, 2008, function 4.20) and the partial Procrustes distances between specimens were compared with the Euclidean distances between specimens on the tangent plane after projecting them either stereographically (Claude, 2008, function 4.22) or orthogonally (Claude, 2008, function 4.23). Similarly, the samples were superimposed using a full Procrustes superimposition (Claude, 2008, function 4.19) and the full Procrustes distances between specimens were compared with the corresponding Euclidean distances on the tangent plane after stereographic or orthogonal projection. The closer the uncentred correlations, and the slope of the regression through the origin, are to one, the greater the equivalence between the distances and the smaller the distortion. This was performed for the baboon sample, the human sample, and the combined sample.

The two samples were superimposed separately. The specimens and, in the case of the human sample, their repeated measures, were aligned using the optimal Procrustes superimposition and projection to the tangent plane. Because each of the human crania were measured twice, the coordinates for that specific specimen were recorded as the average of each configuration and its

repeat, after superimposition, and the recorded size was the average of the centroid sizes calculated for each configuration and its repeat.

3.4.2 Visualisation

Visualisation was aided using wireframe and polygon models, as well as by warping a surface model. A wireframe consists of a few straight lines connecting landmarks in a manner that aids with relating the landmarks back to its biological representation. Figure 3.7 illustrates the wireframe configuration used in the analysis of the baboon crania. Although there have been suggestions of wireframe automation using Delaunay triangulation, it is not ideal as the wireframe representation should relate to anatomical adjacency, where the linking of landmarks depends on the underlying, unrepresented morphology (Klingenberg, 2009).

The surface model was generated by laser surface scanning of an appropriate specimen. Selection of the 'appropriate' specimen was based on the summed scores of the first four principal components, weighted according to the percentage of the total variance accounted for by the respective component. This was used to represent the deviation of each specimen from the mean. A specimen close to the mean for each of the samples was selected and scanned using a NextEngine 3D HD desktop laser scanner (NextEngine, Inc.). The final surface model representation (Figure 3.15, for the baboon sample) was constructed from the merging of five 360º scans, each composed of 12 independent scans. The landmarks digitized on the physical specimen (Table 3.1) were then located on the surface model using Landmark (ver. 3.6; Institute for Data Analysis and Visualization, University of California, Davis; Wiley *et al.,* 2005) and

their coordinates exported as a text document. This particular specimen (Figure 3.15) happened to be a subadult female based on the morphology and size of the permanent canine, as well as the third permanent molars being the only unerupted permanent teeth. This specimen was warped to visualise shape change, but it must be noted that canine morphology, together with tooth number and size, did not play a role in morphological interpretations. Nevertheless, an extension or shortening of the alveolar process of the maxilla may reflect a gain or loss of teeth respectively and interpretations must take this into consideration.



Figure 3.15. Surface model of the specimen used as the basis for visualising shape changes. The specimen was selected on the basis of its proximity to the mean configuration for the sample.

To depict a particular shape-change a target and reference configuration is chosen. When illustrating the shape changes associated with principal components, for example, the mean shape was selected as the reference configuration while the extreme positive or negative score

along the specific principal component would act as the target. Warping of the surface model vertices was performed according to the thin-plate spline procedure for three-dimensions (Bookstein, 1997; as in Mitteroecker *et al.,* 2004). For each representation, the vertices of the surface model are initially warped to the mean shape and then to the target. The reason for the mean shape being the starting point is in order to quantify the shape changes on each triangulation of the surface model. Each triangulation is thus coloured, on a continuous scale, according to percent surface area change between the mean shape and target shape. Colours chosen were blue, to represent reduced surface area, grey for very little or no change, and red for an increase in surface area. The degree to which colour change is associated with percentage surface area change is set as required and presented with each figure.

An introduction to thin plate splines would be incomplete without at least mentioning Thompson's (1917) pioneering work on the transformation of Cartesian coordinates between homologous skeletal elements (Figure 3.16). Unfortunately, it was only in the 1980's when the mathematical application of this method on biological form was first realised (Bookstein, 1997), possibly as a direct result of computers on the field of mathematics and statistics. But Thompson's book was ahead of its time, and although much of our biological understanding and reasoning behind erecting transformation grids has changed (Bookstein, 1996), his publication influenced, if not initiated, much of the work that has brought morphometrics to the point it is now, including Huxley's (1932) proposal of allometric growth (Thompson, 1961; see editor's notes, pg. 268). This notion of drawing grids to illustrate differences between objects was seen originally in the very early work of Albrecht Dürer and used to illustrate geometric variation of the proportions of the human head (as acknowledged in Thompson, 1961).

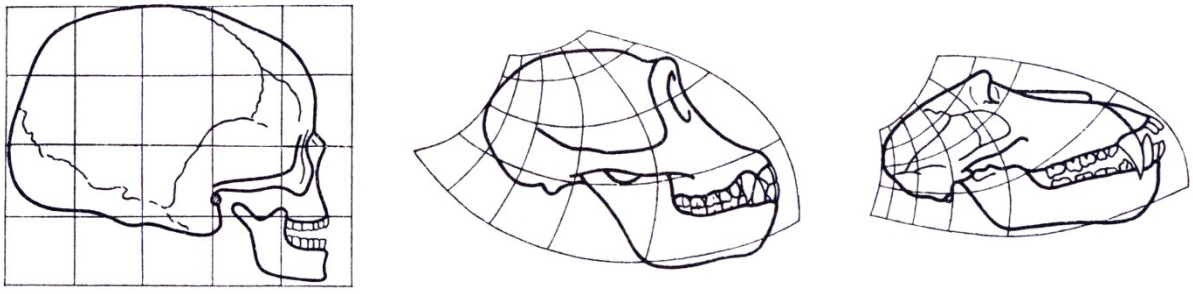


Figure 3.16. Cartesian transformation grids of Thompson (1917). He had used the baboon, on the far right, to depict an extreme of the Cartesian transformation between the human and chimpanzee crania.

Bookstein (1996) established the mathematical procedures for estimating unknown points between sampled data points using principles of interpolation from the fields of physics and engineering. His work resulted in what is referred to as thin plate splines, a method of interpolating the position of a Cartesian grid according to the global and local shape changes between two configurations (Figure 3.17). I will not delve into the mathematics of mapping the Cartesian grid to the target, but I will emphasise that its application can be extended to three-dimensions and be used to map surface models from a reference configuration to a target. This makes logical sense when one considers that a surface model is a suite of points (vertices) in three-dimensional Cartesian space on which polygons are drawn. The thin plate spline determines the new position of these points, depending on the relative positions of the landmarks of the reference configuration and the final position of the landmarks in the target configuration. For greater mathematical detail and discussion, see Bookstein (1997).

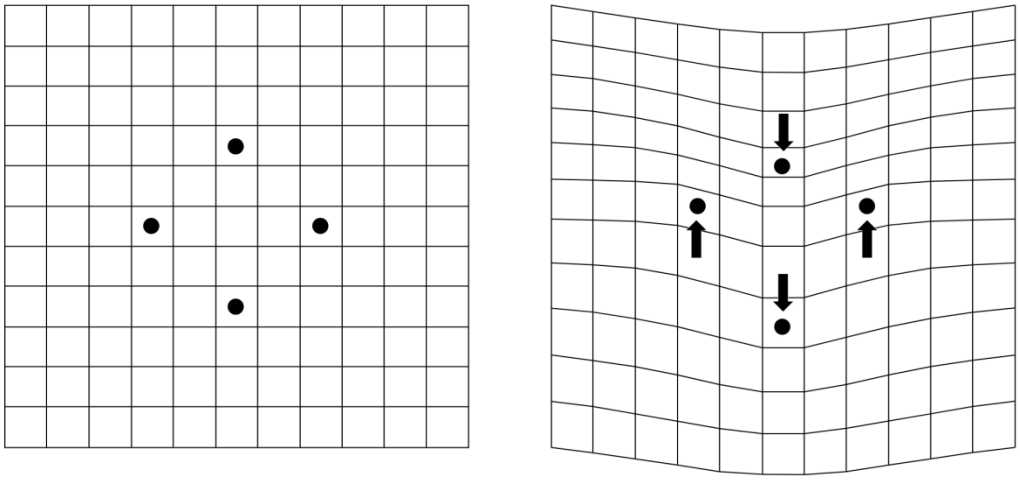


Figure 3.17. Thin plate spline transformation of the vertices of a Cartesian grid. The central and lateral landmarks of the reference configuration on the left are shifted slightly down and up, respectively, to form the target on the right. Modelled from an example in Bookstein (1997) using Microsoft Excel 2007.

3.4.3 General principal component analysis

After applying the appropriate Procrustes superimposition and projecting the data to the tangent plane, they were subjected to a principal component analysis for an initial examination of sample distributions. This method has found favour in shape analyses of this sort. Principal component analysis is a method of ordination, whereby high-dimensional data can be represented by only a handful of variables that preserve most of the variance (Mitteroecker & Huttegger, 2009). Besides being a powerful tool for the analysis of multivariate datasets, the scatterplots of the resulting principal component scores can aid in the assessment of outliers or highlight any mistakes made during the gathering or manipulation of data. A general impression about the data can be gained through plotting the first three of four principal component scores.

Plots depicting the scores of the first three principal components were drawn, and a three-dimensional graph was generated as it has been shown that relevant details may be lost by the reduction of dimensionality to only two axes (Mitteroecker *et al.,* 2004). Principal components are the results of a mathematical manipulation of the data indifferent to the underlying biology, and so relevant details, such as differences between sexes or populations and trends due to growth or interspecific allometry, may not necessarily be recorded by any one of the components alone.

3.5 Aim 1: The role of allometry in morphological integration

The first aim of the study is to assess the role of allometry across different cranial regions in both modern humans and baboons by highlighting regions of differential growth during ontogeny, assessing the effect of allometry on the pattern of morphological integration, and quantifying the proportion of adult, static variation attributable to size. More specifically, the hypotheses state that:

H1) The general pattern of postnatal ontogenetic allometry will be one of slower neural growth and faster facial growth, while the orbits, zygomatic region and cranial base possess an intermediate, possibly isometric growth

H2) Allometry will have a general concealing effect on the pattern of morphological integration, apart from those regions associated with neural versus somatic growth

H3) The proportion of variation attributed to size will be larger in *P. h. ursinus* than *H. s. sapiens*

3.5.1 The pattern of postnatal ontogenetic allometry

The allometric component of shape change in an ontogenetic sample of a single species is generally thought to be represented by the first principal component, primarily because it

accounts for the greatest shared variance of the data, which are usually size and size related shape changes (Jolicoeur & Mosimann, 1960; Jolicoeur, 1963; Collard & O'Higgins, 2001; Klingenberg, 2016). However, as principal components do not suppose a relationship of dependence and independence, but rather model covariation based on variable co-dependence, additional non-allometric variation can be included in the first principal component (Bookstein, 1989; Collard & O'Higgins, 2001). This is logical if one considers that regression of size on Procrustes shape variables would never account for as large a proportion of total variance as the first principal component, and additional variation is plainly evident when plotting the regression of the first principal component on log centroid size, where, although the relationship is strong, centroid size does not explain all the variation seen in the first principal component (for an example, see Collard & O'Higgins, 2001).

Size-shape space

To ensure that the first principal component aligns itself with the information associated with size, Mitteroecker and colleagues (2004) introduced the concept of size-shape space whereby the projected Procrustes residuals are supplemented with the logarithm of centroid size. The remaining components thus account for the non-allometric components of the total variance. Subsequent to the assessment of general principal component analysis, the Procrustes aligned residuals of the samples were supplemented with the logarithm of their centroid size and the principal components of the new dataset were computed to assess the allometric shape changes in each of the samples.

The shape changes associated with first principal component of the size-shape space were evaluated by warping surface models to highlight changes in the relative sizes of surface polygons. Two different warps were performed, firstly between the mean shape and the shape associated with the minimum size, and secondly, between the mean shape and the shape associated with the maximum size. These surface models highlight regions of the cranium that underwent common rates of growth, likely in response to global growth factors.

Although visual assessments are convenient, there needs to be mathematical confirmation of observed patterns. The configurations of landmarks summarising the shape of a particular cranium can be decomposed into several triangles comprising three two-dimensional landmarks – the simplest of geometric shapes (Klingenberg, 2016). During growth, each triangle polygon will change shape to some degree, and those triangles associated through similar underlying growth process should experience a similar amount of change. To explore this, each of these triangular polygons were treated as individual shapes, and after independent superimposition (stereographically projected after partial Procrustes superimposition), a matrix was generated comprising *Rv* coefficients describing the strength of the relationships between all possible pairs of triangles.

3.5.2 The patterning of morphological integration in ontogenetic samples

The following analyses make use of Escoufier's (1973) *Rv* coefficient, which is a multivariate generalization of the coefficient of determination, or the squared Pearson's correlation coefficient, which aims to determine the strength of the association between two multivariate sets

of data (Escoufier, 1973; Robert & Escoufier, 1976; Klingenberg, 2009, 2013). This coefficient is basically a ratio involving the covariance between the two sets of data and the total variance seen in these two sets. The *Rv* coefficient was chosen because the triangles have a common number of landmarks and the relationship is the result of an unobserved latent variable – likely growth given the ontogenetic samples. *Rv* coefficients close to one would describe triangles that change jointly in response to some latent phenomenon, whereas those close to zero probably have little to no common underlying phenomena. The significance of the *Rv* coefficient is established using a permutation procedure introduced by Klingenberg (2009). This involves comparing the coefficient between the two blocks with the frequency distribution obtained by 100,000 permutations, where in each case the rows of the second block are randomly ordered to mimic what could be obtained by chance. Two methods were used to explore the grouping of polygons regarding their associations during allometry. The first clustered the polygons using hierarchical clustering methods and the *Rv* coefficient as a measure of similarity. The second created a network of polygons using the significance of the *Rv* coefficient, after accounting for multiple tests, and attempted to find a "community structure" within the network.

Polygon clustering

The first analysis of the polygon associations clustered individually superimposed triangle configurations using the level of dissociation (1 - *Rv*) as a distance measure. The clustering was performed using an Unweighted Pair Group Method with Arithmetic Mean (UPGMA) hierarchical clustering algorithm (*hclust* function in R). The idea behind this is based on the triangle being the smallest three-dimensional quantifiable shape available for Procrustes superimposition. Those shapes more associated with one another should share similar

developmental underpinnings. The statistical fit of the dendrogram to the underlying data was measured using the cophenetic correlation coefficient, which described the correlation between the branch lengths and the pairwise distances between the variables (Sokal & Rohlf, 1962). The polygon clusters were assigned a colour and a figure was presented to illustrate the distribution of the clusters among the polygons. The number of clusters was established using a modified elbow criterion (Claude, 2008: 123), which plots the number of clusters against the ratio of explained variability. The optimal number of clusters is considered as the last value before the curvature of the graph straightens out from its initial convexity.

Network analysis

The second analysis of the polygon associations involved modelling them as a network. The ideas that originated as graph theory in computer science, and hierarchical clustering in the social sciences, are now being readily applied to the study of networks in diverse biological topics such as metabolism and epidemiology (Newman & Girvan, 2004, and references therein). These methods are being developed primarily to identify an essential property of networks: modularity. The definition of a network module (community structure) parallels that of the biological sense (Bolker, 2000: 773), being a group of nodes (vertices) that possesses greater connections (edges) with each other than with other nodes in the network. The use of network methods to explore and compare anatomical modularity and integration have found popularity in the study of the modular organization of the brain (Chen *et al.,* 2011; Shi *et al*., 2013; Rubinov & Sporns, 2010, provide a review of network methods in measuring brain connectivity). The application of network methods to the analysis of the cranium has being pioneered by Esteve-Altava and colleagues (e.g. Esteve-Altava *et al.,* 2011, 2013a, 2013b; Esteve-Altava & Rasskin-Gutman,

2014). They generated networks with connections (edges) between the various bones of the cranium (nodes) depending on the presence of physical articulations between the bony elements. Although this is a novel and insightful approach, particularly from the perspective of the pathological or a macro-evolutionary gain and loss of elements and articulations, these studies focus primarily on physical approximation of bones and not their patterns of covariation.

The statistical significance of the association between all pairs of polygons was tested by the permutation procedure of the *Rv* coefficient (as per Klingenberg, 2009). Depending of the number of nodes, the significance level was adjusted using the Bonferroni method to reduce the type-I error rate (Holm, 1979). The resulting undirected adjacency matrix describes whether there is an association between a pair of polygons or not, coded as a one or zero respectively, and does not consider the direction of influence or the degree of association. Network modules were detected using the *fastgreedy.community* function in the igraph R package for network analysis (Csardi & Nepusz, 2006). This function tries to detect communities in networks by optimizing the modularity score proposed by Newman and Girvan (2004). This modularity score measures the proportion of the connections in the network that connect nodes within the groups, minus the proportion if the connections between nodes were random whilst keeping the same groupings (Newman & Girvan, 2004). Again, network modules were assigned a particular colour and a figure was provided to illustrate the distribution of the clusters among the polygons.

3.5.3 Allometric proportion of variation

The eigenvalue of the first principal component of the size-shape space and the proportion of variance it accounts for is irrelevant because the addition of size artificially inflates the variability of the sample. Thus, using a combination of the results from this analysis and that of a conventional principal component analysis, the proportions of the variance due to allometric and non-allometric factors among the adult representatives of the samples were calculated.

3.6 Accounting for allometry

Since the allometric effects of growth and development bring about a global integration, its removal and the subsequent analysis of the remaining non-allometric variation is fundamental to uncovering local patterns of integration (Klingenberg, 2010). It is assumed that the general morphological differences between adult female and male baboons results primarily from the extension or prolongation of a common growth trajectory in the latter (Leigh & Cheverud, 1991). In such a case accounting for the effect of allometry and sexual dimorphism can be achieved simply by looking at the residuals after multivariate regression of the Procrustes residuals on the logarithm of centroid size (Monteiro 1999). However, divergent allometric trajectories, albeit minor, may erroneously inflate measures of integration and affect the observed pattern. Thus, the residuals of separate (male and female) second-degree polynomial regressions were used to account for allometry and sexual dimorphism. Juvenile specimens for which sex was not known were included when calculating the allometric trajectories for each of the sexes. The residuals resulting from both regression analyses are then added to the mean shape for visualization and further analysis.

3.7 Aim 2: Patterning of covariation

The second aim is to explore non-allometric patterns of covariation in the crania of the baboon and the modern human samples independently. The purpose was to highlight any departures from an expected pattern of morphological integration and modularity, given the shared developmental basis of each. The analysis of patterns acts as an exploratory procedure that could either support or be at odds with *a priori* patterns of modularity and integration proposed for the general primate cranium. As modules are internally integrated regions that are relatively independent from each other, covariation and the number of connections between cranial modules should be significantly weaker than other random partitions of the cranium. The specific hypothesis states that:

H4) After accounting for allometry and sexual dimorphism, the patterns of covariation in the crania of both *P. h. ursinus* and *H. s. sapiens* will partition into clear morphological modules that fit with current understandings of development

As with the analysis of the allometric pattern of integration, hierarchical clustering and network analyses were used to evaluate the pairwise pattern of covariance and connectivity between all polygons. The method follows the analysis of the *Rv* coefficient, polygon clustering and network analysis outlined under ontogenetic allometry above (section 3.5.1). It must be noted that these analyses of the patterning of covariation were conducted, for this section, on samples for which allometric effects and sexual dimorphism have been accounted for, to highlight more nuanced patterns (Klingenberg, 2014).

3.8 Aim 3: Exploring integration among *a priori* modules

The third aim is to analyse differences in the integration among *a priori* modules in the two species. More specifically it is proposed that:

H5) *P. h. ursinus* and *H. s. sapiens* will possess a general and shared pattern of morphological integration between *a priori* modules, with a few slight differences

Traditional methods of analysing craniofacial modularity and integration involve the *a priori* definition of modules, based on established developmental processes and functional complexes (Moss and Young, 1960; Moss, 1968; Moss & Salentijn, 1969). These methods have typically separated the skull into those parts of mesenchymal and neural crest origin, as well as their mode of ossification (endochondral or intramembranous). The resulting elements are generally referred to as the cranial vault (desmocranium or dermal neurocranium), the facial skeleton (splanchnocranium or viscerocranium), and the cranial base (condrocranium or basicranium).

The landmark configurations were standardised by removing those landmarks that were unique to each and averaging those landmarks representative of pterion. After accounting for allometry and sexual dimorphism (following the methods in section 3.6), the samples were pooled using group-mean subtraction to account for the average differences between the samples (Mitteroecker & Bookstein, 2008). Each landmark was then assigned to the cranial vault, facial skeleton, and the cranial base as presented in Table 3.1 The block describing the facial skeleton and that describing the cranial vault had four landmarks in common: glabella, mid-torus inferior, frontomalare temporal, zygotemporale superior, and zygotemporale inferior. Those describing

the cranial base and cranial vault also shared four landmarks, namely opisthion, porion, asterion and infratemporale. There were no landmarks shared by the facial skeleton and cranial base.

The various configurations underwent separate Procrustes superimposition to eliminate the correlating effect from the initial superimposition on the entire cranium (Lele & Richtsmeier, 2001). The use of geometric morphometric methods in analyses of morphological integration has introduced greater methodological considerations, particularly regarding whether Procrustes alignment is performed on the entire configuration (simultaneous fit) or on the separated blocks of data (separate fit) before running the 2B-PLS (Klingenberg, 2009; Kulemeyer *et al.,* 2009; Baab, 2013). Because the translation, scaling and rotation of configurations during Procrustes superimposition is calculated on all landmarks, a simultaneous fit will preserve information regarding the relative size and orientation between the two blocks of data (Lele & Richtsmeier, 2001). On the other hand, a separate fit will account for the effects of relative size and orientation so that only information regarding shape remains. Because the relative size and orientation between the two blocks of data can generate tremendous amounts of covariance and was not of primary interest in this study, a separate fit was utilised.

Escoufier's (1973) *Rv* coefficient was calculated for each comparison, and significance determined as per Klingenberg (2009). The paired comparisons that were significantly associated were further analysed using the two-block partial least squares (2B-PLS) method. 2B-PLS is used to describe the covariation between different sets of data (Rohlf *et al.*, 2000) and is commonly used to illustrate the covariation among sets of morphological data (e.g. Bookstein *et al*., 2003; Mitteroecker & Bookstein, 2007, 2008; Bastir *et al*., 2008). This method is similar in

concept to principal component analysis (PCA) in that it attempts to find vectors that describe the patterns of a covariance matrix. While PCA deals with a covariance matrix generated between a set of variables and itself, 2B-PLS deals with the covariance matrix generated between two different sets of variables (Mardia *et al*., 1979; Rohlf *et al*., 2000; Mitteroecker & Bookstein, 2007). It is ideal for exploring the association between two Procrustes-aligned landmark datasets by decomposing only that part of the covariance matrix associated with the between-block covariation (Rohlf *et al.*, 2000). The resulting vectors of a 2B-PLS, called partial warps, have more in common with those of principal component analysis in that they are ordered in decreasing magnitude, orthogonal to one another (independent), and can be used to reconstruct and depict the associated shape-changes.

If significant, the scores of the 2B-PLS for the first, second and third partial warps were plotted for each of the comparisons (i.e. between the cranial vault and the facial skeleton, the cranial base and the facial skeleton, and between the cranial base and the cranial vault). Differences between baboons and humans regarding the patterns of covariation were investigated by testing for differences between the major axis slopes drawn for each species using the scores from the 2B-PLS. The major axis slopes were tested using the *sma* function of the smatr package for R. If the slopes differed, the shape-change associated with that particular partial warp was illustrated using wireframes.

RESULTS

The work presented here sought to address different aspects of morphological integration and its modular arrangement in humans and baboons. Landmarks were collected on a number of crania belonging to a sample of baboons, *P. h ursinus*, and modern humans, *H. s. sapiens*. Repeatability was assessed and the effect of various Procrustes superimpositions on the resulting data evaluated. The various aims of the study were then addressed individually. The first aim was to assess the role of allometry across different cranial regions in both these species by highlighting regions of differential growth during ontogeny, assessing its effect on the patterning of integration, and quantifying the proportion of adult variation attributed to size. This was completed by firstly subjecting the data to a size-shape principal component analysis and illustrating the shape changes associated with allometry. Secondly the cranial polygons were clustered and analysed through network methods to assess the effect of allometry on the patterning of integration; and thirdly, the Eigenvalue data from the various principal component analyses were used to estimate the allometric component of variation in the baboon and human samples. The second aim, to explore patterns of morphological integration and modularity, required that the effects of allometry and sexual dimorphism were accounted for. The data were then analysed using clustering and network methods. The third and final aim sought to analyse the differences in morphological integration between *a priori* modules in the two species. This was achieved using a combination of Escoufier's (1973) *Rv* coefficient, the two-block partial least squares method, and major axis regressions.

4.1 Repeatability

Baboon sample

None of the partial Procrustes distances between repeated measurements were large enough to fall within the range of the pairwise partial Procrustes distances. Thus all well below the 5% limit set for this study (Figure 4.1 A). Accounting for allometry and sexual dimorphism reduced overall variability but did not increase the relative degree of measurement error to that observed between any of the specimens (Figure 4.1 B). In addition, plotting of the landmark errors did not highlight any individual landmarks for concern. For these reasons, measurement error in the baboon sample was considered within acceptable limits.

Human sample

Only 18 landmarks had to be estimated or 0.37% of the human dataset. During data collection, visual inspection of the measurement error across individual landmarks revealed that the lambda-pterion landmark possessed an excessive amount of variation (Figure 4.2). It was thus removed for the remainder of the data collection. The resulting error across individual landmarks of the entire human sample is illustrated in Figure 4.3. After accounting for the effect of allometry and sexual dimorphism, the overall degree of measurement error in the human sample mirrored what was observed in the baboon sample (Figure 4.4). All partial Procrustes distances between repeated measurements fell below even the smallest pairwise partial Procrustes distance. Measurement error in the human sample was thus considered acceptable.

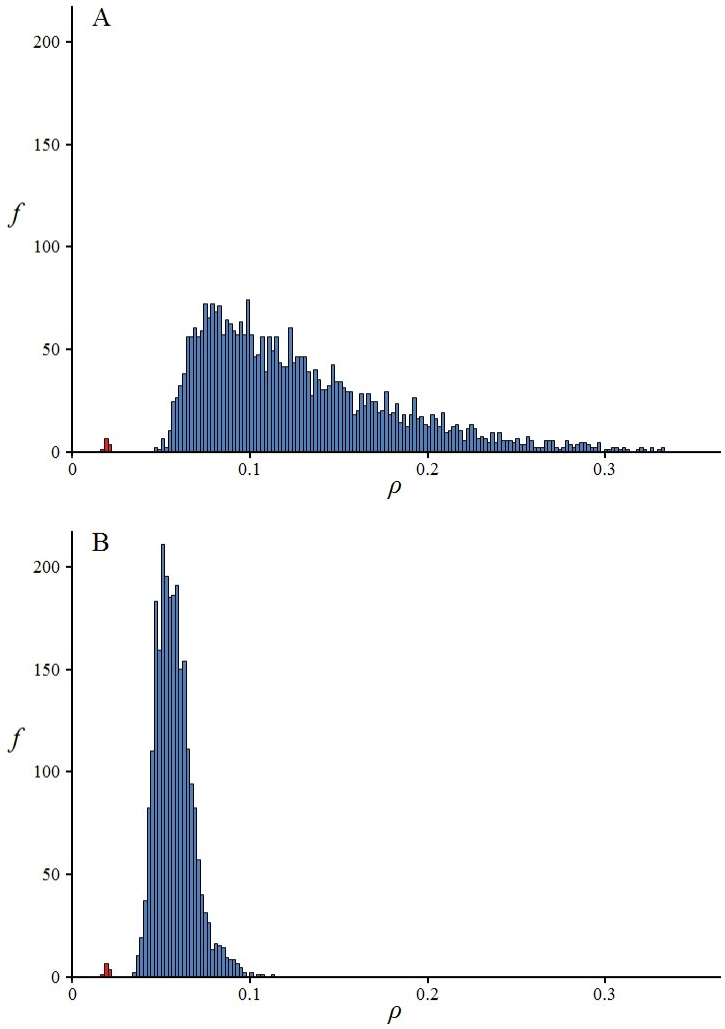


Figure 4.1. Repeatability in the baboon sample. The relative frequencies of Procrustes distances between repeated observations, representing measurement error (red bars), and that between all possible paired specimens, sample variation (blue bars). Specifically, **A** illustrates the measurement error as compared with all paired specimens before accounting for allometry and sexual dimorphism, and **B** after these factors have been 'removed'.

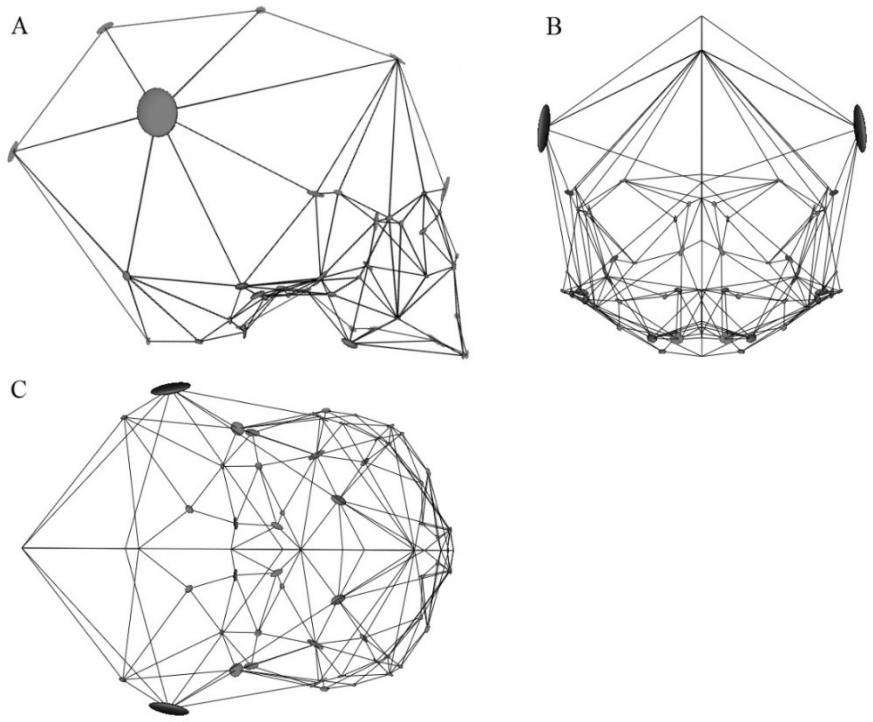


Figure 4.2. Visual representation of measurement error in the first 20 human crania. Ellipses represent the 95% confidence intervals for the superimposed landmarks. There is a high level of error for the lambda-pterion landmark before its removal. Note that this is the symmetrical representation of the data, and thus midline landmarks appear to possess no lateral error. **A**: lateral view; **B**: anterior view; **C**: superior view.

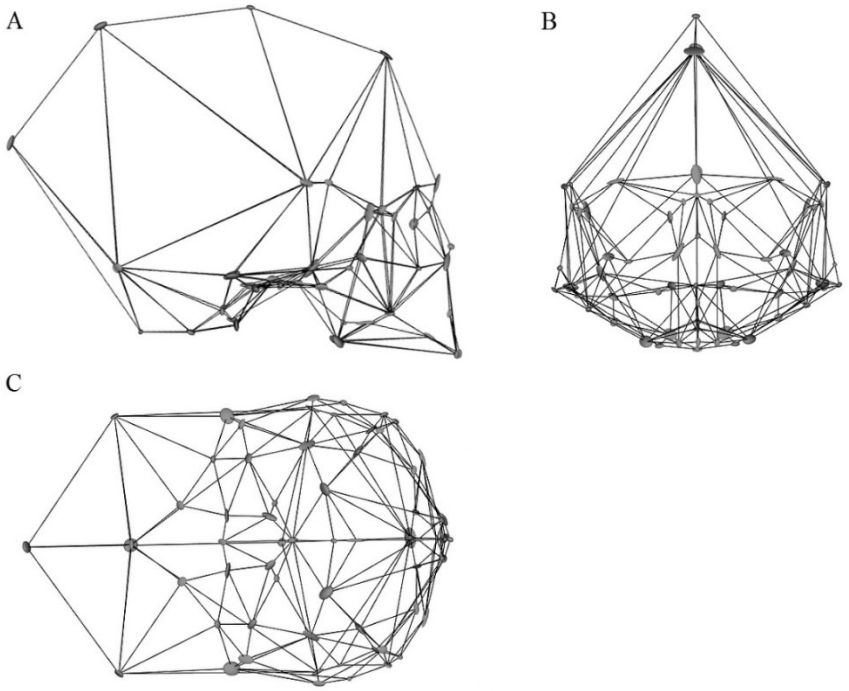


Figure 4.3. Visual representation of measurement error in the entire human sample after removal of the lambda-pterion landmark. **A**: lateral view; **B**: anterior view; **C**: superior view.

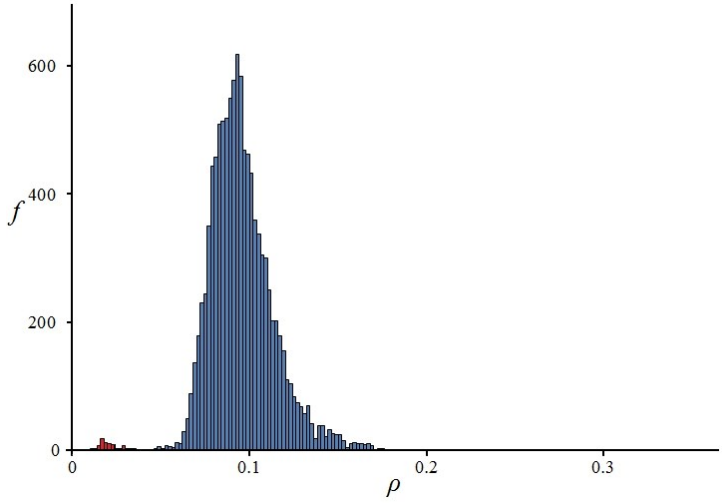


Figure 4.4. Repeatability in the human sample. The frequencies of partial Procrustes distances between repeated observations representing measurement error (red bars), and the pairwise partial Procrustes distances between all possible specimens (sample variation, blue bars), after the effects of allometry and sexual dimorphism have been accounted for.

4.2 Superimposition

Baboon sample

Both partial and full generalised Procrustes analyses were performed on configurations of the baboon crania, and each was subjected to orthogonal and stereographic projection to determine the better method for preserving the original geometry in tangent space. Figure 4.5 shows the scatter plots, regression slopes though the origin, and uncentred correlations between the respective Procrustes distances on the two curved spaces, and the Euclidean distances on the tangent space for the baboon sample. The projection from the two curved spaces to the tangent space is analogous to the projection of the earth's surface to a map in modern cartography. All projections result in unavoidable distortions, but the amount and type of distortion depends on the method of projection. Regarding geometric morphometrics, orthogonal projections project perpendicularly to the tangent plane from either Kendal's shape space or the Procrustes hemisphere. Stereographic projections, on the other hand, project from the 'south pole' of Kendal's shape space, and the 'centre' of the sphere formed by completing the Procrustes hemisphere. Although orthogonal projection to the tangent plane from the Procrustes hemisphere is generally the preferred method of superimposition (Slice, 2001), both the slope of the regression through the origin, and the uncentred Pearson's correlations coefficients suggest that the stereographic projection after partial Procrustes superimposition preserved the composition of the configurations better. A distortion can be observed in the scatterplots of the orthogonal projections from both the Procrustes hemisphere and shape space, particularly when the partial Procrustes distances exceeded 0.25 (Figure 4.5 A & C).

Human sample

The same method, of superimposing the sample to both partial and full generalised Procrustes analyses and subjecting the resulting data to orthogonal and stereographic projection, was performed on the human sample. Figure 4.6 shows the scatter plots, regression slopes though the origin, and uncentred correlations between the partial and full Procrustes distances and the Euclidean distance on the tangent space for the human sample. The slope of the regression through the origin suggests that the stereographic projection of the partial Procrustes superimposed configurations resulted in the least bias; however, the uncentred correlation coefficient of the stereographic projection of the partial Procrustes superimposed data was nearer to one in this sample, albeit only slightly. Given that the stereographic projection of both the partial and full Procrustes superimposed data results in the same tangent plane projection (point G in Figure 3.14), the difference of the initial Procrustes method is immaterial. As with the baboon sample, orthogonal projection appears to distort configurations from both the Procrustes hemisphere and shape space (Figure 4.6 A & C).

Mixed sample

The sample consisting of configurations representing both human and baboon crania were superimposed using partial and full generalised Procrustes analyses and projected orthogonally and stereographically to the tangent plane. Figure 4.7 illustrates the relationships and provides the relevant regression slopes though the origin, and uncentred correlations. Independent of whether the configurations underwent partial or full generalised Procrustes analyses, the orthogonal projection of the data produces noticeable deviations from equivalence with

increasing distance. The regression slope though the origin suggests that a stereographic projection from the Procrustes hemisphere results in the least distortion while the uncentred correlations favour the same projection from after full Procrustes superimposition. As both generate equivalent outcomes, the distinction is inconsequential.

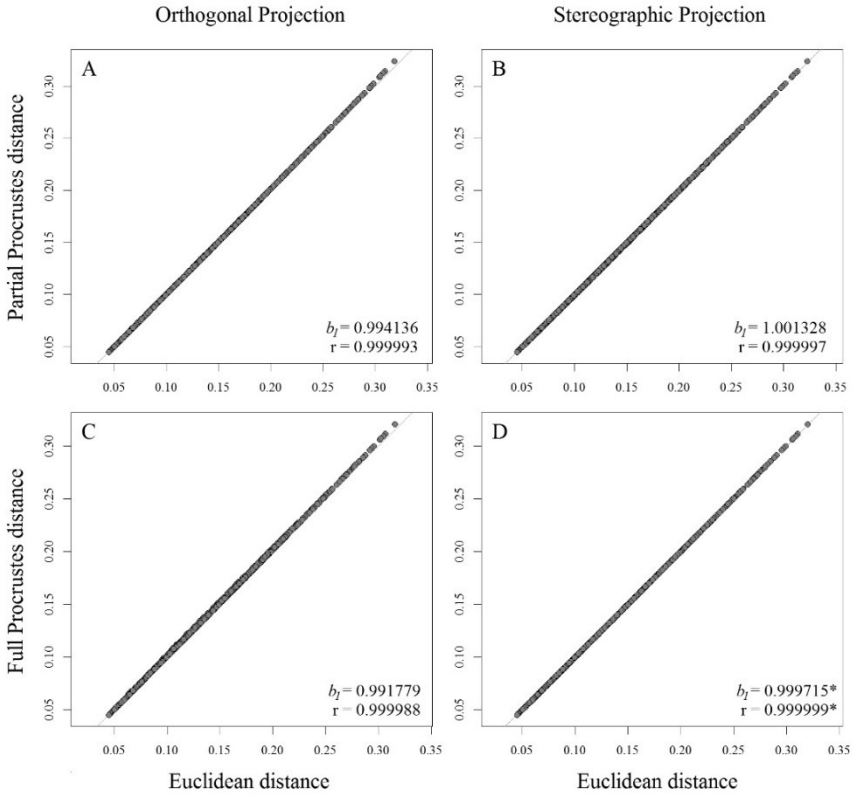


Figure 4.5. Scatterplots illustrating the distortion in configurations of the baboon crania brought about through various projections of Procrustes aligned data to the tangent space. The partial and full Procrustes distances between specimens is compared with the corresponding Euclidean distances in the tangent space. Isometrically spaced data will lie along the diagonal grey line. **A** and **B** depict the orthogonal and stereographic projections of configurations after partial Procrustes alignment respectively. **C** and **D** reflect the results obtained through orthogonal and stereographic projections of configurations after full Procrustes alignment, respectively. *b1* is the slope of the regression through the origin; r is the uncentered Pearson's correlation coefficient. Asterisks are used to highlight slopes and correlation coefficients closest to one.

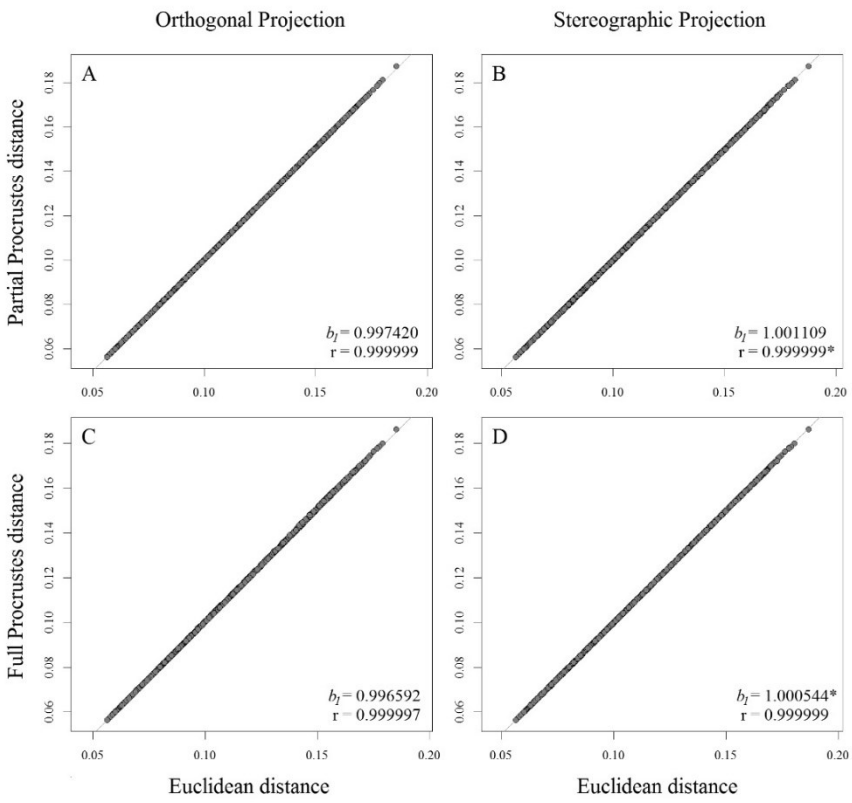


Figure 4.6. Scatterplots illustrating the distortion in configurations of the human crania brought about through various projections of Procrustes aligned data to the tangent space. **A** and **B** depict the orthogonal and stereographic projections of configurations after partial Procrustes alignment respectively. **C** and **D** reflect the results obtained through orthogonal and stereographic projections of configurations after full Procrustes alignment, respectively. *b1* is the slope of the regression through the origin; r is the uncentered Pearson's correlation coefficient. Asterisks are used to highlight slopes and correlation coefficients closest to one.

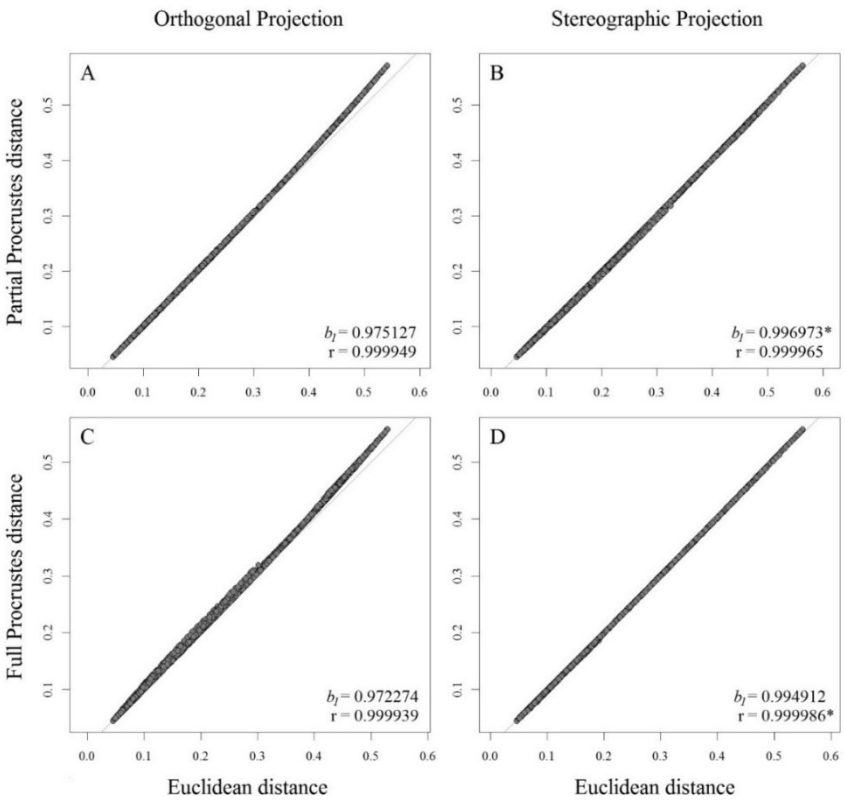


Figure 4.7. Scatterplots illustrating the distortion in configurations of the mixed sample produced by the projections of Procrustes aligned data to the tangent space. **A** and **B** depict the orthogonal and stereographic projections of configurations after partial Procrustes alignment respectively. **C** and **D** reflect the results obtained through orthogonal and stereographic projections of configurations after full Procrustes alignment, respectively. *b1* is the slope of the regression through the origin; r is the uncentered Pearson's correlation coefficient. Asterisks are used to highlight slopes and correlation coefficients closest to one.

Given these results, all samples underwent partial Procrustes superimposition and were stereographically projected to the tangent plane. This method was used whenever configurations of landmarks were to be superimposed.

4.3 General principal component analysis

Principal component analysis (PCA) is a classical multivariate technique that lends itself effectively to geometric morphometrics for the broad visualization of the variability of projected Procrustes configurations. PCA is an important tool for picking out potential outliers and assessing trends in morphometric data with high dimensionality. After superimposing the data each of the samples underwent a general PCA to examine the distribution of each of the datasets.

Baboon sample

The Eigenvalue of each principal component represents the proportion of variance explained by its specific vector or component. As would be expected in an ontogenetic sample the first principal component accounts for a large proportion, about 69%, of the total variance, with the second contributing 6%, the third 2%, and so on (Table 4.1). The main reason for the large disparity among the principal components is that the first is aligned with the greatest variation, which in this case involves the shape changes associated with ontogeny. The possibility that additional non-allometric variation might be included in the first principal component cannot be disregarded. It must be emphasized that principal components are mathematical manipulations of data independent of the underlying biology, and so the first principal component will align itself with the greatest variability without consideration of what that variability represents.

Table 4.1. Proportion of the total variance in the baboon sample accounted for by the first ten principal components. The total is the sum of all Eigenvalues

Principal component	Eigenvalue	Proportion of total variance	Cumulative proportion
PC1	0.005627	0.689	0.689
PC2	0.000518	0.063	0.752
PC3	0.000178	0.022	0.774
PC4	0.000165	0.020	0.794
PC5	0.000148	0.018	0.813
PC6	0.000141	0.017	0.830
PC7	0.000117	0.014	0.844
PC8	0.000105	0.013	0.857
PC9	0.000089	0.011	0.868
PC10	0.000076	0.009	0.877
Remaining PCs	0.001002	0.124	1
Total	0.008166		

Figure 4.8 presents the scores for the principal component analysis of the projected Procrustes residuals of the baboon configurations. The plot of principal components one (PC1) and two (PC2) clearly demonstrate that most of the variation ascribed to the first component is associated with ontogeny, with the juveniles on the one extreme and adult males on the other. The females and young males about midway between (Figure 4.8 A). This would be expected as developmental change usually constitutes the greatest amount of intraspecific variation. Of interest, subadult males have overlapping PC1 scores with subadult and adult female specimens. However, they lie at a lower position along the PC2 axis, suggesting that their development follows a somewhat different trajectory from the females. The male trajectory appears somewhat curved, with adult males possessing more positive PC2 scores than subadult males, almost comparable to what is observed in the subadult females.

The plot of PC2 and PC3 shows a tremendous amount of overlap in PC3 scores for all developmental groups apart from two juvenile and two subadult individuals (Figure 4.8 B). These cranial specimens were visually assessed for any previously unnoticed pathology but as none were found there is insufficient reason to consider their morphology anomalous and possible exclusion.

Figure 4.8 C illustrates the three-dimensional rotation of PC2 and PC3 about PC1 to tease out more information about sample variation that might not be visible when using conventional two-dimensional plots (Mitteroecker *et al*., 2004). The three-dimensional plots illustrate a somewhat divergent and curved ontogenetic trajectory for each of the sexes, but only highlight what was already evident in the two-dimensional plots (Figure 4.8 A & B).

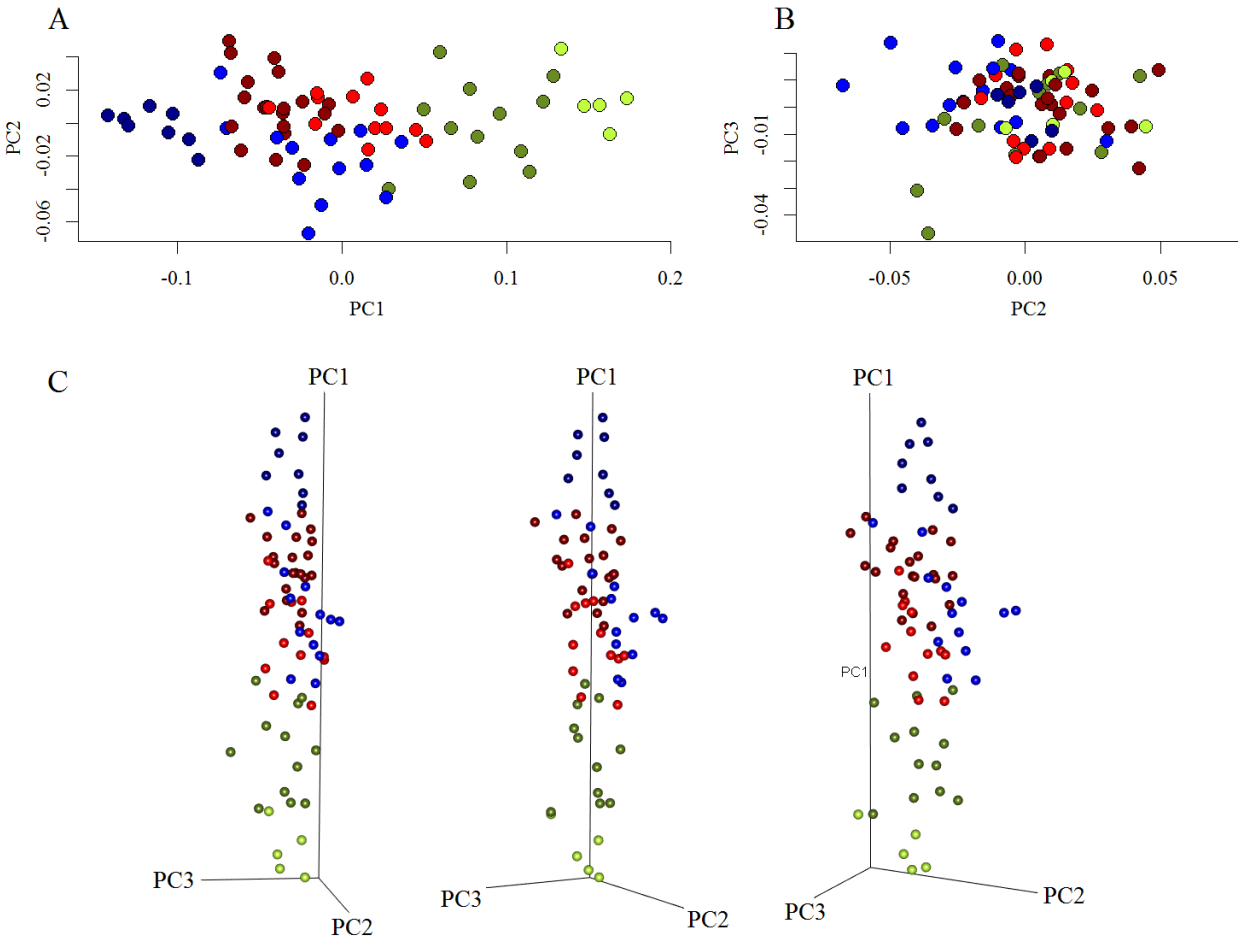


Figure 4.8. Plots of first three principal components scores of shape space of the baboon sample. **A:** Plot of principal components one and two. **B:** Plot of principal components two and three. **C:** Rotation of the first three principal components about the axis of the first principal component. ● *adult male*; ● *subadult male*; ● *adult female*; ● *subadult female*; ● *juvenile*; ● *infant*.

Human sample

The first principal component of the human data accounts for a substantially smaller proportion of the total variance (33%; Table 4.2) than observed in the baboon sample. Not only could this be indicative of relatively greater non-allometric variation or a smaller effect of size in humans,

but the underlying human sample, unlike the baboon sample, is primarily adult. Because variance is an average measure of dispersion, it is very sensitive to sample distribution. The second and third components contribute 9% and 6% to sample variance (Table 4.2).

Table 4.2. Proportion of the total variance in the human sample accounted for by the first ten principal components. The total is the sum of all Eigenvalues.

Principal component	Eigenvalue	Proportion of total variance	Cumulative proportion
PC1	0.001642	0.328	0.328
PC2	0.000470	0.094	0.422
PC3	0.000319	0.064	0.486
PC4	0.000240	0.048	0.534
PC5	0.000226	0.045	0.579
PC6	0.000180	0.036	0.615
PC7	0.000141	0.028	0.643
PC8	0.000135	0.027	0.670
PC9	0.000128	0.025	0.695
PC10	0.000100	0.020	0.715
Remaining PCs	0.001422	0.285	1
Total	0.005003		

The resulting scores of the first three PCs from the principal component analysis on the superimposed human configurations are presented two dimensionally and three dimensionally (Figure 4.9). Although PC1 is clearly associated with ontogeny, with the infant crania and adult crania on either end, the breadth and curvature of the scatter are immediately evident after having observed the preceding plots of the baboon data (Figure 4.8). The adult males and females are almost completely overlapping from every view, indicating that sexual dimorphism of the human cranium is not captured by the vectors presented here. The three-dimensional rotation of PC2 and PC3 about PC1 confirms the observations for the two-dimensional plots: the high level of dispersion, the curved ontogenetic trajectory and the overlap between the male and female adults

(Figure 4.9 C). An earlier plot of the PCA scores, not shown here, revealed a particular cranial specimen (A741) to be isolated from the other specimens. After visually assessing the cranium and the data, it was decided that the specimen was too asymmetrical to be considered normal and excluded from this and further analyses.

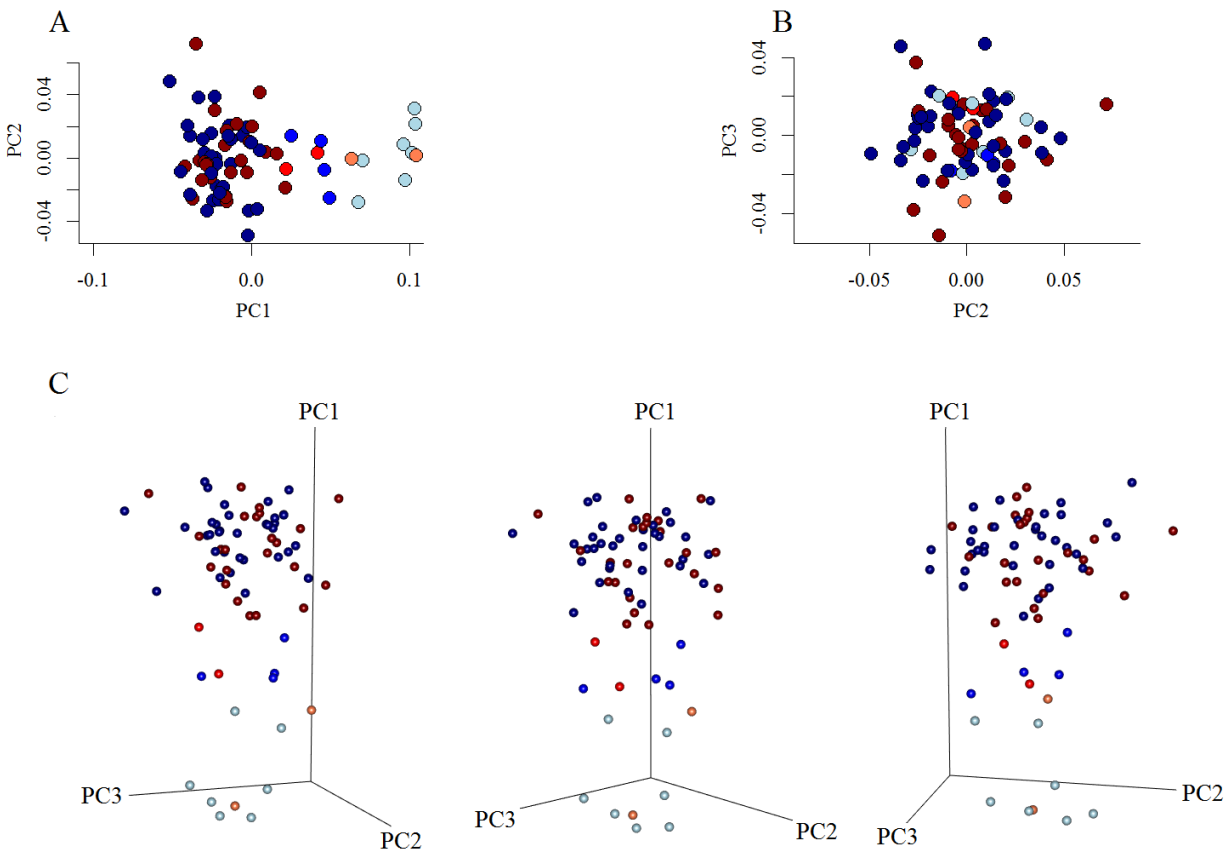


Figure 4.9. Plots of first three principal components scores of shape space of the human sample. **A:** Plot of principal components one and two. **B:** Plot of principal components two and three. **C:** Rotation of the first three principal components about the axis of the first principal component. ● *adult male*; ● *subadult male*; ● *juvenile male*; ○ *infant male*; ● *adult female*; ● *subadult female*; ● *juvenile female*; ○ *infant female*.

4.4 Aim 1: The role of allometry in morphological integration

The first aim of the study was to look at the role of allometry in integrating the cranium by firstly highlighting regions of differential growth during ontogeny using PCA of size-shape space, cluster analysis and network analysis. It also sought to quantify the proportion of the static adult variation attributable to size (section 4.4.3).

4.4.1 Pattern of postnatal ontogenetic allometry

The first part of the allometric analyses sought to highlight regions of the baboon and human cranium that are affected differently during postnatal growth and development. The PCA of size-shape space was used to emphasise regions based on relative size changes, and it is proposed that:

H1) The general pattern of postnatal ontogenetic allometry will be one of slower neural growth and faster facial growth, while the orbits, zygomatic region and cranial base possess an intermediate, possibly isometric growth

In accordance with Mitteroecker and colleagues (2004), an analysis of size-shape space was performed by supplementing the projected Procrustes residuals with the logarithm of centroid size and subjecting the resulting dataset to a principal component analysis. By including size with the Procrustes residuals when generating the covariance matrix on which the components are based, the first component should account for size and size-related (allometric) shape change only, with the remaining components relating to non-allometric variation. The analysis of the

associated shape changes along the first principal component can highlight regions influenced jointly by underlying postnatal growth factors.

Baboon sample

Figure 4.10 presents plots of the first three principal components of the size-shape space in both two-dimensions and three-dimensions. The plot of PC 1 and 2 displays almost the same pattern of variation observed in the equivalent plot of the general PCA (Figure 4.10 A); with PC1 aligning along the ontogenetic series and PC2 displaying some distinction between males and females, and a fair degree of overlap in PC3. The plot between PC2 and PC3 (Figure 4.10 A) shows males to possess more negative PC2 scores and females more positive PC2 scores suggesting that they each follow a somewhat different trajectory. The male morphology is thus not just an extension of a common growth trajectory. The three-dimensional plots of the shape-size space (Figure 4.10 C) illustrate and confirm what is observed in the two-dimensional plots. However, they show that the ontogenetic trajectory of each sex is here more linear and possibly divergent.

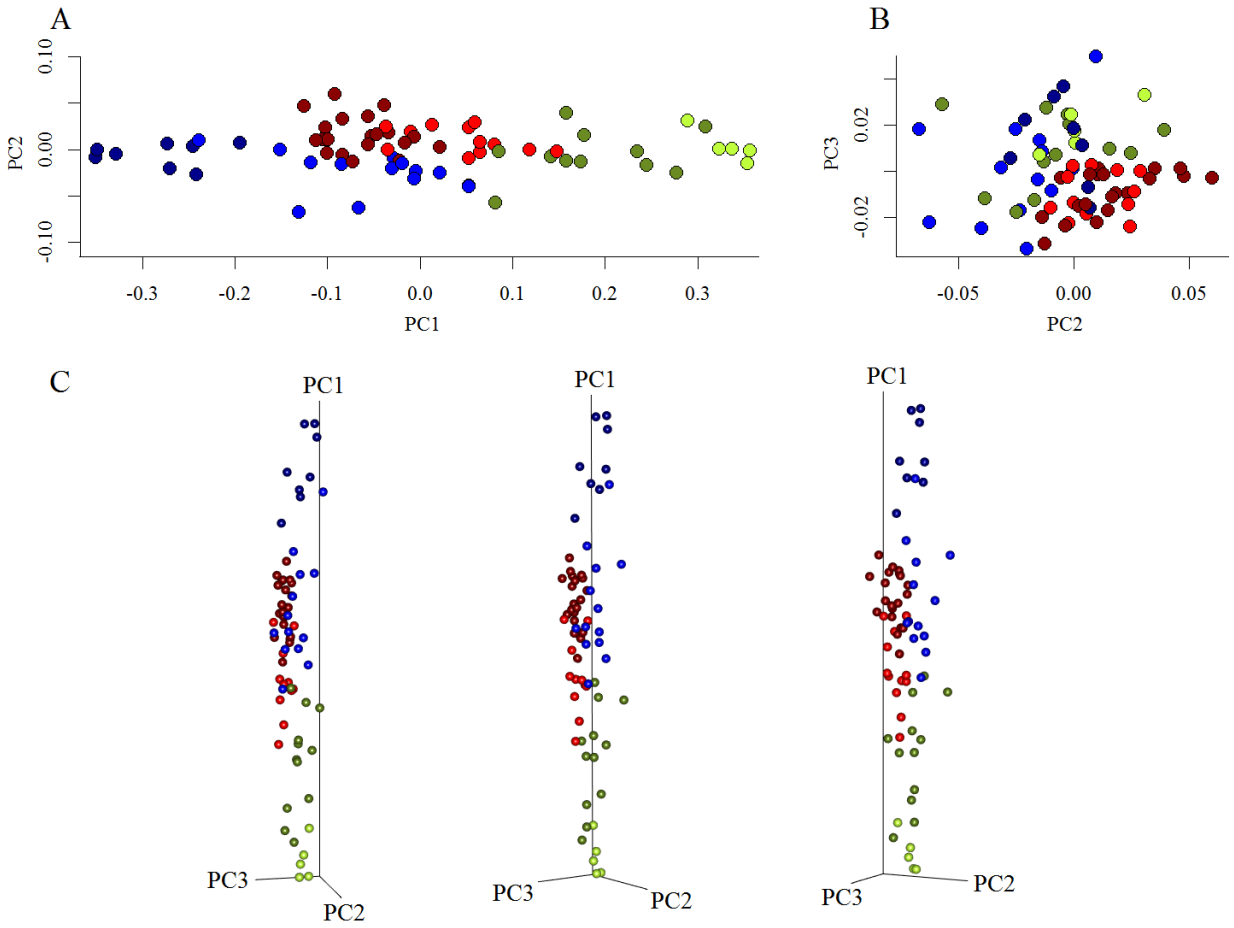


Figure 4.10. Plots of first three principal components scores of size-shape space for the baboon crania. **A:** Plot of principal components one and two. **B:** Plot of principal components two and three. **C:** Rotation of the first three principal components about the axis of the first principal component. ● *adult male*; ● *subadult male*; ● *adult female*; ● *subadult female*; ● *juvenile*; ● *infant*.

The illustrations of shape change associated with PC1 indicate firstly that much of the shape change involves the relative sizes of the neurocranium and muzzle (Figure 4.11). There is a reduction in the contribution of the neurocranium to overall shape in

the adult male, which is taken up by the lengthened muzzle. Interestingly it is not the entire muzzle but more specifically the maxillary component and the nasal bones that seem to contribute to a great deal of the facial growth. The neurocranial shape change is more notably expressed posterior to the foramen magnum, and superiorly over the parietal bones, and includes most of the frontal bone with exception of the orbital portions and supraorbital ridge. In contrast, most of the temporal bone – the mastoidal, petrosal, and even the squamous regions, including the zygomatic process – presents very little relative shape change. The exposed cranial base anterior to foramen magnum also undergoes very little shape change and growth of the palate primarily involves lengthening of its maxillary portion, with little shape change in the horizontal plate of the palatine bone as well as the palatine portion of the premaxilla.

Interestingly, a small region behind the orbit in the temporal fossa between the anterior point of pterion and "landmark x" displays a considerable increase in relative size with decreasing PC1 values (toward the adult male morphology). This region highlights a marked divergence between the two landmarks defining the anterior and posterior limits of the spheno-frontal suture, superior to the greater wing of the sphenoid. The lengthening of the chord between these landmarks possibly relates to an antero-posterior relative broadening of the temporal fossa in older individuals.

The importance of recognising the effect of Procrustes superimposition on interpreting the visual output must be stressed. Procrustes superimposition scales

configurations so that the decrease or increase of an area of the configuration is relative to the decrease or increase of the remaining configuration. For example, a relative decrease in the size of the cranial vault in the adult male baboon does not indicate an absolute reduction in size, but rather that all or some of the other cranial regions have disproportionately increased in size to contribute more to the overall size, leaving the cranial vault relatively smaller. Similarly, no relative shape change does not indicate a lack of absolute change, but rather that this change is isometric.

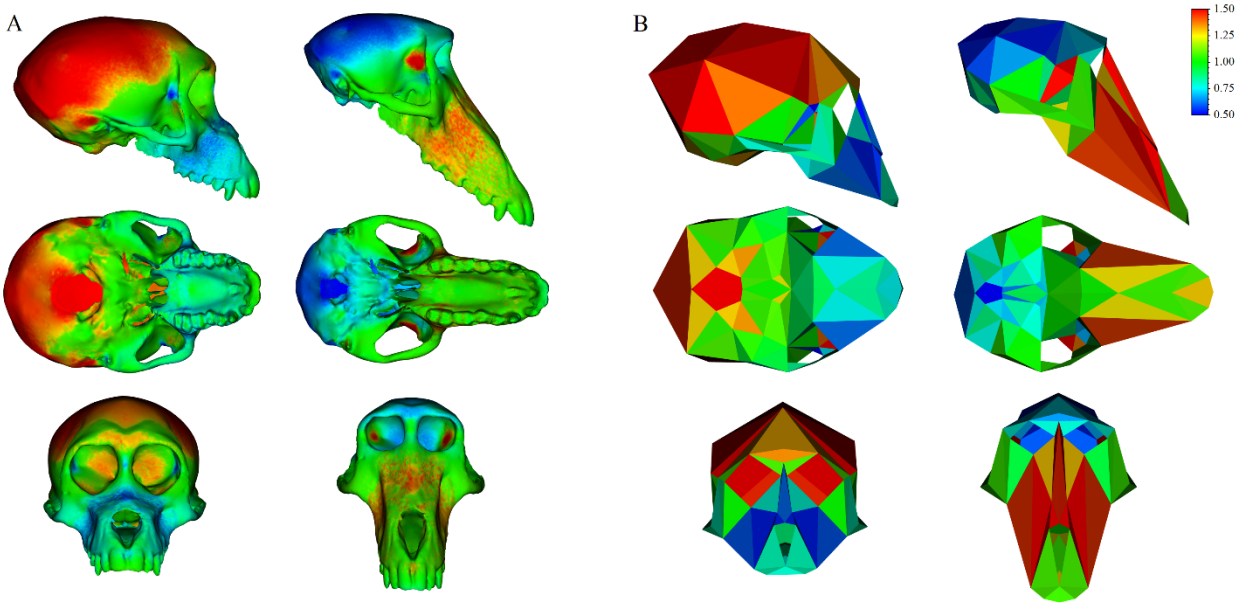


Figure 4.11. Allometric shape change of the baboon cranium as associated with the first Principal component in size-shape space. The images depict shape changes and the relative difference in polygon areas between the smallest and largest individual along the first principal component in size-shape space. Blue indicates a decrease in the polygon area relative to the mean shape, while red indicates an increase in polygon area. **A**: Warped surface scans with lateral, inferior and anterior views from top to bottom. **B**: Polygon models of the shape changes with lateral, inferior and anterior views from top to bottom.

Human sample

Figure 4.12 illustrates the scores of the first three principal components of the size-shape space in both two-dimensions and three-dimensions (Figure 4.12 A, B & C). The most noticeable difference from the regular PCA plots is the relative lengthening of PC1 and a separation of the adult male and female crania along this allometric trajectory (Figure 4.12 A). The ontogenetic series does, however, still possess the curvature noted in the prior analysis, and the male and female points in the plot of PC2 and PC3 are completely overlapping (Figure 4.12 B). The three-dimensional plots of the shape-size space (Figure 4.12 C) support the above observations.

Figure 4.13 demonstrates the shape changes associated with PC1 of size-shape space using warped surface scans and polygon illustrations. The most apparent change involves the relative size of the facial skeleton, with increased relative area along the lateral surface, the frontal process and the alveolar process of the maxilla and the entire bony hard palate. The zygomatic arch and temporal fossa also undergo a substantial relative increase in area. In contrast, the human cranial base, vault and the glabella region underwent a concomitant decrease in relative area with ontogeny. Very little relative change is experienced by the polygons representing the squamous and mastoidal portions of the temporal bone, the squamous part of the frontal bone, the body of the zygomatic bone, the subnasal portion of the maxilla, and the nasal bones.

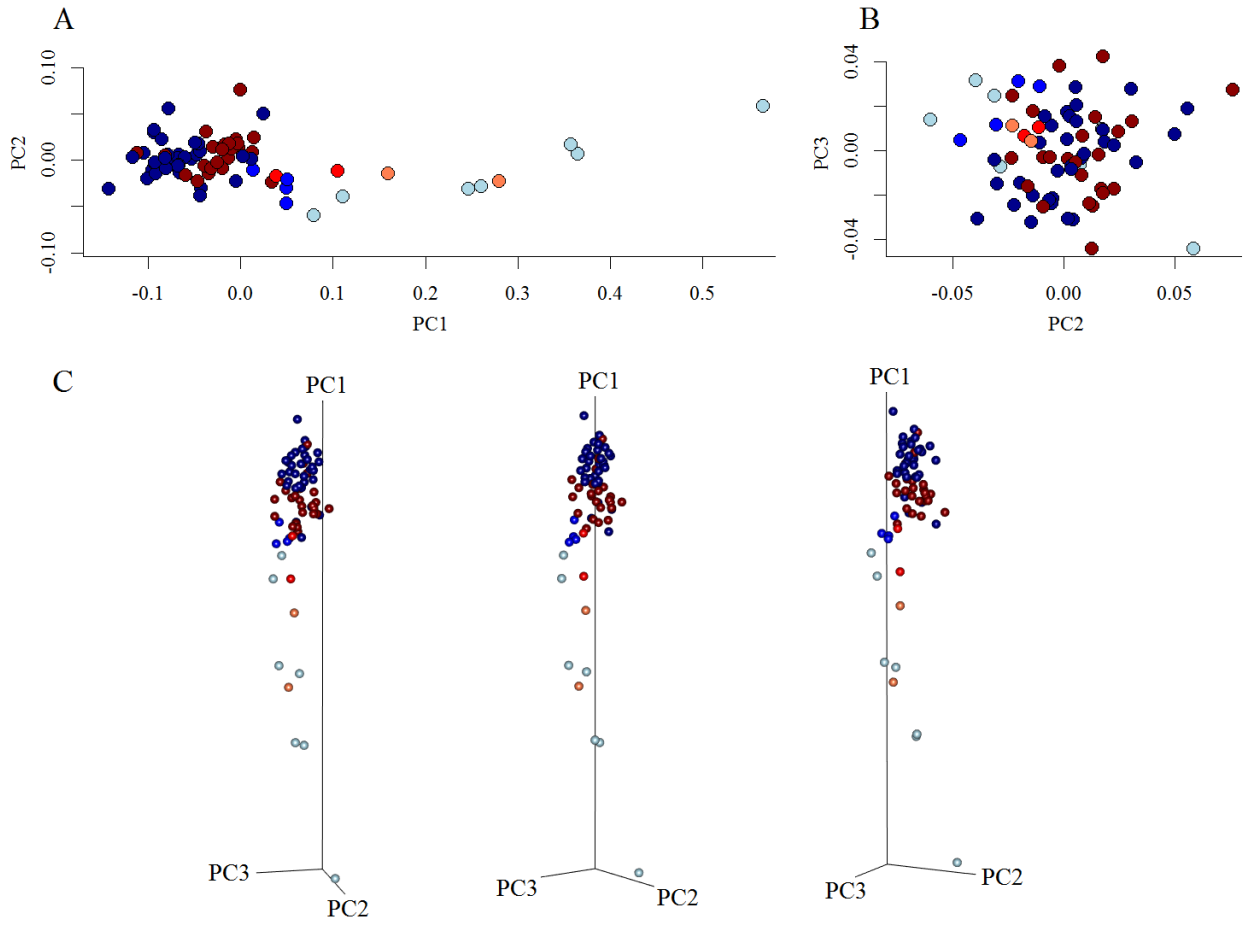


Figure 4.12. A: Plots of first three principal component scores of size-shape space for the human sample. **A:** Plot of principal components one and two. **B:** Plot of principal components two and three. **C:** Rotation of the first three principal components about the axis of the first principal component. ● *adult male*; ● *subadult male*; ● *juvenile male*; ○ *infant male*; ● *adult female*; ● *subadult female*; ● *juvenile female*; ○ *infant female*.

In many ways, the growth of the maxillary region and temporal fossa relative to the cranial vault parallels that observed in the baboon, but to a much lesser extent. Both experience little relative change around the body of the zygomatic bone, the subnasal

region of the maxilla, and the cranial base anterior to foramen magnum. The most distinguishing difference between the two samples appears to involve the zygomatic arch, which experiences little relative change in the baboons but a considerable relative increase in size in the human.

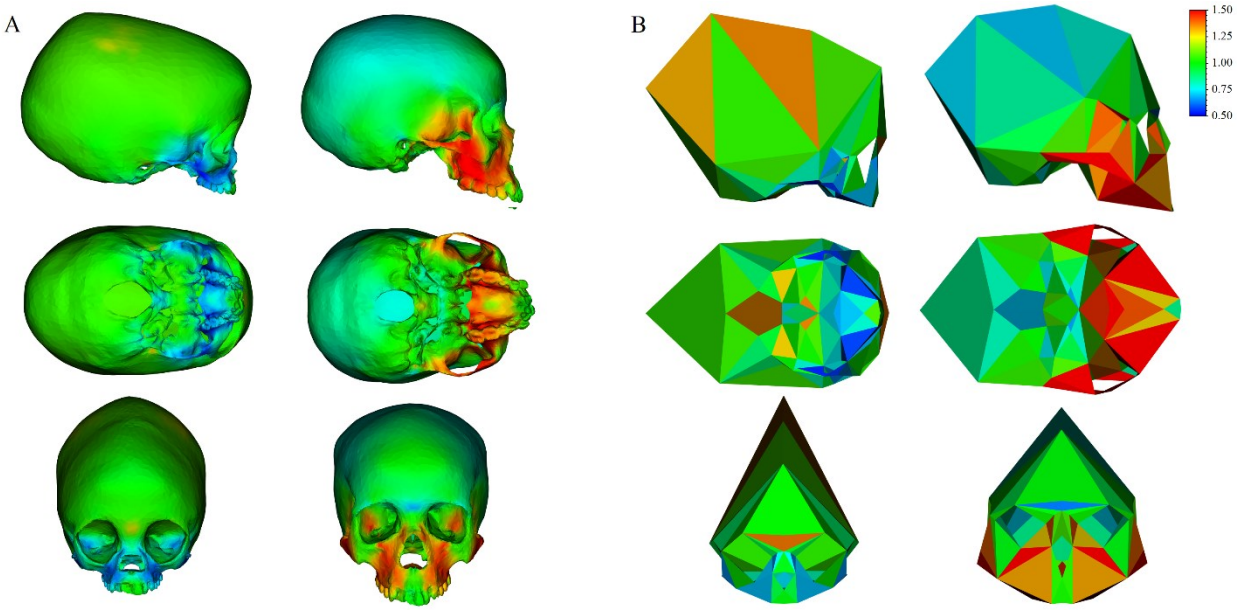


Figure 4.13. Allometric shape change of the human cranium as associated with the first principal component in size-shape space. The images depict shape changes and the relative difference in polygon areas between the smallest and largest individual along the first principal component in size-shape space. Blue indicates a decrease in the polygon area relative to the mean shape, while red indicates an increase in polygon area. **A**: Warped surface scans with lateral, inferior and anterior views from top to bottom. **B**: Polygon models of the shape changes with lateral, inferior and anterior views from top to bottom.

Mixed sample

To compare the ontogenetic trajectories of the two species, the landmarks defining configurations of the human and baboon crania had to correspond. Thus, the landmarks associated with the premaxillary-maxillary suture were removed from the baboon sample, those landmarks comprising pterion were replaced with their mean in both samples, and the landmark between lambda and pterion in the baboon sample was deleted. Group mean subtraction ensured that the plots of PCA scores illustrated the ontogenetic trajectories rather than absolute differences between the baboon and human samples. Figure 4.14 illustrates the scores of the first three principal components of the size-shape space in both two-dimensions and three-dimensions (Figure 4.14 A, B & C). It is clear in Figure 4.14 A that although ontogenetic allometry is accounted for by the first principal component, the trajectories are largely divergent across the second principal component. This observation is supported by the three-dimensional plots of the shape-size space (Figure 4.14 C)

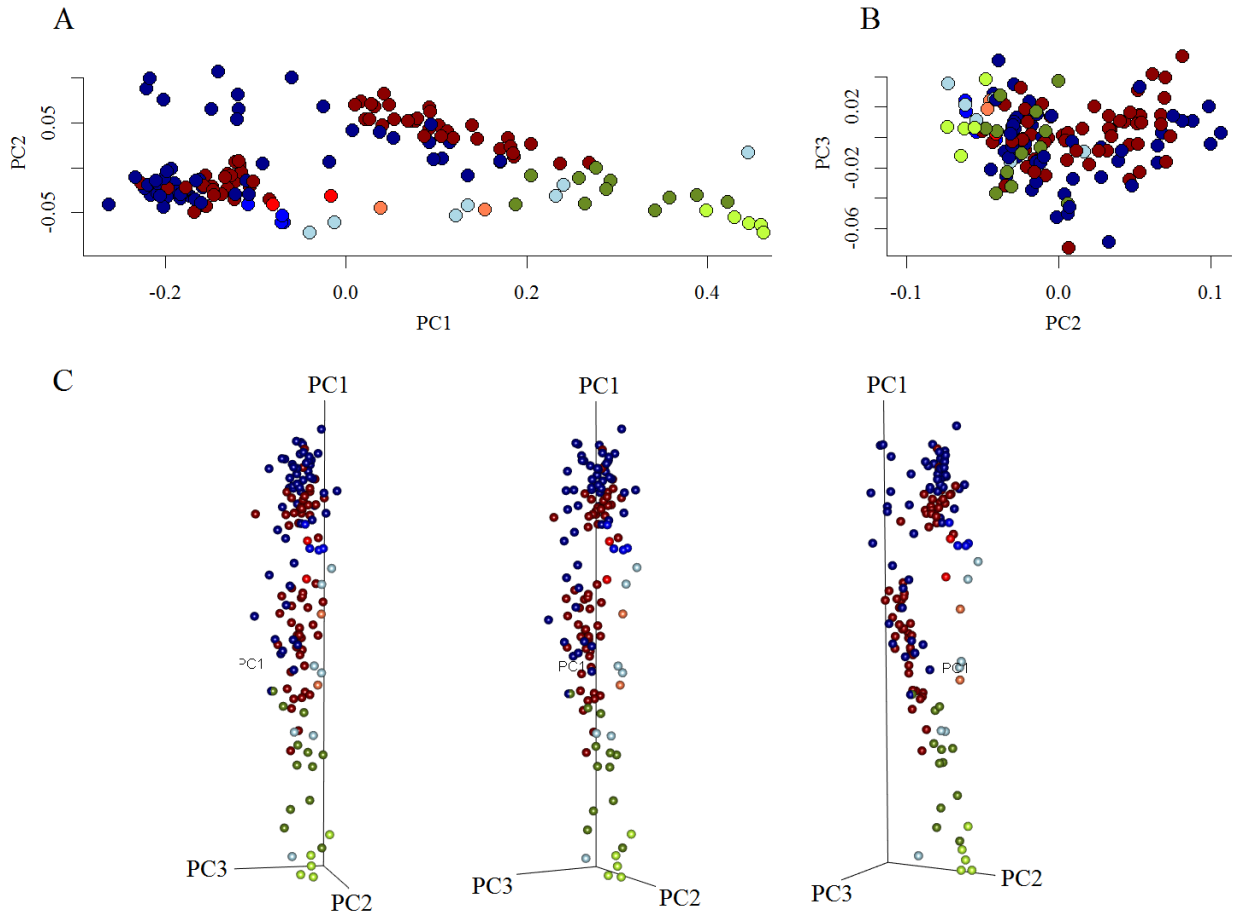


Figure 4.14. A: Plots of first three principal component scores of size-shape space for a pooled baboon and human sample. **A:** Plot of principal components one and two. **B:** Plot of principal components two and three. **C:** Rotation of the first three principal components about the axis of the first principal component. ● *adult male*; ● *subadult male*; ● *juvenile human male*; ○ *infant human male*; ● *adult female*; ● *subadult female*; ● *juvenile human female*; ○ *infant human female*; ● *juvenile baboon*; ● *infant baboon*.

4.4.2 The patterning of morphological integration in ontogenetic samples

This section aimed to assess the effect of ontogenetic allometry on the pattern of morphological integration using clustering and network methods. It is hypothesised that:

H2) Allometry will have a general concealing effect on the pattern of morphological integration, apart from those regions associated with neural versus somatic growth

Polygon clustering of ontogenetic samples

The strength of association between all polygons in the ontogenetic samples was evaluated using Escoufier's (1973) *Rv* coefficient and the statistical significance was tested using the permutation method of Klingenberg (2009) against a Bonferroni adjusted significance level. The *Rv* coefficient was converted to a measure of dissimilarity/distance by subtracting it from one, and used to cluster the polygons using UPGMA hierarchical clustering.

Baboon sample

To illustrate the distribution of the clusters across the baboon cranium, the optimum number of six clusters was selected according the elbow criterion (Figure 4.15) and colours were assigned to those polygons in each of the clusters (Figure 4.16). Hierarchical clustering of the polygons representing the baboon crania during

ontogeny resulted in the dendrogram presented in Figure 4.16. The cophenetic correlation coefficient of r = 0.8891 suggests that this dendrogram is a reliable representation of the underlying data. The larger clusters appear to separate the facial skeleton from the cranial vault although there is significant overlap. There are also smaller clusters of polygons: one involving only the zygomatic arch, the second including the glabella region, the frontal process of the maxilla and the orbit, the third includes only the root of the zygomatic arch, and the last involves some polygons over the temporal fossa. There is an isolated polygon positioned intermediately along the squamosal part of the occipital bone, and another between the petrous temporal and the greater wing of the sphenoid on the cranial base.

Because the strength of the cophenetic correlation coefficient indicates that the dendrogram in Figure 4.16 is representative of the underlying data, the substantial chaining between the nodes of the dendrogram suggests that there are no well-defined clusters in the data. Chaining is where each node of the dendrogram is linked to the next, gradually stepping up with each addition. When chaining is not an artefact of the sampling procedure or the clustering algorithm used, it may suggest that the nodes are associated along a continuous gradient. This might be the case given the ontogenetic status of this sample.

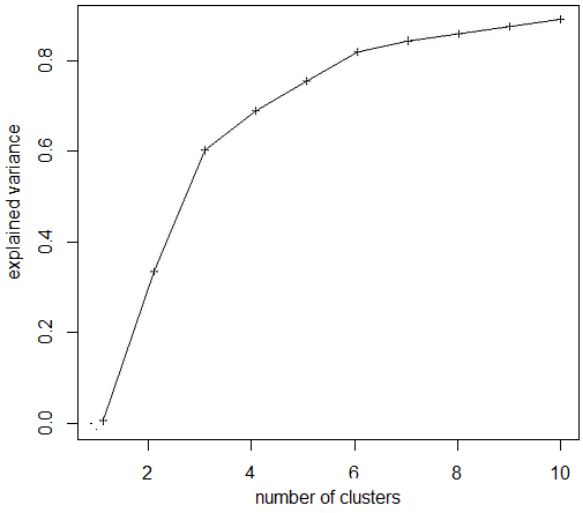


Figure 4.15. Plot between the number of polygon clusters and the proportion of variance explained, representing the baboon cranium during ontogeny. This allows for the elbow criterion to be applied in the selection of the optimal number of clusters.

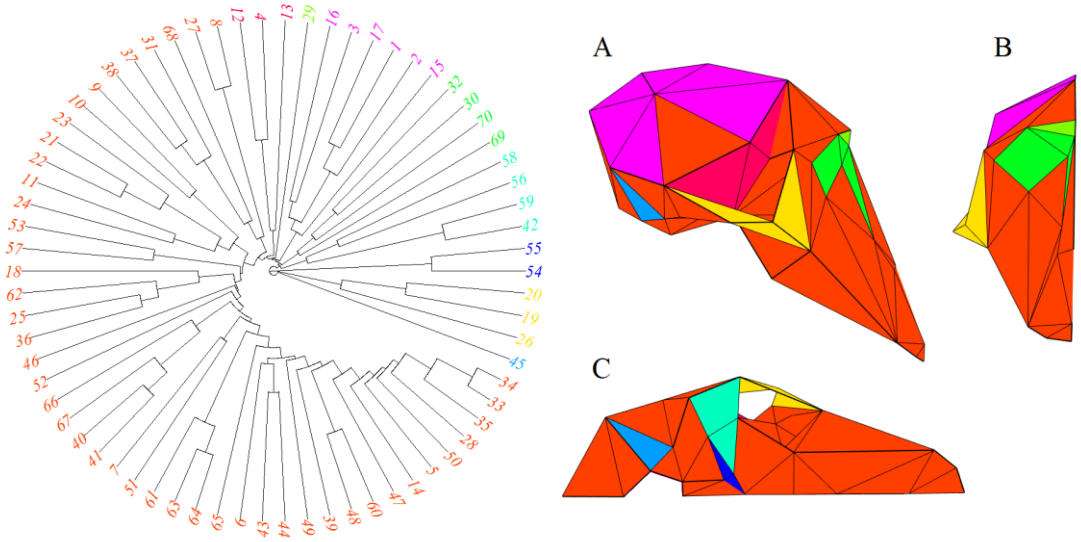


Figure 4.16. The resulting dendrogram and associated polygon clusters of the baboon cranium based on the strength of associations during ontogeny. Colours are assigned to clusters in the dendrogram and illustrated on the polygon representation on the right. **A**: lateral view; **B**: anterior view; **C**: inferior view.

Human sample

After hierarchical clustering of the polygons representing the human cranium, six clusters were selected as being optimal using the elbow criterion (Figure 4.17). The dendrogram presented in Figure 4.18 is considered a reliable representation of the underlying data given the high cophenetic correlation coefficient of r = 0.8105. The extensive chaining evident between the nodes of the dendrogram again suggest that the data possess very little natural clustering, but rather are linked though a continuous latent variable. Nonetheless, the distribution of most of the cranial polygons grouped as a single cluster spread across the entire cranium, except a single polygon on the basioccipital, a handful of polygons on the cranial base, a group over the posterior palate, another group just outside the supero-medial margin of the orbit, and a final polygon over the squamal portion of the frontal bone.

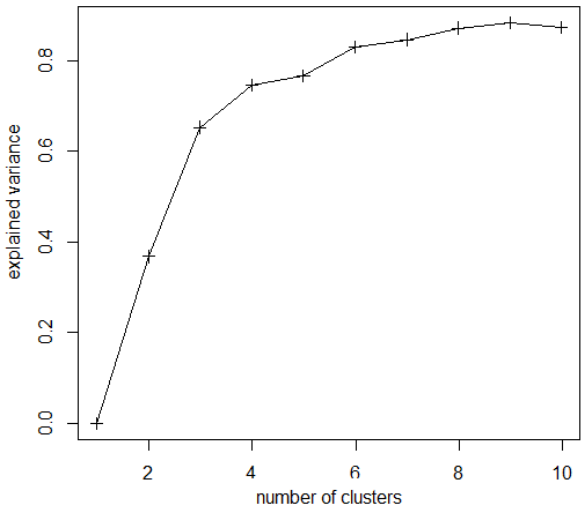


Figure 4.17. Plot between the number of polygon clusters and the proportion of variance explained, representing the human cranium during ontogeny. This allows for the elbow criterion to be applied in the selection of the optimal number of clusters.

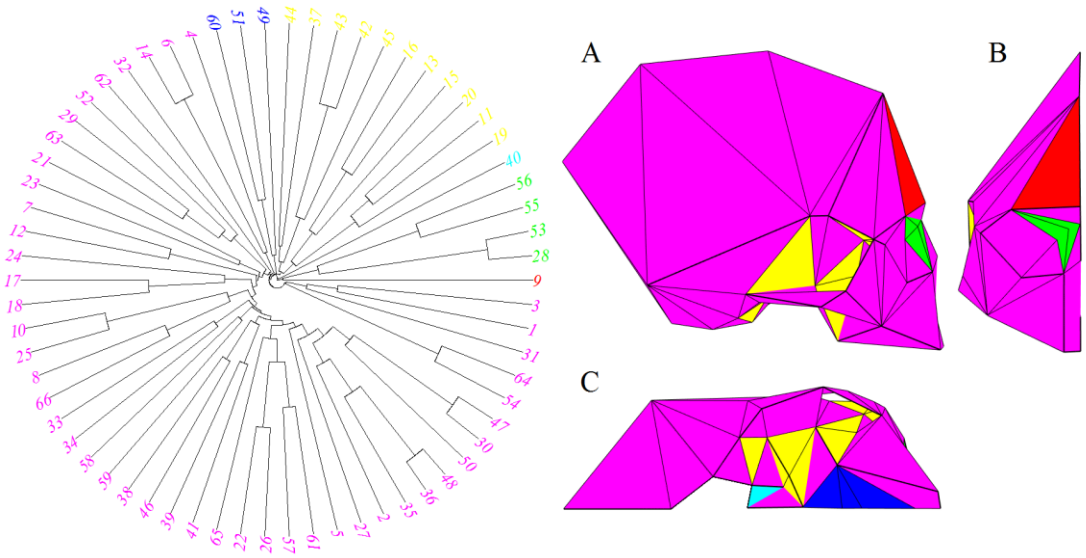


Figure 4.18. The resulting dendrogram and associated polygon clusters of the human cranium, representing ontogenetic associations. Colours are assigned to clusters in the dendrogram and illustrated on the polygon representation on the right. **A**: lateral view; **B**: anterior view; **C**: inferior view.

Network analysis of ontogenetic samples

The second method to assess the pattern of integration in the allometric samples utilised the methods of network analysis. The cranial polygons were modelled as a network by linking those that possess statistically significant covariation during ontogeny, after sequential Bonferroni correction (Holm, 1979). Modules were detected in this network by optimizing the modularity score (Newman & Girvan, 2004) using the greedy optimization algorithm (Csardi & Nepusz, 2006). The modules were assigned a colour and a diagram is provided to illustrate the distribution of the clusters among the polygons.

Baboon sample

Although the network analysis of polygons was partitioned into four groups, the modularity score of only Q = 0.1224 is very weak. Nevertheless, the network and associated polygon illustration of the baboon cranium is provided in Figure 4.19. The graph in Figure 4.19 illustrates a significant amount of overlap between the groupings. The first group includes the polygons associated with the cranial vault, excluding the temporal fossa, and a small region of the posterior cranial base lateral to the foramen magnum. The second grouping includes the squamous portion of the occipital bone, the root of the zygomatic arch and the petrous portion of the temporal bone, the frontal bone (excluding the temporal fossa), the corresponding frontal process of the zygomatic, the nasal bones, the lateral portions of the maxilla, the premaxilla, the nasal aperture, and the bony hard palate. The next grouping included

the zygomatic arch, the orbit, the medial supraorbital region including glabella, as well as the medal portion of the maxilla lateral to the nasal bones and premaxilla. The final cluster grouped the elements of the temporal fossa with the body of the zygomatic, the alveolar process of the maxilla and some elements of the cranial base, including the basi-occipital and petrous portion of the temporal bone.

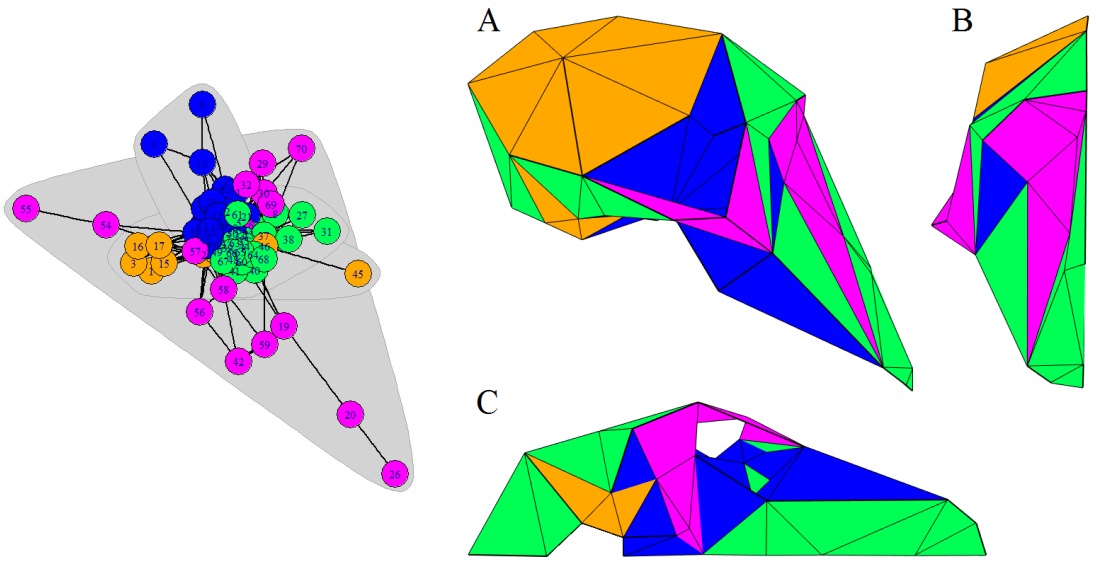


Figure 4.19. The network and associated polygon clusters of the baboon cranium based on the presence and absence of associations during ontogeny. Colours are assigned to the network modules identified in the graph and illustrated on the polygon representation on the right. **A**: lateral view; **B**: anterior view; **C**: inferior view.

Human sample

Clustering of the human ontogenetic data resulted in seven broadly overlapping modules with a weak modularity score of Q = 0.2520 (Figure 4.20). Most of the neurocranium was grouped with polygons from the maxilla, while most of the frontal

bone and temporal fossa clustered together. The nasal aperture, nasal bones, inferior orbit and adjacent bone, as well as the zygomatic bone and arch to the root on the temporal bone all grouped as the third cluster. The posterior palate clusters as a network module, as did the polygons just outside the supero-medial margin of the orbit. The polygons between the petrous temporal and spheno-occipital synchondrosis formed a sixth cluster, while two polygons over the cranial vault formed the last.

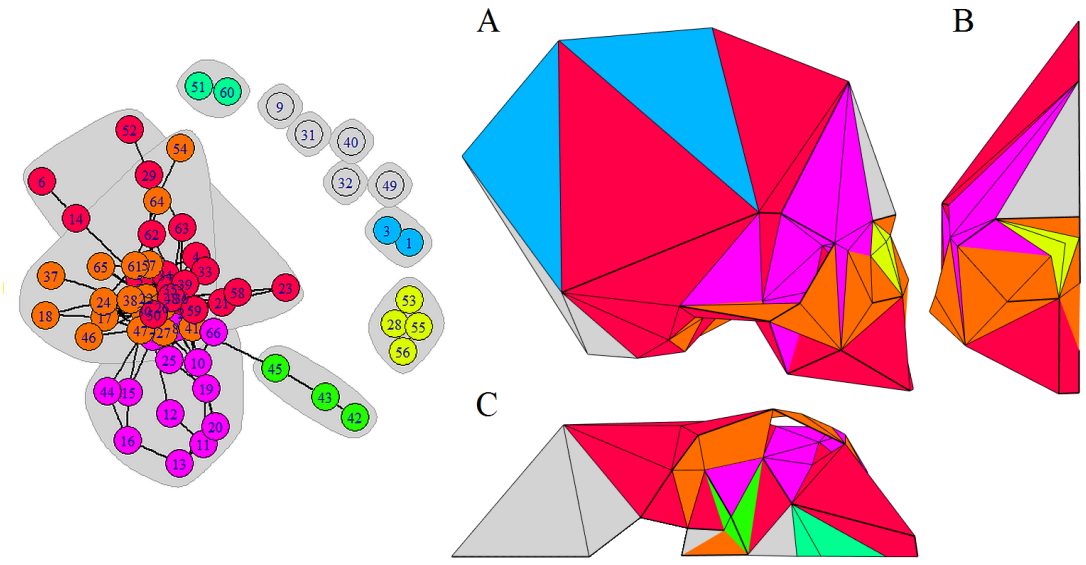


Figure 4.20. The network and associated polygon clusters of the human cranium based on the presence and absence of associations during ontogeny. Colours are assigned to the network modules identified in the graph and illustrated on the polygon representation on the right. Grey polygons are isolated. **A**: lateral view; **B**: anterior view; **C**: inferior view.

4.4.3 Allometric proportion of variation

Allometry is thought to be responsible for generating a high level of integration in the cranium. Across the Primate order, the human cranium has been shown to have relatively low levels of integration, and the baboon the highest. Allometry is thought to be partly responsible for this distinction (Marroig *et al*., 2009; Porto *et al*., 2009). Thus, proportions of variation due to allometric and non-allometric factors among the adult representatives of the samples were calculated using a combination of the Eigenvalues derived from both a PCA on size-shape space and a conventional principal component analysis. The specific hypothesis proposes that:

H3) The proportion of variation attributed to size will be larger in *P. h. ursinus* than *H. s. sapiens*

Baboon sample

Presenting a table demonstrating the proportion of variance accounted for by the first ten principal components of size-shape space would be meaningless because the Eigenvalue and proportion of variance accounted for by the first PC of size-shape space is irrelevant as it has been artificially inflated by the addition of size. The summed Eigenvalues resulting from the principal component analysis of size-shape space is 0.0311, a value nearly four-fold that of the preceding general PCA on the baboon data (Table 4.1). Thus, the Eigenvalue of the first PC of size-shape space is biologically irrelevant, but the remaining eigenvalues should not be affected by the addition of size and account for only the non-allometric component of the total

variance. If we assume that the preceding general PCA on shape space provided a good estimate of total sample variation, and all but the first Eigenvalues of the PCA of size-shape space estimates the non-allometric component of the variation, the proportion of the variation attributed to allometry can be estimated by calculating their difference. Thus, if the sum of the non-allometric Eigenvalues in the size-shape space is 0.0029 and we consider that the variance attributed to shape alone is 0.0082 (as estimated by the earlier general principal component analysis on shape space), the non-allometric variation would constitute approximately 35% of the sample variation, leaving 65% to size-related shape variation (lower than the 69% accounted for by the PC1 of the PCA; Table 4.1). This is quite a significant proportion of the variation and explains why the first component of a general PCA aligns somewhat with allometric variation in an ontogenetic sample. However, the contribution of static allometry to adult variation is of interest here. These same measures, derived from the Eigenvalues from a regular principal component analyses of shape-space using only the adult baboon sub-sample, and one performed on size-shape space of the same sub-sample, indicate that the total variance of the e adult baboon sub-sample is 0.0039, with the non-allometric component contributing 0.0023, or 58% of the total variance. This leaves size responsible for 42% of the shape variation among adult baboons.

Human sample

The total variance from the general PCA of the shape-space of the human data was 0.0050 and the non-allometric Eigenvalues in the size-shape space summed to

0.0037, or approximately 75% of the total variance, leaving only 25% to size-related shape variation. While this value appears small, it is likely due to the large proportion of adult crania in the human dataset. Note again that this value is smaller than the that accounted for by the first principal component in the general PCA of the shape-space (33%), supporting the idea that the first component of a general PCA aligns with a combination of the allometric and non-allometric variation in an ontogenetic sample.

The general PCA and the size-shape PCA were run on the adult subsample of the human data to determine the contribution of static allometry to adult variation. The total variance of the PCA in shape space was 0.0038, and the summed Eigenvalues of the non-allometric portion of the size-shape PCA came to 0.0036. Their difference suggests that size is responsible for only 3% of the shape variation among adult humans, significantly lower than the 42% among adult baboons.

4.5 Accounting for allometry and sexual dimorphism

Both size-related variation and sexual dimorphism inflate craniofacial integration and the removal of the effects of both is necessary to assess the more intrinsic patterns of covariation. However, the results of the general PCA analyses and the PCA on size-shape space suggest that the males and females may perhaps possess divergent allometric trajectories, and that the removal of the common allometric vector would not account for all aspects of sexual morphological dimorphism. For this reason,

second-order polynomial equations were calculated for males and females separately, and were used to account for the effects of allometry and sexual dimorphism in each of the samples.

4.6 Aim 2: Patterning of covariation

The second aim was exploratory in nature, but armed with an extensive background in the potential underlying factors responsible for morphological integration and modularity, I sought to assess the patterning of morphological integration into morphological modules once allometry and sexual dimorphism had been accounted for. The first method hierarchically clustered polygons using a dissimilarity matrix derived from the *Rv* coefficient, while the second created a network of polygons based solely on the presence or absence of association and explored the structure of this network to find network modules. Both these analyses were run after accounting for the effect of size and sexual dimorphism in the samples. It is hypothesised that:

H4) After accounting for allometry and sexual dimorphism, the patterns of covariation in the crania of both *P. h. ursinus* and *H. s. sapiens* will partition into clear morphological modules that fit with current understandings of development

4.6.1 Polygon clustering

The polygons were clustered hierarchically using the UPGMA method on a dissimilarity matrix created by subtracting the respective *Rv* coefficients from one. In

contrast to the analysis of ontogenetic data, the effects of both allometry and sex were accounted for before clustering of the polygons.

Baboon sample

To illustrate the distribution of the clusters across the baboon cranium, an optimum number of eight clusters was selected according the elbow criterion (Figure 4.21). Colours were assigned to each of the eight clusters in the dendrogram as well as their constituent polygons in Figure 4.22. The high cophenetic correlation coefficient (r = 0.8891) implies that this pattern of clustering is a reliable representation of the data and the high separation of the nodes indicates that the data are naturally clustered. The eight clusters included: 1) the cranial vault between the coronal suture and the posterior margin of foramen magnum, excluding the temporal fossa; 2) the squamous temporal and greater wing of the sphenoid in the temporal fossa; 3) the zygomatic arch and the tympanic and articular portions of the temporal bone; 4) the petrous portion of the temporal bone and the polygons of the occipital bone anterior and lateral to the foramen magnum; 5) the frontal and nasal bones, the portion of the maxilla immediately adjacent to the nasal bones, as well as the upper orbit and nasal aperture; 6) the alveolar process of the maxilla, the posterior palate, and the infratemporal fossa; 7) most of the body of the zygomatic bone and adjacent part of the maxilla, together with the lower portion of the orbit; and most interestingly, 8) the premaxilla and the adjacent bony palate clustered with a few polygons from the

anterior basioccipital to where the vomer attaches to the sphenoid body and laterally, between the petrous temporal and the greater wing of the sphenoid.

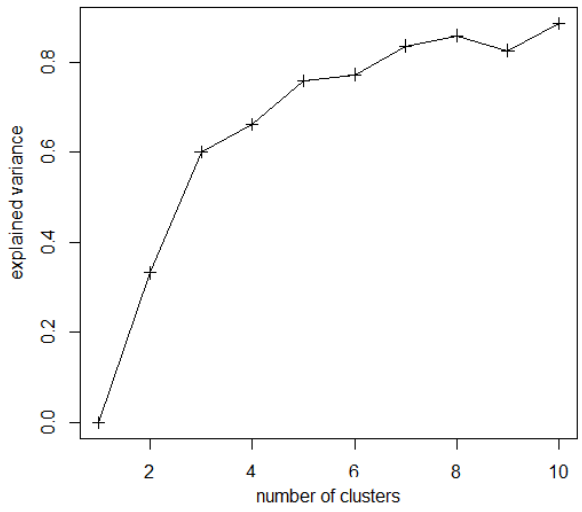


Figure 4.21. Plot between the number of polygon clusters and the proportion of explained variance in the baboon cranium. This allows for the elbow criterion to be applied for the selection of the optimal number of clusters.

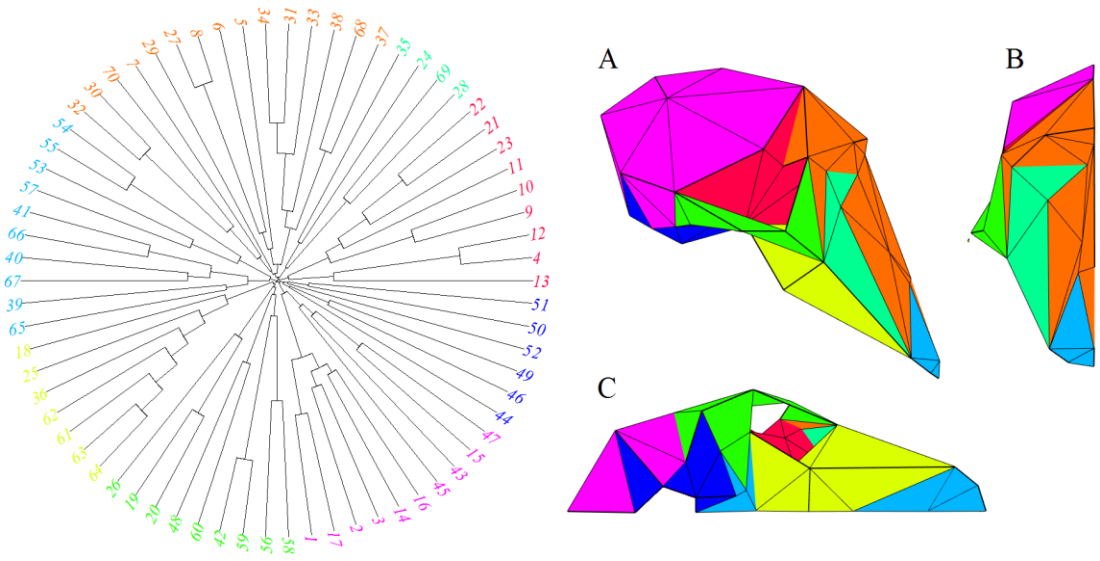


Figure 4.22. The resulting dendrogram based on covariation between polygons and the distribution of clusters on the baboon cranium. Colours are assigned to clusters in the dendrogram and illustrated on the polygon representation on the right. **A**: lateral view; **B**: anterior view; **C**: inferior view.

Human sample

The elbow criterion was again used to select five groupings to illustrate the clustering of polygons across the human cranium (Figure 4.23). The clustering of the dendrogram and the distribution of these polygons on the human cranium are illustrated in Figure 4.24. This pattern of clustering can be considered a reliable representation of the grouping of the data as the cophenetic correlation coefficient is high (r = 0.8763), and the long branch lengths between nodes suggests that the underlying dataset possesses natural groupings.

The five clusters included: 1) most of the cranial vault except the anterior half of the frontal bone, the anterior portion of the squamous temporal, but even includes the mastoidal portion of the temporal bone; 2) the visible portion of the cranial base anterior and lateral to foramen magnum is clustered with the posterior maxilla, the anterior portion of the squamous temporal, the zygomatic arch, the body of the zygomatic bone, the nasal bones, the portion of the squamous frontal between the last cluster, the inferior orbit and the nasal aperture; 3) the lateral portion of the frontal bone and the adjacent greater wing of the sphenoid, the structures making up the superior orbital margin, including the frontal process of the zygomatic bone and the zygomatic process of the frontal bone, the glabella region and the medial margin of the orbit down along the frontal process of the maxilla; 4) the external surface of the maxilla, except for the zygomatic and alveolar processes, but including polygons defining the anterior and lateral palate; and 5) the posterior palate.

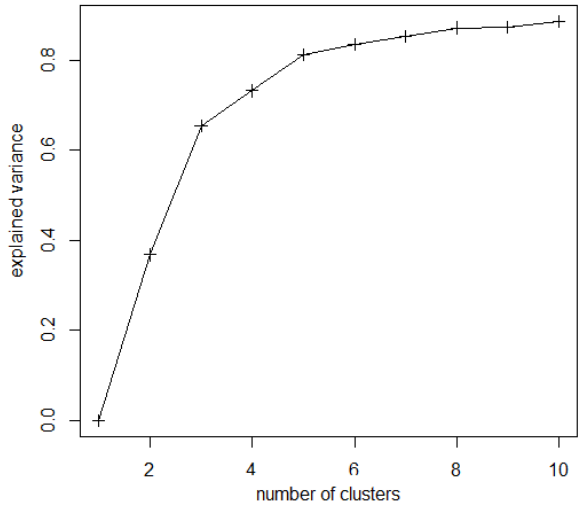


Figure 4.23. Plot between the number of polygon clusters and the proportion of explained variance in the human cranium for the selection of the optimal number of clusters.

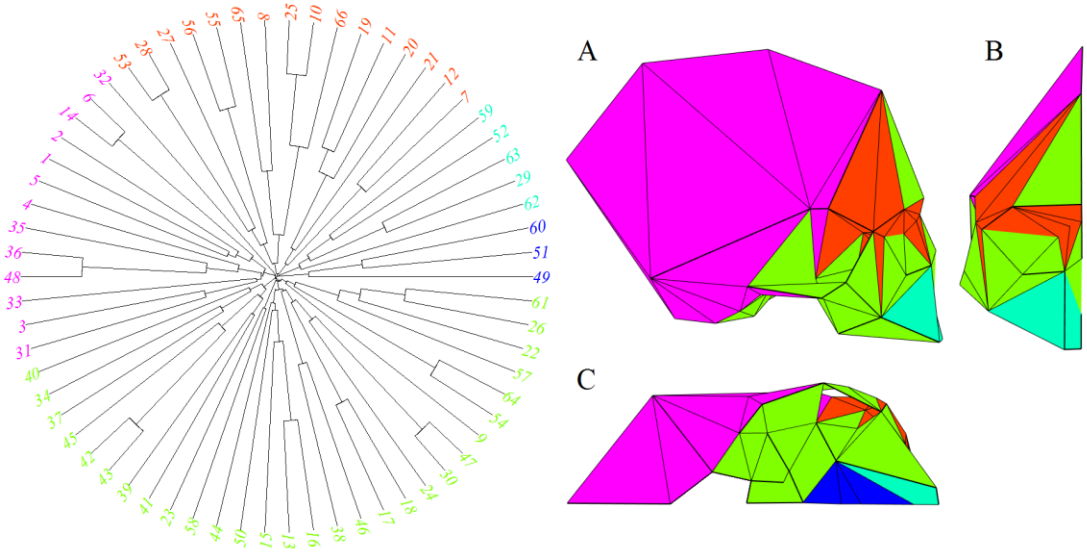


Figure 4.24. A dendrogram based on the strength of covariation between polygons and the distribution of the resulting clusters on the human cranium. Colours are assigned to clusters in the dendrogram and illustrated on the polygon representation on the right. **A**: lateral view; **B**: anterior view; **C**: inferior view.

4.6.2 Network analysis

Baboon sample

In contrast to the network analysis of the baboon sample before accounting for allometry, the modularity score of Q = 0.836 suggests definite groupings of the underlying data. The greedy optimization algorithm could identify 12 groupings of two or more polygons, with seven polygons left unassigned. Colours were allocated to the groupings and used to illustrate their distribution on the baboon cranium (Figure 4.25).

The groupings were 1) the cranial vault between the coronal suture and the posterior margin of foramen magnum, excluding the temporal fossa; 2) the squamous temporal and the superior portion of the greater wing of the sphenoid in the temporal fossa, a part of the frontal bone adjacent to the sphenoid, and the lateral rim of the orbit; 3) the zygomatic arch; 4) the mastoidal and tympanic portions of the temporal bone; 5) the occipital condyle and most of the petrous temporal; 6) the root of the zygomatic arch and the basal portion of the greater wings of the sphenoid; 7) the medial aspect of the frontal bone, superior orbit and its supero-medial margin, and the superior portion of the nasal bones; 8) the inferior portion of the nasal bones, the medial portion of the maxilla immediately adjacent to the nasal bones – from the frontal process to the canines, and the nasal aperture; 9) the lateral portion of the maxilla, the body of the zygomatic bone and the inferior orbit; 10) the premaxilla, inferior to the nasal aperture and the anterior portion of the palatal process of the maxilla; 11) the

alveolar process of the maxilla and the posterior half of the bony hard palate; 11) a small cluster from the anterior basioccipital to where the vomer attaches to the sphenoid body and laterally, between the petrous temporal and the greater wing of the sphenoid. The isolated polygons are located around the lateral part of the frontal bone, the portion of the premaxilla bordering the nasal aperture laterally, the infero-lateral surface of the occipital between glabella and nasion, over the anterior projection of the petrosal, and finally, the basioccipital.

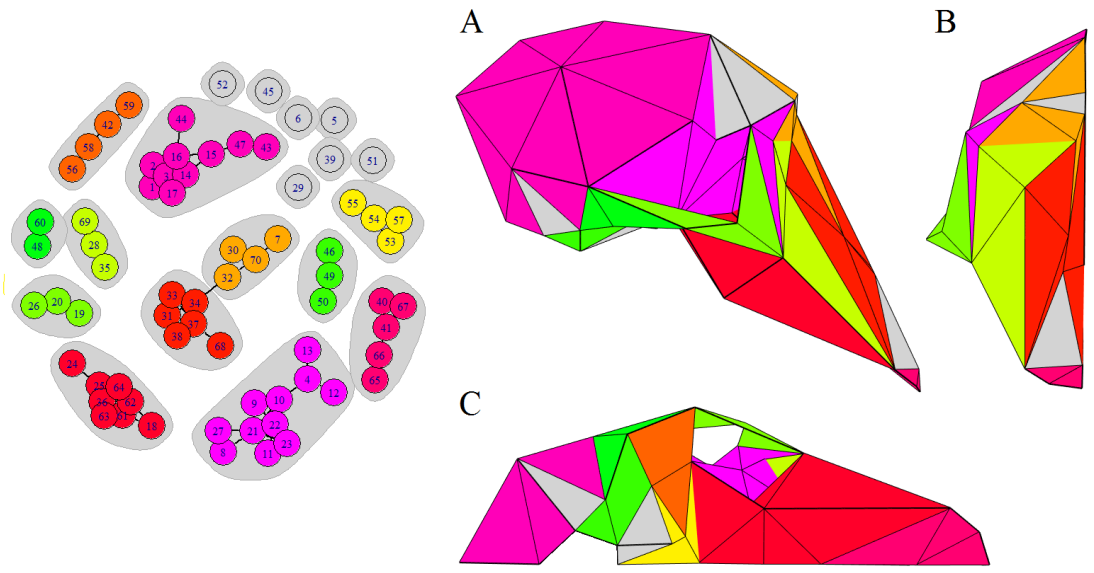


Figure 4.25. The network and associated polygon clusters of the baboon cranium based on the presence and absence of associations. Colours are assigned to the network modules identified in the graph and illustrated on the polygon representation on the right. Grey polygons are isolated. **A**: lateral view; **B**: anterior view; **C**: inferior view.

Human sample

The modularity score of Q = 0.8399 is considerably higher than the value obtained before accounting for allometry and sexual dimorphism in the human sample, and clearly indicates modularity of the network. The greedy optimization algorithm identified 11 groupings of two or more polygons, with six isolated polygons. Colours allocated to the network modules are illustrated on a human cranial diagram in Figure 4.26. The eleven groupings are as follows: 1) almost the entire cranial vault except the frontal bone and the squamous temporal bone; 2) the orbit and most of the frontal bone, the frontal process of the maxillary bone, the frontal process of the zygomatic bone; 3) the portion of the frontal bone in the temporal fossa together with a part of the greater wing of the sphenoid; 4) the mastoidal, the posterior portion of the squamous, and zygomatic process of the temporal bone, with the rest of the zygomatic arch; 5) the bone adjacent to the inferior margin of the orbit grouped together; 6) the anterior maxilla and palate; 7) the posterior palate; 8) the inferior part of the greater wing of the sphenoid, and the anterior portion of the squamous temporal; 9) the anterior petrous temporal and the basioccipital; 10) the exoccipital and a portion of the petrous temporal; and 11) the tympanic portion of the temporal bone.

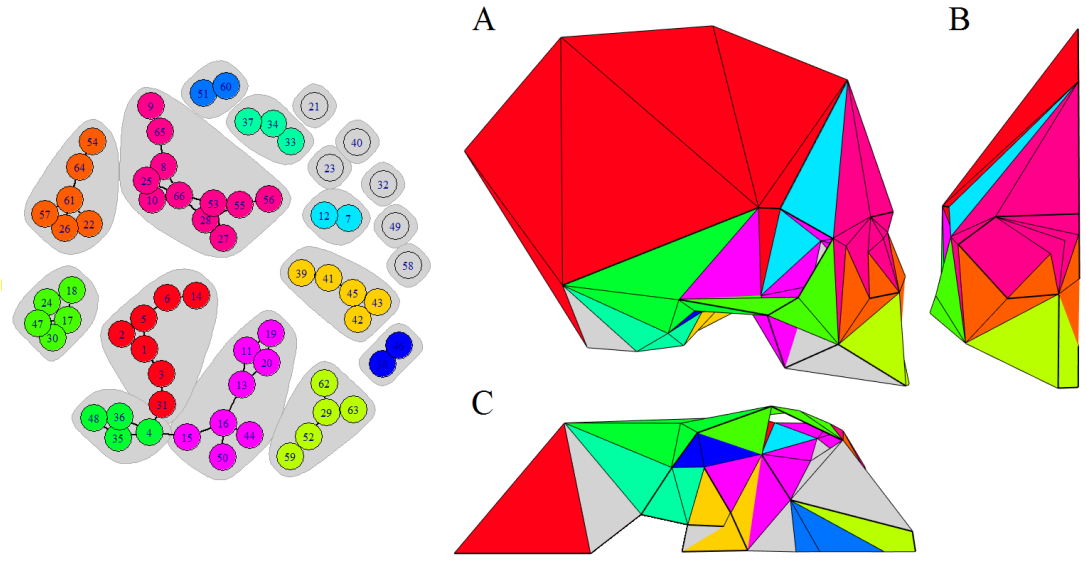


Figure 4.26. The network and associated polygon clusters of the human cranium based on the presence and absence of associations. Colours are assigned to the network modules identified in the graph and illustrated on the polygon representation on the right. Grey polygons are isolated. **A**: lateral view; **B**: anterior view; **C**: inferior view.

4.7 Aim 3: Exploring morphological integration between *a priori* modules

The third aim was to analyse differences in morphological integration between *a priori* modules in the baboon and human cranium with the expectation that:

H4) *P. h. ursinus* and *H. s. sapiens* will possess a general and shared pattern of morphological integration between *a priori* modules, with a few slight differences

The standard method for studies of cranio-facial integration requires that modules be defined based on well-established developmental processes and functional complexes (e.g. Cheverud, 1982; Lieberman *et al*., 2000; Bookstein *et al*., 2003; Bastir & Rosas, 2004, 2006; Mitteroecker & Bookstein, 2008; Singh *et al*., 2012). Typically, the cranium is subdivided into the cranial vault, the facial skeleton, and the cranial base, and the significance, magnitude and pattern of association between these modules are then assessed. To carry out this type of analysis on the sample of humans and baboons, the configurations of landmarks had to be adjusted to make them compatible. This involved removing the landmarks associated with the premaxillary-maxillary suture in the baboon sample, replacing those landmarks comprising pterion with their mean in both samples, and deleting the landmark between lambda and pterion from the baboon sample.

Once the effects of allometry and sexual dimorphism had been accounted for in each of the configurations, mean group subtraction was used to account for the average shape differences between the samples, allowing for a pooled 2B-PLS analysis (Mitteroecker & Bookstein, 2008). Because it is the within-species pattern of covariation that is of interest here, the marked shape differences between the human and baboon cranium would have dominated the analysis had the sample means not been subtracted from each constituent configuration.

Landmarks were assigned to the cranial vault, the facial skeleton, and the cranial base (Table 3.1) and each region was then independently superimposed using generalised partial Procrustes analysis, and stereographically projected to the tangent plane. Escoufier's (1973) *Rv* coefficients and the corresponding statistical significance between the regions, after sequential Bonferroni corrections were applied (Holm, 1979), indicated that all three regions significantly co-varied with one another (Table 4.3). Differences between the strengths are probably influenced by the number of shared landmarks rather than being a true reflection of the strength of the biological association.

Table 4.3: Tests of the integration between *a priori* modules.

Regions		Rv	p
Vault	Face	0.2184	<0.0003
Base	Face	0.1498	0.0005
Base	Vault	0.3523	<0.0003

The 2-block partial least squares (2B-PLS) method was used to explore the association between each of the pairwise comparisons after each region was independently superimposed (Rohlf *et al.*, 2000). The scores of the 2B-PLS analyses for the first three partial warps of each pairwise comparison are plotted in Figure 4.27, together with the major axis slopes describing the association for each sample. 2B-PLS mirrors PCA in many respects, but not least in terms of presenting

components or vectors that explain the variation or covariation in descending magnitude. The first three partial warps of the PLS between the cranial vault and the facial skeleton accounted for 13.0%, 9.1% and 8.5% of the covariance between the two regions. Similarly, the first three partial warps describing the relationships between the cranial base and the facial skeleton account for 11.5%, 10.4% and 9.8% of their covariance. The first three partial warps of the PLS between the the cranial base and cranial vault explains 15.5%, 12.3% and 10.4% of their covariance.

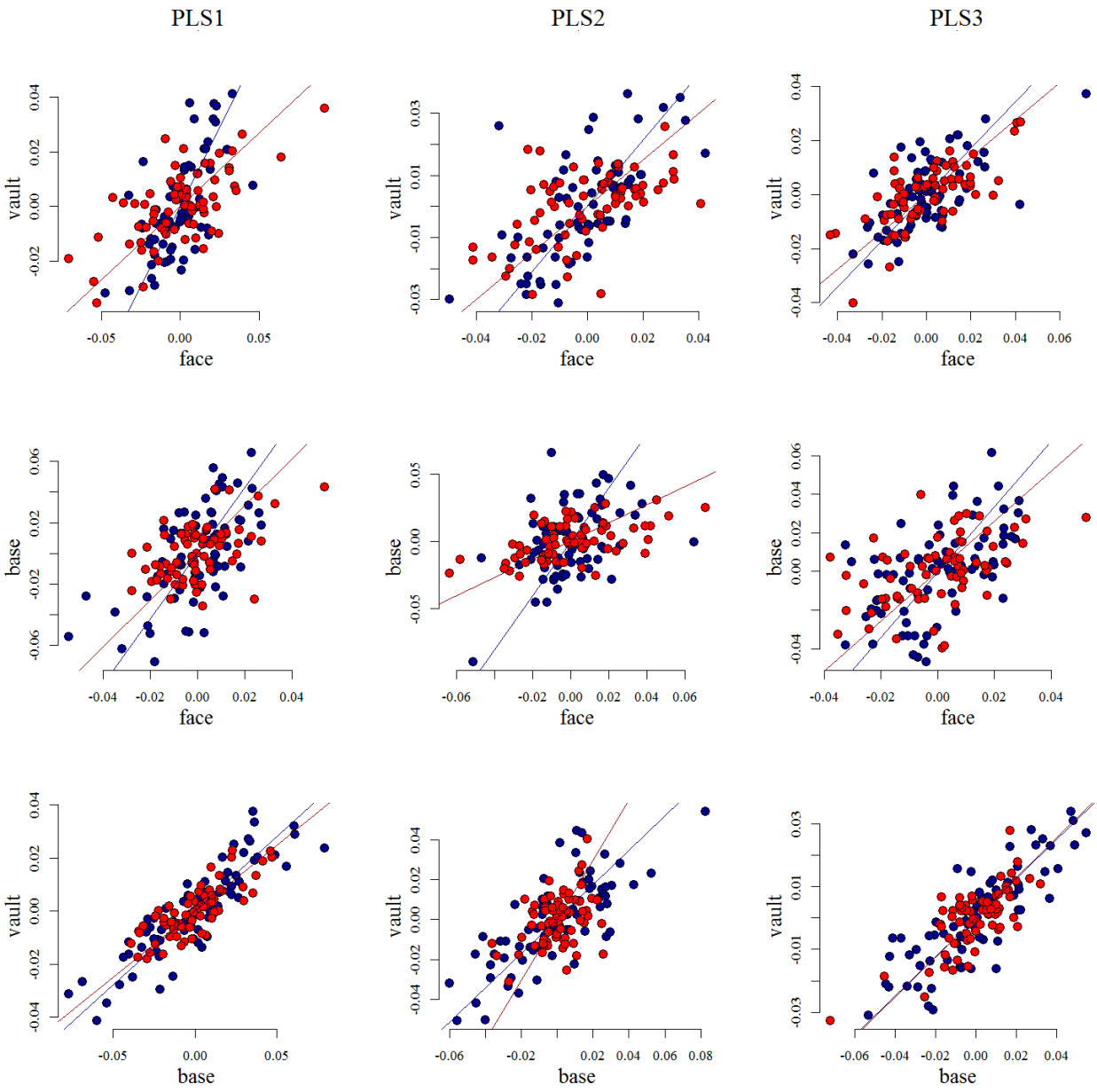


Figure 4.27. Plots of the first partial warp scores from each of the 2B-PLS analyses between the *a priori* defined regions. **A:** between the cranial vault and facial skeleton; **B:** between the cranial base and the facial skeleton and; **C:** between the cranial base and the cranial vault. The scores and slope of the baboon sample are coloured red, and those of the human sample are dark blue.

Differences between the baboon and human crania regarding the integration described by the 2B-PLS was assessed by comparing the major axis slopes drawn for each species using the 2B-PLS scores. Significance was adjusted using the sequential Bonferroni method (Table 4.4). Significant differences in integration between the samples were found between the first two partial warps of the cranial vault and the facial skeleton, and the second partial warp between the cranial base and the facial skeleton. There were no differences detected in the pattern of integration between the cranial base and the vault. The partial warps associated with these differences are illustrated in Figures 4.27, 4.28, and 4.29.

Table 4.4: Tests for differences between the major axis slopes on the 2B-PLS scores of the baboon and human samples.

Regions		Probability of equal slope		
		PLS1	PLS2	PLS3
Vault	Face	0.0000*	0.0038*	0.8755
Base	Face	0.2405	0.0000*	0.2405
Base	Vault	0.2405	0.9230	0.9230

Cranial vault and facial skeleton

Differences between the baboon and human samples were detected in the first partial warp describing the association between the cranial vault and the facial skeleton. The shape changes associated with the first partial warp are illustrated in Figure 4.28.

From the three perspectives, it is evident that projection of the glabella, a sweeping back of the zygomatic arches, and possibly a more airorhynchic palate are associated with a higher, narrower cranium with the concomitant projection of the frontal bone and retraction of the zygomatic process of the temporal bone. This partial warp appears to reflect the relative positioning of the orbits and zygomatic arch associated with the relative orientation of the palate (i.e. airorhynchy versus klinorhynchy). From the first partial warp between the cranial vault and the facial skeleton in Figure 4.27, the human facial skeleton does not undergo as much change as would occur in the baboon for a given shift in the cranium.

The association between the cranial vault and the facial skeleton as described by the second partial warp also proved to be different between the baboon and human samples. Here a posterior and inferior projection of the alveolar process of the maxilla, an increased size of the zygomatic bone and anterior projection of the superior and lateral margins of the orbits is not only associated with the anterior projection of the adjacent frontal bone and a broadening of the zygomatic process, but also with a raising of lambda, giving the posterior cranium a more rounded appearance (Figure 4.29). Regarding this pattern of covariation, the human face observes a greater shift given a unit of change in the cranial vault than what would be observed in the baboon sample. This is illustrated by the second partial warp between the cranial vault and the facial skeleton in Figure 4.27.

Cranial base and facial skeleton

Only the second partial warp proved to differ between the baboon and human samples (Table 4.4). The associated changes described by the second partial warp from these two regions (Figure 4.30) involved a downward displacement of the anterior palate, a raising and posterior movement of the glabella, and a narrowing of the upper facial region across to orbits, producing a longer, narrower facial profile. The associated cranial base changes involved a shortening of the cranial base anterior to the foramen magnum and greater angulation and depth of the posterior cranial fossa.

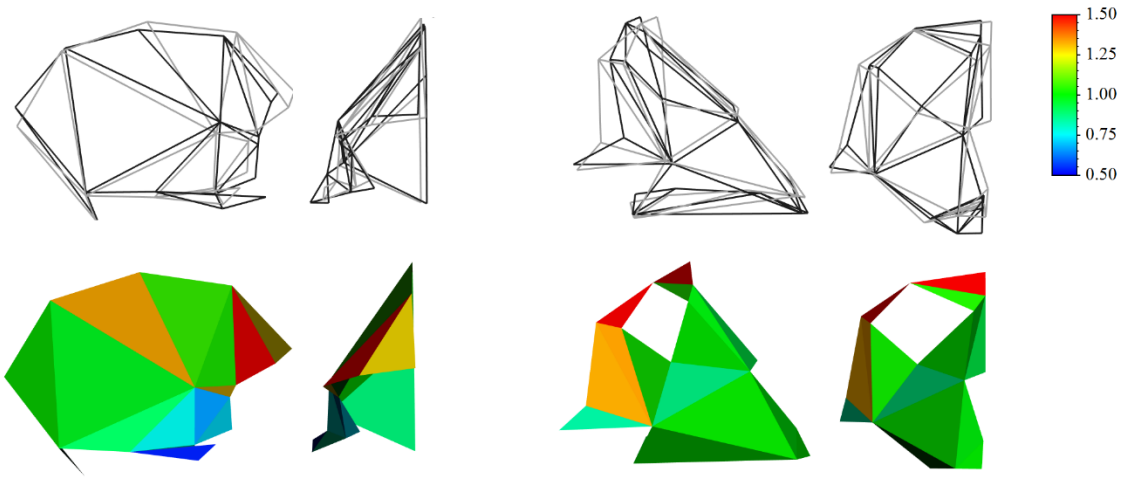


Figure 4.28. Wireframe and polygon models depicting the PLS1 relationship between the cranial vault on the left and the facial skeleton on the right. The darker wireframe relates to the minimum value along the vector, while the lighter represents the maximum. The colour scheme of the polygon models represents relative changes in area. The key is provided, where red indicates regions of area expansion, and blue contraction.

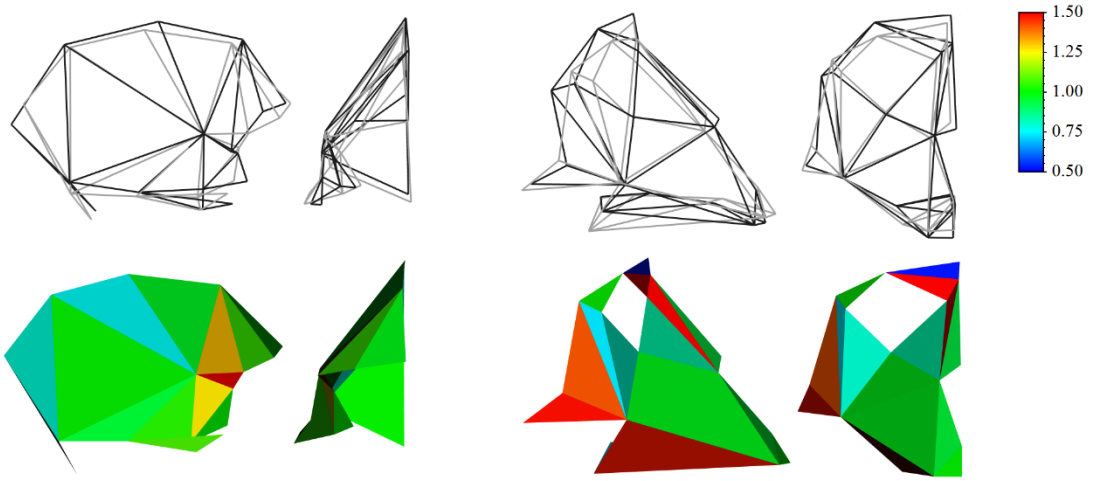


Figure 4.29. Wireframe and polygon models depicting the PLS2 relationship between the cranial vault on the left and the facial skeleton on the right. The darker wireframe relates to the minimum value along the vector, while the lighter represents the maximum. The colour scheme of the polygon models represents relative changes in area. The key is provided.

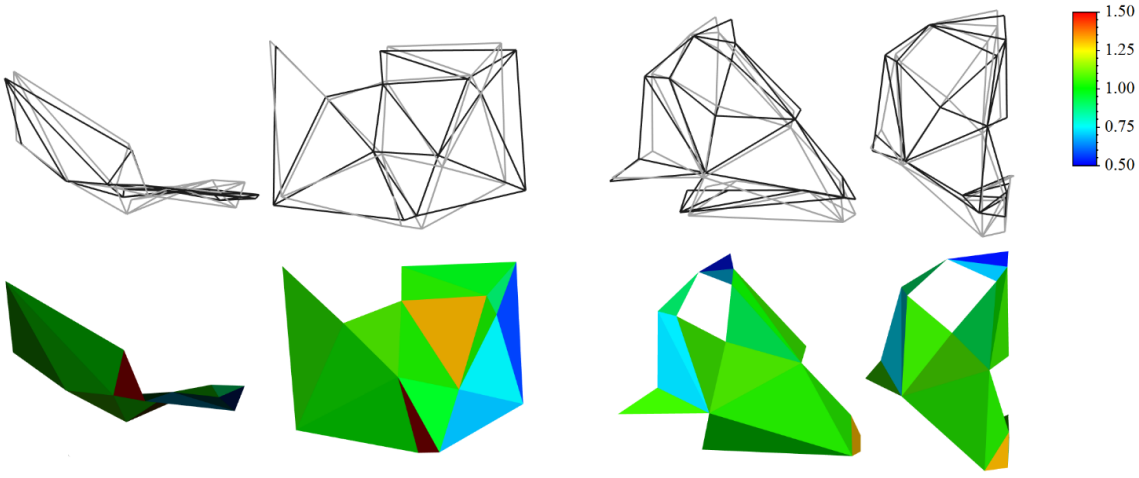


Figure 4.30. Wireframe and polygon models depicting the PLS2 relationship between the cranial base on the left and the facial skeleton on the right. The darker wireframe relates to the minimum value along the vector, while the lighter represents the maximum. The colour scheme of the polygon models represents relative changes in area. The key is provided.

DISCUSSION

> "*Modularity is therefore manifest as the relative independence of parts within the framework of overall integration . . . Fit is a matter of degrees, not all or nothing.*" Klingenberg *et al*. (2003: 522)

5.1 Summary of findings

Morphological integration is the pattern of correlation or covariation among parts due to genetic, developmental and functional processes, and is necessary for the viability of an organism. However, integration among processes is not uniform but forms distinct modules allowing for their independent evolvability (Cheverud, 1996a; Raff, 1996). Understanding integration and its arrangement is central to evolutionary studies because: 1) it constrains evolution by channelling existing variation; 2) understanding patterns of integration is necessary to uncover processes behind the evolution of complex characters; 3) it is an important component of the genotype-phenotype map; and 4) reconstructions of phylogenetic history based solely on morphological traits requires an understanding of character associations.

Studies of morphological integration in the hominin and papionin cranium are necessary because there have been inconsistencies between the genetic and phenotypic phylogenies. Their evolutionary histories are riddled with potential homoplasy, and studies aimed at understanding the evolutionary forces behind the

acquisition of characters in extinct and extant representatives of these taxa need a clear understanding of the pattern of morphological integration. This study thus aimed to assess morphological integration and its patterning in the human and baboon cranium by means of three broad aims. The first sought to study allometry as an integrating factor by analysing shape-change associated with ontogenetic allometry, assessing the patterning of morphological integration in ontogenetic samples, and quantifying the proportion of adult variation attributed to static allometry. The second aim was to assess the patterning of morphological integration into morphological modules once allometry and sexual dimorphism had been accounted for. The third aim assessed differences in the covariation between the cranial base, cranial vault and facial skeleton in baboons and humans.

The findings indicate that ontogenetic allometry in both humans and baboons follows a broad pattern of reduced neural growth and accelerated maxillary growth, but differences exist that cause the trajectories to diverge. The covariance due to this allometry completely obscures any pattern of integration such that there is no meaningful clustering of cranial regions, nor is there any modularity in the networks produced. Static allometry contributes to as much as 42% to the total covariance among adult baboons in comparison to the 3% observed for humans.

After accounting for allometry and sexual dimorphism, further analysis of patterns of integration found significant clustering of the polygons and modularity in the

networks. This approach to morphological integration is novel, but because it is completely exploratory it aims to be a means by which to identify hypothetical cranial modules for future testing. The comprehensive overview of craniofacial embryology and development is necessary to support the *a posteriori* proposal of hypotheses based on the observed clustering and network modules of the polygons. Thus, not all the embryology and development that was introduced will be relevant and require discussion.

The number of clusters and modules suggests that the primate cranium likely comprises many more developmental modules than is generally acknowledged. The final analysis looked at the pattern of integration between the cranial base, vault and facial skeleton in the human and baboon samples. Although integration between these regions is similar in the baboon and human, the relationships involving the facial skeleton are often not identical.

5.2 Technological limitations

Landmark data are not without limitations. The reliable and repeatable positioning of type I and type II landmarks requires that this often occurs at the intersection of structures, resulting in the loss of information concerning the surface composition or the shape of the underlying bone between these landmarks. Thus, the results presented here only concern the processes responsible for the relative positioning of

the landmarks. For example, the removal of the landmark between pterion and lambda resulted in the complete loss of information regarding the curvature of the parietal bone. The remaining landmarks around the parietal bone still record the overall size and extent of the element, but a vital piece of information was lost by having to use reliable and repeatable landmark data, particularly considering that cranial globularity is a key characteristic of the human cranium, among the hominins, and the baboon cranium, among the papionins (Leigh *et al*., 2003).

There are currently landmark-free superimposition and shape analysis techniques being developed to circumvent these issues. Among the new methods is Generalized Procrustes Surface Analysis (Pomidor *et al.*, 2016). While it is readily acknowledged that the scale of morphological detail involved in Procrustes Surface Analysis does not avail itself to most biological investigations, I feel that it is this detail that makes the method particularly suited to the study of morphological integration. Given the current limitations, however, this study used the most practically available methods to investigate a novel approach to the study of morphological integration and modularity.

5.3 Allometry as an integrating factor

5.3.1 Relative cranial growth

It is known that growth and the associated proportional changes are important integrating factors (Lieberman *et al.,* 2008; Hallgrímsson *et al.,* 2007), therefore part of the first aim of this study was to evaluate the role of allometry in both the human and baboon cranium by highlighting regions of differential growth during ontogeny. The specific hypothesis stated that *the general pattern of postnatal ontogenetic allometry will be one of slower neural growth and faster facial growth, while the orbits, zygomatic region and cranial base will possess an intermediate, possibly isometric growth*. The converse of this hypothesis (the putative null hypothesis) is rejected by the general pattern of broad neural versus somatic growth described by the allometric vector in these two species. More specifically, the effect of the reduced postnatal growth of the brain on the cranial vault relative to the increased postnatal growth of the facial skeleton; but are also some key differences between the species.

Growth of the facial skeleton in both species primarily involves the maxilla and palate, as they lengthen and descend relative to the cranial base and vault. The floor of the nasal cavity descends under proposed expansion of the cartilaginous nasal septum (Scott, 1953; Sarnat, 1971; Holton *et al*., 2011; Al Dayeh *et al*., 2013). The entire maxilla is displaced forward and downward due to inter-sutural growth, while subperiosteal depositional processes lengthen the maxilla posteriorly (Enlow, 1990;

Enlow & Hans, 1996). While there are differences in the pattern of subperiosteal growth between human and non-human primates (Duterloo & Enlow, 1970), the persistence of the premaxillary suture suggests that it plays a key role in the anterior extension of the baboon maxilla. Because the direction of sutural growth is perpendicular to its orientation (Richtsmeier & Flaherty, 2013), there is significant extension of the maxilla in the anterior direction. The premaxilla in the baboon, and interestingly the corresponding region in the human, appears to grow isometrically, in sharp contrast to the surrounding maxilla.

Growth of the periorbital region of the facial skeleton appears to be mixed neural and somatic. Although the eyeballs are outgrowths of the embryonic forebrain and are thus considered to have a neural growth pattern of fast *in utero* and slower postnatal growth (Sperber, 2001), and the pressure exerted by the eyeballs on the surrounding bone does affect growth of the orbits, this effect is mediated by the surrounding muscles and connective tissue (Lieberman, 2011b). Not only do these muscles and connective tissues grow at a higher postnatal rate than the eyeball, but they probably have a greater effect on the immediately adjacent bone. The frontal processes of the maxilla in both species undergo positive allometry like the rest of the maxilla, probably as a result of the expanding nasal capsule below. The supraorbital region experiences negative allometry as it is situated adjacent to, and is probably under the influence of, the slowly growing brain and surrounding structures. Finally, the body of the zygomatic bone, making up the inferolateral margin of the orbits, experiences

isometric growth in both humans and baboons. This suggests that growth at the zygomatico-maxillary suture, like the premaxillary suture, contributes principally to maxillary growth through displacement.

The temporal fossa in both the baboon and human cranium experiences positive allometry, particularly between the anterior and posterior limits of the spheno-frontal suture, suggesting that the greater wing of the sphenoid contributes primarily to the growth of the temporal fossa. On the other hand, a principal difference in the growth of this region in the baboon and human involves the enlargement of the zygomatic arch. Unexpectedly, growth in this structure is positively allometric in the human, but isometric in the baboon. This likely relates to the available space for the developing temporalis muscle. As you move up the human cranium from the temporal fossa, the cranial vault quickly expands laterally so that the fossa is hidden if viewed from above. The developing muscle thus quickly occupies the available space, placing tensile pressure on, and initiating growth at, the zygomatico-temporal suture as well as subperiosteal resorption along the inner surface and deposition along the outer surface of the arch. Although the baboons possess relatively large brains among the papionins (Leigh *et al*., 2003), the cranium has marked postorbital constriction and the developing temporalis muscles easily find purchase higher up along the cranial vault. This is particularly evident in large males where the temporalis muscles eventually meet in the midline to develop a sagittal crest. Thus, in baboons there is reduced pressure from the temporalis muscles on the zygomatic arches to develop

laterally. Finally, the results regarding growth of the basicranium support those of Leigh and colleagues (2003) as it appears to be negatively allometric to isometric.

The shape changes associated with growth suggest a dissociation between the cranial vault and the facial skeleton, with the basicranium, the zygomatic arch and the upper orbital region acting almost as mediators between the two regions. In terms of growth differences and their possible effects on patterns of integration, the premaxillary suture is an additional growth site in the baboons and will likely shift the pattern of covariation between the facial skeleton and the rest of the cranium, when compared with humans. In addition, while the role of the zygomatic arch is primarily masticatory, I propose that its observed positive allometric growth in the human cranium results from additional pressures from the expanded cranial vault, likely affecting its integration with the facial skeleton and the cranial vault.

5.3.2 Clustering and networks during ontogeny

While allometry is an important integrating factor, it has been argued that it obscures the finer details of morphological integration related to specific genetic or developmental processes (Klingenberg, 2008; Mitteroecker *et al*., 2012). Besides the rough separation of polygons into a cranial vault group and a facial skeleton group in some of the results, possibly from differences of somatic and neural growth, the lack of definite modularity in both the dendrograms and networks based on the pattern of

covariation in the ontogenetic samples attests to the overarching and blurring effect of allometry. In the current work, the resulting dendrograms suffered from significant chaining, generally suggestive of a continuous underlying factor, while the networks had low modularity and many overlapping groupings. Thus, the findings of this analysis generally support the proposal (Hypothesis 2) that the patterns of covariation resulting from allometry do not necessarily reflect genetic and developmental integration (Klingenberg, 2008; Mitteroecker *et al*., 2012), and that the effect of allometry should be accounted for before testing for morphological integration (Klingenberg, 2008). Although Marroig and colleagues (2009) found the boundaries between modules to be obscured in mammalian species possessing a large proportion of allometric variation, both the human and the baboon cranium were affected equally from the incorporation of allometry in their analysis.

5.3.3 Role of allometry in static variation

The second part of the first aim was to quantify the role of allometry in static variation in baboons and humans. Allometry plays a significant role in adult baboon morphology, contributing to around 42% of the shape variation among adult baboons, which is in strong contrast to the 3% observed among adult humans. The null hypothesis was is easily rejected, lending support to the proposal that the proportion of variation attributed to size will be larger in baboons than humans (Hypothesis 3). The proportion of variation attributed to allometry has been implicated as the factor responsible for increased cranial integration in the baboons (Marroig *et al.*, 2009),

and is purported to constrain intra- and interspecific variation among the Papionini primarily along allometric directions (Singleton, 2002; Frost *et al*., 2003). Conversely, allometry does not explain all morphological differences among the papionins. Although allometry has played an important role in confusing primate taxonomists, there are many non-allometric factors (Collard & O'Higgins, 2001) and even strong evidence of 'decoupling' between the broad cranial regions in this group (Leigh *et al*., 2003).

This brings into question how allometry is related to integration, evolutionary constraints and evolvability. Firstly, allometry brings about a broad pattern of covariation through shared and differential responses to global signals. This covariation is independent of genetic, developmental and functional integration (Klingenberg, 2008; Mitteroecker *et al*., 2012), which are linked to many types of evolutionary constraints (Maynard Smith *et al*., 1985; Richardson & Chipman, 2003). Unless the allometry follows a particular pattern resulting from the relationship between size and functional constraints, there is no reason to suppose that allometry would constrain evolution.

Secondly, allometry should increase evolvability in size-related features only through the range of variation available for selection and the ease with which selection can act on this variation. This effect is readily evident in the morphological diversity of dogs and cats due to artificial selection. Cats do not possess a wide range of size variation

while dogs do, and the range of morphological diversity among the dog breeds attests to the ability of allometry to offer up an assortment for selection. This can be tested. If selection and stochastic processes act equally on the non-allometric component of variation, we would expect the extent and pattern of integration to be very similar once the effects of allometry have been accounted for. Fortunately, measures of the non-allometric variation in both humans and baboons were available to assess this. The non-allometric Eigenvalues of the baboon summed to 0.0023, while in the human it was 0.0036, about 50 percent greater than in the baboon. Thus, the reduced allometric variation in humans is associated with an increase in non-allometric variation. From this it can be confirmed that, in terms of evolvability, size-related variation does offer a path of least resistance, as proposed by Marroig and Cheverud (2005, 2010).

5.4 Exploration of modules

The second aim of the current work used novel methods to explore patterns of covariation. Specifically, it explored covariation in the baboon and human cranium to assess the patterning of morphological integration into morphological modules once allometry and sexual dimorphism had been accounted for. Because this method diverts from the generally accepted hypothesis-driven method of empirical investigation, caution must be taken when interpreting the results *a posteriori*, and a thorough theoretical framework should be provided on which findings can be discussed. *A posteriori* hypotheses can provide the impetus for future studies and the findings here are offered as potential units of morphological change, needing future

rigorous testing. Given these necessary caveats, and the extensive overview of development in the background chapter, the present hypothesis states that after accounting for allometry and sexual dimorphism, the patterns of covariation in the crania of both *P. h. ursinus* and *H. s. sapiens* will partition into clear morphological modules that fit with current understandings of development (Hypothesis 4).

Although the removal of allometry substantially enhanced the ability of clustering and network methods to discern morphological modules in the baboon and human cranium, it remains to be seen whether these patterns fit with existing knowledge of development. Nonetheless, the significant clustering and high modularity scores lends further support to the proposition that the effect of allometry obscures the intrinsic pattern of morphological integration (Mitteroecker & Bookstein, 2007; Klingenberg, 2009, 2013), and should be accounted for before hypothesis testing (Porto *et al*., 2009).

There were a few groupings shared in both the baboon and human samples involving both the clustering and the network analyses. All analyses consistently grouped the polygons of the cranial vault to the exclusion of those of the anterior frontal, which were consistently associated with the upper orbit and interorbital region. The premaxilla and associated palatal region also formed an isolated grouping in the baboon analyses, as did a comparable region in the human maxilla. There were, however, several differences. While the posterior palate grouped with the alveolar

process of the maxilla in the baboon sample, the two regions formed separate groupings in the human sample. Another distinction involved the zygomatic arch, which separated out from other structures in the baboon but not in the human. The zygomatic arch in the human cranium was integrated with the temporal bone and, in the case of the cluster analysis, with the entire cranial base anterior and lateral to the foramen magnum. The temporal fossa also formed its own isolated group in the baboon but was split between the frontal bone and the cranial base in the human. The baboon maxilla divided into a nasal part, a lateral part, and an alveolar part, with the lateral portion of the maxilla integrating with the inferior orbit. Although differences between configurations in the maxillary region precluded this type of resolution in the human sample, the lateral zygomatic process of the human maxilla was similarly integrated with the inferior orbit in the cluster analysis.

The cranial base polygons of the baboon sample consistently formed three groupings, one lateral to foramen magnum, including the exoccipital and the petrous temporal, one involving the basioccipital and the adjacent sphenoid, and the third involving the articular portion of the temporal bone. However, the clustering method in the human sample grouped the cranial base with the zygomatic arch and squamous temporal, while the network analysis separated it into four different units.

Studies testing *a priori* hypotheses of modularity based on Moss' (Moss & Young, 1960; Moss, 1968; Moss & Salentijn, 1969) functional matrix hypothesis (e.g.

Cheverud, 1996b; Ackermann & Cheverud, 2000; Marroig & Cheverud, 2001; González-José *et al*., 2004; Hallgrímsson, *et al*., 2004; Marroig *et al*., 2004, 2009; Ackerman, 2005; Porto *et al*., 2009, 2013; Shirai & Marroig, 2010; Willmore *et al*., 2012) have consistently found support for a cranial vault module and an oral region module. While the current study supports the cranial vault as a module, the results suggest that the oral region should, at the very least, be subdivided into anterior and posterior groups, with the possibility of a third, alveolar, module. Villmoare and colleagues (2014) provide strong evidence supporting this splitting of the oral region into anterior and posterior groups, suggesting that the primate palate is a module comprising two smaller modules: the premaxilla on the one hand, and the maxillae and palatines on the other. This proposal fits with the observations here but does not explain the isolation of the alveolar process in some instances. A solution may lie in the study by Paradis *et al*. (2013), who compared the mandibles of normal mice with a mutant bred to possess failed tooth development. The agenesis of teeth affected primarily the alveolar process, with almost no difference in the rest of the mandible between the mutant and normal mice. This is not to say that the exact same processes regulate development of the maxillary and mandibular jaws, but often they are equivalent and possess comparable structure as a result of functional integration (Boughner & Hallgrímsson, 2008; Lieberman, 2011a; Polly, 2011). Thus, I would hypothesise that the alveolar process of the maxilla is a module, if only for future testing. Besides differences in arrangement of landmarks, inconsistencies in the lateral portions of the maxilla between baboons and humans may result from presence of sinuses in humans, and their complete absence in baboons. The human maxillary

sinuses have recently been shown to mediate the integration between the inner functional capsules and the external morphology of the facial skeleton (Maddux & Butaric, 2017). Some observations of the external maxillary surface (i.e. its separation into a nasal part, a lateral part, and an alveolar part) might reflect strong integration with the underlying nasal and oral capsules.

While studies (Cheverud, 1982, 1995, 1996; Ackermann & Cheverud, 2000; Marroig & Cheverud, 2001; Marroig *et al*., 2004; Ackermann, 2005) have consistently supported the vault and the oral regions as independent modules, they have, with few exceptions, found the zygomatic to possess relatively weak internal integration. This leaves little justification for proposing that the zygomatic arch is an independent module. Besides the inconsistent results between the baboon and human, the zygomatic arch forms a bridge between the neurocranium and facial skeleton, lies over the temporalis muscle, and primarily acts as to anchor the masseter muscle and the temporal fascia. Likewise, the orbital portion of the frontal bone forms a superior intersection between the cranial vault and the maxilla, and much of its morphology probably relates to the arrangement of the facial skeleton, neurocranium, orbits and nasal capsule, rather than forming a module on its own. Even the orbits themselves were often divided in this study, forming modules with the frontal bone superiorly and the lateral maxilla inferiorly.

While hypotheses describing the cranial base as a module have almost never received statistical support, the evidence here suggests that this might be due to the cranial base comprising many, functionally independent structures. Many of the elements vary in function, from auditory to mastication, and from supporting the brain to supporting the entire cranium on two condyles. It is important to note that the number of elements comprising the primate skull is reduced, with many of the elements fusing pre- and postnatally from hundreds of condensations (Kardong, 2002; Esteve-Altava *et al*., 2013a). I propose here that the portion of the cranial base studied be subdivided into the petrosal, the articular temporal, the exoccipital, the basioccipital-basisphenoid, and the infratemporal portion of the greater wings of the sphenoid for further testing. Each of these regions appeared to separate out in at least two of the analyses, and they each have different functions in the cranial base.

Recent studies of the mammalian mandible have divided it into between two and five developmental and functional modules (Klingenberg *et al*., 2003; Willmore *et al*., 2009) on the premise that modules be defined by mesenchymal cell condensations possessing different cellular properties (Atchley & Hall, 1991). Studies of the cranial base, such as the current study, are restricted by the resolution of the measurements taken. There are probably very localised structures, at the scale of Atchley and Hall's (1991) mesenchymal cell condensations, that arise through partially independent developmental programs and exhibit all the attributes of a developmental module. By using these broad-brush strokes and consistently separating the cranium into large *a*

priori modules we may miss some finer but important details regarding morphological integration.

5.5 Study of integration among *a priori* modules

The third and final part of this thesis aimed to analyse differences in morphological integration between *a priori* modules in the two species by assigning the landmarks to the cranial vault, the facial skeleton, and the cranial base, and comparing the patterns of covariation. The premise is that baboons and humans possess a shared general pattern of morphological integration between *a priori* modules, with a few slight differences (Hypothesis 5).

Although pooling the data forces the axes of the 2B-PLS analyses to line up with commonalities among the species, it also allows for comparison and statistical testing between the two species. 2B-PLS, like PCA, assigns vectors according to the characteristics of the covariance and/or variance matrices, and not necessarily with any biological factor. The species-specific 2B-PLS analyses can, however, serve as exploratory tools for identifying the strongest patterns of integration among regions. Although not specifically addressing this aim, exploring the integration for each species independently has the potential to reveal marked distinctions in the patterns of integration, where they exist, and will be considered for future analyses.

All relationships between the facial skeleton, the cranial vault and cranial base proved significant; however, the nature of the relationship in baboons and in humans differed significantly in some instances, supporting the above hypothesis. These findings are comparable to those of Mitteroecker and Bookstein (2008) and Singh *et al*. (2012) who found that humans share similar, but not identical, patterns of integration with the other apes. The similarities between the patterns of integration were likely due to shared developmental processes among the primates (Klingenberg *et al*., 2003; Marroig *et al*., 2004; Hallgrímsson *et al*., 2007a) and even mammals (Cheverud, 1996a), while differences in the nature of the relationship result from changes in cranial functional relationships. For example, the biomechanical and functional demands of increased muzzle length in the baboon will not be experienced by the human cranium, and will likely affect the functional demands on the baboon cranial vault.

According to Lieberman (2011b), there are four primary factors responsible for the unique pattern of integration in the human cranium involving the development of four key features:

1) A relatively large brain and globular cranial vault
2) A greatly flexed cranial base
3) A more anteriorly positioned foramen magnum and horizontally positioned nuchal plane
4) A relatively diminished and non-prognathic facial skeleton

Given this list of unique characteristics, it is not unreasonable to suppose that the nature of morphological integration between these three regions would differ from that in the baboon cranium.

Those patterns that were investigated more thoroughly revealed that the integration between the cranial vault and the facial skeleton primarily involves points of intersection, namely the supraorbital and zygomatic regions. A large component of non-allometric variation among the primates involves craniofacial halfting, and specifically the differences involved in developing airorhynchic and klinorhynchic morphologies. The upward or downward rotation of the facial skeleton relative to the cranial vault and base necessarily involves the supraorbital region, the orbits, the zygomatic arches, the shape of the mandible and cranial base flexion. Similarly, although not clear in these illustrations, integration between these regions typically follows the traditionally recognised brachycephalic versus dolichocephalic pattern identified by Retzius (1842). Generally, a short, broad basicranium and vault is associated with a shorter and wider facial skeleton, while a long narrow basicranium and vault is associated with a narrower and taller facial skeleton. Although usually attributed to human crania (e.g. Enlow, 1968) these patterns of integration are readily apparent among the apes (Mitteroecker & Bookstein, 2008; Singh *et al*., 2012).

To summarise these findings, humans and baboons share an overall pattern of integration between the cranial vault, cranial base and facial skeleton because of

shared developmental processes among the primates and mammals. There are, however, differences that involve the relationships between the cranial vault and facial skeleton, and the cranial base and the facial skeleton, that likely reflect distinct functional demands given their unique physical attributes. Most of the integration between *a priori* regions involves their relative positioning and proportions, and affects areas directly involved with their attachment to one another. This interdependence has, nonetheless, been used to infer complete and pervasive integration of the human cranium

5.6 Pervasive integration

The idea of total morphological integration was originally proposed by Cheverud (1995), but more recent studies (Lieberman *et al*., 2000; Strait, 2001; Hallgrímsson *et al*., 2002; González-Jose´ *et al*., 2004) have suggested complete integration of morphological traits. The argument I put forward here readily acknowledges that pervasive integration is necessary because there needs to be coherence among processes and the resulting structures for an organism to be viable. Even so, this does not rule out the possibility of modularity.

I will begin by outlining two important factors responsible for the pervasive integration of the human cranium, to rouse Moss' (1968) original propositions. The first is that the object under study is the cranium, the remaining framework after all

the organs have been removed. Because cranial growth is largely governed by the soft tissues of the head rather than inherent growth mechanisms of the bone, Moss (1968) believed that studies of the head should focus on the soft tissues rather than on the skeletal material. The modules of the head are each of the individual organs and functional spaces that compete for territory in a tightly-packed region. These organs and spaces are supported by a framework of bone and connective tissue. It is this framework that forms the basis of many studies of integration and modularity.

The second factor is that while organs are highly functional units probably under strong selective pressures (often stabilising), the arrangement between them is mostly stochastic; and it is primarily this arrangement that is recorded by the bony framework (hence the general congruence between genetics and cranial measures; Harvati & Weaver, 2006; von Cramon-Taubadel & Smith, 2012). Cheverud (1982) recognised the importance of stochastic processes in bringing about non-functional correlations between cranial regions. Selection, unless diversifying, would result in decreased variation within the organs and spaces, and stochastic processes (in a large population) would result in increased variation between the organs and spaces.

Measures of covariation are dependent on the underlying variance (Mitteroecker *et al.*, 2012), and it is the measure of this covariation between the organs and spaces, relative to the total amount of variation, that is the basis for the argument for pervasive integration of the human cranium. While the variation of epigenetic

packaging and arrangement of modules is likely as heritable as the genetic structures responsible for the growth and regulation of organs themselves, is this then the type of integration we want to be measuring? Yes and no. If the question is to identify the effects of selection on one structure on overall cranial morphology, all genetic and epigenetic integration must be considered. If the question involves the evolvability of a structure, then the associations that come about through spatial packing are not necessarily that important. And so, recognising the total integration of the cranium and its dissociability are equally important.

Integration of the genetic control of development

There are some recent developments regarding the molecular regulation of development that adds to the debate regarding total integration of the cranium. It is readily acknowledged that variation in protein-coding genetic sequences accounts for very little non-pathological phenotypic variation. Most viable phenotypic variation results from variation in enhancer sequences. Craniofacial shape has moderate to high levels of heritability in both humans (e.g. Byard *et al*., 1985; Sherwood *et al*., 2008a) and the papionins (e.g., Cheverud and Buikstra, 1982; Sherwood *et al*., 2008b), yet very little is known about the genetic basis of normal facial variation. Studies of quantitative trait loci in the human (Boehringer *et al*., 2011; Liu *et al*., 2012; Paternoster *et al*., 2012) and baboon (Sherwood *et al*., 2008b) have revealed that very few coding genes are associated with regular non-detrimental craniofacial variation (in the human orthologous regions). Those genes that are have generally been

associated with known syndromes. For example, a single nucleotide polymorphism in the PAX3 gene is associated with the prominence and height of nasion, yet other variants of this gene are involved in the deleterious Waardenburg syndrome characterised by deafness, pigmentary abnormalities, and a broad nasal bridge (Paternoster *et al*., 2012). These studies have highlighted that DNA variants in genes essential for craniofacial development play a very small role in patterning normal human facial variation.

The fact that coding genes themselves are relatively invariant and play little role in normal variation has shifted the research focus to regulators sequences, and specifically enhancers, which have recently come to the forefront in evolutionary developmental biology (Attanasio *et al*., 2013). The vast numbers of enhancer sequences are hypothesised to regulate the spatio-temporal pattern and level of gene expression during development, and although the enhancer and the gene it affects are located on the same chromosome they may be separated by hundreds of kilobase-pairs (Pennacchio *et al*., 2013). This focus on regulatory genes has not gone unnoticed by the theoretical biologists, and Stern (2000) has looked at the new-found role of enhancer sequences and proposed that the effect pleiotropy has in constraining diversity had been overestimated, that integration was overplayed, and that the phenotype is more mosaic than predicted.

Recent studies have, however, shown that regulatory elements are as pleiotropic as the genes they regulate, and enhancers have been co-opted into various developmental networks across multiple regions (Attanasio *et al*., 2013). Gene regulation is a multifaceted process by which cells in multicellular organisms differentiate based on their extracellular environment. It is an epigenetic process that involves a complex gene regulatory network. Evolution generally co-opts existing processes in the development of novel structures and thus conserved enhancer sequences should naturally be involved with the regulation of multiple developmental processes.

I argue throughout this thesis that, although "*integration cannot be reliably studied through phenotypic covariance patterns alone*" (Hallgrímsson *et al*., 2009: 355), the exploration of covariance patterns can offer a unique perspective from which hypotheses can be erected for future testing. It is not a means to an end but rather the means by which we arrive at the beginning. Just as new methods are being developed to decipher archaeological palimpsests (e.g. Mocella *et al*., 2015), work on the palimpsest of morphological integration should proceed, and new methods developed. The study of morphological integration requires both a bottom-up and top-down approach, where bottom-up refers to experimental procedures and measures of resulting shifts in integration, and top-down, where observed patterns can provide the hypotheses for future experimentation.

CONCLUSION

The study of morphological integration and modularity is central to the study of biological evolution. This thesis set out to address three broad aims regarding integration of the baboon and human cranium, namely to: 1) study allometry as an integrating factor, 2) assess the patterning of morphological integration into morphological modules once allometry and sexual dimorphism had been accounted for, and 3) assess differences in the covariation between the cranial base, cranial vault and facial skeleton in these two species.

The findings suggest that allometry can be considered a nuisance factor in the study of morphological integration when it reflects only developmental dissociation (but not functional demands or constraints) as it overshadows the more nuanced patterns of possibly genetic or developmental integration. Allometry among cranial regions is unlikely a constraining factor regarding evolutionary diversity but rather a path of least resistance. Once the effects of allometry and sexual dimorphism were accounted for, novel methods of exploring character covariance patterns using clustering and network techniques uncovered regions of the cranium that appear to be modules. Theoretical support was at least provided regarding the modularity of the cranial vault and possibly the subdivision of the oral region into premaxillary and maxillary/palatal modules. Rigorous testing is nevertheless necessary for empirical support. Additionally, I hypothesise that the cranial base be further subdivided into multiple modules based on the results presented and the separate developmental and functional

processes involved with each, subject to rigorous scientific scrutiny. Finally, it is worth considering that just because something is globally expressed, does not mean it is not locally modulated.

The analysis of integration between the cranial base, cranial vault and facial skeleton supported the findings of Mitteroecker and Bookstein (2008) and Singh and colleagues (2012) suggesting that humans share a similar pattern of integration with the non-human primates and the differences likely reflect shared developmental processes among the primates and mammals (Cheverud, 1996a; Klingenberg *et al*., 2003; Marroig *et al*., 2004; Hallgrímsson *et al*., 2007a). Integration between these regions primarily involves their relative positioning and proportions; relating the concepts of airorhynchy and klinorhynchy as well as brachycephaly and dolichocephaly, respectively.

The nature of the cranium is responsible for the broad integration observed. The living organs and functional capsules had competed for limited space and all we are left with is the skeletal framework that mediated this accommodating and compensatory development between organs. Future studies should look to landmark-free superimposition and shape analysis techniques so that inferences are not limited to the arrangement of distantly spaced landmarks, but that integration of the surfaces and shapes of the elements themselves can be studied.

REFERENCES

Ackermann, R.R. (2002). Patterns of covariation in the hominoid craniofacial skeleton; implications for paleoanthropological models. *J. Hum. Evol.*, 43: 167-187.

Ackermann, R.R. (2005). Ontogenetic integration of the hominoid face. *J. Hum. Evol.*, 48(2): 175-197.

Ackermann, R.R. & Cheverud, J.M. (2000). Phenotypic covariance structure in tamarins (genus *Saguinus*): a comparison of variation patterns using matrix correlation and common principal component analysis. *Am. J. Phys. Anthropol.*, 111(4): 489-501.

Adams, A., McBratney-Owen, B., Newby, B., Bowen, M.E., Olsen, B.R. & Warman, M.L. (2013). Presphenoidal synchondrosis fusion in DBA/2J mice. *Mamm. Genome*, 24(1-2): 54-62.

Adams, D.C. & Otárola-Castillo, E. (2013). geomorph: an R package for the collection and analysis of geometric morphometric shape data. *Methods in Ecology and Evolution*, 4(4): 393-399.

Al Dayeh, A.A., Rafferty, K.L., Egbert, M. & Herring, S.W. (2013). Real-time monitoring of the growth of the nasal septal cartilage and the nasofrontal suture. *Am. J. Orthod. Dentofacial Orthop.*, 143(6): 773-783.

Alberch, P., Gould, S.J., Oster, G. & Wake, D. (1979). Size and shape in ontogeny and phylogeny. *Paleobiol.*, 5: 296-317.

Albert, A.M., Ricanek Jr, K. & Patterson, E. (2007). A review of the literature on the aging adult skull and face: Implications for forensic science research and applications. *Forensic Sci. Int.*, 172(1), 1-9.

Albertson, R.C., Streelman, J.T., Kocher, T.D. & Yelick, P.C. (2005). Integration and evolution of the cichlid mandible: The molecular basis of alternate feeding strategies. *Proc. Natl. Acad. Sci. U.S.A.*, 102(45): 16287-16292.

Altenberg, L. (1994) The evolution of evolvability in genetic programming. In Kinnear Jr., K.E. ed. *Advances in Genetic Programming 3*. Cambridge: MIT Press. pp. 47-74.

Altenberg, L. (2005). Modularity in evolution: some low-level questions. In Callebaut, W. & Rasskin-Gutman, D. eds. *Modularity: Understanding the Development and Evolution of Complex Natural Systems.* Cambridge: MIT Press. pp. 99-128.

Altmann, J. & Alberts, S.C. (2005). Growth rates in a wild primate population: ecological influences and maternal effects. *Behav. Ecol. Sociobiol.*, 57(5): 490-501.

Altmann, J., Altmann, S. & Hausfater, G. (1981). Physical maturation and age estimates of yellow baboons, *Papio cynocephalus*, in Amboseli National Park, Kenya. *Am. J. Primatol.*, 1(4): 389-399.

Ammerman A.J. & Cavalli-Sforza, L.L. (1984). *The Neolithic Transition and the Genetics of Populations in Europe*. Princeton: Princeton Univ. Press.

Arbour, J.H. & Brown, C.M. (2014). Incomplete specimens in geometric morphometric analyses. *Methods in Ecology and Evolution*, 5(1): 16-26.

Arther, W. (2002). The emerging conceptual framework of evolutionary developmental biology. *Nature*, 415: 757-764

Atchley, W.R. (1984). Ontogeny, timing of development and genetic variance-covariances structure. *Am. Nat.*, 123(4): 519-540.

Atchley, W.R. & Hall, B.K. (1991). A model for development and evolution of complex morphological structures. *Biol. Rev*., 66(2): 101-157.

Attanasio, C., Nord, A. S., Zhu, Y., Blow, M. J., Li, Z., Liberton, D. K., Morrison, H., Plajzer-Frick, I., Holt, A., Hosseini, R., Phouanenavong, S., Akiyama, J.A., Shoukry, M., Afzal, V., Rubin, E.M, FitzPatrick, D.R., Ren, B., Hallgrímsson,

B., Pennacchio, L.A. & Visel, A. (2013). Fine tuning of craniofacial morphology by distant-acting enhancers. *Science*, 342(6157): 1241006.

Baab, K.L., McNulty, K.P. & Rohlf, F.J. (2012). The shape of human evolution: a geometric morphometrics perspective. *Evol. Anthr.*, 21(4): 151-165.

Bass, W.M. (1995). *Human Osteology: A Laboratory and Field Manual*. Springfield: Missouri Archaeological Society.

Bastir, M. & Rosas, A. (2004). Facial heights: evolutionary relevance of postnatal ontogeny for facial orientation and skull morphology in humans and chimpanzees. *J. Hum. Evol.*, 47(5): 359-381.

Bastir, M. & Rosas, A. (2005). Hierarchical nature of morphological integration and modularity in the human posterior face. *Am. J. Phys. Anthropol.*, 128(1): 26-34.

Bastir, M. & Rosas, A. (2006). Correlated variation between the lateral basicranium and the face: a geometric morphometric study in different human groups. *Arch. Oral. Biol.*, 51(9): 814-824.

Bastir, M. & Rosas, A. (2016). Cranial base topology and basic trends in the facial evolution of *Homo*. *J. Hum. Evol.*, 91: 26-35.

Bastir, M., Rosas, A., Lieberman, D. E. & O'Higgins, P. (2008). Middle cranial fossa anatomy and the origin of modern humans. *Anat. Rec.*, 291(2): 130-140.

Bastir, M., Rosas, A., Stringer, C., Cuétara, J.M., Kruszynski, R., Weber, G.W., Ross, C.F. & Ravosa, M.J. (2010). Effects of brain and facial size on basicranial form in human and primate evolution. *J. Hum. Evol.*, 58(5): 424-431.

Bhat, M., & Enlow, D.H. (1985). Facial variations related to headform type. *Angle Orthod*., 55(4): 269-280.

Bigoni, L., Velemínská, J. & Bruzek, J. (2010). Three-dimensional geometric morphometric analysis of cranio-facial sexual dimorphism in a Central European sample of known sex. *Homo*, 61(1): 16-32.

Blackith, R.E. (1960) A Synthesis of Multivariate Techniques to Distinguish Patterns of Growth in Grasshoppers. *Biometrics*, 16(1): 28-40.

Bock, W.J. (1960). A critique of "Morphological integration". *Evolution*, 14(1): 130-132.

Boehringer, S., van der Lijn, F., Liu, F., Günther, M., Sinigerova, S., Nowak, S., Ludwig, K.U., Herberz, R., Klein, S., Hofman, A., Uitterlinden, A.G., Niessen, W.J., Breteler, M.M., van der Lugt, A., Würtz, R.P., Nöthen, M.M., Horsthemke, B., Wieczorek, D., Mangold, E. & Kayser, M. (2011). Genetic determination of human facial morphology: links between cleft-lips and normal variation. *Eur. J. Hum. Genet.*, 19(11):1192-1197.

Bogin, B. & Smith, B.H. (1996). Evolution of the human life cycle. *Am. J. Hum. Biol.*, 8(6): 703-716.

Bolker, J.A. (2000). Modularity in development and why it matters to Evo-Devo. *Am. Zool.*, 40(5): 770-776.

Bookstein, F.L. (1989). "Size and shape": A comment on semantics. *Syst. Zool.*, 38(2): 173-180.

Bookstein, F.L. (1991). *Morphometric tools for landmark data.* Cambridge: Cambridge University Press.

Bookstein, F.L. (1996). Biometrics, biomathematics and the morphometric synthesis. *Bull. Math. Biol.*, 58(2): 313-365.

Bookstein, F.L. (1997). *Morphometric tools for landmark data: Geometry and Biology.* Cambridge: Cambridge University Press.

Bookstein, F.L., Schäfer, K., Prossinger, H., Seidler, H., Fieder, M., Stringer, C., Weber, G.W., Arsuaga, J.-L., Slice, D.E., Rohlf, F.J. & Recheis, W. (1999). Comparing frontal cranial profiles in archaic and modern *Homo* by morphometric analysis. *Anat. Rec.*, 257(6): 217-224.

Bookstein, F.L. Gunz, P., Mitteroecker, P., Prossinger, H., Schæfer, K. & Seidler, H. (2003). Cranial integration in *Homo*: singular warps analysis of the midsagittal plane in ontogeny and evolution. *J. Hum. Evol.*, 44(2): 167–187.

Boughner, J.C. & Hallgrímsson, B. (2008). Biological spacetime and the temporal integration of functional modules: a case study of dento-gnathic developmental timing. *Dev. Dynam.*, 237(1): 1-17.

Breuker, C.J., Debat, V. & Klingenberg, C.P (2006). Functional evo-devo. *Trends Ecol. Evol.*, 21(9): 488–492.

Bruner, E., Martin- Loeches, M. & Colom, R. (2010). Human midsagittal brain shape variation: patterns, allometry and integration. *J. Anat*., 216(5): 589-599.

Bulmer, M.G. (2003). *Francis Galton: pioneer of heredity and biometry*. Baltimore: Johns Hopkins University Press.

Burke, A.C, Nelson, C.E., Morgan, B.A. & Tabin, C. (1995). Hox genes and the evolution of vertebrate axial morphology. *Development*, 121: 333-346.

Byard, P.J., Poosha, D.V., Satyanarayana, M. & Rao, D.C. (1985). Family resemblance for components of craniofacial size and shape. *J. Craniofac. Genet.*, 5: 229-238.

Carmody, K.A., Mooney, M.P., Cooper, G.M., Bonar, C.J., Siegel, M.I., Dumont, E.R. & Smith, T.D. (2008). Relationship of premaxillary bone and its sutures to deciduous dentition in nonhuman primates. *Cleft Palate Craniofac. J.*, 45(1): 93-100.

Chai, Y., Jiang, X., Ito, Y., Bringas, P., Han, J., Rowitch, D.H., Soriano, P., McMahon, A.P. & Sucov, H.M. (2000). Fate of the mammalian cranial neural crest during tooth and mandibular morphogenesis. *Development*, 127(8), 1671-1679.

Chen, H., Liu, C.T. & Yang, S.S. (1981). Achondrogenesis: A review with special consideration of achondrogenesis type II (Langer-Saldino). *Am. J. Med. Genet*., 10: 379-394.

Chen, Z.J., He, Y., Rosa-Neto, P., Gong, G. & Evans, A.C. (2011). Age-related alterations in the modular organization of structural cortical network by using cortical thickness from MRI. *Neuroimage*, 56(1): 235-245.

Chernoff, B. & Magwene, P.M. (1999). Morphological Integration: Forty Years Later. In Olsen, E.C. & Miller, R.L. eds. *Morphological Integration*. Chicago: University of Chicago Press. pp. 319-353.

Cheverud, J.M. (1982). Phenotypic, genetic and environmental morphological integration in the cranium. *Evolution*, 36: 499-516.

Cheverud, J.M. (1984). Quantitative genetics and developmental constraints on evolition and selection. *J. Theor. Biol.*, 110: 155-171.

Cheverud, J.M. (1988). A comparison of genetic and phenotypic correlations. *Evolution*, 42: 958-968.

Cheverud, J.M. (1989). A comparative analysis of morphological variation patterns in the papionins. *Evolution*, 43: 1737-1747.

Cheverud, J.M. (1995). Morphological integration in the saddle-back tamarin (*Saguinus fuscicollis*) cranium. *Am. Nat.*, 145: 63-89.

Cheverud, J.M. (1996a). Developmental integration and the evolution of pleiotropy. *Am. Zool.*, 36(1): 44-50.

Cheverud, J.M. (1996b). Quantitative genetic analysis of cranial morphology in the cotton-top (*Saguinus oedipus*) and saddle-back (*S. fuscicollis*) tamarins. *J. Evol. Biol.*, 9: 5-42.

Cheverud, J.M., Buikstra, J.E., 1982. Quantitative genetics of skeletal nonmetric traits in the rhesus macaques of Cayo Santiago. III. Relative heritability of skeletal nonmetric and metric traits. *Am. J. Phys. Anthropol.*, 59: 151-155.

Cheverud, J.M., Dow, M.M. & Leutenegger, W. (1985). The quantitative assessment of phylogenetic constraints in comparative analyses: sexual dimorphism in body weight among primates. *Evolution*, 39(6): 1335-1351.

Cheverud, J.M., Kohn, L.A.P., Konigsberg, L.W. & Leigh, S.R. (1992). Effects of fronto-occipital artificial cranial vault modification on the cranial base and face. *Am. J. Phys. Anthropol.*, 88: 323-345.

Cheverud, J.M., Rutledge, J. & Atchley, W. (1983). Quantitative genetics of development: Genetic correlations among age-specific trait values and the evolution of ontogeny. *Evolution*, 37: 895-905.

Cheverud, J.M., Wagner, G. & Dow, M. (1989). Methods for the comparative analysis of variation patterns. *Syst. Zool*., 38: 201-213.

Cheverud, J.M., Schmitz, A. & Roseman, C. (2009). Parallel evolution of papionin craniofacial morphology. *Am. J. Phys. Anthropol*., 138(S48): 105.

Clarke, B. (2008). Normal Bone Anatomy and Physiology. *Clin. J. Am. Soc. Nephrol.*, 3(S3): S131-S139.

Clarke, J.D.W. & Tickle, C. (1999). Fate maps old and new. *Nat. Cell Biol.*, 1(4): E103- E109.

Clarke, S.L. (2013). *Developmental Enhancers: Ancient Origins, Neofunctionalization and Pleiotropy.* PhD Theses, Department of Genetics, Stanford University.

Claude, J. (2008). *Morphometrics with R*. New York: Springer.

Cock, A.G. (1966) Genetical aspects of metrical growth and form in animals. *Q Rev Biol*, 41: 131-190.

Collard, M. & O'Higgins, P. (2001). Ontogeny and homoplasy in the *papionin* monkey face. *Evol. Dev.*, 3(5): 322-331.

Corruccini, R.S. (1976). The interaction between neurocranial and facial shape in hominid evolution. *Homo*, 26: 136-140.

Corruccini, R.S. (1977). Integration of occluding structures in hominoid molars. *J. Dent. Res.*, 56(2): 190-190.

Couly, G.F., Cotley, P.M., Le Douarin, N.M. (1992). The developmental fate of the cephalic mesoderm in quail-chick chimeras. *Development*, 114: 1-15.

Csardi, G. & Nepusz, T. (2006). The igraph software package for complex network research, *InterJournal, Complex Syst.*, 1695.

Darwin, C. (1859) *On the Origin of Species by Means of Natural Selection, Or, the Preservation of Favoured Races in the Struggle for Life*. London: J. Murray.

Dayal, M.R., Kegley, A.D., Štrkalj, G., Bidmos, M.A., & Kuykendall, K.L. (2009). The history and composition of the Raymond A. Dart Collection of Human Skeletons at the University of the Witwatersrand, Johannesburg, South Africa. *Am. J. Phys. Anthropol*., 140(2): 324-335.

Disotell, T.R., Honeycutt R.L. & Ruvolo M. (1992). Mitochondrial DNA phylogeny of the Old-World monkey tribe *Papionini*. *Mol. Biol. Evol.*, 9(1): 1-13.

Dryden, I.L. & Mardia, K.V. (1998). *Statistical Shape Analysis*. Chichester: John Wiley and Sons.

Duterloo, H.S., & Enlow, D.H. (1970). A comparative study of cranial growth in Homo and Macaca. *Am. J. Anat.*, 127(4): 357-367.

Echelard, Y., Epstein, D.J., St-Jacques, B., Shen, L., Mohler, J., McMahon, J.A. & McMahon, A.P. (1993). Sonic hedgehog, a member of a family of putative signaling molecules, is implicated in the regulation of CNS polarity. *Cell*, 75 (7): 1417-1430.

Eldredge, N. (1972). Systematics and evolution of *Phacops rana* (Green, 1832) and *Phacops iowensis* Delo, 1935 (Trilobita) from the Middle Devonian of North America. *Bull. Am. Mus. Nat. Hist.*, 147: 45–114.

Enlow, D.H. (1968). *The Human Face: An Account of the Postnatal Growth and Development of the Craniofacial Skeleton*. New York: Hoeber Medical Division, Harper & Row.

Enlow, D.H. (1990). *Facial growth*, 3rd Edition. Philadelphia: W B. Saunders.

Enlow, D.H. & Azuma, M. (1975) Functional growth boundaries in the human and mammalian face. In: Bergsma, D., Langman, J. & Paul, N.W., editors. *Morphogenesis and Malformation of the Face and the Brain*. New York: Alan R. Liss. pp. 217–230.

Enlow, D.H. & Hans, M.G. (1996). *Essentials of Facial Growth*. Philadelphia: W.B. Saunders Company.

Enlow, D.H. & McNamara Jr, J.A. (1973). The neurocranial basis for facial form and pattern. *Angle Orthod*., 43(3): 256-270.

Enlow, D.H., Moyers, R.E., Hunter, W.S. & McNamara Jr,.J.A. (1969) A procedure for the analysis of intrinsic facial form and growth: An equivalent-balance concept. *Am. J. Orthod*., 56(1): 6-23.

Enlow, D.H., Kuroda, T. & Lewis, A.B. (1971a). Intrinsic craniofacial compensations. *Angle Orthod*., 41(4): 271-285.

Enlow, D.H., Kuroda, T. & Lewis, A.B. (1971b). The morphological and morphogenetic basis for craniofacial form and pattern. *Angle Orthod*., 41(3): 161-188.

Enlow, D.H., DiGangi, D., McNamara, J.A. & Mina, M. (1988). An evaluation of the morphogenic and anatomic effects of the functional regulator utilizing the counterpart analysis. *Eur. J. Orthodont*., 10(1): 192-202.

Escoufier, Y. (1973). Le Traitement des Variables Vectorielles. *Biometrics*, 29(4): 751-760.

Esteve-Altava, B., Rasskin-Gutman, D. (2014) Theoretical morphology of tetrapod skull networks. *C. R. Palevol.*, 13(1): 41-50.

Esteve-Altava, B., Marugán-Lobón, J., Botella, H. & Rasskin-Gutman, D. (2011). Network Models in Anatomical Systems. *J. Anthropol. Sci*., 89: 1-10.

Esteve-Altava, B., Marugán-Lobón, J., Botella, H., Bastir, M., Rasskin-Gutman, D. (2013a). Grist for Riedl's Mill: A network model perspective on the integration and modularity of the human skull. *J. Exp. Zool. (Mol. Dev. Evol.*), 320(8): 489-500.

Esteve-Altava, B., Marugán-Lobón, J., Botella, H. & Rasskin-Gutman, D. (2013b). Structural constraints in the evolution of the tetrapod skull complexity: Williston's law revisited using network models. *Evol. Biol.*, 40(2), 209-219.

Fleagle, J.G., Gilbert, C.C. & Baden, A.L. (2010). Primate cranial diversity. *Am. J. Phys. Anthropol*., 142(4): 565-578.

Forey, P.L. (1998). *History of the Coelacanth Fishes*. New York : Chapman & Hall.

Fowlkes, J.L., Thrailkill, K.M., Liu, L., Wahl, E.C., Bunn, R.C., Cockrell, G.E., Perrien, D.S., Aronson, J. & Lumpkin, C.K. Jr. (2006). Effects of systemic and local administration of recombinant human IGF-I (rhIGF-I) on de novo bone formation in an aged mouse model. *J. Bone Miner. Res.*, 21: 1359-1366.

Freedman, L. (1962). Growth of muzzle length relative to calvaria length in *Papio*. *Growth*, 26: 117-128.

Freeman, S. & Herron, J.C. (2004) *Evolutionary Analysis* (3rd edition). Upper Saddle River: Pearson Prentice Hall.

Frost, S.R., Marcus, L.F., Bookstein, F.L., Reddy, D.P. & Delson, E. (2003). Cranial allometry, phylogeography and systematics of large-bodied *papionins* (primates: *Cercopithecinae*) inferred from geometric morphometric analysis of landmark data. *Anat. Rec. A Discov. Mol. Cell Evol. Biol.*, 275(2): 1048-1072.

Funatsu, M., Sato, K. & Mitani, H. (2006). Effects of Growth Hormone on Craniofacial Growth. *Angle Orthod.*, 76(6): 970-977.

Galton, F. (1888). Co-relations and their measurement, chiefly from anthropometric data. *Proc. R. Soc.*, 45: 135-145.

Gans C (1993) Evolutionary origins of the vertebrate skull. In Hanken, J. & Hall, B.K. *The Vertebrate Skull vol. II. Patterns of Structural and Systematic Diversity.* Chicago: The University of Chicago Press. pp. 1-35.

Gans, C. & Northcutt, R.G. (1983). Neural crest and the origin of vertebrates: a new head. *Science*, 220: 268-273.

Gavan, J.A. & Hutchinson, T.C. 1973. The problem of age estimation: A study using rhesus monkeys (*Macaca mulatta*). *Am. J. Phys. Anthropol.*, 38(1): 69-81.

Gayon, J. (2000). History of the concept of allometry. *Amer. Zool.*, 40: 748-758.

Gilbert, C.C. (2007). Craniomandibular morphology supporting the diphyletic origin of mangabeys and a new genus of the *Cercocebus/Mandrillus* clade, *Procercocebus*, *J. Hum. Evol.*, 53(1): 69-102.

Gingerich, P.D. & Winkler, D.A. (1979). Patterns of variation and correlation in the dentition of the red fox, Vulpes vulpes. *J. Mammal.*, 60(4): 691-704.

Giustina, A., Mazziotti, G. & Canalis, E. (2008). Growth Hormone, Insulin-Like Growth Factors, and the Skeleton. *Endocr. Rev.*, 29(5): 535-559.

Gonzalez, P.N., Kristensen, E., Morck, D.W., Boyd, S. & Hallgrímsson, B. (2013). Effects of growth hormone on the ontogenetic allometry of craniofacial bones. *Evol. Dev.*, 15(2): 133–145.

González- José, R., Van der Molen, S., González- Pérez, E. & Hernandez, M. (2004). Patterns of phenotypic covariation and correlation in modern humans as viewed from morphological integration. *Am. J. Phys. Anthropol.*, 123(1): 69-77.

Goodrich, E.S. (1958). Studies on the Structure and Development of Vertebrates. New York: Dover Publications.

Gould, S.J. (1967). Evolutionary patterns in pelycosaurian reptiles: a factor-analytic study. *Evolution*, 21(2): 385-401.

Gould, S.J. (1970). Evolutionary paleontology and the science of form. *Earth-Sci. Rev.*, 6(2): 77-119.

Gould, S.J. (1971). Muscular mechanics and the ontogeny of swimming in scallops. *Palaeontology*, 14: 61-94.

Gould, S.J. (1974). The origin and function of "bizarre" structures: antler size and skull size in the "Irish Elk", *Megaloceros giganteus*. *Evolution*, 28(2): 191-220.

Gould, S.J. (1977). *Ontogeny and Phylogeny*. Belknap Press: Cambridge, MA.

Gould, S.J. (1980a). Is a new and general theory of evolution emerging? *Paleobiology*, 6(1):119-130.

Gould, S.J. (1980b). The evolutionary biology of constraint. *Daedalus*, 109(2): 39-52.

Gould, S.J. & Garwood, R.A. (1969). Levels of integration in mammalian dentitions: an analysis of correlations in *Nesophontes micrus* (Insectivora) and *Oryzomys couesi* (Rodentia). *Evolution*, 23(2): 76-300.

Gould, S.J. & Lewontin, R.C. (1979). The spandrels of San Marco and the Panglossian paradigm: a critique of the adaptationist programme. *Proc. R. Soc. B*, 205(1161): 581-598.

Gross, J.B. & Hanken, J. (2008). Review of fate-mapping studies of osteogenic cranial neural crest in vertebrates. Dev. Biol., 317(2), 389-400.

Groves, C.P. (2001). *Primate Taxonomy*. Washington DC: Smithsonian Institution Press.

Grubb, P., Butynski, T.M., Oates, J.F., Bearder, S.K., Disotell, T.R., Groves, C.P. & Struhsaker, T.T. (2003). Assessment of the Diversity of African Primates. *Int. J. Primatol.*, 24(6): 1301-1357.

Gunz, P., Mitteroecker, P., Bookstein, F.L. & Weber, G.W. (2004). Computer aided reconstruction of incomplete human crania using statistical and geometrical estimation methods. *Enter the Past: Computer Applications and Quantitative Methods in Archaeology*. BAR International Series 1227. Oxford: Archaeopress: 92-94.

Gunz, P., Mitteroecker, P., Neubauer, S., Weber, G.W. & Bookstein, F.L. (2009). Principles for the virtual reconstruction of hominin crania. *Journal of Human Evolution*, 57(1): 48-62.

Hall, B.K. & Gillis, J.A. (2013). Incremental evolution of the neural crest, neural crest cells and neural crest-derived skeletal tissues. *J. Anat.*, 222(1): 19-31.

Hallgrímsson, B., Wilmore, K. & Hall, B.K.H. (2002). Canalization, Developmental Stability, and Morphological Integration in Primate Limbs. *Am. J. Phys. Anthropol.* (Yearbook) S45: 131-158.

Hallgrímsson, B., Dorval, C.J., Zelditch, M.L., & German, R.Z. (2004). Craniofacial variability and morphological integration in mice susceptible to cleft lip and palate. *J. Anat*., 205(6), 501-517.

Hallgrímsson B., Lieberman, D.E., Liu, W., Ford-Hutchinson, A.F., Jirik, F.R. (2007a). Epigenetic interactions and the structure of phenotypic variation in the cranium. *Evol. Dev*., 9: 76-91.

Hallgrímsson, B., Lieberman, D.E, Young, N.M. Parsons, T. & Wat, S. (2007b). Evolution of covariance in the mammalian skull. In: Bock, G. & Goode, J., editors. Tinkering: The Microevolution of Development: Novartis Foundation Symposium 284. Chichester: Wiley. pp. 164-190.

Hallgrímsson, B., Jamniczky, H., Young, N.M., Rolian, C., Parsons, T.E., Boughner, J.C. & Marcucio, R.S. (2009). Deciphering the palimpsest: studying the relationship between morphological integration and phenotypic covariation. *Evol. Biol.*, 36(4): 355-376.

Harvati, K. & Weaver, T.D. (2006). Human cranial anatomy and the differential preservation of population history and climate signatures. *Anat. Rec.* 288A: 1225-1233.

Heuzé, Y., Boyadjiev, S.A., Marsh, J.L., Kane, A.A., Cherkez, E., Boggan, J.E. & Richtsmeier, J.T. (2010). New insights into the relationship between suture closure and craniofacial dysmorphology in sagittal nonsyndromic craniosynostosis. *J. Anat*., 217(2): 85-96.

Holland, D., Chang, L., Ernst, T.M., Curran, M., Buchthal, S.D., Alicata, D., Skranes, J., Johansen, H., Hernandez, A., Yamakawa, R., Kuperman, J.M. & Dale, A.M. (2014). Structural Growth Trajectories and Rates of Change in the First 3 Months of Infant Brain Development. *JAMA Neurol.* Prepublished online. doi:10.1001/jamaneurol.2014.1538.

Holland, L.Z., Albalat, R., Azumi, K., Benito-Gutiérrez, È., Blow, M.J., Bronner-Fraser, M., Brunet, F., Butts, T., Candiani, S., Dishaw, L.J., Ferrier, D.E.K., Garcia-Fernàndez, J., Gibson-Brown, J.J., Gissi, C., Godzik, A., Hallböök, F., Hirose, D., Hosomichi, K., Ikuta, T., Inoko, H., Kasahara, M., Kasamatsu, J., Kawashima, T., Kimura, A., Kobayashi, M., Kozmik, Z., Kubokawa, K., Laudet, V., Litman, G.W., McHardy, A.C., Meulemans, D., Nonaka, M., Olinski, R.P., Pancer, Z., Pennacchio, L.A., Pestarino, M., Rast, J.P., Rigoutsos, I., Robinson-Rechavi, M., Roch, G., Saiga, H., Sasakura, Y., Satake, M., Satou, Y., Schubert, M., Sherwood, N., Shiina, T., Takatori, N., Tello, J., Vopalensky, P., Wada, S., Xu, A., Ye, Y., Yoshida, K., Yoshizaki, F., Yu, J., Zhang, Q., Zmasek, C.M., de Jong, P.J., Osoegawa, K., Putnam, N.H., Rokhsar, D.S., Satoh, N. & Holland, P.W.H. (2008). The amphioxus genome illuminates vertebrate origins and cephalochordate biology. *Genome Res.*, 18(7): 1100-1111.

Holm, S. (1979). A simple sequentially rejective multiple test procedure. *Scand. J. Stat.*. 6(2): 65-70.

Holton, N.E., Franciscus, R.G., Marshall, S.D., Southard, T.E. & Nieves, M.A. (2011). Nasal septal and premaxillary developmental integration: implications for facial reduction in *Homo*. *Anat. Rec.*, 294(1): 68-78.

Huxley, J.S. (1932). *Problems of Relative Growth*. London: Methuen.

Huxley, T.H. (1863). *Evidence as to Man's Place in Nature*. London: Williams and Norgate.

Ito, T., Nishimura, T.D., Hamada, Y. & Takai, M. (2015). Contribution of the maxillary sinus to the modularity and variability of nasal cavity shape in Japanese macaques. *Primates*, 56(1): 11-19.

Jacobson, A.G. (1993). Somitomeres: Mesodermal Segments of the Head and Trunk. in Hanken, J. & Hall, B.K. eds. *The Skull. Volume 1. Development*. Chicago: University of Chicago Press. Pp. 42-76.

Jeffery, N. (2002). Differential regional brain growth and rotation of the prenatal human tentorium cerebelli. *J. Anat*., 200(2): 135-144.

Jiang, X., Iseki, S., Maxson, R.E., Sucov, H.M. & Morriss-Kay, G.M. (2002) Tissue Origins and Interactions in the Mammalian Skull Vault, Dev. Biol. 241(1): 106-116.

Jolicoeur, P. & Mosimann J.E. (1960). Size and shape variation in the painted turtle, a principal component analysis. *Growth*, 24: 339-354.

Jolicoeur, P. (1963). The multivariate generalization of the allometry equation. *Biometrics*, 19(3): 497-499.

Jolly, C.J. (1993). Species, subspecies and baboon systematics. In: Kimbel, W.H. & Martin, L.B., editors. *Species, Species Concepts and Primate Evolution*. New York: Plenum Press. pp. 67-107.

Jolly, C.J. (2003). Cranial anatomy and baboon diversity. *Anat. Rec. A Discov. Mol. Cell Evol. Biol.*, 275A:1043-1047.

Kahumbu, P. & Eley R.M. (1991). Teeth emergence in wild olive baboons in Kenya and formulation of a dental schedule for aging wild baboon populations. *Am. J. Primatol.*, 23: 1-9.

Kardong, K. V. (2002). *Vertebrates: comparative anatomy, function, evolution*. Boston: McGraw-Hill.

Kendall, D.G. (1984). Shape manifolds, procrustean metrics, and complex projective spaces. *Bull. London Math. Soc.*, 16(2): 81-121.

Klingenberg, C.P. (2008) Morphological integration and developmental modularity. *Annu. Rev. Ecol. Evol. Syst.*, 39: 115-132

Klingenberg, C.P. (2009). Morphometric integration and modularity in configurations of landmarks: tools for evaluating *a priori* hypotheses. *Evol. Dev*,.11(4): 405-421.

Klingenberg, C.P. (2010). Evolution and development of shape: integrating quantitative approaches. *Nat. Rev. Genet.*, 11(9): 623-635.

Klingenberg, C.P. (2013). Cranial integration and modularity: insights into evolution and development from morphometric data. *It. J. Mammal*., 24(1): 43-58.

Klingenberg, C.P. (2014). Studying morphological integration and modularity at multiple levels: concepts and analysis. *Phil. Trans. R. Soc. B*, 369: 20130249.

Klingenberg, C.P. (2016). Size, shape, and form: concepts of allometry in geometric morphometrics. *Dev. Genes Evol.*, 226(3): 113-137.

Klingenberg, C.P. & Marugán-Lobón, J. (2013). Evolutionary covariation in geometric morphometric data: analyzing integration, modularity, and allometry in a phylogenetic context. *Syst. Biol.*, 62(4): 591-610.

Klingenberg, C.P., Mebus, K. & Auffray, J.-C. (2003). Developmental integration in a complex morphological structure: how distinct are the modules in the mouse mandible? *Evol. Dev.*, 5(5): 522-531.

Knußmann, R., editor. (1988). *Anthropologie. Handbuch der vergleichenden Biologie des Menschen*. Stuttgart: Fischer.

Kohn, L.A.P., Leigh, S.R., Jacobs, S.C. & Cheverud, J. (1993). Effects of annular cranial vault modification on the cranial base and face. *Am. J. Phys. Anthropol.*, 90:147-168.

Koyabu, D., Maier, W & Sánchez-Villagra, M.R. (2012). Paleontological and developmental evidence resolve the homology and dual embryonic origin of a mammalian skull bone, the interparietal. *Proc. Natl. Acad. Sci. U.S.A.*, 109(35): 14075-14080.

Krogman, W.M. & İşcan, Y.M. (1986). *The Human Skeleton in Forensic Medicine*. Springfield, IL: Charles C. Thomas.

Kulemeyer, C., Asbahr, K., Gunz, P., Frahnert, S. & Bairlein, F. (2009). Functional morphology and integration of corvid skulls - a 3D geometric morphometric approach. *Front. Zool.*, 6:2.

Kuratani, S. (2004) Evolution of the vertebrate jaw: comparative embryology and molecular developmental biology reveal the factors behind evolutionary novelty. *J. Anat.*, 205(5): 335-347.

Kuratani, S. & Schilling, T. (2008). Head segmentation in vertebrates. *Integr. Comp. Biol.*, 48(5): 604-610.

Kuratani, S., Adachi, N., Wada, N. Oisi, Y. & Sugahara, F. (2013). Developmental and evolutionary significance of the mandibular arch and prechordal⁄premandibular cranium in vertebrates: revising the heterotopy scenario of gnathostome jaw evolution. *J. Anat.*, 222: 41-55.

Kuykendall, K.L. (1992). Dental Development in Chimpanzees (Pan troglodytes) and Implications for Dental Development Patterns in Fossil Hominids. PhD Theses, Department of Anthropology, Washington University.

Lande, R. (1979). Quantitative genetic analysis of multivariate evolution, applied to brain: body size allometry. *Evolution*, 33(1): 402-416.

Larsen, W.J (2001). *Human Embryology* (3rd edition). London: Churchill Livingstone.

Leamy, L. (1977). Genetic and environmental correlations of morphometric traits in randombred house mice. *Evolution*, 31: 357-369.

Leigh, S.R. (2006). Cranial ontogeny of Papio baboons (*Papio hamadryas*). *Am. J. Phys. Anthropol.*, 130: 71-84.

Leigh, S.R. (2007). Homoplasy and the evolution of ontogeny in papionin primates. *J. Hum. Evol.*, 52(5): 536-558.

Leigh, S.R. & Cheverud, J.M. (1991). Sexual dimorphism in the baboon facial skeleton. *Am. J. Phys. Anthropol.*, 84(2): 193-208.

Leigh, S.R., Shah, N.F. & Buchanan, L.S. (2003). Ontogeny and phylogeny in papionin primates. *J. Hum. Evol.*, 45(4): 285-316.

Lele, S. & Richtsmeier, J.T. (1991). Euclidean distance matrix analysis: A coordinate‐free approach for comparing biological shapes using landmark data. *American Journal of Physical Anthropology*, 86(3): 415-427.

Lele, S. & Richtsmeier, J.T. (2001). *An Invariant Approach to Statistical Analysis of Shapes*. London: Chapman and Hall-CRC press.

Lieberman, D. (2011a). Epigenetic integration, complexity, and evolvability of the human head. In: Hallgrímsson, B. & Hall, B.K., editors. *Epigenetics: Linking Genotype and Phenotype in Development and Evolution*. Berkeley: University of California Press.

Lieberman, D. (2011b). *The evolution of the human head*. Cambridge: Harvard University Press.

Lieberman, D.E. & McCarthy, R.C. (1999). The ontogeny of cranial base angulation in humans and chimpanzees and its implications for reconstructing pharyngeal dimensions. *J. Hum. Evol.*, 36: 487-517.

Lieberman D.E., Mowbray K.M. and Pearson O.M. (2000a) Basicranial influences on overall cranial shape. *J. Hum. Evol.*, 38: 291-315.

Lieberman, D.E., Ross, C.F. & Ravosa, M.J. (2000b). The primate cranial base: ontogeny, function and integration. *Am. J. Phys. Anthropol.*, 113(s 31): 117-169.

Lieberman, D.E., McBratney, B.M. & Krovitz, G. (2002). The evolution and development of cranial form in *Homo sapiens*. *Proc. Natl. Acad. Sci. U.S.A.*, 3(99): 1134-1139.

Lieberman, D.E., Hallgrímsson, B., Liu, W., Parsons, T.E. & Jamniczky, H.A. (2008). Spatial packing, cranial base angulation, and craniofacial shape variation in the mammalian skull: testing a new model using mice. *J. Anat.*, 212(6): 720-735.

Liu, F., van der Lijn, F., Schurmann, C., Zhu, G., Chakravarty, M.M., Hysi, P.G., Wollstein, A., Lao, O., de Bruijne, M., Ikram, M.A., van der Lugt, A., Rivadeneira, F., Uitterlinden, A.G., Hofman, A., Niessen, W.J., Homuth, G., de Zubicaray, G., McMahon, K.L., Thompson, P.M., Daboul, A., Puls, R., Hegenscheid, K., Bevan, L., Pausova, Z., Medland, S.E., Montgomery, G.W., Wright, M.J., Wicking, C., Boehringer, S., Spector, T.D., Paus, T., Martin, N.G., Biffar, R. & Kayser, M. (2012). A genome-wide association study identifies five loci influencing facial morphology in Europeans. *PLoS Genet.*, 8(9):e1002932.

Liu, Z.J., Shcherbatyy, V., Gu, G. & Perkins, J.A. (2008). Effects of tongue volume reduction on craniofacial growth: A longitudinal study on orofacial skeletons and dental arches. *Arch. Oral Biol.*, 53(10): 991-1001.

Lockwood, C.A. (2007). Adaptation and functional integration in primate phylogenetics. *J. Hum. Evol.*, 52(5): 490-503.

Lofsvold, D. (1986). Quantitative genetics of morphological differentiation in *Peromyscus*. I. Tests of the homogeneity of genetic covariance structure among species and subspecies. *Evolution*, 40(3): 559-573.

Maddux, S.D. & Butaric, L.N. (2017). Zygomaticomaxillary morphology and maxillary sinus form and function: How spatial constraints influence pneumatization patterns among modern humans. Anat. Rec., 300(1): 209-225.

Mantel, N. (1967). The detection of disease clustering and a generalized regression approach. *Cancer Res.*, 27(2): 209–220.

Marcus, L., Hingst-Zaher, E. & Zaher, H. (2000). Application of landmark morphometrics to skulls representing the orders of living mammals. *Hystrix*, 11(1): 27-47.

Mardia, K.V., Kent, J.T. & Bibby, J.M. (1979). *Multivariate Analysis*. New York: Academic Press.

Marroig, G and Cheverud, J.M. (2001) A comparison of phenotypic variation and covariation patterns and the role of phylogeny, ecology and ontogeny during cranial evolution of New World Monkeys. *Evolution*, 55: 2576-2600.

Marroig, G. & Cheverud, J.M. (2005) Size as a line of least resistance: diet and adaptive morphological radiation in New World monkeys? *Evolution*, 59(5): 1128-1142.

Marroig, G. & Cheverud, J.M. (2010) Size as a line of least resistance II: direct selection on size or correlated response due to constraints? *Evolution*, 64(5): 1470-1488.

Marroig, G. de Vivo, M. & Cheverud, J.M. (2004). Cranial evolution in sakis (Pithecia, Platyrrhini) II: evolutionary processes and morphological integration. *J. Evol. Biol.*, 17: 144-155.

Marroig, G., Shirai, L.T., Porto, A., de Oliveira, F.B. & De Conto, V. (2009). The evolution of modularity in the mammalian skull II: evolutionary consequences. *Evol. Biol.*, 36(1): 136-148.

Martin, R.D. (1983). *Human Brain Evolution in an Ecological Context*. New York: American Museum of Natural History.

Martínez-Abadías, N., Esparza, M., Sjøvold, T., González‐José, R., Santos, M., & Hernández, M. (2009a). Heritability of human cranial dimensions: comparing the evolvability of different cranial regions. *Journal of Anatomy*, 214(1): 19-35.

Martínez-Abadías, N., Paschetta, C., de Azevedo, S., Esparza, M., & González-José, R. (2009b). Developmental and genetic constraints on neurocranial globularity: insights from analyses of deformed skulls and quantitative genetics. *Evol. Biol.*, 36(1): 37-56.

Martínez-Abadías, N., Heuze, Y., Wang, Y., Jabs, E.W., Aldridge, K. & Richtsmeier, J.T. (2011). FGF/FGFR signaling coordinates skull development by modulating magnitude of morphological integration: evidence from Apert syndrome mouse models. *PLoS ONE*, 6(10): e26425.

Martínez-Abadías, N., Esparza, M., Sjøvold, T., González-José, R., Santos, M., Hernández, M. & Klingenberg, C.P. (2012). Pervasive genetic integration directs the evolution of human skull shape. *Evolution*, 66(4): 1010-1023.

Maynard Smith, J., Burian, R.M., Kaufmann, S.A., Alberch, P., Campbell, J., Goodwin, B.C., Lande, R., Raup, D. & Wolpert, L. (1985). Developmental constraints and evolution: A perspective from the Mountain Lake conference on development and evolution. Quarterly Review of Biology, 60, 265-287.

Mayr, E. (1991). One Long Argument: Charles Darwin and the Genesis of Modern Evolutionary Thought. Cambridge: Harvard University Press.

McBratney-Owen, B., Iseki, S., Bamforth, S.D., Olsen, B.R. & Morriss-Kay, G.M. (2008). Development and tissue origins of the mammalian cranial base. *Dev. Biol.*, 322(1): 121-132.

McCarthy, R.C. & Lieberman, D.E. (2001). Posterior maxillary (PM) plane and anterior cranial architecture in primates. *Anat. Rec*., 264: 247-260.

McCollum, M.A., Sherwood, C.C., Vinyard, C.J., Lovejoy, C.O. & Schachat, F. (2006). Of muscle-bound crania and human brain evolution: The story behind the MYH16 headlines. *J. Hum. Evol.*, 50(2): 232-236.

Menegaz, R.A., Sublett, S.V., Figueroa, S.D., Hoffman, T.J., Ravosa, M.J. & Aldridge, K. (2010). Evidence for the influence of diet on cranial form and robusticity. *Anat. Rec*., 293(4): 630-641.

Meyer, M., Fu, Q., Aximu-Petri, A., Glocke, I., Nickel, B., Arsuaga, J.L., Martínez, I., Gracia, A., de Castro, J.M., Carbonell E. & Pääbo, S. (2014). A mitochondrial genome sequence of a hominin from Sima de los Huesos. *Nature*, 505(7483): 403-406.

Mezey, J.G., Cheverud, J.M., & Wagner, G.P. (2000). Is the genotype-phenotype map modular?: a statistical approach using mouse quantitative trait loci data. *Genetics*, 156(1): 305-311.

Mitteroecker, P. (2009). The developmental basis of variational modularity: insights from quantitative genetics, morphometrics, and developmental biology. *Evol. Biol.*, 36: 377–385.

Mitteroecker, P. & Bookstein, F. (2007). The conceptual and statistical relationship between modularity and morphological integration. *Syst. Biol*., 56(5): 818-36.

Mitteroecker, P. & Bookstein, F. (2008). The evolutionary role of modularity and integration in the hominoid cranium. *Evolution*, 62(4): 943-958.

Mitteroecker, P. & Huttegger, S.M. (2009). The concept of morphospaces in evolutionary and developmental biology: mathematics and metaphors. *Biol. Theory*, 4(1): 54-67.

Mitteroecker, P., Gunz, P., Bernhard, M., Schaefer, K. & Bookstein, F.L. (2004). Comparison of cranial ontogenetic trajectories among great apes and humans. *J. Hum. Evol.*, 46(6): 679-698.

Mitteroecker, P., Gunz, P., Neubauer, S. & Müller, G. (2012). How to explore morphological integration in human evolution and development? *Evol. Biol.*, 39(4): 536-553.

Mocella, V., Brun, E., Ferrero, C., & Delattre, D. (2015). Revealing letters in rolled Herculaneum papyri by X-ray phase-contrast imaging. *Nat. commun*., 6: 5895.

Monteiro, L.R. (1999). Multivariate regression models and geometric morphometrics: the search for causal factors in the analysis of shape. *Syst. Biol.*, 48(1): 192-199.

Morriss-Kay, G.M. (2001). Derivation of the mammalian skull vault. *J. Anat.*, 199(1-2): 143-151.

Morriss-Kay, G.M. & Wilkie, A.O.M. (2005) Growth of the normal skull vault and its alteration in craniosynostosis: insights from human genetics and experimental studies. *J. Anat.*, 207(5): 637-653.

Moss, M. L. (1968). A theoretical analysis of the functional matrix. Acta Biotheoretica, 18(1): 195-202.

Moss, M. L. (1997a). The functional matrix hypothesis revisited. 1. The role of mechanotransduction. Am. J. Orthod. Dentofacial Orthop., 112(1): 8-11.

Moss, M. L. (1997b). The functional matrix hypothesis revisited. 2. The role of an osseous connected cellular network. Am. J. Orthod. Dentofacial Orthop., 112(2), 221-226.

Moss, M. L. (1997c). The functional matrix hypothesis revisited. 3. The genomic thesis. Am. J. Orthod. Dentofacial Orthop., 112(3), 338-342.

Moss, M. L. (1997d). The functional matrix hypothesis revisited. 4. The epigenetic antithesis and the resolving synthesis. Am. J. Orthod. Dentofacial Orthop., 112(4), 410-417.

Moss, M. L., & Salentijn, L. (1969). The primary role of functional matrices in facial growth. American journal of orthodontics, 55(6), 566-577.

Moss, M. L., & Young, R. W. (1960). A functional approach to craniology. American journal of physical anthropology, 18(4), 281-292.

Müller, F. & O'Rahilly, R. (1991). Development of anencephaly and its variants. *Am. J. Anat.*, 190(3): 193-218.

Neaux, D., Guy, F., Gilissen, E., Coudyzer, W., Vignaud, P., & Ducrocq, S. (2013). Facial orientation and facial shape in extant great apes: a geometric morphometric analysis of covariation. *PloS ONE*, 8(2): e57026.

Needham, J. (1933). On the dissociability of the fundamental processes in ontogenesis. *Biol. Rev*., 8(2): 180-223.

Needham, J. (1936). *Order and life*. New Haven: Yale university press.

Neubauer, S., Gunz, P. & Hublin, J. J. (2009). The pattern of endocranial ontogenetic shape changes in humans. *J. Anat.*, 215(3): 240-255.

Newman, J.L. (1997). *The peopling of Africa: a geographic interpretation*. Yale University Press: New Haven.

Newman, M.E. & Girvan, M. (2004). Finding and evaluating community structure in networks. *Physical review E*, 69(2): 026113.

Newman, T.K., Jolly, C.J. & Rogers, J. (2004). Mitochondrial phylogeny and systematics of baboons (*Papio*). *Am. J. Phys. Anthropol.*, 124(1): 17-27.

Northcutt, R.G. (2005). The new head hypothesis revisited. *J Exp. Zool. Part B: Mol. Dev. Evol.*, 304(4): 274-297.

Northcutt, R.G. (2008). Historical hypotheses regarding segmentation of the vertebrate head. *Integr. Comp. Biol.*, 48(5): 611-619.

Northcutt, R.G. & Gans, C. (1983). The genesis of neural crest and epidermal placodes: a reinterpretation of vertebrate origins. *Quart Rev. Biol*. 58: 1–28.

Olson, E.C. & Miller, R.L. (1951). Relative Growth in Paleontological Studies. *J. Paleo.*, 25(2): 212-223

Olson, E.C. & Miller, R.L. (1958). *Morphological Integration*. Chicago University Press: Chicago. (Reprinted 1999).

O'Regan, H.J. & Kitchener, A.C. (2005). The effects of captivity on the morphology of captive, domesticated and feral mammals. *Mammal Rev.*, 35(3-4): 215-230.

Page, S.L. & Goodman, M. (2001). Catarrhine phylogeny: noncoding DNA evidence for a diphyletic origin of the mangabeys and for a human-chimpanzee clade. *Mol. Phylogenet. Evol.*, 18(1): 14-25.

Paradis, M.R., Raj, M.T. & Boughner, J.C. (2013). Jaw growth in the absence of teeth: the developmental morphology of edentulous mandibles using the p63 mouse mutant. *Evol. Dev.*, 15(4): 268-279.

Parker, J. (2011). Morphogens, nutrients, and the basis of organ scaling. *Evol. Dev.*, 13: 304-314.

Parsons, T.E., Kristensen, E., Hornung, L., Diewert, V.M., Boyd, S.K., German, R.Z. & Hallgrímsson, B. (2008). Phenotypic variability and craniofacial dysmorphology: increased shape variance in a mouse model for cleft lip. *J. Anat.*, 212(2): 135-143.

Paternoster, L., Zhurov, A.I., Toma, A.M., Kemp, J.P., St Pourcain, B., Timpson, N.J., McMahon, G., McArdle, W., Ring, S.M., Smith, G.D., Richmond, S. & Evans, D.M. (2012). Genome-wide association study of three-dimensional

facial morphology identifies a variant in PAX3 associated with nasion position. *Am. J. Hum. Genet.*, 90(3):478-85.

Pearson, K. (1896). Mathematical contributions to the theory of evolution. III. Regression, heredity and panmixia. *Phil. Trans. R. Soc. A.*, 187: 253-318

Pearson, K. (1903). Mathematical contributions to the theory of evolution. XI. On the influence of natural selection on the variability and correlation of organs. *Phil. Trans. R. Soc. A.*, 200: 1-66.

Pearson, O.M. & Lieberman, D.E. (2004). The aging of Wolff's "law": ontogeny and responses to mechanical loading in cortical bone. *Am. J. Phys. Anthropol.*, 125(S39): 63-99.

Pélabon, C., Bolstad, G. H., Egset, C. K., Cheverud, J. M., Pavlicev, M., & Rosenqvist, G. (2013). On the relationship between ontogenetic and static allometry. *Am. Nat.*, 181(2): 195-212.

Pennacchio, L.A., Bickmore, W., Dean, A., Nobrega, M.A. & Bejerano, G. (2013). Enhancers: Five essential questions. *Nat. Rev. Genet.*, 14(4): 288.

Peterson, J., & Dechow, P. C. (2002). Material properties of the inner and outer cortical tables of the human parietal bone. *Anat. Rec.*, 268(1): 7-15.

Phillips-Conroy, J.E. & Jolly, C.J. (1988). Dental eruption schedules of wild and captive baboons. *Am. J. Primatol.*, 15: 17-23.

Polanski, J.M & Franciscus, R.G. (2006) Patterns of Craniofacial Integration in Extant Homo, Pan, and Gorilla. *Am. J. Phys. Anthropol*., 131: 38-49.

Polly, P.D. (2011). Movement adds bite to the evolutionary morphology of mammalian teeth. *BMC Biol.*, 10:69.

Pomidor, B.J., Makedonska, J. & Slice, D.E. (2016). A Landmark-Free Method for Three-Dimensional Shape Analysis. *PloS ONE*, 11(3): e0150368.

Porto, A., de Oliveira, F.B., Shirai, L.T., De Conto, V. & Marroig, G. (2009). The evolution of modularity in the mammalian skull I: morphological integration patterns and magnitudes. *Evol. Biol.*, *36*(1): 118-135.

Porto, A., Shirai, L.T., Oliveira, F.B., & Marroig, G. (2013). Size variation, growth strategies, and the evolution of modularity in the mammalian skull. *Evolution*, 67(11): 3305-3322.

Presley, R. (1993). Development and the phylogenetic features of the middle ear region. In: Szalay, F.S., Novacek, M.J. & McKenna, M.C., editors. *Mammal Phylogeny*. New York: Springer. pp. 21-29

Presely, R. & Steel, F.L. (1976). On the homology of the alisphenoid. *J. Anat.*, 121(3): 441-459.

Pyeritz, R.E. (1989). Pleiotropy revisited: molecular explanations of a classic concept. *Am. J. Med. Genet.*, 34(1): 124-34.

Rada-Iglesias, A., Prescott, S.L. & Wysocka, J. (2013). Human genetic variation within neural crest enhancers: molecular and phenotypic implications. *Phil. Trans. R. Soc. B*, 368(1620): 20120360.

Rae, T.C. (2008) Paranasal pneumatization in extant and fossil Cercopithecoidea. *J. Hum. Evol.*, 54(3): 279-286.

Raff, R.A. (1996). *The Shape of Life: Genes, Development and the Evolution of Animal Form.* Chicago: University of Chicago Press.

Randhawa, R., & Cohen, P. (2005). The role of the insulin-like growth factor system in prenatal growth. *Mol. Genet. Metab.*, 86(1): 84-90.

Retzius, A.A. (1842). Mémoire sur les formes du crâne des habitants du Nord. *Ann. Sci Nat. 3rd series, Zoologie*, 6: 133-171.

Richardson, M.K., & Chipman, A.D. (2003). Developmental constraints in a comparative framework: a test case using variations in phalanx number during amniote evolution. *J. Exp. Zool. B*, 296(1): 8-22.

Richtsmeier, J.T. (2002) Cranial Vault Dysmorphology and Growth in Mooney, M.P. & Siegel, M.I. eds, Craniosynostosis, in *Understanding Craniofacial Anomalies*. Hoboken: John Wiley & Sons, Inc.

Richtsmeier, J.T. & Flaherty, K. (2013). Hand in glove: brain and skull in development and dysmorphogenesis. *Acta Neuropathol.*, 125(4): 469–489.

Riedl, R. (1978). *Order in Living Organisms: A Systems Analysis of Evolution*. New York: Wiley.

Riska, B. (1986). Some models for development, growth and morphometric correlation. *Evolution*, 40(6): 1303-1311.

Riska, B. (1989). Composite traits, selection response and evolution. *Evolution*, 43(6): 1172-1191.

Robert, P., & Escoufier, Y. (1976). A unifying tool for linear multivariate statistical methods: the RV-coefficient. *Appl. Stat.*, 25(3): 257-265.

Rohlf, F.J. (1999). Shape Statistics: Procrustes Superimpositions and Tangent Spaces. *J. Classif.*, 16(2): 197-223.

Rohlf, F.J. (2001). Comparative methods for the analysis of continuous variables: geometric interpretations. *Evolution*, 55(11): 2143-2160.

Rohlf, F.J. (2003). Bias and error in estimates of mean shape in geometric morphometrics. *J. Hum. Evol.*, 44(6): 665-683.

Rohlf, F.J. & Slice, D. (1990). Extensions of the Procrustes method for the optimal superimposition of landmarks. *Syst. Zool.*, 39(1): 40-59.

Rohlf, F.J., Corti, M. & Olmstead, R. (2000). Use of two-block partial least-squares to study covariation in shape. *Systematic Biol.*, 49(4): 740-753.

Rolian, C. & Willmore, K.E (2009). Morphological integration at 50: patterns and processes of integration in biological anthropology. *Evol. Biol.*, 6(1): 1-4.

Rosen, C.J., Dimai, H.P., Vereault, D., Donahue, L.R., Beamer, W.G., Farley, J., Linkhart, S., Linkhart, T., Mohan, S. & Baylink, D.J. (1997). Circulating and skeletal insulin-like growth factor-I (IGF-I) concentrations in two inbred strains of mice with different bone mineral densities. *Bone*, 21: 217-223.

Ross, C.F., & Ravosa, M.J. (1993). Basicranial flexion, relative brain size, and facial kyphosis in nonhuman primates. *Am. J. Phys. Anthropol.*, 91(3): 305-324.

Rubinov, M. & Sporns, O. (2010). Complex network measures of brain connectivity: uses and interpretations. *Neuroimage*, 52(3): 1059-1069.

Russell, E.S. (1916). *Form and Function: A Contribution to the History of Animal Morphology*. John Murray: London.

Ruvolo, M. (1997). Molecular phylogeny of the hominoids: inferences from multiple independent DNA sequence data sets. *Mol. Biol. Evol.*, 14(3): 248-265.

Ruvolo, M., Disotell, T.R., Allard, M.W., Brown, W.M. & Honeycutt, R.L. (1991). Resolution of the African hominoid trichotomy by use of a mitochondrial gene sequence. *Proc. Natl. Acad. Sci. U.S.A.*, 88(4): 1570-1574.

Salles, F., Anchieta, M., Costa Bezerra, P., Torres, M.L., Queiroz, E. & Faber, J. (2008). Complete and isolated congenital aglossia: case report and treatment of sequelae using rapid prototyping models. *Oral Surg. Oral Med. Oral Pathol. Oral Radiol. Endod.*, 105(3): e41-e47.

Santagati, F. & Rijli, F.M. (2003) Cranial neural crest and the building of the vertebrate head. *Nat. Rev. Neurosci.*, 4: 806-818.

Sarnat, B.G. (1971). Surgical experimentation and gross postnatal growth of the face and jaws. *J. Dent. Res.*, 50(60): 1462-1476.

Schaefer, K., Mitteroecker, P., Gunz, P., Bernhard, M. & Bookstein, F.L. (2004). Craniofacial sexual dimorphism patterns and allometry among extant hominids. *Ann. Anat*., 186(5): 471-478.

Scheuer, L. & Black, S. (2000). *Developmental Juvenile Osteology*. London: Academic Press.

Schlebusch, C.M., Lombard, M. & Soodyall, H. (2013). MtDNA control region variation affirms diversity and deep sub-structure in populations from southern Africa. *BMC Evol. Biol.*, 13: 1-21.

Schlosser, G. (2004). The role of modules in development and evolution. In Schlosser, G. & Wagner, G.P. (eds.) *Modularity in Development and Evolution*. Chicago University Press: Chicago.

Schlosser, G. & Wagner, G.P. (2004). Introduction: the modularity concept in developmental and evolutionary biology. In Schlosser, G. & Wagner, G.P. (eds.) *Modularity in Development and Evolution*. Chicago University Press: Chicago.

Schultz, A.H. (1935). Eruption and decay of the permanent teeth in primates. *Am. J. Phys. Anthropol.*, 19(4): 489-581.

Schumacher, G.-H. (1997). Muscles, Blood Vessels, and Craniofacial Growth: Some Experimental Approaches. In Dixon, A.D., Hoyte, D.A., & Ronning, O eds. *Fundamentals of craniofacial growth*. New York: CRC Press. 463-486.

Scott, J.H. (1953). The cartilage of the nasal septum. *Br. Dent. J.*, 95: 37-43.

Seier, J. (2003). Supply and use of nonhuman primates in biomedical research: a South African perspective. IN: *National Research Council. International Perspectives: The Future of Nonhuman Primate Resources, Proceedings of the Workshop Held April 17-19, 2002.* National Academies Press: Washington.

Seko Y, Azuma N, Takahashi Y, Makino H, Morito T, et al. (2008) Human Sclera Maintains Common Characteristics with Cartilage throughout Evolution. *PLoS ONE*, 3(11): e3709.

Setchell, J.M., Wickings, E.J. & Knapp, L.A. (2006). Life history in male mandrills (*Mandrillus sphinx*): Physical development, dominance rank and group association. *Am. J. Phys. Anthropol.*, 131(4): 498-510.

Sherwood, R.J., Duren, D.L., Demerath, E.W., Czerwinski, S.A., Siervogel, R.M. & Towne, B. (2008a). Quantitative genetics of modern human cranial variation. *J. Hum. Evol.*, 54(6), 909.

Sherwood, R.J., Duren, D.L., Havill, L.M., Rogers, J., Cox, L.A., Towne, B. & Mahaney, M.C. (2008b). A Genomewide Linkage Scan for Quantitative Trait Loci Influencing the Craniofacial Complex in Baboons (*Papio hamadryas* spp.) *Genetics*, 180: 619–628.

Shi, F., Wang, L., Peng, Z., Wee, C.Y., & Shen, D. (2013). Altered modular organization of structural cortical networks in children with autism. *PLoS ONE*, 8(5): e63131.

Shirai, L.T., & Marroig, G. (2010). Skull modularity in neotropical marsupials and monkeys: size variation and evolutionary constraint and flexibility. *J. Exp. Zool. B Mol. Dev. Evol.*, 314(8): 663-683.

Singh, N., Harvati, K., Hublin, J.J. & Klingenberg, C.P. (2012). Morphological evolution through integration: a quantitative study of cranial integration in Homo, Pan, Gorilla and Pongo. *J. Hum. Evol.*, 62(1): 155-164.

Singleton, M. (2002). Patterns of cranial shape variation in the *Papionini* (Primates: Cercopithecinae). *J. Hum. Evol.*, 42(5): 547-578.

Singleton, D.A., Buschang, P.H., Behrents, R.G. & Hinton, R.J. (2006). Craniofacial growth in growth hormone-deficient rats after growth hormone supplementation. *Am. J. Orthod. Dentofacial Orthop.*, 130(1): 69-82.

Sithaldeen, R., Bishop, J.M. & Ackermann, R.R. (2009). Mitochondrial DNA analysis reveals Plio-Pleistocene diversification within the chacma baboon. *Mol. Phylogenet. Evol.*, 53: 1042-1048.

Sithaldeen, R., Ackermann, R.R. & Bishop, J.M. (2015). Pleistocene aridification cycles shaped the contemporary genetic architecture of southern African Baboons. *PloS ONE*, 10(5): e0123207.

Skelton, R.R. & McHenry, H.M. (1992). Evolutionary relationships among early hominids. *J. Hum. Evol.*, 23(4): 309-349.

Slice, D.E. (2001). Landmark coordinates aligned by Procrustes analysis do not lie in Kendall's shape space. *Syst. Biol.*, 50(1): 141-149.

Small, C., Brits, D. & Hemingway, J. (2015). Assessing the effects of tooth loss in adult crania using geometric morphometrics. *Int. J. Legal Med.*, 1174: 1-11.

Sokal, R.R., & Rohlf, F.J. (1962). The comparison of dendrograms by objective methods. *Taxon*, 11: 33-40.

Sperber, G.H., Sperber, S.M. & Guttman, G.D. (2010). *Craniofacial Embryogenetics and Development.* Shelton: PMPH-USA.

Spoor, F. (1997). Basicranial architecture and relative brain size of Sts 5. *S. Afr. J. Sci.*, 93, 182-186.

Standring, S. (2005). *Gray's Anatomy: The Anatomical Basis of Clinical Practice* (49th edition). London: Elsevier Churchill Livingston.

Stearns, S.C. (1989). Comparative and experimental approaches to the evolutionary ecology of development. *Geobios mémoire spécial*, 12: 349-355.

Stearns, F.W. (2010). One Hundred Years of Pleiotropy: A Retrospective. *Genetics*, 186(3): 767–773.

Stemple, D.L. (2005). Structure and function of the notochord: an essential organ for chordate development. *Development*, 132(11): 2503-2512.

Stern, D.L. (2000). Perspective: Evolutionary Developmental Biology and the Problem of Variation. *Evolution*, 54(4): 1079-1091.

Stern, C.D., Downs, K.M. (2012). The hypoblast (visceral endoderm): an evo-devo perspective. *Development*, 139(6):1059-1069.

Strait, D.S. (2001). Integration, phylogeny and the hominid cranial base. *Am. J. Phys. Anthropol.*, 114(4):273-297.

Swindler, D.R. & Orlosky, F.J. (1974). Metric and morphological variability in the dentition of colobine monkeys. *J. Hum. Evol.*, 3(2): 135-160.

Szalay, F.S. & Delson, E. (1979). *Evolutionary History of the Primates*. New York: Academic Press.

Takakura, M. & Kuroda, T. (1998). Morphologic analysis of dentofacial structure in patients with acromegaly. *Int. J. Adult Orthod. Orthognath. Surg.*, 13: 277-288.

Tan, S.S. & Morriss-Kay, G.M. (1985). The development and distribution of the cranial neural crest in the rat embryo. *Cell Tiss. Res.*, 240: 403-416.

Terentjev, P.V. 1931. Biometrische Untersuchungen über die morphologischen Merkmale von *Rana ridibunda* Pall. (Amphibia, Salientia). *Biometrika* 23: 23-51.

Thompson, D.W. (1917). *On Growth and Form*. Cambridge: Cambridge University Press.

Thompson, D.W. (1961). *On Growth and Form*. Cambridge: Cambridge University Press.

Trinkaus, E. (1990). Cladistics and the hominid fossil record. *Am. J. Phys. Anthropol*., 83(1): 1-11.

VandeBerg, J.R., Buschang, P.H. & Hinton, R.J. (2004a). Absolute and relative growth of the rat craniofacial skeleton. *Arch. Oral Biol.*, 49(6): 477-484.

VandeBerg, J.R., Buschang, P.H., & Hinton, R.J. (2004b). Craniofacial growth in growth hormone-deficient rats. *Anat. Rec. A Discov. Mol. Cell Evol. Biol.*, 278(2): 561-570.

Vanderschueren, D., Vandenput, L., Boonen, S., Lindberg, M.K., Bouillon, R., & Ohlsson, C. (2004). Androgens and bone. *Endocr. Rev*., 25(3): 389-425.

Van Valen, L. (1962). Growth fields in the dentition of Peromyscus. *Evolution*, 16:272-277.

Van Valen, L. (1965). The Study of Morphological Integration. *Evolution*, 19(3): 347-349.

Van Valen, L. (1970). An analysis of developmental fields. *Dev. Biol*., 23(3): 456-477.

Van Valen, L. (1973). Festschrift. *Science*, 180: 488.

Villmoare, B.A., Dunmore, C., Kilpatrick, S., Oertelt, N., Depew, M.J. & Fish, J.L. (2014). Craniofacial modularity, character analysis, and the evolution of the premaxilla in early African hominins. *J. Hum. Evol.*, 77: 143-154.

von Cramon-Taubadel, N. & Smith, H.F. (2012). The relative congruence of cranial and genetic estimates of hominoid taxon relationships: implications for the reconstruction of hominin phylogeny. J. *Hum. Evol*. 62: 640-653.

Wagner, G.P. (1984). On the eigenvalue distribution of genetic and phenotypic dispersion matrices: Evidence for a nonrandom organization of quantitative character variation. *J. Math. Biol.*, 21:77-95.

Wagner, G.P. (1988). The influence of variation and of developmental constraints on the rate of multivariate phenotypic evolution. *J. Evol. Biol.*, 1(1): 45-66.

Wagner, G.P. (1990). A comparative study of morphological integration in *Apis mellifera* (Insecta, Hymenoptera). *J. Zool. Syst. Evol. Res.*, 28(1):48-61.

Wagner, G.P. (1996). Homologues, natural kinds, and the evolution of modularity. *Am. Zool.*, 36: 36-43.

Wagner, G.P. (2007). The developmental genetics of homology. *Nat. Rev. Genet.*, 8(6): 473-479.

Wagner G.P. & Altenberg, L. (1996). Complex adaptations and the evolution of evolvability. *Evolution*, 50(3): 967-976.

Wagner, G.P & Mezey, J.G. (2004) The Role of Genetic Architecture Constraints in the Origin of Variational Modularity. In Schlosser, G. & Wagner, G.P. (eds.) *Modularity in Development and Evolution.* Chicago University Press: Chicago, IL.

Wagner, G.P. & Zhang, J. (2011). The pleiotropic structure of the genotype–phenotype map: the evolvability of complex organisms. *Nat. Rev. Genet.*, 12(3): 204-213.

Wagner, G.P., Pavlicev, M. & Cheverud, J.M. (2007) The road to modularity. *Nat. Rev. Genet.*, 8(12): 921-931.

Wayne, R.K. (1986). Cranial morphology of domestic and wild canids: the influence of development on morphological change. Evolution, 40(2): 243-261.

Weidenreich, F. (1941). The brain and its rôle in the phylogenetic transformation of the human skull. *Trans. Am. Philos. Soc*., 31(5): 320-442.

Weidenreich, F. (1946). Generic, specific and subspecific characters in human evolution. *Am. J. Phys. Anthropol*., 4(4): 413-432.

Weidenreich, F. (1947). Some particulars of skull and brain of early hominids and their bearing on the problem of the relationship between man and anthropoids. *Am. J. Phys. Anthropol*., 5(4): 387-428.

White, T.D., Black, M.T. & Folkens, P.A. (2012). *Human Osteology*. San Diego: Academic Press.

Wiley, D.F., Amenta, N., Alcantara, D.A., Ghosh, D., Kil, Y.J., Delson, E., Harcourt-Smith, W., Rohlf, F.J., St. John, K. & Hamann, B. (2005). *Evolutionary Morphing. Proceedings of IEEE Visualization*, 23-28 Oct. 2005: 431-438.

Willmore, K.E., Roseman, C.C., Rogers, J., Cheverud, J.M. & Richtsmeier, J.T. (2009). Comparison of mandibular phenotypic and genetic integration between baboon and mouse. *Evol. Biol.*, 36(1): 19-36.

Willmore, K.E., Buikstra, J.E., Cheverud, J.M., & Richtsmeier, J.T. (2012). Developmental origins of and covariation between metric and nonmetric cranial traits. In Wang, Q. ed. *Bones, genetics, and behavior of Rhesus macaques:* Macaca mulatta *of Cayo Santiago and beyond*. New York: Springer. pp. 61-84.

Wright, S. (1918). On the nature of size factors. *Genetics*, 3: 367-374.

Wright, S. (1932). General, group and special size factors. *Genetics*, 15: 603-619.

Wright, S. (1934). The method of path coefficients. *Ann. Math. Stat.*, 5: 161-215.

Yoshida, T., Vivatbutsiri, P., Morriss-Kay, G., Saga, Y. & Iseki, S. (2008). Cell lineage in mammalian craniofacial mesenchyme. *Mech. Dev*., 125(9): 797-808.

Young, N.M., & Hallgrímsson, B. (2005). Serial homology and the evolution of mammalian limb covariation structure. *Evolution*, 59(12): 2691-2704.

Zelditch, M.L. (1987). Evaluating Models of Developmental Integration in the Laboratory Rat Using Confirmatory Factor Analysis. *Syst. Biol.*, 36(4): 368-380.

Zelditch, M.L. (1988). Ontogenetic Variation in Patterns of Phenotypic Integration in the Laboratory Rat. *Evolution*, 42(1): 28-41.

Zelditch, M.L. & Carmichael, A.C. (1989). Growth and intensity of integration through postnatal growth in the skull of *Sigmodon fulviventer*. *J. Mammal*., 70(3): 477-484.

Zelditch, M.L., Swiderski, D.L., Sheets, H.D. & Fink, W.L. (2004). *Geometric Morphometrics for Biologists: A Primer*. New York: Elsevier Academic Press.